The role of specific adhesins in the regulation of other adhesin genes associated with *Mycobacterium tuberculosis* pathogenicity

Johannes Nkanyiso Mthembu

Submitted in fulfilment of the requirements for the degree of Masters in Medical Science (Medical Microbiology)

The discipline of Medical Microbiology

School of Laboratory Medicine and Medical Sciences

College of Health Sciences

University of KwaZulu-Natal

South Africa

2022

Supervisor: Professor Manormoney Pillay

Co-supervisor: Dr Sibusiso Senzani

Plagiarism declaration

DECLARATION:

I, Johannes Mthembu (Student number:214539650) declare that all work presented in this dissertation is my original work which is being submitted for the first time to this University and has not been submitted to any other University. The work of others has been indicated and acknowledged throughout this dissertation to the best of my knowledge.

Signed:

JN Mthembu

_____ 2nd September 2022

Supervisor: Professor Manormoney Pillay Date

_____ 01/09/2022

Sibusiso Senzani Date

DEDICATION

To all those who are first graduates at home and who are meant to break their family generational curses. Aluta continues.

ACKNOWLEDGEMENTS

To my Supervisor Prof MP, thank you so much for giving me a chance to be part of your research group. I have learned a lot from you and your professionalism. I would say I came to Medical School, clueless about life. However, I've looked at myself and reflected on the growth. There is a lot that I have learned. Thank you so much, I appreciate it.

I would like to acknowledge the project funding provided by the National Research Foundation (Grantholder-linked and DST-NRF Innovation Masters Bursary) and the UKZN College of Health Sciences.

To my Co-supervisor, Dr. Sibusiso Senzani, you made the research fascinating.

To Inga Elson and Zareena Solwa thank you so much for being there for me in hard times. To Inga, there are no words that can describe how you played a role the times I had a break-in at res and the time they attempted to mug me. I lost hope and I suffered from depression, you came in and played the role of a parent. Thank you so much for the Laptop and the cell phone as part of my gift. I appreciate you a lot. Once again, thank you so much for giving me a chance to assist you in the Laboratory. There is a lot that I've learned from you.

To Nonhle Mkhwanazi, thank you so much for being the best friend I met in Medical School. You have been there for me and that is what friends are for. To Asanda Nyide, thank you so much friend for being a true person. The world needs people like you. Your motivation, your words of encouragement, and constant check-ups meant a lot to me.

To Tumelo Mzenda, thank you so much Tumrisho for being there for me. There are no words that can describe how you played a part in my life as a friend. Thank you so much for believing in me. Also, I cannot forget Minenhle Nxumalo and Khethelo Nxumalo, homies thank you so much for welcoming me back to Durban. You guys offered me shelter and food while I was still sorting out the funding with Prof MP. I appreciate both of you. To my family, thanks guys. I would like to thank my family for their continuous love, support, and encouragement to follow my dreams.

TABLE OF CONTENTS

LIST OF TABLES

LIST OF FIGURES

LIST OF ABBREVIATIONS

AES	Allelic exchange substrate
Apa	Alanine-proline rich antigen
Ag85A	Antigen 85A
AIDS	Acquired immunodeficiency syndrome
cDNA	Complementary deoxyribonucleic acid
CFU	Colony forming unit
CO_2	Carbon dioxide
ºC	Degrees Celsius
Cpn60.2	Chaperone protein 60.2
DEPC	Diethyl pyrocarbonate
DNA	Deoxyribonucleic acid
ECM	Extracellular matrix
FAP	Fibronectin Attachment protein
FBS	Fetal bovine serum
g	G-Force/ Relative Centrifugal Force
HBHA	Heparin-binding hemagglutinin adhesin
Δ*hbhA*	Heparin-binding hemagglutinin knockout mutant
hbhA-complement	Complemented heparin-binding hemagglutinin knockout strain
HIV	human immunodeficiency virus
HRP	Horseradish peroxidase
INF	Interferon
IgG	Immunoglobulin G
IL	Interleukin
kDa	kilo dalton
KZN	KwaZulu-Natal
LAM	Lipoarabinomannan
LTBI	Latent tuberculosis infection
LpqH	lipoglycoprotein antigen
MOPS	3-(N-morpholino) propane sulfonic acid

MDR	Multidrug-resistant
min	Minutes
mL	Millilitre
MOI	Multiplicity of infection
M. tuberculosis	*Mycobacterium tuberculosis*
MTBC	*Mycobacterium tuberculosis* complex
MTP	*Mycobacterium tuberculosis* curli pili
Δ*mtp*	*Mycobacterium tuberculosis* curli pili knockout mutant
mtp-complement	*Mycobacterium tuberculosis* curli pili complemented *mtp*
Δ*mtp-hbhA*	*Mycobacterium tuberculosis* curli pili- Heparin-binding hemagglutinin knockout mutant
mtp-hbhA-complement	*Mycobacterium tuberculosis* curli pili- Heparin-binding hemagglutinin complemented knockout strain
OADC	Oleic acid-albumin-dextrose-catalase
OD	Optical density
PBS	Phosphate buffered saline
PCR	Polymerase chain reaction
POC	Point of care
Psts-1	Phosphate binding transporter protein
RNA	Ribonucleic acid
rpm	Rotations per minute
RT-qPCR	Real time reverse transcription quantitative polymerase chain reaction
s	Second
SA	South Africa
TB	Tuberculosis
TDR	Total drug-resistant
TLR	Toll-like receptor
TNF-α	Tumour necrosis factor alpha
µL	Microlitre
V	Volts

v/v	Volume/ volume
WHO	World Health Organization
WT	Wild-type
XDR	Extensively drug-resistant

ABSTRACT

Background/Aim: Tuberculosis (TB), caused by *Mycobacterium tuberculosis* (*M. tuberculosis*), remains one of the most common causes of death throughout the world. The lack of rapid diagnostics, effective vaccines, and drugs contributes to the high number of deaths recorded every year. The presence of multiple surface adhesins is critical for *M. tuberculosis* survival because they initiate and sustain host-pathogen interactions. Amongst other adhesins is the *M. tuberculosis* curli pili (MTP), which aid in the adhesion/invasion of host cells and the development of biofilms. The heparin-binding haemagglutinin adhesin (HBHA) facilitates the spread of *M. tuberculosis* away from the site of infection. Since L, D-transpeptidase (Ldt), which is encoded by *Rv0309*, has been shown to bind to laminin and fibronectin and to be an adhesin, it may serve as a biomarker for the development of novel therapeutic approaches. Studying the impact triggered by the three adhesins, MTP, HBHA, and Rv0309, on the regulation of other adhesins that bind to macrophages; 19-kilodalton (19 kDa), *M. tuberculosis* Phosphate-binding protein (PstS-1), Chaperone chaperonin 60.2 (Cpn 60.2), Alanine and proline-rich antigenic glycoprotein (Apa), antigen 85 complexes (Ag85A), chaperone DnaK, and *M. tuberculosis* type IV pili, will further substantiate their use in biomarker development. Therefore, the purpose of this study was to elucidate the role of MTP, HBHA, and Rv0309 adhesins in regulating adhesins that bind to macrophages during infection. This was achieved using *in vitro* infection assays with gene knockout and complemented mutant strains of *M. tuberculosis*, real-time quantitative PCR (RT-qPCR), and a dot blot assay.

Methods: *M. tuberculosis* wild-type, *mtp*-deletion mutant (Δ*mtp*), *hbhA*-deletion mutant (Δ*hbhA*), *mtp-hbhA*-deletion mutant (Δ*mtp-hbhA*), Δ*Rv0309* mutant and the respective complemented strains that had been constructed in previous studies, were confirmed using polymerase chain reaction (PCR). The strains were individually cultured in supplemented Middlebrook 7H9 broth till an optical density of 600 $(OD)_{600}$ of 1 was reached. THP-1 monocytic cells were differentiated into macrophages and infected at a multiplicity of infection (MOI) of five. At the end of 4-h and 24-h post-infection, cells were lysed with TritonX-100. The lysate from the infected cells was collected for RNA extraction and bacterial protein extraction. To quantify the internalized bacteria, serial dilutions of the lysate from the infected cells were plated on 7H11 agar plates for CFUs. To confirm MOI, the bacterial inoculum was serially diluted and plated for CFUs. Intracellular pathogen RNA was extracted using the TriZol method and converted into cDNA using the High Capacity cDNA Reverse Transcription kit. Primers for adhesin genes: *Rv0350, Rv0440, Rv0934, Rv1860, Rv3660, Rv3763,* and

Rv3804 were designed using Primer3plus web. To assess the impact triggered by MTP, HBHA, and Rv0309 adhesin on the expression of *Rv0350, Rv0440, Rv0934, Rv1860, Rv3660, Rv3763,* and *Rv3804*, RT-qPCR- was performed using 2X SYBR green supermix in a 7500 RT-qPCR Detection System. The gene expression data was normalized using 16S rRNA and analysed using the absolute quantification method. Proteins were isolated using the TriZol method and resuspended in 0.1 % SDS. Extracted proteins were resolved in SDS-PAGE. Western blot was attempted with Cpn60.2 and PstS-1 primary antibodies used against the Goat anti-mouse HRP secondary antibody. Dot blot was used to determine the optimal antibody dilutions and protein concentration. GraphPad Prism version 8 software was used to determine significance values.

Results and Discussion: Infection with mutant *mtp* resulted in a decrease in the number of bacteria that infected THP-1 cells at both 4-h ($p < 0.001$) and 24-h ($p = 0.002$) time points compared to the wild-type. At 4-h post-infection, four of the seven genes, *Rv3763*, *Rv3804*, *Rv1860* and *Rv0440*, were expressed in all three strains. The expression of three of these genes, *Rv3763* ($p = 0.049$), *Rv3804* ($p = 0.003$) and *Rv0440* ($p = 0.004$), was significantly increased in the Δ*mtp* compared to the wild-type strains. *Rv3660* was expressed in the Δ*mtp* but not in the wild-type ($p = 0.012$). At 24-h post infection. the expression of five genes was significantly increased in the wild-type compared to the Δ*mtp* strain; *Rv3763* ($p = 0.049$), *Rv0934* ($p = 0.006$), *Rv3804* ($p = 0.005$), *Rv0350* ($p = 0.012$) and *Rv0440* ($p = 0.004$). The *mtp* mutant strain induced lower expression of the genes at 24-h (*Rv3763*, *Rv0934*, *Rv3804*, *Rv1860* and *Rv0440*) in contrast to 4-h. Low expression of the genes *Rv3763, Rv0934, Rv1860* and *Rv3804* in the mutant *mtp* strain are associated with cell wall activities and are important virulence factors of *M. tuberculosis*. The decrease in the CFUs and altered gene expression in the mutant suggests that *mtp* is required for the expression of the genes associated with cell wall processes and that the deletion of the *mtp* gene may result in a decrease in cell wall activities. The deficiency of *mtp* gene in the mutant resulted in the reduced capability of the strain in infecting the THP-1 cells implying a decrease in the virulence of the strain.

Infection with the *hbhA* mutant resulted in a decrease in the number of bacteria that infected THP-1 cells at both 4-h ($p = 0.049$) and 24-h ($p = 0.034$) time points compared to the wild-type. At 4-h post-infection, five of the seven genes, *Rv3763*, *Rv0934*, *Rv3804*, *Rv1860* and *Rv0440*, were expressed in all three strains. The *hbhA* mutant induced the expression of all the genes at both 4-h and 24-h. *Rv3660* ($p = 0.001$) and *Rv0350* ($p < 0.001$) were expressed in the Δ*hbhA* but not by the wild-type at 4-h. At 24-h, all seven genes, *Rv3763, Rv0934, Rv3804, Rv0350, Rv3660, Rv1860* and *Rv0440,* were expressed across all strains. The expression of four of these

genes was significantly increased in the wild-type compared to the Δ*hbhA* strain *Rv3763* (p=0.023), *Rv0934* (p=0.001), *Rv3804* (p=0.002), *Rv1860* (p=0.017). The deletion of *hbhA* induced the expression of all the adhesin genes to compensate for the loss of this gene in the mutant.

There was a significant reduction in the number of bacteria that infected THP-1 cells in the Δ*mtp-hbhA* compared to the wild-type at the 4-h (p =0.002) and 24-h (p =0.047) time points. The double knockout induced a low expression of *Rv3763, Rv0934, Rv0350, Rv3804,* and *Rv3660* at 4-h. The expression of *Rv3763* (p=0.039), *Rv0934* (p = 0.002) and *Rv3804* (p=0.000) was significantly increased in the wild-type strains compared to the Δ*mtp-hbhA*. There was a higher expression of *Rv1860* and *Rv0440* in the mutant at 4-h compared to the 24-h time point. At 24-h, all seven genes, *Rv3763*, *Rv0934*, *Rv3804*, *Rv0350*, *Rv3660*, *Rv1860* and *Rv0440*, were expressed across all strains. The expression of these genes was significantly increased in the wild-type compared to the Δ*mtp-hbhA. Rv3763* expression was higher in the mutant at 24-h compared to the 4-h. The observed expression in the mutant suggests the importance of both *hbhA* and *mtp* in the virulence of *M. tuberculosis.* Deletion of *mtp-hbhA* resulted in a decrease in the capability of *M. tuberculosis* in initiating infection in THP-1 cells.

There was a significant difference in *Rv0309* mutant in infecting THP-1 cells in comparison to the wild-type strains at the 4-h and 24-h time points (p = 0.001). This suggests that deletion of the *Rv0309* gene in the mutant might have reduced the infecting capability of the strains. There was an upregulation of the *Rv3763, Rv0934*, *Rv1860*, *Rv3804,* and *Rv0440* in the mutant at 4-h. Upregulation of these genes suggests that *Rv0309* is an important virulence factor of *M. tuberculosis*. *Rv1860* expression at 24-h was doubled compared to the expression of 4-h in the mutant to compensate for the loss of *Rv0309* in the mutant. This may suggest that in the absence of *Rv0309*, the *M. tuberculosis* expresses *Rv1860* which binds to laminin and fibronectin to promote infection.

Confirmatory studies by protein detection using anti-Cpn 60.2 and anti-PstS1 antibodies with western blot failed. Numerous attempts for troubleshooting were conducted using the dot blot assay and optimisation of various factors, such as the use of positive control, different antibody dilutions, protein concentration, and optimized buffers. This showed that the purchased antibodies did not work.

Conclusion: The findings demonstrated that MTP, HBHA and Rv0309 play a role in the regulation of other adhesin genes, as evidenced by the deletion of the three major genes that

may have disrupted several metabolic and cell wall processes, potentially reducing the virulence of the *M. tuberculosis* strain. The findings of this work add to the growing evidence that the adhesins, MTP, HBHA, and Rv0309 as well as the related adhesins they interact with during macrophage infection, are promising targets for TB diagnostic or therapeutic interventions.

Introduction

Tuberculosis (TB), caused by *Mycobacterium tuberculosis* (*M. tuberculosis*), remains one of the most common causes of death throughout the world (WHO, 2021), especially amongst the most vulnerable populations (WHO, 2021). In people with TB, human immune deficiency virus (HIV) co-infection promotes the progression of latent TB to active disease (Iliyasu and Babashani, 2009). Globally, close to 1.5 million deaths were caused by TB in 2020 (WHO, 2021). Despite combinatorial antibiotic treatment and widespread vaccination, the global incidence of TB in 2020 was estimated to be around 10 million annually (8.2 % in people living with HIV) (WHO, 2021). About 86 % of TB infections were reported in resource-poor countries where there is a rapid re-emergence due to poor strategies to control TB (WHO, 2021).

In addition to HIV, the limitations of current diagnostic methods and the emergence of drug resistance, including multi-(MDR), extensively-(XDR) and total-(TDR) drug-resistant *M. tuberculosis* strains pose a serious threat to TB control due to the ineffectiveness of the standard TB regimes (WHO, 2018). Recent advances in diagnostics, such as Xpert MTB/RIF (Cepheid, Sunnyvale, CA) and first-line probe assays (e.g., GenoType MTBDRplus and Nipro NTM+MDRTB detection kit 2, (referred to as "Nipro", Tokyo, Japan) enable rapid drug-susceptibility testing for rifampicin (RIF) and isoniazid (INH) resistance (WHO, 2021). Despite these advances, therapeutic strategies are still not enough to reach the end goal of TB elimination by 2050. In addition to this, the current standard TB treatment regime entails taking a combination of multiple drugs for at least 6 months, all of which have side effects and hence represent considerable obstacles to patient compliance (WHO,2021). This further results in treatment cessation due to the lengthy treatment duration and adverse effects due to toxicity of the drugs. This factor, when paired with an incorrect drug prescription, contributes greatly to the formation and spread of multidrug-resistant and extensively drug-resistant *M. tuberculosis* strains in the population, necessitating more complex treatment regimens for a much longer period of time (WHO, 2021). Thus, novel strategies are urgent needed to combat the global TB pandemic.

There have been significant advancements in TB diagnostic technologies, but they are frequently prone to error, expensive, lack the essential sensitivity or accuracy and, most importantly, are not adequately portable, making them ineffective in isolated, rural areas where they are most needed (MacGregor-Fairlie *et al*., 2020). In addition to this, the slow laboratory

turnaround times lead to the inability to initiate treatment timeously, thus contributing to increased transmission rates (Tsara *et al*., 2009; Engel *et al.,* 2015; Musewa *et al*., 2021). Therefore, there is a need to develop new therapeutics and rapid, accurate diagnostic tools and this relies on the discovery of suitable, novel biomarkers (Parsons *et al.,* 2011).

One of the greatest challenges in TB control is the lack of effective vaccines. In the past 100 years, Bacillus Calmette Guerin (BCG) vaccine has been the only licensed vaccine that is available to the public (Luca and Mihaescu, 2013; WHO, 2014). The BCG vaccine is used to prevent childhood TB meningitis and miliary TB in many countries with a high prevalence of TB (Trunz *et al*., 2006). However, the BCG vaccine is effective only in infancy and not protective in adults (Trunz *et al.,* 2006). As part of the WHO strategy to end the global TB epidemic by 2035, new vaccine candidates are in clinical trials (WHO, 2021). The introduction of efficacious vaccines would be needed for the elimination of 90 % of TB mortality and 95 % of TB incidence rates by 2035 (WHO, 2014). In addition to this, new vaccine candidates need to be safer than the BCG vaccine and offer protection from new-born to adulthood (Scriba *et al.,* 2020). However, effective vaccine development relies on biomarkers that can be used as therapeutic targets.

The lack of suitable biomarkers has hindered the design of rapid TB diagnostics and therapeutics (Murray, 2007; Govender, 2018). Despite considerable research, not many biomarkers have been shown to be suitable targets for point of care (POC) tests, vaccines, and drugs. Inflammation-based biomarkers such as the C-reactive protein lack predictive value for clinical use due to their non-specific nature (Wallis *et al*., 2013). The most reliable biomarkers capture the effects of various types of interventions on clinical outcomes by measuring important elements related to the pathological processes of the disease being treated (Maertzdorf *et al.,* 2011). Molecules originating from the intracellular, extracellular, or cell surface of *M. tuberculosis* such as metabolites, DNA, and protein, can be exploited as possible targets for TB detection in a variety of tests (Martin *et al*., 2021). The *M. tuberculosis* extracellular proteins such as adhesins and virulence factors such as fibronectin-binding protein A (*FbpA*), B (*FbpB*) and C (*Fpb*C) (Viljoen *et al*., 2020) are promising TB biomarkers that can be used for the development of rapid diagnostics and therapeutics.

While other respiratory pathogens such as *Streptococcus* and *Mycoplasma* express their virulence through a single powerful toxin, *M. tuberculosis* has been shown to secrete different proteins that function to deactivate macrophages (Barnett *et al.,* 2015). One of these proteins

includes adhesins, which are externally located in most pathogenic bacteria, and can be used as targets in diagnosis, drug, and vaccine development (Kumar *et al.,* 2013). *Mycobacterium tuberculosis* has been reported to harbour multiple adhesins, which may play a role in the epidemiological success of this pathogen. The majority of the adhesins secreted by *M. tuberculosis* are surface located. These include the well-known Heparin-binding hemagglutinin adhesin (HBHA) (Pethe *et al.,* 2001), Malate Synthase (Kinhikar *et al*., 2006), Apa (alanine-proline-rich antigen) (Ragas *et al.,* 2007), and curli pili (MTP) (Alteri *et al.,* 2007). Since adhesins are externally located, they may be useful as biomarkers in TB diagnostics (Telford *et al*., 2006). Adhesins are also the first point of contact between the host and pathogen, and therefore, may be suitable targets for the design of novel, effective drugs. In addition to this, some adhesins have been reported to induce host response, such as HBHA (Pethe *et al.,* 2001) and MTP (Alteri *et al*., 2007), and are therefore potential vaccine candidates.

Among the studied adhesins, an important target for diagnostic, vaccine and drug development is MTP (Rv3312A), a virulence factor and prospective diagnostic/therapeutic target (Alteri *et al*., 2007). *Mycobacterium tuberculosis* curli pili binds to laminin and has been shown to react with IgG antibodies in the sera of TB patients (Alteri *et al*., 2007). Functional genomics research has shed light on the role MTP plays in the adhesion and invasion of THP-1 macrophages (Ramsugit and Pillay, 2014) and A549 epithelial cells (Ramsugit *et al*., 2016). Heparin-binding hemagglutinin (*Rv0475*) is present in the early stages of TB infection and is the first point of contact with epithelial cells (Pethe *et al*., 2001). Additionally, the pathogen's binding to epithelial cell glycoconjugates was discovered to be aided by HBHA (Pethe *et al.*, 2001). A study by Menozzi *et al*., (2006) suggested that HBHA could constitute a macrophage-independent extra pulmonary dissemination mechanism that leads to *M. tuberculosis* infection. The *Rv0309* gene which encodes L, D-transpeptidase, an enzyme that plays a role in cell division and separation, as well as biofilm formation (Muniram, 2018), has been identified as a potential adhesin (Kumar *et al*., 2013). However, not much has been reported on its role as adhesin and invasin. The emerging research on *M. tuberculosis* adhesins as potential biomarkers justifies further study for their use in TB diagnostics and therapeutics.

Globally, diagnosis and successful treatment of TB prevents millions of deaths each year with an estimated 54 million lives from 2000 to 2017 (WHO, 2018). However, there is still a large and persistent gap in detection and treatment (WHO, 2018). Whilst anti-TB strategies are available, novel and rapid approaches are urgently required for the diagnosis, treatment, and prevention of TB, to reduce global TB burdens. The success of *M. tuberculosis* as a global

pathogen may be attributable to the presence of multiple adhesins that enable the initial interaction with host cells. The current study proposes to elucidate whether deletion of the selected identified adhesins, MTP, HBHA and Rv0309, will result in a compensatory up- or down regulation of the reported multiple adhesins during TB pathogenesis in a THP-1 infection model. The findings will increase current knowledge of the role of adhesins in TB pathogenesis, and support the inclusion of multiple adhesins in the design of diagnostics, vaccines and drugs that may potentially block the initial crucial attachment between pathogen and host.

Chapter 1: Literature Review

1.1 The global picture of TB and HIV/AIDS

Tuberculosis (TB) is a serious global health problem and is listed as one of the most common causes of death (WHO, 2021). Despite the significant scientific effort that has been made to better understand this disease, global prevalence rates remain high with 150-600 cases per 100 000 population in a number of the 30 high TB burden countries (WHO, 2020). The disease affects child health directly and indirectly as most of the disease victims are parents of young children. Its effects are mostly recognized in low-income, poor countries where there is a lack of TB control strategies (WHO, 2021). In many countries in Sub-Saharan Africa and South Asia, escalating rates of TB were due to the human immunodeficiency virus (HIV) epidemic (WHO, 2021). In 2020, there were an estimated 10 million new cases of TB world wide, of which 5.6 million were men, 3.3 million were women and 1.1 million were children (WHO, 2021). People living with HIV accounted for 9 % of the total cases (WHO, 2021). Globally, the incidence of TB is decreasing at a rate of roughly 2 % per year, with a total reduction of 11 % between 2015 and 2020 (WHO, 2021). This was more than halfway to the End TB Strategy's goal of a 20 % reduction in TB cases between 2015 and 2020 (WHO, 2021).

The number of TB deaths decreased by 9.2 % between 2015 and 2020, only about a fourth of the way to the target (WHO, 2021). The increase in TB mortality in 2020 due to disruptions in diagnosis and treatment-induced by the COVID-19 pandemic jeopardized the progress made up to 2019 (14 % drop from 2015 to 2019 and a 41 % reduction from 2000 to 2019) (WHO, 2021). To have achieved the first milestone of the End TB strategy of 2020, the incidence rate should have declined between 4-5 % per annum, with the case fatality ratio declining to 10 % (WHO, 2018).

1.2 Association of TB with HIV

Studies have shown that the HIV epidemic enhanced the TB pandemic and caused a shortage of effective TB treatment (Ducati *et al.*, 2006; Keshavjee and Farmer, 2012). The combined impact of HIV and TB is fatal, with each speeding up the progression of the other (Schlipköter and Flahault, 2010; Kwan and Ernst, 2011; WHO, 2021). It has been observed that HIV-infected individuals are most likely to develop TB (Kwan and Ernst, 2011), presumably due to the weakened immune system that makes it more difficult to fight the TB pathogen (Ducati *et al.*, 2006; WHO, 2021). Around 214 000 people died from HIV-related TB globally in 2020 (WHO, 2021). In 2020, only 73 % of notified TB patients globally had a recorded HIV test result, up from 70 % in 2019 (WHO, 2020). Overall in 2020, 88 % of TB patients known to be living with HIV were on anti-retroviral therapy (ART) (WHO, 2021). About 85 % of TB patients in the WHO African Region, where the burden of HIV-associated TB is highest, had a documented HIV test result (WHO, 2021). The HIV-compromised immune system provides a conducive environment for acquiring new infections as well as for reactivation of latent bacilli into a vegetative form which then causes active disease (Kana *et al.*, 2008). Infection with *M. tuberculosis* can speed up the progression of HIV into acquired immune deficiency syndrome (AIDS) making TB the leading cause of death in HIV-infected individuals (Schlipköter and Flahault, 2010).

1.3 Tuberculosis and HIV in South Africa

South Africa is listed among the 30 countries of the world with a high burden of TB (WHO, 2021). Incidence rates of TB in South Africa have increased from less than 301 per 100 000 population in 1990 to 576 per 100 000 population in 2000 (WHO, 2002) and continued to increase to more than 900 per 100 000 population in 2009 (WHO, 2010). The World Health Organization (WHO) reported an estimated incidence of 328 000 cases of active TB in 2020 compared to an incidence of 500 000 cases in the year 2011 (WHO, 2021). This statistic is significantly lower than the WHO prediction of 360 000 people estimated in 2019 and the findings of South Africa's first national TB prevalence survey (390 000). The apparent drop in TB diagnoses reflects the global fall in TB notifications caused by the COVID-19 pandemic's influence on TB screening and testing (WHO, 2021). The WHO provided an estimate of 61 000 people who died from TB in South Africa in 2020 (WHO, 2021). In addition to this, of the

61 000 people estimated, 36 000 were reported to have been co-infected with TB/HIV and the other 25 000 died from TB disease alone (WHO, 2021).

1.4 Drug-resistant *M. tuberculosis*

The best estimate of the percentage of patients receiving an MDR/RR-TB diagnosis for the first time has remained at around 3-4 % for more than a decade, and at about 18–21 % for TB that has already been treated (WHO, 2021). Globally, 470,000 people fall ill with a TB that does not respond to at least isoniazid and rifampicin (MDR/RR-TB) and about 180,000 die from this form of TB each year (WHO, 2021). Rifampicin resistance was detected in 71 % (2.1/3.0 million) of patients diagnosed with bacteriologically proven pulmonary TB in 2020, up from 61 % (2.2/3.6 million) in 2019 and 50 % (1.7/3.4 million) in 2018 (WHO, 2021). Globally, there were 132 222 cases of MDR/RR TB and 25 681 cases of pre-XDR-TB or XDR-TB in 2020 (WHO, 2021). This was a significant decrease (22 %) from the total of 201 997 people diagnosed with MDR/RR TB in 2019, and it was consistent with similarly significant decreases in the total number of people newly diagnosed with TB (18 %) and the total number of people diagnosed with bacteriologically confirmed pulmonary TB (17 %) between 2019 and 2020 (WHO, 2021).

Globally, the average proportion of MDR-TB patients with *M. tuberculosis* strains also resistant to one of the fluoroquinolones was 20.1 % (95 % confidence interval 15.5–25.0 %) based on data from 105 countries and territories (WHO, 2020). Figure 1.1 shows three major populations that predominantly contribute to the current MDR-TB epidemic since they account for almost half of global TB recorded cases (WHO, 2020). Despite the fact that countries have been increasing diagnostic capacity and detecting more patients with rifampicin resistance in recent years, only 201 997 patients (44 % of the estimated total) were notified globally, indicating that drug susceptibility testing coverage is severely inadequate.

The prevalence and incidence rates of drug-resistant TB in KwaZulu-Natal province were the highest in South Africa (Kapwata *et al*., 2017). An outbreak of XDR TB in the Tugela Ferry region, uMzinyathi district, was reported in 2006 (Gandhi *et al*., 2006). Multi drug resistant TB was found in 221 out of 1539 individuals, including 53 HIV-infected patients who had XDR-TB in 2005 (Gandhi *et al*., 2006). In 2004, there were 584 laboratory-diagnosed cases of MDR-TB in the KwaZulu-Natal province, followed by an increase in 2012 to 6630 cases

(Gandhi *et al.*, 2012). Massyn *et al.*, (2016) reported that in KwaZulu-Natal, 3603 TB patients started drug-resistant TB (DR-TB) treatment in 2015 and 84 (2 %) of the patients were children.

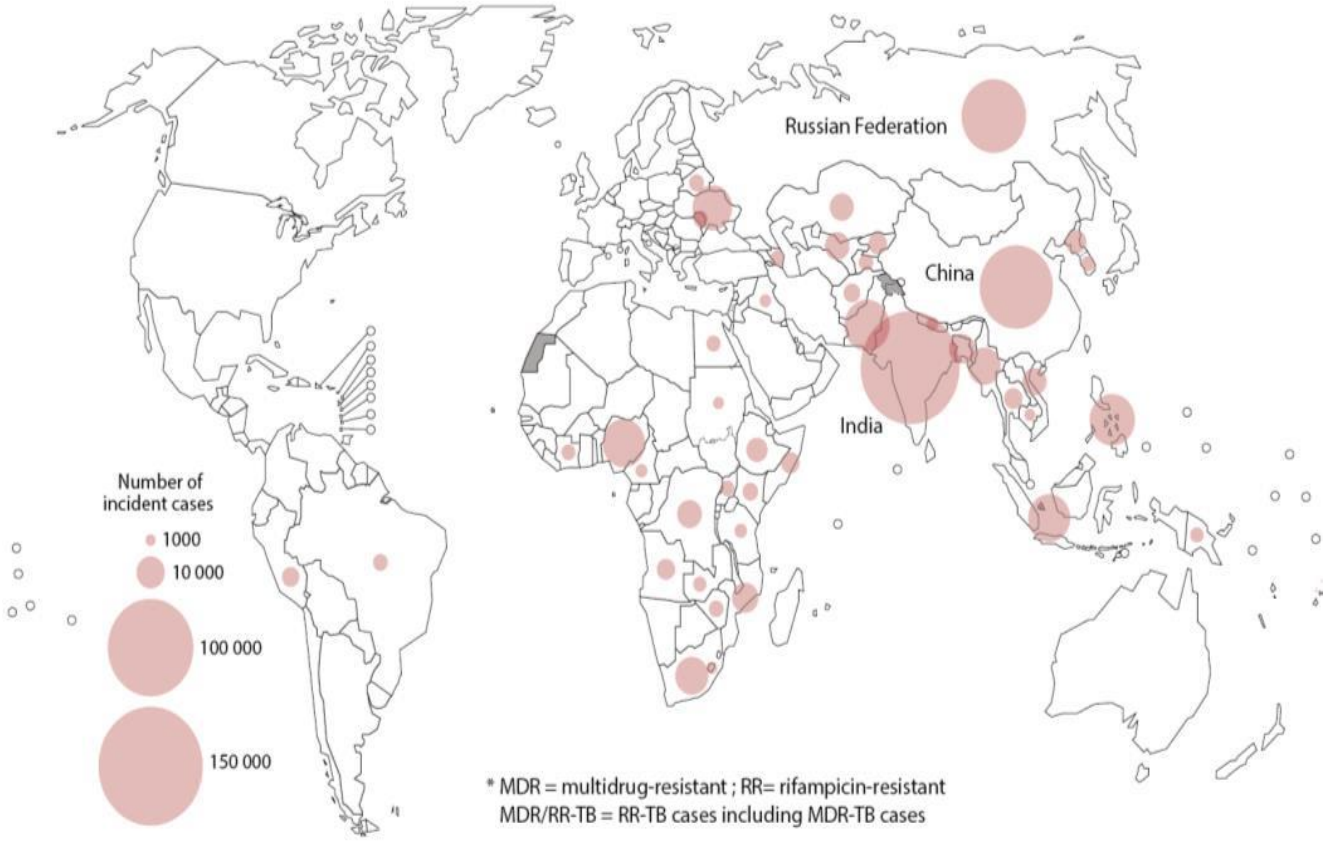

Figure 1.1: The estimated incidence of MDR/RR-TB in 2020, for countries with at least 1000 incident cases (WHO, 2020)

The figure above indicates 3 major populations as the most significant contributors to the rising prevalence of MDR-TB; India, Russia, and China. Image sourced from WHO Global Tuberculosis Report, 2020.

1.5 General description of *M. tuberculosis*.

Mycobacterium tuberculosis belongs to the *Mycobacterium tuberculosis* complex (MTBC) that includes *Mycobacterium africanum*, *Mycobacterium bovis*, *Mycobacterium caprae*, *Mycobacterium microti*, *Mycobacterium pinnipedii*, *Mycobacterium origis*, *Mycobacterium mungi*, *Mycobacterium suricattae* (Alexander *et al*., 2010; Coscolla *et al*., 2013; Parsons *et al*., 2013, Gupta *et al*., 2018; Riojas *et al*., 2018; Lipworth *et al*., 2019). The MTBC were classified using the IS6110 Restriction fragment length polymorphism (RFLP) analysis that groups clinical strains according to genotype families (Filliol *et al*., 2006; Gutacker *et al*., 2006). The methods of large sequence polymorphism (LSP) and whole genome sequencing (WGS) were used to divide human-adapted clinical strains into seven lineages that are spread around the globe (Tsolaki *et al*., 2005; Homolka *et al*., 2012; Stucki *et al*., 2012). These lineages are referred to as lineages 1 through 7, and they are phylogenetically linked together based on genomic deletions known as region of difference (RD) and *M. tuberculosis*-specific deletion 1 region (TbD1). The MTBC's human-adapted lineages have a specific geographic distribution, with certain "generalist" lineages like Lineage (L) 2 and L4 appearing all over the world and others, like L5, L6, and L7, having regionally confined "specialist" lineages (Coscolla and Gagneux, 2014; Stucki *et al.,* 2016). Africa is the only continent where all seven human-adapted lineages may be found, including three "specialist" lineages found nowhere else. According to current research, the MTBC started in Africa (Gagneux, 2018) and spread over the world as a result of human migration.

Mycobacterium tuberculosis is an acid-fast bacillus that is an intracellular, facultative anaerobe. It is a non-encapsulated, rod-shaped, and spore-forming bacterium (Talip *et al*., 2013). The bacillus ranges from 1.5 µm to 4.0 µm in length and 0.3 µm to 0.5 µm in diameter (Talip *et al*., 2013). *Mycobacterium tuberculosis* is a slow-growing pathogen with a doubling time of 12-h to 24-h under the most favourable conditions (Welin, 2011). Its cell wall provides a strong impermeable barrier to drugs and plays a fundamental role in virulence. *Mycobacterium tuberculosis* possesses a complex cell wall that is made of three components (Abrahams and Besra, 2018). These include the plasma membrane, the cell wall core which is made up of peptidoglycan–arabinogalactan complex, and the outermost layer (Bansal-Mutalik and Nikaido 2014). The outer membrane components of the cell wall resemble that of Gram-negative bacteria (Dahl, 2004). The inner and the outer membrane form a periplasmic space with the peptidoglycan that is covalently linked to lipoarabinomannan and arabinogalactan

(Paul and Beveridge, 1992). In turn, lipoarabinomannan and arabinogalactan are bound to mycolic acid (Alderwick *et al*., 2015). The mycolic layer, which is found beneath the outermost mycoside layer (Kumar, 2015), is made up of lengthy -alkyl and -hydroxy fatty acids that are ester-bonded to the arabinose terminal units of arabinogalactan (Kumar, 2015). Mycolic acids, which are hydrophobic, make up half of the mycobacterial cell membrane (Todar, 2012). Mycolic acids also formed a protective barrier within the phagocytic granule, protecting the cell from oxygen radicals, cationic proteins, and lysozymes (Todar, 2012). The pathogen's cell shape and stiffness are maintained by arabinogalactan, which is found outside of the innermost peptidoglycan layer (Kumar, 2015).

1.6 *Mycobacterium tuberculosis* genetics

Elucidation of the complete genomic sequence of the *M. tuberculosis* H37v strain (Cole *et al.*, 1998) provided a strong foundation for improving the understanding of TB pathogenesis and was followed by the full genome sequencing of strains belonging to different lineages (Casali *et al.*, 2014). The complete sequence of the laboratory virulent strain *M. tuberculosis* H37v showed that its genome contains 4 411 529 base pairs associated with more than 4 008 genes that encode 3906 proteins together with 70 stable ribonucleic acids (RNA's) (National Centre for Biotechnology Information (NCBI), 2018). Over 200 genes were annotated as encoding enzymes that play a significant role in the metabolism of fatty acids (Cole *et al*., 1998). Among these enzymes, close to 100 were estimated to function in β oxidation of fatty acids (Cole *et al*., 1998). This differs from *E. coli* which only contains 50 enzymes that are involved in the metabolism of fatty acids (Cole *et al.*, 1998). Many enzymes found in *M. tuberculosis* may contribute to the ability of this pathogen to survive and grow in the tissue of the infected host (Cole *et al*., 1998). Construction of physical maps has enabled estimation of the genome size of *M. tuberculosis* H37v. The integration of previously constructed maps and the new physical maps led to the identification of a 4.41 megabase (Mb) genome size (Figure 1.2) with a single circular chromosome (Cole *et al.*, 1998).

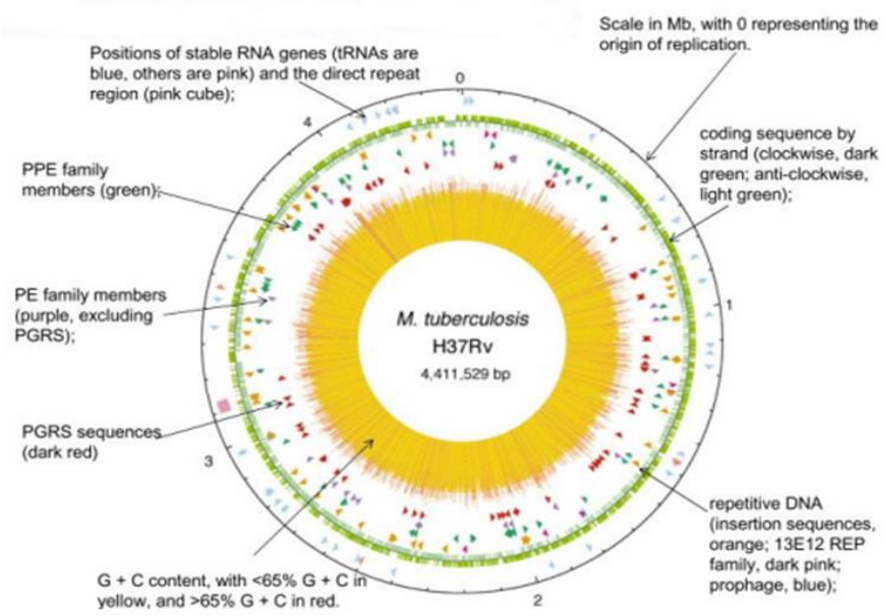

Figure 1.2 : Circular diagram representing *M. tuberculosis* H37Rv genome (adapted from Cole *et al*., 1998). The diagram depicts the outer scale in megabases, as well as the positions of the stable ribonucleic acid genes, direct repeat region, coding sequence, repetitive deoxyribonucleic acid sequences, proline-proline-glutamate family members and polymorphic GC-rich sequences sequences. The guanine and cytosine content is shown by the histogram in the centre.

One of the notable features of the genome of the *M. tuberculosis* H37v strain is the high percentage of GC-rich sequences and the large number of genes that are involved in the synthesis of fatty acids. The high GC content of *M. tuberculosis* H37v suggested that there was an over-representation of amino acid components such as proline, alanine, and glycine (Cole *et al.,* 1998). This differs from amino acids that are encoded by the adenine and thymine (A+T)-rich region which were found in low amounts (Cole *et al.,* 1998). Close to 95% of *M. tuberculosis's* genome consists of the two unrelated gene families that are named PE and PPE (Cole *et al.,* 1998). These names come from the presence of conserved Pro-Glu (PE) and Pro-Pro-Glu (PPE) found near the conserved N-terminal region of the predicted family (Cole *et al*., 1998). Pro-Glu and Pro-Pro-Glu genes are not unique to members of the MTBC (Cole *et al*., 1998). *Mycobacterium leprae* for example has 26 genes from these two unrelated gene families and only 19 of the genes are pseudogenes (Cole *et al*., 1998). *Mycobacterium. tuberculosis* is

distinct from other bacteria in that it devotes a significant percentage of its coding capacity to the production of lipogenesis and lipolysis enzymes, as well as two unique families of glycine-rich proteins the PE and PPE with a repeating structure that could be a source of antigenic diversity (Cole *et al*., 1998).

1.7 Tuberculosis pathogenesis

Mycobacterium tuberculosis has adopted many ways of infecting the human host by invading and replicating in the lungs of susceptible individuals. Infection with *M. tuberculosis* occurs when the droplets containing tubercle bacilli from an individual with active pulmonary TB or latent TB are dispersed in the air and reach the alveoli of the healthy host (Delogu *et al*., 2013). Here the *M. tuberculosis* bacilli contact the epithelial cells of alveoli (Ahmad, 2011), the macrophages, and dendritic cells (Cooper, 2009). Inside the alveoli, the bacilli are engulfed by macrophages through phagocytosis (Guirado *et al*., 2013). Those bacilli that survive the phagocytosis process are transported to the lung tissue and remain within the macrophages (Guirado *et al*., 2013).

In some cases, an immune response in the lung is triggered in the individual who inhales bacilli which helps to inhibit the growth of the pathogen inside the lungs (Thillai *et al.*, 2014). This ultimately leads to bacteria inside the lungs becoming dormant and this is known as latent TB infection. Individuals with latent TB infection who are immune-competent show no symptoms of TB and cannot transmit the disease to other individuals (WHO, 2014). The survival of a pathogen following phagocytosis and its transportation to the macrophages results in a pathogen engaging with different mechanisms of the host cell (Weiss and Schaible, 2015). This involves mechanisms such as inhibiting the fusion of the phagosome with the lysosome (Pieters, 2008). In most cases, the presence of bacilli in the phagosomes results in granuloma formation. This occurs as the immune response attempts to separate the infected tissue from the healthy tissue (Lin *et al*., 2014, Pai *et al*., 2016). The bacteria then replicate within the expanding granuloma, and when the bacterial burden becomes too high, the granuloma can no longer contain the infection. Thereafter, the bacteria spread to the local lymph nodes and other organs, including the brain (Lin *et al*., 2014, Pai *et al*., 2016). The bacteria can re-enter the respiratory tracts to be discharged or reach the circulation system at this stage in the infection,

rendering the host infectious and symptomatic, allowing active TB to proceed (Lin *et al*., 2014, Pai *et al*., 2016).

1.8 The role of macrophages during TB infection.

Macrophages and monocytes are cells that belong to the innate immune compartment (Chanput *et al*., 2014). These cells are associated with the recognition of pathogens such as bacteria and viruses through the interaction of their surface structures with different receptors (Hjort *et al.,* 2003; Si-Tahar *et al*., 2009). Macrophages are among the largest phagocytic cells and are capable of engulfing more than 100 bacteria (Guyton and Hall, 2006). Infection of macrophages is regarded as the first step which results in diffusion of the pathogen, development of granuloma, and TH1 type immunity initiation (Flynn *et al*., 2011; Silva Miranda *et al*., 2012). Activated dendritic cells present the processed antigens to $CD^{+}4$ T-cells which initiates an immune cascade (Dreher and Nicod, 2002). This results in activated lymphocytes and infected macrophages responding rapidly to inflammatory signals from chemokines, cytokines, and sensitization of white blood cells (Leemans *et al*., 2005) which results in granuloma formation where *M. tuberculosis* is contained (Kapoor *et al*., 2013). The contained *M. tuberculosis* enters the drug-resistant state of dormancy inside the granulomas (Kapoor *et al.,* 2013). The transcriptional profile for intracellular *M. tuberculosis* in the THP-1 model did not respond to a low-iron environment as observed for intracellular *M. tuberculosis* in the mouse macrophage model suggesting variability between mouse and human macrophage model results (Fontán *et al*., 2008). Transcriptional analysis of intracellular *M. tuberculosis* in the THP-1 model has shown that the major transcriptional changes were related to the metabolism of lipids, cell envelope, PE/PPE, the early secretory antigenic target (ESAT)-6-like families of proteins and twin arginine translocation (TAT) system of secretion suggesting that secretion and expression of surface components and cell wall structure are altered in intracellular *M. tuberculosis* (Fontán *et al*., 2008). Therefore, there is a need to study surface structures that are associated with *M. tuberculosis* pathogenicity.

1.9 Host immune response to *M. tuberculosis* infection

In the course of human infection with *M. tuberculosis,* two cell types are confronted by the bacteria viz, the alveolar macrophages and epithelial cells (Bermudez and Goodman, 1996). *Mycobacterium tuberculosis* can infect the macrophages via two different routes. The first is the opsonic pathway, in which some host chemicals attach to bacteria and serve as a bridge for microbe recognition by phagocytic cell surface receptors (Esparza *et al*., 2015). The second pathway encompasses adhesins present on the bacterial surface that are explicitly identified by macrophage receptors (Esparza *et al*., 2015). Infection of host macrophage and epithelial cells by *M. tuberculosis* bacilli leads to the initiation of a cascade of defined inflammatory events, primarily regulated by the production of inflammatory molecules such as Interferon gamma (IFN-γ) and Interleukin-2 (IL-2) by activated thymus cells (T-cells) (Cooper, 2009; Sasindran and Torrelles, 2011). This promotes the secretion of inflammatory cytokines such as interleukin-(IL)-12, IL-6, IL-10, and IL-23, tumor necrosis factor-α (TNF-α) along with a variety of chemokines such as (C-C) motif ligand 2 (CCL2), chemokine CC motif ligand 4 (CCL4) and (C-X-C) motif ligand 8 (CXCL8) from infected alveolar and tissue macrophages (Algood *et al*., 2003; Sasindran and Torrelles, 2011).

1.10 Tuberculosis diagnostics: current techniques and their disadvantages

Despite several nations' increased efforts to enhance TB diagnosis, the gap between newly diagnosed people (2.9 million) and those projected to have developed TB (10 million) remained substantial in 2020 (WHO, 2021). This substantial discrepancy was attributed to underreporting of diagnosed individuals and/or underdiagnoses due to a lack of access to healthcare or, if available, inaccurate diagnosis (WHO, 2020). Several techniques have been used to diagnose TB, including chest X-rays, tuberculin skin tests, sputum smear microscopy, and culture (MacGregor-Fairlie *et al*., 2020). Sputum smear microscopy remains the most commonly used diagnostic test for pulmonary TB in countries with a high rate of infection (WHO, 2021). This approach, however, has poor sensitivity in HIV-coinfected patients and cannot distinguish between susceptible and drug-resistant *M. tuberculosis* (Vassall *et al*., 2017). Lipoarabinomannan (LAM) antigen detection is a potential POC test proposed by the WHO for HIV-co-infected patients who are sputum smear negative (Pai *et al*., 2016).

The interferon gamma release assay (IGRA) as used in QuantiFERON®-TB Gold In-Tube (Qiagen, Hilden, Germany), and the Mantoux tuberculin skin test (TST) (Sanofi Pasteur, Lyon, France), are still used to identify TB infection, although neither can discriminate between the active and latent forms (Pai *et al*., 2016). The QuantiFERON®-TB Gold (Qiagen, Hilden, Germany) diagnostic test measures interferon gamma (IFN-γ) production in response to ESAT-6 and culture filtrate protein 10 (CFP-10). Despite its low cost, ease of use, and speed, the QuantiFERON®-TB (Qiagen, Hilden, Germany) Gold exhibits cross-reactivity with other mycobacterial species such as *M. marinum, M. sulzgai, and M. kansassi* (Helmy *et al*., 2012). Both QuantiFERON®-TB (Qiagen, Hilden, Germany) and Mantoux tuberculin skin test (Sanofi Pasteur, Lyon, France) have low predictive values and are unable to distinguish between re-infections and new infections (Rangaka *et al*., 2012). The IGRA, demonstrated capability of discriminating between BCG-induced infection and *M. tuberculosis* infection (Sia and Rengarajan, 2019).

The development of novel diagnostic procedures for TB has made great progress, resulting in the increase of the pipeline of new diagnostic techniques. Tuberculosis is currently diagnosed using a variety of serological, genotypic, and phenotypic approaches (WHO, 2021). The WHO has suggested the quick test GeneXpert MTB/RIF Ultra (Cepheid, California, USA), an automated molecular assay, for TB diagnosis due to its superior degree of accuracy (WHO, 2020). Within 2 hours, the GeneXpert (Cepheid, California, USA), near-patient cartridge-based assay detects both TB and RR-TB using real-time quantitative polymerase chain reaction (RT-qPCR) (WHO, 2021). The DNA-based diagnostic assays for MDR-TB found genetic alterations in as little as 24 to 48 hours (WHO, 2016). This is a considerable improvement over the prior three-month turnaround time. Multidrug-resistant TB can be detected more quickly, allowing infected people to start treatment with appropriate second-line medications sooner (WHO, 2016).

Determine TB-LAM diagnostic test (Alere Incorporated, California, USA), is an appealing point-of-care choice, due to its cost effectiveness, user friendliness, and quick turnaround time (Lawn *et al*., 2013). To diagnose TB, this diagnostic assay looks for *M. tuberculosis* antigen LAM in urine samples (Lawn *et al*., 2013). However, when compared to the GeneXpert molecular diagnostic assay, it has a lower sensitivity (Lawn *et al*., 2013).

The GenoType® MTBDRplus test (Hain Life Science) is a DNA strip assay that detects *M. tuberculosis*, simultaneously with isoniazid (INH) and Rifampin (RIF) resistance mutations in

the enoyl reductase (*inhA*), catalase-peroxidase enzyme (*katG*), and beta subunit of RNA polymerase (*rpoB*) genes using polymerase chain reaction (PCR) and reverse hybridization (Hillemann *et al*., 2007; Huang *et al*., 2009;). In addition to this, the GenoType® MTBDRplus version 2.0 test (Hain Life Science) detects the specific mutations that are linked to resistance of fluoroquinolones and second-line injectable drugs (Theron *et al*., 2016).

1.11 Tuberculosis drugs: current treatment regimes

Tuberculosis treatment involves different combinatorial drugs. These drugs differ in their mode of action. Drug-sensitive TB requires six months of anti-microbial drug use (WHO, 2021). This involves two months of treatment with first-line drugs (isoniazid (INH), rifampicin (RIF), ethambutol (EMB) and pyrazinamide (PZA)) and four months of treatment with second-line drugs (Zumla *et al.*, 2013). Combined drug therapy is more effective compared to monotherapy (WHO, 2021). The treatment of drug-resistant TB has always been more difficult than drug-susceptible TB treatment (WHO, 2018). Drug-resistant TB treatment has required the use of second-line drugs (levofloxacin, moxifloxacin, bedaquiline (BDQ), delamanid (DLM) and linezolid (LZD) (WHO, 2021). These second-line drugs are costlier and result in more side effects in patients (WHO, 2018). In addition to this, second-line drugs must be taken for up to two years (WHO, 2021). The toxic side effects and long treatment duration promote patience non-compliance (WHO, 2021).

The WHO currently advises that all oral regimens should be used as the preferred choice for the majority of patients (WHO, 2022). The fact that most patients won't need to use injectable medications is a significant advancement in the treatment of people with drug-resistant TB. Since some patients find injections to be exceedingly painful and challenging, it is imperative that this be put into practice as soon as possible.

A small number of novel medications have been studied as an add-on therapy to the current drug resistance treatment. Delamanid, linezolid and bedaquiline are some of the drugs have been studied (WHO, 2018, Solodovnikova *et al*., 2021). These antimicrobial medications have a variety of side effects, including nausea, hepatitis, neurotoxicity, vestibular toxicity, and jaundice, despite their promise (Garcia-Prats *et al*., 2016). In addition to this, MDR-TB is now treated with two different therapy regimens. The first regimen consists of a nine to eleven-month injectable-free alternative. The second regimen consists of an 18 to 20-month injectable-

free period (WHO, 2019). Moreover, treatment may be changed from the initial short treatment to the lengthier regimen depending on the patient's response.

Initial treatment for drug-resistant TB consists of a four-month rigorous phase that could be prolonged to six months if sputum tests are positive for the disease at the end of month four (WHO, 2021). This regimen is followed by a five-month fixed continuation phase (WHO, 2021). Bedaquiline is a significant anti-TB medicine in the shorter regimen, outperforming the injectable drugs in terms of efficacy and treatment of RR-TB and MDR-TB (Tack *et al.*, 2021). The WHO has reclassified linezolid as a Group A medicine for the treatment of XDR-TB and MDR-TB, indicating that it should be included in the regimen for all patients unless contraindicated (WHO, 2021). The shorter regimen also includes clofazimine (CFZ) and levofloxain (LFX), which replaces moxifloxacin (MFX) (Ahmad *et al*., 2018, WHO, 2021). Para-aminosalicylic acid is used as an alternative for injectables in children under the age of six (WHO, 2021). Delamanid is preferred as a substitute for injectables in children aged six to twelve (WHO, 2021). This regimen's intense phase includes a high dose of INH, EMB, and PZA (WHO, 2019). Treatment for rifampicin-resistant -TB/ multidrug-resistance -TB comprises rifabutin and rifamycin, which are given for six months and can cause neutropenia and uveitis, as well as RIF, which cannot be given with BDQ (WHO, 2019).

Five antimicrobials are given during the intense phase and three are given during the continuation phase in the lengthier regimen for treatment of MDR/RR TB (WHO, 2020). A six-month intensive phase is required, which can be extended to eight months if patients have delayed culture conversion, modest clinical responses to treatment, or bilateral lung illness with significant cavitation (WHO, 2018). The 12-month continuation phase is specified in this regimen (WHO, 2018). The treatment plan is broken into three groups: A, B, and C. The antimicrobials MFX/LFX, LZD, and BDQ are favoured in group A. Terizidone/cycloserine and CFZ are in Group B. (WHO, 2018). Because of the significant risk of relapse and treatment failure, capreomycin and kanamycin in group C are not indicated (WHO, 2019).

1.12 Vaccines: current vaccine and those in the pipeline

The Bacillus Calmette-Guérin (BCG) vaccine has been used in the treatment of TB for the past 100 years and is still the only licensed vaccination against disseminated and meningeal TB in children. (McShane, 2011). The BCG vaccine was designed from an attenuated strain of *Mycobacterium bovis* (*M. bovis*) (Buddle *et al.,* 1999). It is estimated that the BCG vaccine prevents close to 120 000 childhood deaths per year (Harris *et al*., 2016). The BCG offers highly variable protection against pulmonary TB in adolescents and adults (WHO, 2014). In patients with immunosuppressive conditions such as HIV, BCG poses a risk of dissemination of TB (Colditz *et al*., 1994). Administration of BCG in infancy does not protect against adult pulmonary TB (Mangtani *et al*., 2014; Roy *et al.,* 2014; WHO, 2014). The reactivation of latent TB to an active state after successful completion of TB treatment suggests that the host immune response to the pathogen is complex (Mack *et al.,* 2009), and further supports the need for developing multiple epitope vaccines against TB (Barker *et al.,* 2011). New TB vaccines that could offer protection in infancy and extend to adulthood are urgently required to prevent new infection and achieve zero TB deaths (Ottenhoff and Kaufmann, 2012; Davenne and McShane, 2016). One of the biggest limiting factors in TB vaccine development is the lack of suitable biomarkers that can be used and the lack of adequate information regarding a protective host immune response to *M. tuberculosis* (Barker *et al.,* 2011).

Over the last five years, a few vaccine candidates have failed at the early clinical trials stage, and very few that entered pre-clinical trials have moved to the TB vaccine pipeline. In addition to this, only a few of those vaccines that have entered the TB vaccine pipeline have slowly progressed to the vaccine development stage. There is a need to develop a broad and dynamic pipeline to accelerate the goal of new TB vaccine development (Frick, 2013). This requires more knowledge of the different antigens. Some vaccine technologies, including the cytomegalovirus (CMV) vector, have shown bigger promise in pre-clinical studies (Frick, 2013). The CMV is attenuated and a live persistent viral vector that has been shown to express multiple *M. tuberculosis* antigens (Voss *et al.,* 2018). Construction of this vector leads to low-level replication of the virus which results in sustained antigen expression (Voss *et al.,* 2018) and long-term immunity. These findings suggest that this technology is highly attractive in vaccine development (Früh and Picker, 2017).

Vaccine technologies under development for pandemic flu could also be applied to TB (Wong and Gao, 2017). These technologies use mRNA vectors that generally produce high levels of

antigen (Ag) expression *in vivo,* are relatively simple to manufacture, and can be tested against different pathogens with no difficulty (Voss *et al*., 2018). There is a need to increase the speed at which candidate vaccines enter and move through the pipeline. However, robust and transparent criteria that could be used to fast-forward the pace of TB vaccine candidate development were previously reviewed (Voss *et al.,* 2018). In TB-endemic nations, MTBVAC (Aguilo *et al*., 2016) as a BCG replacement vaccine (in neonates) and booster vaccine (in adults) has been poised to enter Phase 3 efficacy trials (Martín *et al*., 2021, WHO, 2021). ChAdOx1 85A (Wilkie *et al.,* 2020) generated a strong antigen 85A (Ag85A)-specific CD4+ and CD8+ T cell responses were increased by MVA85A vaccination (Wilkie *et al*., 2020). In addition to this, ChAdOx1 85A is well tolerated when administered alone or in combination with MVA85A in phase I clinical trials (Wilkie *et al*., 2020). In phase IIb clinical trials, MVA85A vaccine candidate showed an increased antigen-specific CD4 T-cell response, but no improved protection against TB in new-borns (Tameris *et al*., 2013). A phase IIb clinical trial carried out in Kenya, South Africa, and Zambia on people with signs of latent TB infection revealed that the M72/AS01E (GlaxoSmithKline) was strongly protective against TB illness (Tait *et al*., 2019). Over almost three years of follow-up, the point estimate for vaccine effectiveness was found to be 50 % (Tait *et al*., 2019). Both latent and actively infected patients produced interferon gamma and specific lymphoproliferation in response to the M72/AS01E vaccination (Tait *et al*., 2019). Additionally, it demonstrated safety and produced humoral and cell-mediated immunity in healthy and HIV-positive persons, *M. tuberculosis* infected adults, children, and new-borns who had received the BCG vaccine (Tait *et al*., 2019). Phase I and Phase IIa clinical studies of VPM1002 have demonstrated its immunogenicity and safety in both adults and new-borns (Grode *et al*., 2013; Loxton *et al*., 2017). The VPM1002, a live recombinant vaccine candidate, was attempted to boost BCG immunogenicity and vaccination potential (Grode *et al*., 2013). To do this, BCG was engineered to avoid the phagosome by expressing listeriolysin and allowing perforation of the phagosomal membrane, hence increasing major histocompatibility complex (MHC) class I antigen presentation to CD8-T cells (Grode *et al*., 2013, WHO, 2020). A more effective vaccine is required to stop millions of deaths caused by TB every year.

1.13 Biomarkers for tuberculosis therapeutics and diagnostics development:

New tools and approaches are required for the diagnosis and treatment of TB. This includes the evaluation of novel host and pathogen key elements in response to infection in the search for novel accurate targets that can be included in the development of POC diagnostics, effective drugs and vaccine. Biomarkers are defined as any biological characteristic that can be measured and monitored to indicate normal or pathogenic processes (Maertzdorf *et al.*, 2011). Biomarkers can serve as surrogate endpoints in clinical trials and can be used to improve treatment outcomes by informing therapeutic decisions for individual patients (Wallis and Peppard, 2015). In addition to this, biomarkers can aid in the predictive risk of disease progression and have the potential to speed up clinical trials.

1.14 *Mycobacterium tuberculosis* adhesins as biomarkers

Many pathogenic bacteria express structures that allow adherence to the host cell. Adhesins are extracellular structures or molecules that are present on bacterial cell surfaces and aid in the initial host-pathogen interaction. Adhesins are involved in the attachment of bacteria to the host cell receptors and colonization (Mandlik, *et al.*, 2008; Kumar *et al*., 2013). Attachment of *M. tuberculosis* to the epithelium causes perturbation and the formation of membrane extensions that promote adherence to the respiratory epithelium (Pessolani *et al*., 2003). Membrane extensions facilitate the adhesion and attachment of the bacteria to the host cell (Pessolani *et al.*, 2003). Attachment of bacteria to host cells is important for bacterial invasion, survival, and colonization (Mandlik *et al.*, 2008). This results in the change of host cell signaling which facilitates the dissemination of the pathogen and evades the host immune response (Pethe *et al*., 2001). Invasion of a host cell by a bacterium is a complex process that involves the interaction of host cell determinants and bacteria (Bermudez and Goodman, 1996; Danelishvili *et al.*, 2003).

Studies have demonstrated that adhesion molecules are also important for bacterial cell aggregation allowing cell-to-cell contact which ultimately leads to biofilm formation that contributes to microbial persistence (Barnhart and Chapman, 2006). It has been discovered that several *M. tuberculosis* adhesin molecules attach to and interact with mammalian host cells and tissues (Menozzi *et al*., 1998; Diaz-Silvestre *et al*., 2005; Alteri *et al*., 2007). Only a few

of these adhesins have been thoroughly studied and identified as having possible adhesin-binding activities (Figure 1.3) (Bisht and Meena, 2019).

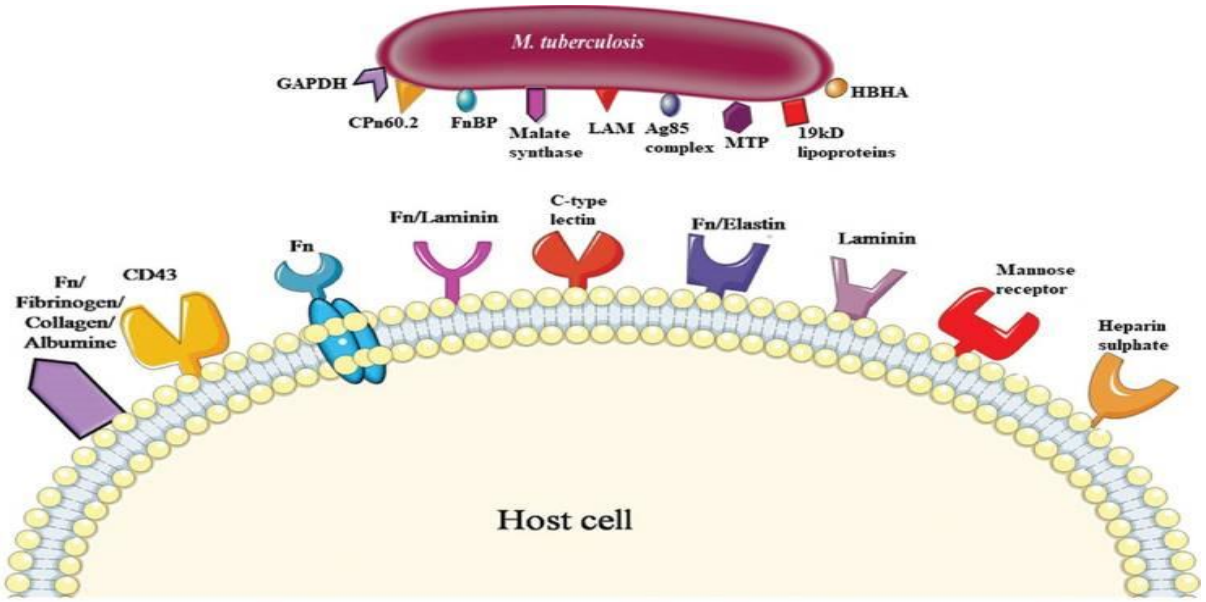

Figure 1.3: Diagrammatic representation of different adhesion molecules used by *M. tuberculosis* and the receptors (Bisht and Meena, 2019).

1.15 *Mycobacterium tuberculosis* adhesins

Mycobacterium tuberculosis antigens that bind with receptors on mammalian host cells have been identified as adhesins in several studies. The discovery of heparin binding hemagglutinin adhesin (HBHA), a surface-exposed adhesin required for the bacterial attachment to the lungs as well as the bacteria's extra pulmonary dispersion, was described by Pethe *et al.,* 2001. *Mycobacterium tuberculosis* pili (MTP), an important component of the pathophysiology of the disease and a possible anti-TB biomarker, was described by Alteri *et al*., (2007). Kinhikar *et al*. (2006) showed that malate synthase may bind to the human extracellular matrix proteins laminin and fibronectin by an unidentified method of cell wall attachment. Malate synthase is hence referred to as an "anchorless adhesin" (Kumar *et al*., 2013). Govender *et al.* (2014) explored the potential of adhesins as biomarkers that may be targeted for the development of therapies. With the use of *in vitro* infection assays, growth kinetics, RT-qPCR, metabolomics and RNA sequencing, there has been a number of studies that aimed to elucidate *M. tuberculosis* adhesion (Nyawo, 2016, Dlamini, 2016, Muniram, 2018, unpublished; Govender, *et al*., 2018; Ashokcoomar *et al*., 2020, Reedoy *et al.,* 2020 and Naidoo, 2021).

1.15.1 Heparin-binding hemagglutinin adhesin (HBHA)

Heparin-binding hemagglutinin adhesin is encoded by the *hbhA* gene located in the locus Rv0475 (Kapopoulou *et al.,* 2011). The *hbhA* gene is 600 base pairs (bp) long (Kapopoulou *et al.*, 2011) with a molecular weight of 28 kDa (Menozzi *et al.,* 1998). The *hbhA* gene is a core mycobacterial gene and is conserved in many *Mycobacterium* strains (Marmiesse *et al.,* 2004). The HBHA protein contains a N-terminal signal sequence (Marmiesse *et al*., 2004, Veyron-Churlet *et al.,* 2018). The HBHA contains a high number of lysine motifs in the C-terminal region that binds to heparin sulfate (Menozzi *et al.,* 1998). Methylation of HBHA at the C-terminal lysine residues influences both the immunological and biochemical properties of HBHA protein (Menozzi *et al.,* 1998). The HBHA mediates the adhesion of *M. tuberculosis* to epithelial cells (Menozzi *et al.,* 1996; Pethe *et al*., 2001). It also aids in the rapid spread of the pathogen to areas outside the lungs (Pethe *et al*., 2001). Menozzi *et al*., (2006) showed that binding of HBHA to proteoglycans causes epithelial transcytosis which promotes the dissemination of *M. tuberculosis.* Using an HBHA-deficient strain, Mueller-Oritz *et al*. (2002)

supported the findings of Pethe *et al*., (2001), indicating that HBHA was necessary for extrapulmonary dispersion but not for *M. tuberculosis* adhesion to, or growth in macrophages (Mueller-Ortiz *et al*., 2002). Delogu *et al*., (2006) used real time PCR (RT-PCR) to measure the expression of *hbhA* at different phases of *in vitro* and *in vivo M. tuberculosis* infection. The expression levels of *hbhA* increased during the early stationary phase of an axenic culture, but remained constant during the early stages of infection (Delogu *et al***.,** 2006). In contrast to low or steady *hbhA* expression in bone marrow-derived macrophages and the mice's spleen, A549 human pneumocytes and the mice's lungs showed elevated *hbhA* expression (Delogu *et al*., 2006).

Few studies have been done on the adhesion of HBHA to macrophages since the original study by Pethe *et al*., (2001). A study by Mueller-Ortiz *et al*., (2001) revealed that the *M. tuberculosis* C3 binding protein matched the amino acid sequence of HBHA and was shown to attach selectively to the cell membrane. Additionally, HBHA-coated polystyrene beads were phagocytosed and adhered to J774.A1 macrophages with improved efficiency (Mueller-Ortiz *et al*., 2001). These results showed that HBHA may use C3 and C3 binding receptors to facilitate *M. tuberculosis* phagocytosis and adhesion to macrophage (Mueller-Ortiz *et al*., 2001). Moreover, it was discovered that HBHA might stimulate household contacts' CD4+ T cells to co-express IFN-γ, IL-2, and IL-17, but not in active TB patients (Loxton *et al.*, 2012). In a mouse infection model, Kuvar (2016) showed that HBHA regulates host-pathogen interactions and immune response causing differential gene regulation (unpublished).

Moodley (2018) showed that single deletion of *hbhA* in V9124 strain had a minimal role in binding of *M. tuberculosis* to THP-1 cells (unpublished). Transcriptomic studies on the combined effect of MTP and HBHA on adhesion and invasion in a THP-1 human macrophage model revealed that these adhesins influence transcriptional alterations favouring adhesion and subsequent macrophage invasion (Moodley, 2018, unpublished). This data is consistent with functional genomic studies that found MTP and HBHA to be important in aiding bacterial growth and biomass generation (Govender *et al*., 2018, unpublished). Naidoo (2021) analysed the transcriptomic perturbations in the strains lacking the MTP adhesin, HBHA adhesin or both MTP-HBHA adhesins and their respective complements. Among the deletion mutants, 43 genes were significantly differently expressed (Naidoo, 2021). Moreover, Naidoo (2021) found that changes in iron and copper regulation were seen in the absence of HBHA, indicating that the adhesin may have a function in the regulation of these metals. These findings provide

evidence that HBHA can be an important biomarker for the development of POC TB diagnostics and vaccine.

1.15.2 *Mycobacterium tuberculosis* curli pili

Mycobacterium tuberculosis produces cell surface adhesive organelles that facilitate attachment and successful colonization of the host cell (Alteri *et al.,* 2007). The *M. tuberculosis* pili (MTP) encoded by *Rv3312A* (*mtp*), are curli cell surface and structural amyloid fibres that are highly sticky, proteinaceous, and hydrophilic bacterial structures composed of repeating subunits called pilin (Proft and Baker, 2009). The *mtp* gene is located between the gene region *adenosine deaminase* (*add*), *deoxyribose A* (*deo A*), *cytidine deaminase* (*cdd*)) that is involved in intermediary metabolism and mycobacterial gene *Rv3312c* (Ramsugit *et al*., 2013). The *Rv3312c* is a *Mycobacterium* gene with no known function (Ramsugit *et al*., 2013). The *mtp* gene appeared to be extremely conserved among different *M. tuberculosis* clinical strains (Naidoo *et al*., 2014). *Mycobacterium tuberculosis* curli pili is suggested to have adhesive properties that facilitate binding with the extracellular proteins (Alteri *et al*., 2007).

Mycobacterium tuberculosis curli pili has been proposed to be a major *M. tuberculosis* adhesin and invasin of macrophages (Ramsugit and Pillay, 2014) and epithelial cells (Ramsugit *et al.,* 2016). Wild-type and *mtp*-mutant strains induced a similar concentration of chemokines and cytokines in A549 epithelial cells, which suggested that MTP had no significant influence on cytokine response in epithelial cells (Ramsugit *et al.,* 2016). Naidoo *et al.* (2014) studied the *mtp*-encoded pilin subunit protein's potential as a diagnostic biomarker. The *mtp* gene was found to be lacking in non-tuberculous mycobacteria and other respiratory organisms but present in all clinical isolates examined from the MTBC. As a result, it was concluded that the pilin subunit protein of *M. tuberculosis* could be employed as a biomarker for POC diagnostics (Naidoo *et al*., 2014). A study by Naidoo *et al*., (2018) looked into MTP's capacity to react with Immunoglobulin G (IgG) in TB patients, including HIV-uninfected and co-infected individuals, for future use in a POC test. Serum or plasma samples were screened in a slot blot assay employing an MTP synthetic peptide, exhibiting an accuracy of 97 % in the identification of anti-MTP IgG antibodies, confirming the expression of MTP during *M. tuberculosis* infection (Naidoo *et al*., 2018).

The MTP has been shown by Dlamini (2016) to be essential for epithelial cell gene regulation and to affect host immune responses by altering signalling pathways during infection. These findings showed that MTP can modify immunological responses, indicating that it needs to be further studied as a potential vaccine candidate (unpublished). Moreover, Nyawo (2016) found that MTP is involved in the proliferation of *M. tuberculosis* under *in vitro* settings and plays a significant role in host-pathogen interactions by inducing inflammatory and innate immunological responses, consequently affecting host immune responses vital to host defence (unpublished). Using MTP-proficient and MTP-deficient of *M. tuberculosis* V9124 strains, a metabolomics study was conducted to examine the function of MTP in modulating *M. tuberculosis* metabolism (Ashokcoomar *et al*., 2020). Metabolites from *M. tuberculosis* were analysed using two-dimensional gas chromatography time-of-flight mass spectrometry and bioinformatics techniques. The findings showed that a total of 28 metabolites related with cell wall biogenesis, decreased amino acid synthesis, and fatty acid hydrolysis were substantially different in the MTP-deficient strain compared to the wild-type (Ashokcoomar *et al*., 2020). Naidoo (2021) found the significant changes in expression levels of genes linked with cell wall production and structure in MTP-deficient strains. Moreover, a bioinformatics analysis combined with gene expression and a bioluminescence experiment revealed bacterial transcriptome changes caused by the deletion of the *mtp* and *hbhA* genes in *M. tuberculosis* (Naidoo, 2021). An overall increase in ATP synthase expression was seen in *mtp*, indicating that the mutant strain attempted to boost ATP synthesis, which could perhaps be attributable to changes in the proton motive force (Naidoo, 2021). Collectively these findings indicate the potential of MTP as a TB biomarker or novel target for a POC diagnostic test, vaccine, and drug developments.

1.15.3 L, D-transpeptidase (Ldt)

The *Rv0309* gene, located at the 377 931bp position, is 657 bp in length (Kapopoulou *et al.*, 2011) and encodes an enzyme called L, D-transpeptidase (Ldt) (Lavollay *et al*., 2008). The L, D-transpeptidases are important components of all bacterial cell walls. The L, D-transpeptidases have been identified as adhesin (Kumar *et al*., 2013) and may be a potential biomarker for anti-TB therapeutics. Using functional genomics, a study by Muniram (unpublished, 2018) further elucidated the function of Ldt in growth, biofilm formation, and cellular morphology. Muniram (unpublished, 2018), showed reduced growth of the *Rv0309* mutant compared to the wild-type strain during two different growth phases *in vitro*. Biofilm forming ability was significantly lower in the *Rv0309* mutant with a 55.75% reduction compared to the V9124 wild-type strain ($p=0.03$). The complemented strain showed an almost complete restoration to wild-type when compared to the mutant and was also significantly higher than the mutant ($p=0.024$) (Muniram, unpublished 2018). Furthermore, Muniram found an elongated filamentous phenotype in mutant strains where cells showed incomplete cell division and non-polar budding. The overall study by Muniram, (unpublished, 2018) demonstrated that Ldt is important for *in-vitro* growth, cellular and biofilm production. In addition to this, the overall study by Muniram (unpublished, 2018) suggested that the *Rv0309* gene is important in *M. tuberculosis* pathogenesis in *in-vitro*. This further suggested that Ldt should therefore be further studied to determine its adhesin/invasin function, as well as the full potential of this protein as an anti-TB biomarker and therapeutic target.

1.16 Adhesins that mediate binding to macrophages.

Mycobacteria have numerous surface proteins with primary and secondary adhesin functions that engage with host cell receptors (Menozzi *et al*., 2006). Pethe *et al*. (2002) discovered laminin binding protein which is important in cyto-adherence. The glyoxalate pathway enzyme, malate synthase (*glcB; Rv1837c*), has been demonstrated by Kinhikar *et al*., (2006) to bind to the human extracellular matrix (ECM) proteins, laminin and fibronectin and function as an anchorless adhesin. THP-1 macrophage-like cells are the favoured site of binding for the 19-kDa lipoprotein antigen (*Rv3763*) that is found on the cell wall (Diaz-Silvestre *et al*., 2005). The cell surface glycoprotein Apa (*Rv1860*) has been demonstrated to transiently associate with the cell wall to enable attachment to the pulmonary surfactant protein-A (PSP-A) (Ragas *et al*., 2007). Effective bacterial association with macrophages appears to require the presence of the molecular chaperone protein Cpn60.2 (*GroEL2*; *Rv0440*), which is thought to play a role in bacterial pathogenicity and is crucial for cell survival (Stokes *et al*., 2004).

Mycobacterium tuberculosis possess multiple adhesins, which may promote its success as a pathogen (Kumar *et al*., 2013). It is possible that inactivation of specific adhesins may lead to the pathogen upregulating other existing adhesins which may assist in its survival and success. Moreover, studies on the regulatory mechanism in the absence or presence of specific adhesin, can be crucial because they may provide an insight into the initial pathogen interaction with the host cell. This could help in the development of novel vaccines and other anti-TB therapeutics.

1.16.1 The lipoglycoprotein antigen (LpqH)

The 19 kilodaltons (19-kDa) lipoglycoprotein antigen (LpqH) is a glycosylated lipoprotein with several functions (Diaz-Silvestre *et al.*, 2005). Lipoglycoprotein antigen is only expressed by slow-growing pathogens such as *M. tuberculosis* and *M. vaccae* (Yeremeev *et al.*, 2000). Lipoglycoprotein antigen is a prominent *M. tuberculosis* cell wall antigen with a 21-amino-acid secretion signal peptide that targets the Sec protein export pathway (Herrmann *et al.*, 1996). Many mycobacterial genomes contain LpqH homologs (Wilkinson *et al.*, 2009). To date, no similar gene products have been reported to have the unique features of *M. tuberculosis* LpqH that contribute to the pathogenicity of *M. tuberculosis* and the associated MTBC mycobacteria. The *M. tuberculosis* LpqH has a pleiotropic modulatory influence on the infected host's antimicrobial immune response boosting neutrophil and $CD4^+$ T cell activation (Neufert *et.al*, 2001). It interacts with macrophages via Toll-like receptor 2 (TLR2) and induces IL-2 and TNF-α production or apoptosis (Diaz-Silvestre *et al.*, 2005). The LpqH is also responsible for the binding of the macrophage mannose receptor, facilitating the uptake of mycobacteria (Diaz-Silvestre *et al.*, 2005). Additionally, the LpqH is considered to help *M. tuberculosis* evade the immune system and spread by causing TLR2-dependent macrophage death (López *et al.*, 2003). Furthermore, the LpqH aids in the transfer of nutrients through the cell wall of mycobacteria, which aids in their survival. A study by Ciaramella *et al.*, (2000) demonstrated that the 19 kDa proteins primarily promote apoptosis in monocytes or macrophages by activating LpqH, which then activates TLR2, which upregulates the death receptor and signalling molecule, so initiating the death receptor signalling cascade. These data demonstrate the importance of LpqH in the infectivity of *M. tuberculosis.*

1.16.2 Alanine- and proline-rich antigen (Apa)

The most suitable targets for developing a novel subunit vaccination against TB are antigenic proteins actively released during *M. tuberculosis* infection (Kaufmann, 2020). The alanine- and proline-rich antigen (Apa) is a 45 - 47 kDa secretory protein and elicits a mostly Th1 type of T-cell response in healthy humans (Kumar *et al.*, 2003). It binds to mouse macrophages via mannose residues (Romain, 1999). It has been proposed to be a promising candidate for future vaccine development against TB (Satchidanandam *et al.*, 2016). Alanine- and proline-rich antigen has been described as an adhesin molecule that interacts with surfactant protein A in the lungs, and this contact is reliant on APA glycosylation (Ragas *et al*., 2007). Similarly, APA is a fibronectin attachment protein (FAP) that adheres to bladder tumor cells and plays a vital role in the treatment of bladder cancer, as well as being a viable alternative to BCG in the treatment of TB (Sinn *et al.*, 2008).

1.16.3 *Mycobacterium tuberculosis* phosphate-binding protein PstS-1

The phosphate specific transporter (Pst) lipoprotein is a membrane-associated complex that belongs to the ATP-binding cassette (ABC) transporter superfamily (Braibant *et al.*, 2000). In *M. tuberculosis*, three putative Pst operons i.e. *pstS-1*, *pstS-2*, and *pstS-3* have been identified, which likely represent a subtle biochemical adaptation of this microorganism for its growth and survival under different phosphate-limiting conditions during its infectious cycle (Lefèvre *et al*., 1997). The three genes that code for PstS-1, PstS-2 and PstS-3 proteins are substantially similar (approximately 75 % similarity between *pstS-1* and *pstS-2* or *pstS-3* and 94 % similarity between *pstS-2* and *pstS-3*), and they all have a lipoprotein consensus signal (Lefèvre *et al*., 1997). The *M. tuberculosis* phosphate-binding protein (PstS-1) is a 38 kDa glycosylated lipoprotein that binds with the macrophage mannose receptor and promotes phagocytosis (Vyas *et al*., 2003). *Mycobacterium tuberculosis* PstS-1 is known to cause adaptive protective immunity in mice and humans by inducing a robust immunological response (Palma *et al.*, 2011). The *in vivo* multiplication of *M. tuberculosis* was reduced when genes encoding PstS-1 were disrupted, demonstrating that the high-affinity phosphate-specific transporters are also virulence factors for *M. tuberculosis* and *M. bovis* (Peirs *et al*., 2005). The *M. tuberculosis* PstS-1 specific immunity has been found in TB patients, and PstS-1specific antibodies (Abs)

were found useful as an aid in the serodiagnosis of active TB (Imaz, *et al*., 2004). Thus, PstS-1 as a major adhesin that facilitates binding of *M. tuberculosis* to THP-1 cells, maybe a suitable biomarker candidate for the development of a POC TB test.

1.16.4 Cpn60.2 molecular chaperone

Chaperones are proteins that have a significant role in maintaining cellular viability by promoting protein folding (Saibil, 2013). One of the most prevalent *M. tuberculosis* adhesins, albeit poorly described, is the chaperone Cpn60.2 also known as (GroEL 2, Hsp 65). Chaperone Cpn60.2 is one of the two chaperones (Cpn60.1 and Cpn60.2) found on the outer surface of the *M. tuberculosis* cell wall (Stokes, 2013). Chaperone Cpn60.2 mediates the binding of *M. tuberculosis* to the $CD^{+}43$ receptor, a large sialylated glycoprotein bound on the surface of macrophages (Hickey *et al*., 2010). In addition to this, Cpn60.2 is a heat-shock protein that facilitates the survival of *M. tuberculosis* inside the host cell during harsh conditions (Sharma *et.al*, 2016). Experimental evidence showed that deletion of Cpn60.1 does not affect growth as opposed to deletion of Cpn60.2 which was lethal to bacterial cells (Hu *et al*., 2008). A study by Hickey *et al*., (2010) found that recombinant Cpn60.2 hindered 57 % of bacterial association with macrophages. In addition, it has recently been shown that Cpn60.2 prevented macrophage apoptosis by interacting with mitochondrial mortalin (Joseph *et al*., 2017). The presence of Cpn 60.2 has been reported to stimulate human peripheral blood macrophages which results in the stimulation and production of cytokines that activate B and T cells (Henderson *et al*., 2010). Additionally, a recent study by Vargas-Romero *et al*., (2016) found a link between *M. tuberculosis* virulence and Cpn60.2 secretions which is consistent with a previous study that found Cpn60.2 in the cerebral fluid of patients with TB meningitis (Mudaliar *et al*., 2006). Thus, Cpn60.2, may be a suitable biomarker candidate for the development of a POC TB test and vaccine development.

1.16.5 The DnaK molecular chaperone

The DnaK molecular chaperone is an important protein encoded by the common operon (*groE*) in *Escherichia coli*, *groEL* (L for large) and chaperonin *groES* (S for small) in prokaryotes (Qamra *et al*., 2004). These two genes are called chaperonin (*cpn60*) and chaperonin (*cpn10*) both of which mediate correct assembly, folding, transport, and degradation of other proteins *in vivo* (Qamra *et al*., 2004; Shahar *et al*., 2011). In the *M. tuberculosis* cell wall, DnaK is also a surface molecule (Rawat and Monu, 2015). Over expression of DnaK in *M. tuberculosis* leads to improved pathogen clearance in a mouse model, implying that higher DnaK synthesis primes the host's immune system (Stewart *et al*., 2001). This shows that the pathogen carefully controls and maintains the expression of endogenous heat shock protein to utilize it to its advantage during the invasion. Thus, DnaK maybe a suitable biomarker candidate for the development of a POC TB test.

1.16.6 Antigen 85 (Ag85) complex

The antigen 85 complex is a secretory protein released by *M. tuberculosis.* It constitutes three abundantly secreted proteins fibronectin-binding protein 85A (fbpA), 85B (fbpB) and 85C (fbpC) encoded by *Rv3804c*, *Rv1886c* and *Rv0129c* respectively, in *M. tuberculosis* (Wiker *et al*., 1990). The antigen 85 complex has been described as a potential cell surface marker of the pathogen which contributes to host-pathogen interaction (Rawat and Monu, 2015). Ratliff *et al*., (1988) found that *M. tuberculosis* binds exclusively to fibronectin and not to the other pure extracellular matrix proteins that were examined. The capacity to bind fibronectin and other extracellular matrix proteins have been shown to increase the pathogenicity of pathogenic organisms, particularly staphylococci and streptococci (Patti *et al*., 1994). Armitige *et al*., (2000) showed that disrupting genes of the Ag85 complex in *M. tuberculosis* strains impacts cell wall production. The surface Ag85 complex has been found to have cell wall mycolyl transferase activity during infection, in addition to its role in cell wall biosynthesis (Belisle *et al.,* 1997). Collectively, these data from these studies suggest that the Ag85 complex should be further studied as it may be a potential biomarker for drug and vaccine development.

1.17 Techniques to study gene and protein expression

Recent technical advancements have improved the chances of figuring out how bacteria regulate their genes. Microarrays, quantitative real-time polymerase chain reaction (RT-qPCR) and RNA sequencing are all cutting-edge approaches for examining gene regulation during host-microbe interactions.

1.17.1 Quantitative real-time polymerase chain reaction (RT-qPCR)

Pathogens rely on the expression of certain gene products to survive in the host cell. Environmental pressures control the expression of these genes (Fuchs *et al*., 2012). Understanding the pattern of gene up and down regulation provides crucial information about a bacterium's properties, which could lead to new therapeutic targets. Quantitative real-time polymerase chain reaction has a higher sensitivity than conventional PCR, which is valuable for analysing gene expression in macrophage cultures and infected tissues with minimal *M. tuberculosis* mRNA (Fraga *et al*., 2008). One of the drawbacks associated with RT-qPCR is that it can be inhibited by the presence of certain biological components such as urea and haemoglobin (Deepak *et al.,* 2007). This can be prevented by using samples that are free from urea and haemoglobin and the use of inhibitors. To get the best results, RNA needs to be treated with DNase treatment to remove any traces of genomic DNA. In addition to this, the number of genes that may be analysed in a single PCR assay is restricted. This weakness was solved by microarray technology (McLoughlin, 2011).

The RT-qPCR has been used in *M. tuberculosis* gene expression studies. Ryndak *et al*., (2015) used RT-qPCR to verify genes that showed differential expression in microarray technology. Their study revealed that among the studied genes, transcripts of the 23S Ribosomal ribonucleic acid (rRNA) which were used as a negative control did not show differential expression by RT-qPCR confirming macro array technology. Moreover, Ryndak *et al*., (2015) also found that transcripts for ESAT-6 were upregulated ~3.8 fold by microarray and ~4.8 fold by RT-qPCR. Their data proved that RT-qPCR is useful in determining and confirming gene expression studies in *M. tuberculosis*. Ashokcoomar et *al*., 2020 investigated the role of MTP in modulating the metabolome in an *in vitro* bacterial model. Moreover, Ashokcoomar *et al.,* (2020) used RT-qPCR to confirm the metabolomics data. The RT-qPCR transcriptomic data from Ashokcoomar *et al*., (2020) supported the metabolomics data which revealed a similar pattern, where the Δ*mtp* strain produced various metabolites, related to the respective pathways

associated with *glf, glmU, fadD32* and *glpK,* in increased concentrations compared to the wild-type strain. These findings reveal that during host infection, amino acid, carbon, and fatty acid metabolism are changed in the absence of MTP, indicating that MTP plays an important role in TB pathogenesis by modulating host metabolic activities.

1.17.2 RNA sequencing

The RNA sequencing (RNA Seq) approaches (which are based on ultra-high throughput sequencing of total RNA and meticulous counts of all expressed transcripts) have gained popularity and allow researchers to bypass many of the limitations of microarray technology (Kukurba and Montgomery, 2015). RNA-Sequencing approaches, in contrast to hybridization-based methods, are more sensitive and allow for unbiased strand-specific identification of common and novel transcripts, as well as additional information to be deduced from the RNA (Wang *et al*., 2009). It also allows for the positive identification of both lowly expressed and highly expressed genes in a single RNA-Seq experiment, providing a platform for the investigation of unbiased, fully qualitative and quantitative transcriptomic profiles of host cells following mycobacterial infection (Nalpas *et al*., 2013).

Transcriptome analysis evaluates global changes in gene expression profiles in tissue, organs, cells, or complete organisms, providing a dynamic link between the genome and the proteome (Parida and Kaufmann, 2010). Mvubu *et al*., (2016) used transcriptomics to identify differential gene expression and strain-specific molecular signatures in pulmonary epithelial cells induced by different *M. tuberculosis* strains, including F15/LAM4/ KZN, F28, Beijing, and F11, as well as unique genotypes that were investigated using RNA sequencing. The results showed that gene expression varied among the strains, but that a subset of 292 genes was stimulated by all of them (Mvubu *et al*., 2016). Moreover, Mvubu *et al.,* (2016) found that a total of 240 genes were up-regulated, whereas 52 genes were down-regulated, out of the 292 typically stimulated genes. This research established that epithelial cells play an important role in the innate and adaptive immune responses (Mvubu *et al*., 2016). Furthermore, the virulent strains' genetic variety stimulates strain-specific and differential immune host responses, which may have an impact on clinical outcome, granuloma formation, and downstream alterations (Mvubu *et al*., 2016). The molecular signatures discovered in this work could be exploited to develop supplementary immunotherapies for TB infection and host-associated biomarkers.

Global changes in transcriptional response have shed light on the molecular activities that take place within the host during *M. tuberculosis* infection establishment. The transcriptional responses to *M. tuberculosis* infection have been studied in a number of ways (Dlamini, 2016, Kuvar, 2017; Nyawo, 2016; Moodley, 2018). Using MTP-proficient and MTP-deficient *M. tuberculosis* V9124 strains, a global transcriptome analysis in a mouse model of infection explored the significance of MTP in pathogenesis by analysing its role in host-pathogen interactions and host immune responses (Nyawo, 2016). Growth experiments found that the MTP-deficient strain grew at a considerably slower rate than the wild-type strain, implying that MTP aids the pathogen's growth rate (Nyawo, 2016; Dlamini, 2016). In addition, MTP plays a key role in host-pathogen interactions that lead to infection, prompting inflammatory and innate immune responses that are critical to the host's defence. MTP is also linked to immune response modulation by cytokines and transcriptional factors (Nyawo, 2016). MTP was found to be a strong immunogen (Nyawo, 2016).

In a THP-1 human macrophage model, previous investigations looked at the combined effect of HBHA and MTP on adhesion and invasion (Moodley, 2018, unpublished). The MTP-deficient strain had a lower bacillary load than the wild type at all studied intervals, including 4-h after infection (Moodley, 2018, unpublished). The findings suggested that these coupled adhesins induce transcriptional alterations that favour macrophage adherence and invasion (Moodley, 2018, unpublished).

RNA sequencing of A549 lung epithelial cells infected by MTP-proficient and MTP-deficient *M. tuberculosis* V9124 strains was used to investigate the role of MTP in inducing host immune response *in vitro* (Dlamini, 2016). According to the findings, *mtp* has an effect on gene regulation in A549 alveolar epithelial cells, and its presence allows for increased production of host immune response genes including cell surface receptors (Dlamini, 2016).

1.18 Techniques used to study protein expression

1.18.1 Dot blot technique

Dot-blot is a straightforward method for detecting the presence of a protein of interest in a sample. The dot-blot is similar to the other blotting techniques in that it does not reveal the size of the hybridized fragment. Based on RNA Dot-blot, the dot-blot immunoassay was developed in 1982 (Hawkes *et al*., 1982) and validated for large-scale absence/presence screening of protein markers in bacteriology, immunology, and epidemiological research. Enzyme-linked immunosorbent assay (ELISA) was invented and scientifically confirmed for protein quantification ten years before dot-blot and is now a widely used technology. Some studies used dot-blot instead of ELISA due to technical requirements such as protein solubility (Yamada *et al*., 2004; Teimouri *et al*., 2019; Smart *et al*., 2021). The validation of a large number of different proteins requires the use of dot-blot rather than ELISA for practical and time-consuming reasons. (Guillemin *et al*., 2009). Furthermore, the dot-blot technique is quite similar to the Western-blot technique, and it is a compromise between the benefits of the protein-array approach and those of the Western-blot technique. As the antibody settings (dilutions, incubation duration) are similar in dot-blot and Western-blot, antibody specificity can be ensured in a dot-blot quantification following a Western-blot validation of the antibody (Guillemin *et al*., 2009). There is no technical or biological validation of dot-blot other than a specific use in a study context for one or two proteins due to the low rate of dot-blot use for protein quantification. (De Lisle, 1991; Duffy *et al*., 1999). As a result, the validation of many protein markers necessitates a broader dot-blot validation (Guillemin *et al*., 2009).

1.18.2 Western-blot

Western blotting has many applications in protein research, including investigating regulatory molecular events that support metabolism and protein turnover (Bass *et al.*, 2017). It can be used in protein research to investigate protein abundance, cellular localization, protein-protein interactions and methylation (Voelkel *et al*., 2013). Western-blot is mainly conducted on complex samples such as cell extract and tissues but can also be used to detect protein in less complex samples (Gomes *et al.*, 2009). Picogram levels of protein can be detected by Western blot (Coorssen *et al.*, 2000). The sensitivity and specificity of Western-blots are due to the separation of proteins of different sizes, charges, and conformation by gel electrophoresis (Ghosh *et al*., 2014). Western-blot is also associated with some limitations, one of which is that it can only be carried out if a primary antibody against the protein of interest is available (Péré-Brissaud *et al*., 2015). Antibodies for different projects can be expensive and if the primary antibodies are not present, it will not be possible to detect a protein using the Western-blot (Ghosh *et al.*, 2014). Other Western-blotting limitations include the need for each antibody to be independently optimized and the cost of modern western blotting equipment such as advanced digital imagers (Ghosh *et al*., 2014). Integrating transcriptomic data with proteomics data will enhance our understanding of *M. tuberculosis* adhesins genes functionality at the phenotypic level.

1.19 Significance of this study

Despite global efforts to understand the pathogenesis of *M. tuberculosis*, there is still insufficient knowledge about the adherence mechanism used by this pathogen. *Mycobacterium tuberculosis* possesses multiple adhesins, which are likely to enhance this microbe's success in TB pathogenesis and contribute to it being such a successful pathogen. The present study would increase the understanding of which, if not all, of the selected adhesins are regulated in the absence of major adhesins. This knowledge could potentially support the use of blocking agents against these major adhesins or the upregulated adhesins, as adjunctive therapy in conjunction with conventional anti-TB treatment. The emerging research on *M. tuberculosis* adhesins as potential biomarkers justifies that adhesins should be explored as novel biomarkers for TB diagnostics and therapeutics. The significance of this study will be the validation of adhesins as targets for TB diagnostics, drug and vaccine development.

1.20. Research design

1.20.1 Aims

This study aims to elucidate the role of selected adhesin genes on the regulation of specific adhesins genes of *M. tuberculosis* in a THP-1 infection model.

1.18.2 Objectives

1. To infect THP-1 cells with adhesin gene proficient, deficient, and complemented strains of *M. tuberculosis*.

2. To extract *M. tuberculosis* RNA from infected THP-1 cells post adhesion and at different intervals post-infection.

3. To use RT-qPCR to investigate the regulation of adhesin and non-adhesin genes.

4. To confirm gene expression by performing phenotypic functional assays by evaluating specific protein expression during infection using western blot.

Dissertation outline

This dissertation comprises 3 chapters. Chapter 1 reviewed the relevant literature. Chapter 2 presents Manuscript 1 which investigated the individual role of HBHA, MTP and Rv0309 and the combined role of MTP and HBHA in the regulation of other adhesin genes employed by *M. tuberculosis* during the infection process in a THP-1 infection model, using *M. tuberculosis* V9124, Δ*mtp*, Δ*hbhA*, Δ*Rv0309* and Δ*mtp-hbhA* deletion mutants and their respective complemented strains. Chapter 3 presents protein work and troubleshooting that was performed in trying to confirm phenotypic expression of the studied genes. The important findings from the literature review and the manuscript are summarized in Chapter 4, along with the manuscript's limitations, conclusions, and recommendations for further research.

1.21 References

Abrahams, K.A. and Besra, G.S., 2018. Mycobacterial cell walls biosynthesis: a multifaceted antibiotic target. *Parasitology*, 145(2), pp.116-133.

Aguilo, N., Uranga, S., Marinova, D., Monzon, M., Badiola, J. and Martin, C., 2016. MTBVAC vaccine is safe, immunogenic and confers protective efficacy against *Mycobacterium tuberculosis* in newborn mice. *Tuberculosis*, *96*, pp.71-74.

Ahmad, S., 2011. Pathogenesis, immunology, and diagnosis of latent *Mycobacterium tuberculosis* infection. *Clinical and Developmental Immunology*, *2011*.

Ahmad, N., Ahuja, S.D., Akkerman, O.W., Alffenaar, J.C., Anderson, L.F. and Baghaei, P., 2018. Collaborative Group for the Meta-Analysis of Individual Patient Data in MDR-TB treatment–2017. Treatment correlates of successful outcomes in pulmonary multidrug-resistant tuberculosis: an individual patient data meta-analysis. *Lancet*, 392(10150), pp.821-834.

Alderwick, L.J., Harrison, J., Lloyd, G.S. and Birch, H.L., 2015. The mycobacterial cell wall—peptidoglycan and arabinogalactan. *Cold Spring Harbor Perspectives In Medicine*, 5(8), p.a021113.

Alexander, K. A., Laver, P. N., Michel, A. L., Williams, M., van Helden, P. D., Warren, R. M., & van Pittius, N. C. G. (2010). Novel *Mycobacterium tuberculosis* complex pathogen, *M. mungi*. *Emerging Infectious Diseases*, 16(8), 1296.

Algood HM, Chan J, Flynn JL. Chemokines and tuberculosis. *Cytokine and Growth Factor Reviews*. 2003 Dec 1;14(6):467-77.

Alteri, C.J., Xicohténcatl-Cortes, J., Hess, S., Caballero-Olín, G., Girón, J.A. and Friedman, R.L., 2007. *Mycobacterium tuberculosis* produces pili during human infection. *Proceedings of the National Academy of Sciences*, 104(12), pp.5145-5150.

Armitige, L.Y., Jagannath, C., Wanger, A.R. and Norris, S.J., 2000. Disruption of the genes encoding antigen 85A and antigen 85B of *Mycobacterium tuberculosis* H37Rv: effect on growth in culture and in macrophages. *Infection and Immunity*, 68(2), pp.767-778.

Ashokcoomar, S., Reedoy, K.S., Senzani, S., Loots, D.T., Beukes, D., Van Reenen, M., Pillay, B. and Pillay, M., 2020. *Mycobacterium tuberculosis* curli pili (MTP) deficiency is associated

with alterations in cell wall biogenesis, fatty acid metabolism and amino acid synthesis. *Metabolomics*, 16(9), pp.1-15.

Bansal-Mutalik, R. and Nikaido, H., 2014. Mycobacterial outer membrane is a lipid bilayer and the inner membrane is unusually rich in diacyl phosphatidylinositol dimannosides. *Proceedings of the National Academy of Sciences*, 111(13), pp.4958-4963.

Barker, L. F., Leadman, A. E., and Clagett, B. (2011). The challenges of developing new tuberculosis vaccines. *Health Affairs*, 30(6), 1073-1079.

Barnett, T. C., Cole, J. N., Rivera-Hernandez, T., Henningham, A., Paton, J. C., Nizet, V., and Walker, M. J. (2015). Streptococcal toxins: role in pathogenesis and disease. *Cellular Microbiology*, 17(12), 1721-1741.

Barnhart, M.M. and Chapman, M.R., 2006. Curli biogenesis and function. *Annu. Rev. Microbiol.*, 60, pp.131-147.

Bass, J.J., Wilkinson, D.J., Rankin, D., Phillips, B.E., Szewczyk, N.J., Smith, K. and Atherton, P.J., 2017. An overview of technical considerations for Western blotting applications to physiological research. *Scandinavian Journal of Medicine and Science In Sports*, 27(1), pp.4-25

Belisle, J.T., Vissa, V.D., Sievert, T., Takayama, K., Brennan, P.J. and Besra, G.S., 1997. Role of the major antigen of *Mycobacterium tuberculosis* in cell wall biogenesis. *Science*, 276(5317), pp.1420-1422.

Bermudez, L.E. and Goodman, J., 1996. *Mycobacterium tuberculosis* invades and replicates within type II alveolar cells. *Infection and Immunity*, 64(4), pp.1400-1406.

Bisht, D. and Meena, L.S., 2019. Adhesion molecules facilitate host-pathogen interaction and mediate *Mycobacterium tuberculosis* pathogenesis. *The Indian Journal of Medical Research*, 150(1), p.23.

Braibant, M., Gilot, P. and Content, J., 2000. The ATP binding cassette (ABC) transport systems of *Mycobacterium tuberculosis*. *FEMS Microbiology Reviews*, 24(4), pp.449-467.

Buddle, B.M., Parlane, N.A., Keen, D.L., Aldwell, F.E., Pollock, J.M., Lightbody, K. and Andersen, P., 1999. Differentiation between *Mycobacterium bovis BCG*-vaccinated and *M. bovis*-infected cattle by using recombinant mycobacterial antigens. *Clinical and Diagnostic Laboratory Immunology*, 6(1), pp.1-5.

Casali, N., Nikolayevskyy, V., Balabanova, Y., Harris, S. R., Ignatyeva, O., Kontsevaya, I, and Horstmann, R. D. (2014). Evolution and transmission of drug-resistant tuberculosis in a Russian population. *Nature Genetics*, 46(3), 279.

Ciaramella, A., Martino, A., Cicconi, R., Colizzi, V. and Fraziano, M., 2000. Mycobacterial 19-kDa lipoprotein mediates *Mycobacterium tuberculosis*-induced apoptosis in monocytes/macrophages at early stages of infection. *Cell Death and Differentiation*, 7(12), pp.1270-1272.

Chanput, W., Mes, J.J. and Wichers, H.J., 2014. THP-1 cell line: an *in vitro* cell model for immune modulation approach. *International Immunopharmacology*, *23*(1), pp.37-45.

Colditz, G. A., Brewer, T. F., Berkey, C. S., Wilson, M. E., Burdick, E., Fineberg, H. V., and Mosteller, F. (1994). Efficacy of BCG vaccine in the prevention of tuberculosis: meta-analysis of the published literature. *Jama*, 271(9), 698-702.

Cole, S., Brosch, R., Parkhill, J., Garnier, T., Churcher, C., Harris, D., Gordon, S.V., Eiglmeier, K., Gas, S., Barry Iii, C.E. and Tekaia, F., 1998. Deciphering the biology of *Mycobacterium tuberculosis* from the complete genome sequence. *Nature*, 393(6685), p.537.

Cooper, A.M., 2009. Cell-mediated immune responses in tuberculosis. *Annual Review of Immunology*, 27, pp.393-422.

Coorssen, J. R., Blank, P. S., Albertorio, F., Bezrukov, L., Kolosova, I., Backlund Jr, P. S., and Zimmerberg, J. (2002). Quantitative femto-to attomole immunodetection of regulated secretory vesicle proteins critical to exocytosis. *Analytical Biochemistry*, 307(1), 54-62.

Coscolla, M., Lewin, A., Metzger, S., Maetz-Rennsing, K., Calvignac-Spencer, S., Nitsche, A.and Couacy-Hymann, E. (2013). Novel *Mycobacterium tuberculosis* complex isolate from a wild chimpanzee. *Emerging Infectious Diseases*, 19(6), 969.

Coscolla, M. and Gagneux, S., 2014, December. Consequences of genomic diversity in *Mycobacterium tuberculosis*. In *Seminars in Immunology* (Vol. 26, No. 6, pp. 431-444). Academic Press.

Dahl, J. L. (2004). Electron microscopy analysis of *Mycobacterium tuberculosis* cell division. *FEMS Microbiology Letters*, 240(1), 15-20.

Danelishvili, L., McGarvey, J., Li, Y.J. and Bermudez, L.E., 2003. *Mycobacterium tuberculosis* infection causes different levels of apoptosis and necrosis in human macrophages and alveolar epithelial cells. *Cellular Microbiology*, 5(9), pp.649-660.

Davenne, T., and McShane, H. (2016). Why don't we have an effective tuberculosis vaccine yet?. *Expert Review of Vaccines*, 15(8), 1009-1013.

De Lisle, R.C., 1991. A quantitative dot-blot immunoassay for integral membrane proteins: preparation of pancreatic plasma membranes containing apical and basolateral domains. *Analytical Biochemistry*, 192(1), pp.1-5.

Deepak, S. A., Kottapalli, K. R., Rakwal, R., Oros, G., Rangappa, K. S., Iwahashi, H., and Agrawal, G. K. (2007). Real-time PCR: revolutionizing detection and expression analysis of genes. *Current Genomics*, 8(4), 234-251.

Delogu G, Sanguinetti M, Posteraro B, Rocca S, Zanetti S and Fadda G (2006) The *hbhA* gene of *Mycobacterium tuberculosis* is specifically upregulated in the lungs but not in the spleens of aerogenically infected mice. *Infection and Immunology*, 74: 3006–3011.

Delogu, G., Sali, M. and Fadda, G., 2013. The biology of *mycobacterium tuberculosis* infection. *Mediterranean Journal of Hematology and Infectious Diseases*, 5(1).

Diaz-Silvestre, H., Espinosa-Cueto, P., Sanchez-Gonzalez, A., Esparza-Ceron, M. A., Pereira-Suarez, A. L., Bernal-Fernandez, G and Mancilla, R. (2005). The 19-kDa antigen of *Mycobacterium tuberculosis* is a major adhesin that binds the mannose receptor of THP-1 monocytic cells and promotes phagocytosis of mycobacteria. *Microbial Pathogenesis*, 39(3), 97-107.

Dlamini, M. T. 2016. 'Whole transcriptome analysis to elucidate the role of mtp in gene regulation of pulmonary epithelial cells infected with *Mycobacterium tuberculosis*.' Unpublished Masters thesis. University of KwaZulu-Natal, Durban, South Africa.

Dreher, D. and Nicod, L.P., 2002. Dendritic cells in the mycobacterial granuloma are involved in acquired immunity. *American Journal of Respiratory and Critical Care Medicine.* 165(12):1577-1578.

Ducati, R.G., Ruffino-Netto, A., Basso, L.A. and Santos, D.S., 2006. The resumption of consumption: a review on tuberculosis. *Memórias do Instituto Oswaldo Cruz*, 101(7), pp.697-714.

Duffy, L.K., Scofield, E., Rodgers, T., Patton, M. and Bowyer, R.T., 1999. Comparative baseline levels of mercury, Hsp 70 and Hsp 60 in subsistence fish from the Yukon-Kuskokwim delta region of Alaska. *Comparative Biochemistry and Physiology Part C: Pharmacology, Toxicology and Endocrinology*, 124(2), pp.181-186.

Engel, A., Renema, J.J., Il'in, K. and Semenov, A., 2015. Detection mechanism of superconducting nanowire single-photon detectors. *Superconductor Science and Technology*, 28(11), p.114003.

Esparza, M., Palomares, B., García, T., Espinosa, P., Zenteno, E. and Mancilla, R., 2015. PstS-1, the 38-kDa *Mycobacterium tuberculosis* Glycoprotein, is an Adhesin, Which Binds the Macrophage Mannose Receptor and Promotes Phagocytosis. *Scandinavian Journal of Immunology*, 81(1), pp.46-55.

Filliol, I., Motiwala, A.S., Cavatore, M., Qi, W., Hazbón, M.H., Bobadilla del Valle, M., Fyfe, J., García-García, L., Rastogi, N., Sola, C. and Zozio, T., 2006. Global phylogeny of *Mycobacterium tuberculosis* based on single nucleotide polymorphism (SNP) analysis: insights into tuberculosis evolution, phylogenetic accuracy of other DNA fingerprinting systems, and recommendations for a minimal standard SNP set. *Journal of Bacteriology*, 188(2), pp.759-772.

Flynn, J.L., Chan, J. and Lin, P.L., 2011. Macrophages and control of granulomatous inflammation in tuberculosis. *Mucosal Immunology*, *4*(3), pp.271-278.

Fontán P, Aris V, Ghanny S, Soteropoulos P, andSmith I (2008) Global transcriptional profile *of Mycobacterium tuberculosis* during THP-1 human macrophage infection. *Infection and Immunology*, 76: 717-725.

Fraga, D., Meulia, T. and Fenster, S., 2008. Real-time PCR. *Current Protocols Essential Laboratory Techniques*, (1), pp.10-3.

Frick, M. (2013). The TB vaccines pipeline. *Clayden P, Collins S, Daniels C, et al.; i-Base/Treatment Action Group*.

Früh, K., & Picker, L. (2017). CD8+ T cell programming by cytomegalovirus vectors: applications in prophylactic and therapeutic vaccination. *Current Opinion in Immunology*, 47, 52-56.

Fuchs, T.M., Eisenreich, W., Heesemann, J. and Goebel, W., 2012. Metabolic adaptation of human pathogenic and related nonpathogenic bacteria to extra-and intracellular habitats. *FEMS Microbiology Reviews*, 36(2), pp.435-462.

Gagneux, S. and Small, P.M., 2007. Global phylogeography of *Mycobacterium tuberculosis* and implications for tuberculosis product development. *The Lancet Infectious Diseases*, 7(5), pp.328-337.

Gagneux, S., 2018. Ecology and evolution of *Mycobacterium tuberculosis*. *Nature Reviews Microbiology*, *16*(4), pp.202-213.

Gandhi, N. R., Moll, A., Sturm, A. W., Pawinski, R., Govender, T., Lalloo, U.and Friedland, G. (2006). Extensively drug-resistant tuberculosis as a cause of death in patients co-infected with tuberculosis and HIV in a rural area of South Africa. *The Lancet*, 368(9547), 1575-1580.

Gandhi, N. R., Andrews, J. R., Brust, J. C., Montreuil, R., Weissman, D., Heo, M., and Shah, N. S. (2012). Risk factors for mortality among MDR-and XDR-TB patients in a high HIV prevalence setting. *The International Journal of Tuberculosis and Lung Disease*, 16(1), 90-97.

Garcia-Prats, A.J., Schaaf, H.S. and Hesseling, A.C., 2016. The safety and tolerability of the second-line injectable antituberculosis drugs in children. *Expert Opinion on Drug Safety*, 15(11), pp.1491-1500.

Ghosh, R., Gilda, J.E. and Gomes, A.V., 2014. The necessity of and strategies for improving confidence in the accuracy of western blots. *Expert Review of Proteomics*, 11(5), pp.549-560.

Global tuberculosis report, 2022. Geneva: World Health Organization; 2022. Licence: CC BY-NC-SA 3.0 IGO

Gomes, A. V., Young, G. W., Wang, Y., Zong, C., Eghbali, M., Drews, O., and Ping, P. (2009). Contrasting proteome biology and functional heterogeneity of the 20 S proteasome complexes in mammalian tissues. *Molecular and Cellular Proteomics*, 8(2), 302-315.

Govender, V.S., Ramsugit, S. and Pillay, M., 2014. *Mycobacterium tuberculosis* adhesins: potential biomarkers as anti-tuberculosis therapeutic and diagnostic targets. *Microbiology*, 160(9), pp.1821-1831.

Govender, V. S., Jain, P., Larsen, M. H. & Pillay, M. 2018. '*Mycobacterium tuberculosis* heparin binding hemagglutinin adhesin (HBHA) and curli pili (MTP) are essential for *in vitro* growth, but not viability and biofilm production.' Unpublished Manuscript from the PhD thesis. University of Kwa-Zulu- Natal, Durban, South Africa

Grode, L., Ganoza, C.A., Brohm, C., Weiner 3rd, J., Eisele, B. and Kaufmann, S.H., 2013. Safety and immunogenicity of the recombinant BCG vaccine VPM1002 in a phase 1 open-label randomized clinical trial. *Vaccine*, 31(9), pp.1340-1348.

Gupta, R.S., Lo, B. and Son, J., 2018. Phylogenomics and comparative genomic studies robustly support division of the genus *Mycobacterium* into an emended genus *Mycobacterium* and four novel genera. *Frontiers in Microbiology*, *9*, p.67.

Guillemin, N., Meunier, B., Jurie, C., Cassar-Malek, I., Hocquette, J.F., Levéziel, H. and Picard, B., 2009. Validation of a Dot-Blot quantitative technique for large scale analysis of beef tenderness biomarkers. *Journal of Physiology and Pharmacology*, 60(supplement 3), pp.91-97.

Guirado, E., Schlesinger, L.S. and Kaplan, G., 2013, September. Macrophages in tuberculosis: friend or foe. *In Seminars in immunopathology* (Vol. 35, No. 5, pp. 563-583). Springer Berlin Heidelberg.

Gutacker, M.M., Mathema, B., Soini, H., Shashkina, E., Kreiswirth, B.N., Graviss, E.A. and Musser, J.M., 2006. Single-nucleotide polymorphism–based population genetic analysis of *Mycobacterium tuberculosis* strains from 4 geographic sites. *The Journal of infectious diseases*, *193*(1), pp.121-128.

Guyton, A. and J. Hall. 2006. *Textbook of Medical Physiology*. 11th ed., United State of America.

Harris, R. C., Dodd, P. J., & White, R. G. (2016). The potential impact of BCG vaccine supply shortages on global paediatric tuberculosis mortality. *BMC Medicine*, 14(1), 138.

Hawkes, R., Niday, E. and Gordon, J., 1982. A dot-immunobinding assay for monoclonal and other antibodies. *Analytical Biochemistry*, 119(1), pp.142-147.

Helmy, N., Kamel, M.M., Ashour, W. and El Kattan, E., 2012. Role of Quantiferon TB gold assays in monitoring the efficacy of antituberculosis therapy. *Egyptian Journal of Chest Diseases and Tuberculosis*, 61(4), pp.329-336.

Henderson, B., Lund, P.A. and Coates, A.R., 2010. Multiple moonlighting functions of mycobacterial molecular chaperones. *Tuberculosis*, 90(2), pp.119-124.

Herrmann, J.L., O'Gaora, P., Gallagher, A., Thole, J.E. and Young, D.B., 1996. Bacterial glycoproteins: a link between glycosylation and proteolytic cleavage of a 19 kDa antigen from *Mycobacterium tuberculosis*. *The EMBO Journal*, 15(14), pp.3547-3554

Hickey, T. B., Ziltener, H. J., Speert, D. P., and Stokes, R. W. (2010). *Mycobacterium tuberculosis* employs Cpn60. 2 as an adhesin that binds CD43 on the macrophage surface. *Cellular Microbiology*, 12(11), 1634-1647.

Hillemann, D., Rüsch-Gerdes, S. and Richter, E., 2007. Evaluation of the GenoType MTBDRplus assay for rifampin and isoniazid susceptibility testing of *Mycobacterium tuberculosis* strains and clinical specimens. *Journal of Clinical Microbiology*, 45(8), pp.2635-2640.

Hjort, M.R., Brenyo, A.J., Finkelstein, J.N., Frampton, M.W., LoMonaco, M.B., Stewart, J.C., Johnston, C.J. and D'Angio, C.T., 2003. Alveolar epithelial cell-macrophage interactions affect oxygen-stimulated interleukin-8 release. *Inflammation*, 27(3), pp.137-145.

Homolka, S., Projahn, M., Feuerriegel, S., Ubben, T., Diel, R., Nübel, U. and Niemann, S., 2012. High resolution discrimination of clinical *Mycobacterium tuberculosis* complex strains based on single nucleotide polymorphisms. *PloS one*, *7*(7), p.e39855.

Hu, Y., Henderson, B., Lund, P.A., Tormay, P., Ahmed, M.T., Gurcha, S.S., Besra, G.S. and Coates, A.R., 2008. A *Mycobacterium tuberculosis* mutant lacking the groEL homologue cpn60. 1 is viable but fails to induce an inflammatory response in animal models of infection. *Infection and Immunity*, 76(4), pp.1535-1546.

Huang, W.L., Chen, H.Y., Kuo, Y.M. and Jou, R., 2009. Performance assessment of the GenoType MTBDR plus test and DNA sequencing in detection of multidrug-resistant *Mycobacterium tuberculosis*. *Journal of Clinical Microbiology*, 47(8), pp.2520-2524.

Iliyasu, Z., and Babashani, M. (2009). Prevalence and predictors of tuberculosis coinfection among HIV-seropositive patients attending the Aminu Kano Teaching Hospital, northern Nigeria. *Journal of Epidemiology*, 0903030070-0903030070.

Imaz, M.S., Comini, M.A., Zerbini, E., Sequeira, M.D., Latini, O., Claus, J.D. and Singh, M., 2004. Evaluation of commercial enzyme-linked immunosorbent assay kits for detection of tuberculosis in Argentinean population. *Journal of Clinical Microbiology*, 42(2), pp.884-887.

Joseph, S., Yuen, A., Singh, V. and Hmama, Z., 2017. *Mycobacterium tuberculosis* Cpn60. 2 (GroEL2) blocks macrophage apoptosis via interaction with mitochondrial mortalin. *Biology Open*, *6*(4), pp.481-488.

Kana, B.D., Gordhan, B.G., Downing, K.J., Sung, N., Vostroktunova, G., Machowski, E.E., Tsenova, L., Young, M., Kaprelyants, A., Kaplan, G. and Mizrahi, V., 2008. The resuscitation-promoting factors of *Mycobacterium tuberculosis* are required for virulence and resuscitation from dormancy but are collectively dispensable for growth in vitro. *Molecular Microbiology*, 67(3), pp.672-684.

Kapoor, N., Pawar, S., Sirakova, T.D., Deb, C., Warren, W.L. and Kolattukudy, P.E., 2013. Human granuloma *in vitro* model, for TB dormancy and resuscitation. *PloS One*, 8(1), p. e53657.

Kapopoulou, A., Lew, J. M. and Cole, S. T. 2011. The MycoBrowser portal: A comprehensive and manually annotated resource for mycobacterial genomes. *Tuberculosis,* 91, 8-13.

Kapwata, T., Morris, N., Campbell, A., Mthiyane, T., Mpangase, P., Nelson, K.N., Allana, S., Brust, J.C., Moodley, P., Mlisana, K. and Gandhi, N.R., 2017. Spatial distribution of extensively drug-resistant tuberculosis (XDR TB) patients in KwaZulu-Natal, South Africa. *PLoS One*, 12(10), p. e0181797.

Kaufmann, S.H., 2020. Vaccination against tuberculosis: revamping BCG by molecular genetics guided by immunology. *Frontiers in Immunology*, 11, p.316.

Keshavjee, S. and Farmer, P.E., 2012. Tuberculosis, drug resistance, and the history of modern medicine. *New England Journal of Medicine*, 367(10), pp.931-936.

Kinhikar, A.G., Vargas, D., Li, H., Mahaffey, S.B., Hinds, L., Belisle, J.T. and Laal, S., 2006. *Mycobacterium tuberculosis* malate synthase is a laminin-binding adhesin. *Molecular Microbiology*, 60(4), pp.999-1013.

Kukurba, K.R. and Montgomery, S.B., 2015. RNA sequencing and analysis. *Cold Spring Harbor Protocols*, 2015(11), pp.pdb-top084970.

Kumar, P., Amara, R.R., Challu, V.K., Chadda, V.K. and Satchidanandam, V., 2003. The Apa protein of *Mycobacterium tuberculosis* stimulates gamma interferon-secreting CD4+ and CD8+ T cells from purified protein derivative-positive individuals and affords protection in a guinea pig model. *Infection and Immunity*, 71(4), pp.1929-1937.

Kumar, S., Puniya, B.L., Parween, S., Nahar, P. and Ramachandran, S., 2013. Identification of novel adhesins of *M. tuberculosis* H37Rv using integrated approach of multiple computational algorithms and experimental analysis. *PLoS One*, 8(7), p.e69790

Kumar, S., 2015. *Essentials of microbiology*. JP Medical Ltd.

Kuvar, S (2016) The role of *hbhA* in gene regulation *in vivo* using a *hbhA* knockout mutant of *M. tuberculosis*. Masters Dissertation, University of KwaZulu-Natal.

Kwan, C.K. and Ernst, J.D., 2011. HIV and tuberculosis: a deadly human syndemic. *Clinical Microbiology Reviews*, 24(2), pp.351-376.

Lavollay, M., Arthur, M., Fourgeaud, M., Dubost, L., Marie, A., Veziris, N., Blanot, D., Gutmann, L. and Mainardi, J.L., 2008. The peptidoglycan of stationary-phase *Mycobacterium tuberculosis* predominantly contains cross-links generated by L, D-transpeptidation. *Journal of Bacteriology*, 190(12), pp.4360-4366.

Lawn, S.D., Dheda, K., Kerkhoff, A.D., Peter, J.G., Dorman, S., Boehme, C.C. and Nicol, M.P., 2013. Determine TB-LAM lateral flow urine antigen assay for HIV-associated tuberculosis: recommendations on the design and reporting of clinical studies. *BMC Infectious Diseases*, 13(1), pp.1-9.

Leemans, J.C., Thepen, T., Weijer, S., Florquin, S., Van Rooijen, N., Van de Winkel, J.G. and Van der Poll, T., 2005. Macrophages play a dual role during pulmonary tuberculosis in mice. *The Journal of Infectious Diseases*, 191(1), pp.65-74.

Lefèvre, P., Braibant, M., De Wit, L., Kalai, M., Röeper, D., Grötzinger, J., Delville, J.P., Peirs, P., Ooms, J., Huygen, K. and Content, J., 1997. Three different putative phosphate transport receptors are encoded by the *Mycobacterium tuberculosis* genome and are present at the surface of *Mycobacterium bovis* BCG. *Journal of Bacteriology*, 179(9), pp.2900-2906.

Lin, P.L., Ford, C.B., Coleman, M.T., Myers, A.J., Gawande, R., Ioerger, T., Sacchettini, J., Fortune, S.M. and Flynn, J.L., 2014. Sterilization of granulomas is common in active and latent

tuberculosis despite within-host variability in bacterial killing. *Nature Medicine*, 20(1), pp.75-79.

Lipworth, S., Jajou, R., de Neeling, A., Bradley, P., van der Hoek, W., Maphalala, G., Bonnet, M., Sanchez-Padilla, E., Diel, R., Niemann, S. and Iqbal, Z., 2019. SNP-IT tool for identifying subspecies and associated lineages of *Mycobacterium tuberculosis* complex. *Emerging Infectious Diseases*, *25*(3), p.482.

López, M., Sly, L.M., Luu, Y., Young, D., Cooper, H. and Reiner, N.E., 2003. The 19-kDa *Mycobacterium tuberculosis* protein induces macrophage apoptosis through Toll-like receptor-2. *The Journal of Immunology*, 170(5), pp.2409-2416.

Loxton, A.G., Black, G.F., Stanley, K. and Walzl, G., 2012. Heparin-binding hemagglutinin induces IFN-γ+ IL-2+ IL-17+ multifunctional CD4+ T cells during latent but not active tuberculosis disease. *Clinical and Vaccine Immunology*, 19(5), pp.746-751.

Loxton, A.G., Knaul, J.K., Grode, L., Gutschmidt, A., Meller, C., Eisele, B., Johnstone, H., van der Spuy, G., Maertzdorf, J., Kaufmann, S.H. and Hesseling, A.C., 2017. Safety and immunogenicity of the recombinant Mycobacterium bovis BCG vaccine VPM1002 in HIV-unexposed newborn infants in South Africa. *Clinical and Vaccine Immunology*, 24(2), pp. e00439-16.

Luca, S. and Mihaescu, T., 2013. History of BCG vaccine. *Maedica*, 8(1), pp.53-58.

MacGregor-Fairlie, M., Wilkinson, S., Besra, G.S. and Goldberg Oppenheimer, P., 2020. Tuberculosis diagnostics: overcoming ancient challenges with modern solutions. *Emerging Topics in Life Sciences*, 4(4), pp.435-448.

Mack, U., Migliori, G. B., Sester, M., Rieder, H. L., Ehlers, S., Goletti, D., and Arend, S. M. (2009). LTBI: latent tuberculosis infection or lasting immune responses to *M. tuberculosis*? A TBNET consensus statement. *European Respiratory Journal*, 33(5), 956-973.

Maertzdorf, J., Repsilber, D., Parida, S. K., Stanley, K., Roberts, T., Black, G., and Kaufmann, S. H. (2011). Human gene expression profiles of susceptibility and resistance in tuberculosis. *Genes and Immunity*, 12(1), 15.

Maertzdorf, J., Repsilber, D., Parida, S. K., Stanley, K., Roberts, T., Black, G., and Kaufmann, S. H. (2011). Human gene expression profiles of susceptibility and resistance in tuberculosis. *Genes and Immunity*, 12(1), 15.

Mandlik, A., Swierczynski, A., Das, A. and Ton-That, H., 2008. Pili in Gram-positive bacteria: assembly, involvement in colonization and biofilm development. *Trends in microbiology*, 16(1), pp.33-40.

Mangtani, P., Abubakar, I., Ariti, C., Beynon, R., Pimpin, L., Fine, P. E., Rodrigues, L. C., Smith, P. G., Lipman, M. and Whiting, P. F. 2014. Protection by BCG vaccine against tuberculosis: a systematic review of randomized controlled trials. *Clinical Infectious Diseases*, 58, 470-480.

Marmiesse, M., Brodin, P., Buchrieser, C., Gutierrez, C., Simoes, N., Vincent, V., and Brosch, R. (2004). Macro-array and bioinformatic analyses reveal mycobacterial 'core'genes, variation in the ESAT-6 gene family and new phylogenetic markers for the *Mycobacterium tuberculosis* complex. *Microbiology*, 150(2), 483-496.

Martín, C., Marinova, D., Aguiló, N. and Gonzalo-Asensio, J., 2021. MTBVAC, a live TB vaccine poised to initiate efficacy trials 100 years after BCG. *Vaccine*, 39(50), pp.7277-7285.

Massyn, N., Peer, N., English, R., Padarath, A., Barron, P. and Day, C.E., 2016. District health barometer 2015/16. *Durban: Health Systems Trust*.

McLoughlin, K.S., 2011. Microarrays for pathogen detection and analysis. *Briefings in Functional Genomics*, 10(6), pp.342-353.

McShane, H. (2011). Tuberculosis vaccines: beyond bacille Calmette–Guérin. *Philosophical Transactions of the Royal Society B: Biological Sciences*, 366(1579), 2782-2789.

Menozzi, F. D., Rouse, J. H., Alavi, M., Laude-Sharp, M., Muller, J., Bischoff, R and Locht, C. (1996). Identification of a heparin-binding hemagglutinin present in mycobacteria. *Journal of Experimental Medicine*, 184(3), 993-1001.

Menozzi, F. D., Bischoff, R., Fort, E., Brennan, M. J., and Locht, C. (1998). Molecular characterization of the mycobacterial heparin-binding hemagglutinin, a *mycobacterial* adhesin. *Proceedings of the National Academy of Sciences*, 95(21), 12625-12630.

Menozzi, F. D., Reddy, V. M., Cayet, D., Raze, D., Debrie, A.-S., Dehouck, M.-P., Cecchelli, R. and Locht, C. 2006. *Mycobacterium tuberculosis* heparin-binding hemagglutinin adhesin

(HBHA) triggers receptor-mediated transcytosis without altering the integrity of tight junctions. *Microbes and Infection,* 8**,** 1-9.

Moodley, S. 2018. "The role of heparin binding haemaggluttin adhesin and curli pili on the pathogenicity of *Mycobacterium tuberculosis*.' Unpublished PhD thesis, University of Kwa-Zulu- Natal, Durban, South Africa.

Mudaliar, A.V., Kashyap, R.S., Purohit, H.J., Taori, G.M. and Daginawala, H.F., 2006. Detection of 65 kD heat shock protein in cerebrospinal fluid of tuberculous meningitis patients. *BMC Neurology*, 6(1), pp.1-7.

Mueller-Ortiz SL, Wanger AR, and Norris SJ (2001) Mycobacterial protein HbhA binds human complement component C3. *Infection and Immunity* 69: 7501–7511.

Mueller-Ortiz, S.L., Sepulveda, E., Olsen, M.R., Jagannath, C., Wanger, A.R. and Norris, S.J., 2002. Decreased infectivity despite unaltered C3 binding by a Δ*hbhA* mutant of *Mycobacterium tuberculosis*. *Infection and Immunity*, 70(12), pp.6751-6760.

Muniram S. (2018). *Mycobacterium tuberculosis L, D-Transpeptidase Promotes In-Vitro Growth, Biofilm Production and Septum Formation During Cell Division* (Masters thesis). University of KwaZulu-Natal, Durban, South Africa.

Musewa, A., Bulage, L., Maganda, J.F. and Ario, A.R., 2021. Turnaround Time for Microbiological Testing of Tuberculosis in Routine Clinical Practice and Time to Patient Initiation on Treatment, Iganga Hospital, Uganda: 2012-2017.

Murray, P.J., 2007. The JAK-STAT signaling pathway: input and output integration. *The Journal of Immunology*, 178(5), pp.2623-2629.

Mvubu, N.E., Pillay, B., Gamieldien, J., Bishai, W. and Pillay, M., 2016. *Mycobacterium tuberculosis* strains exhibit differential and strain-specific molecular signatures in pulmonary epithelial cells. *Developmental and Comparative Immunology*, *65*, pp.321-329.

Naidoo, N., Ramsugit, S. and Pillay, M. 2014. *Mycobacterium tuberculosis* pili (MTP), a putative biomarker for a tuberculosis diagnostic test. *Tuberculosis*, 94, 338-345.

Naidoo, N., Pillay, B., Bubb, M., Pym, A., Chiliza, T., Naidoo, K., Ndung'u, T., Kasprowicz, V. O. and Pillay, M. 2018. Evaluation of a synthetic peptide for the detection of anti

Mycobacterium tuberculosis curli pili IgG antibodies in patients with pulmonary tuberculosis. *Tuberculosis*, 109, 80-84.

Naidoo, T.J., 2021. The role of *Mycobacterium tuberculosis* curli pili (MTP) and heparin-binding hemagglutinin adhesin (HBHA) on global *in vitro* bacterial transcriptomics (Mastersdissertation).

Nalpas, N.C., Park, S.D., Magee, D.A., Taraktsoglou, M., Browne, J.A., Conlon, K.M., Rue-Albrecht, K., Killick, K.E., Hokamp, K., Lohan, A.J. and Loftus, B.J., 2013. Whole-transcriptome, high-throughput RNA sequence analysis of the bovine macrophage response to *Mycobacterium bovis* infection *in vitro*. *BMC Genomics*, 14(1), pp.1-19.

National Centre for Biotechnology Information (NCBI), *Mycobacterium tuberculosis*. (Accessed 27 March 2018) Available: https://www.ncbi.nlm.nih.gov/geno me/166

Neufert, C., Pai, R.K., Noss, E.H., Berger, M., Boom, W.H. and Harding, C.V., 2001. *Mycobacterium tuberculosis* 19-kDa lipoprotein promotes neutrophil activation. *The Journal of Immunology*, 167(3), pp.1542-1549.

Nyawo, G. R. 2016. 'The role of *Mycobacterium tuberculosis* pili in pathogenesis: growth and survival kinetics, gene regulation and host immune response, and *in vitro* growth kinetics.' Masters dissertation. University of KwaZulu- Natal, Durban, South Africa.

Ottenhoff, T. H., and Kaufmann, S. H. (2012). Vaccines against tuberculosis: where are we and where do we need to go? *PLoS Pathogens*, 8(5), e1002607.

Pai, M., Behr, M.A., Dowdy, D., Dheda, K., Divangahi, M., Boehme, C.C., Ginsberg, A., Swaminathan, S., Spigelman, M., Getahun, H. and Menzies, D., 2016. Tuberculosis. *Nature Reviews. Disease Primers* 2, 16076.

Palma, C., Spallek, R., Piccaro, G., Pardini, M., Jonas, F., Oehlmann, W., Singh, M. and Cassone, A., 2011. The *M. tuberculosis* phosphate-binding lipoproteins PstS1 and PstS3 induce Th1 and Th17 responses that are not associated with protection against *M. tuberculosis* infection. *Clinical and Developmental Immunology*, 2011.

Parida, S.K. and Kaufmann, S.H., 2010. The quest for biomarkers in tuberculosis. *Drug discovery today*, *15*(3-4), pp.148-157.

Parsons, L.M., Somoskövi, Á., Gutierrez, C., Lee, E., Paramasivan, C.N., Abimiku, A.L., Spector, S., Roscigno, G. and Nkengasong, J., 2011. Laboratory diagnosis of tuberculosis in resource-poor countries: challenges and opportunities. *Clinical Microbiology Reviews*, 24(2), pp.314-350.

Parsons, S. D., Drewe, J. A., van Pittius, N. C. G., Warren, R. M., and Van Helden, P. D. (2013). Novel cause of tuberculosis in meerkats, South Africa. *Emerging Infectious Diseases*, 19(12), 2004.

Patti, J.M., Allen, B.L., McGavin, M.J. and Höök, M., 1994. MSCRAMM-mediated adherence of microorganisms to host tissues. *Annual Reviews in Microbiology*, 48(1), pp.585-617.

Paul, T. R., and Beveridge, T. J. (1992). Reevaluation of envelope profiles and cytoplasmic ultrastructure of mycobacteria processed by conventional embedding and freeze-substitution protocols. *Journal of Bacteriology*, 174(20), 6508-6517.

Peirs, P., Lefevre, P., Boarbi, S., Wang, X.M., Denis, O., Braibant, M., Pethe, K., Locht, C., Huygen, K. and Content, J., 2005. *Mycobacterium tuberculosis* with disruption in genes encoding the phosphate binding proteins PstS1 and PstS2 is deficient in phosphate uptake and demonstrates reduced *in vivo* virulence. *Infection and Immunity*, 73(3), pp.1898-1902.

Pessolani, M.C.V., de Melo Marques, M.A., Reddy, V.M., Locht, C. and Menozzi, F.D., 2003. Systemic dissemination in tuberculosis and leprosy: do mycobacterial adhesins play a role? *Microbes and Infection*, 5(7), pp.677-684.

Pethe, K., Alonso, S., Biet, F., Delogu, G., Brennan, M.J., Locht, C. and Menozzi, F.D., 2001. The heparin-binding haemagglutinin of *M. tuberculosis* is required for extrapulmonary dissemination. *Nature*, 412(6843), p.190

Pethe K, Bifani P, Drobecq H, Sergheraert C, Debrie AS, Locht C, Menozzi FD (2002) Mycobacterial heparin-binding hemagglutinin and laminin-binding protein share antigenic methyllysines that confer resistance to proteolysis. *Proc Natl Acad Sci U S A* 99: 10759–10764.

Pieters, J., 2008. *Mycobacterium tuberculosis* and the macrophage: maintaining a balance. *Cell Host and Microbe*, 3(6), pp.399-407.

Proft, T., and Baker, E. N. (2009). Pili in Gram-negative and Gram-positive bacteria—structure, assembly and their role in disease. *Cellular and Molecular Life Sciences*, 66(4), 613.

Qamra, R., Srinivas, V., and Mande, S. C. (2004). *Mycobacterium tuberculosis GroEL* homologues unusually exist as lower oligomers and retain the ability to suppress aggregation of substrate proteins. *Journal of Molecular Biology*, 342(2), 605-617.

Ragas A, Roussel L, Puzo G, and Riviere M (2007) The *Mycobacterium tuberculosis* cell-surface glycoprotein Apa as a potential adhesin to colonize target cells via the innate immune system pulmonary C-type lectin surfactant protein A. *J Biol Chem* 282:5133-42.

Ramsugit, S., Guma, S., Pillay, B., Jain, P., Larsen, M. H., Danaviah, S. and Pillay, M. 2013. Pili contribute to biofilm formation *in vitro* in *Mycobacterium tuberculosis*. *Antonie Van Leeuwenhoek*, 104, 725-735.

Ramsugit, S. and Pillay, M. 2014. *Mycobacterium tuberculosis* pili promote adhesion to and invasion of THP-1 macrophages. *Japanese Journal of Infectious Diseases*, 67, 476-478.

Ramsugit, S., Pillay, B. and Pillay, M. 2016. Evaluation of the role of Mycobacterium tuberculosis pili (MTP) as an adhesin, invasin, and cytokine inducer of epithelial cells. *The Brazilian Journal of Infectious Diseases*, 20, 160-165.

Rangaka, M.X., Wilkinson, K.A., Glynn, J.R., Ling, D., Menzies, D., Mwansa-Kambafwile, J., Fielding, K., Wilkinson, R.J. and Pai, M., 2012. Predictive value of interferon-γ release assays for incident active tuberculosis: a systematic review and meta-analysis. *The Lancet Infectious Diseases*, 12(1), pp.45-55.

Ratliff, T.L., McGARR, J.A., Abou-zeid, C., Rook, G.A., Stanford, J.L., Aslanzadeh, J. and Brown, E.J., 1988. Attachment of mycobacteria to fibronectin-coated surfaces. *Microbiology*, 134(5), pp.1307-1313.

Rawat, R. and Monu, M.L. 2015. Adhesion molecules A potent surface marker of *Mycobacterium* play key role in host-pathogen interaction and pathogenesis. *Adv Res J Biochem Biotechnol*, 2, pp.41-6.

Reedoy, K.S., 2020. *Mycobacterium tuberculosis* pili (MTP) modulates pathogen and host metabolomic changes in an A549 epithelial cell model of infection (Masters dissertation).

Romain, F., Horn, C., Pescher, P., Namane, A., Riviere, M., Puzo, G., Barzu, O. and Marchal, G., 1999. Deglycosylation of the 45/47-kilodalton antigen complex of *Mycobacterium tuberculosis* decreases its capacity to elicit *in vivo* or *in vitro* cellular immune responses. *Infection and Immunity*, 67(11), pp.5567-5572.

Riojas, M.A., McGough, K.J., Rider-Riojas, C.J., Rastogi, N. and Hazbón, M.H., 2018. Phylogenomic analysis of the species of the *Mycobacterium tuberculosis* complex demonstrates that *Mycobacterium africanum*, *Mycobacterium bovis*, *Mycobacterium caprae*, *Mycobacterium microti* and *Mycobacterium pinnipedii are* later heterotypic synonyms of *Mycobacterium tuberculosis*. *International Journal of Systematic and Evolutionary Microbiology*, *68*(1), pp.324-332.

Roy, A., Eisenhut, M., Harris, R., Rodrigues, L., Sridhar, S., Habermann, S., Snell, L., Mangtani, P., Adetifa, I. and Lalvani, A. 2014. Effect of BCG vaccination against *Mycobacterium tuberculosis* infection in children: systematic review and meta-analysis. *BMJ*, 349, g4643.

Ryndak, M.B., Singh, K.K., Peng, Z. and Laal, S., 2015. Transcriptional profile of *Mycobacterium tuberculosis* replicating in type II alveolar epithelial cells. *PloS One*, 10(4), p. e0123745.

Saibil, H., 2013. Chaperone machines for protein folding, unfolding and disaggregation. *Nature reviews Molecular Cell Biology*, 14(10), pp.630-642.

Sasindran, S.J. and Torrelles, J.B., 2011. *Mycobacterium tuberculosis* infection and inflammation: what is beneficial for the host and for the bacterium. *Frontiers in Microbiology*, 2, p.2.

Satchidanandam, V., Kumar, N., Biswas, S., Jumani, R. S., Jain, C., Rani, R., and Sridharan, A. (2016). The Secreted Protein Rv1860 of *Mycobacterium tuberculosis* Stimulates Human Polyfunctional CD8+ T Cells. *Clin. Vaccine Immunol*., 23(4), 282-293.

Schlipköter, U. and Flahault, A., 2010. Communicable diseases: achievements and challenges for public health. *Public Health Reviews*, 32(1), pp.90-119.

Scriba, T.J., Netea, M.G. and Ginsberg, A.M., 2020, August. Key recent advances in TB vaccine development and understanding of protective immune responses against *Mycobacterium tuberculosis*. *In Seminars in Immunology* (Vol. 50, p. 101431). Academic Press.

Shahar, A., Melamed-Frank, M., Kashi, Y., Shimon, L., and Adir, N. (2011). The dimeric structure of the Cpn60. 2 chaperonin of *Mycobacterium tuberculosis* at 2.8 Å reveals possible modes of function. *Journal of Molecular Biology*, 412(2), 192-203.

Sharma, A., Rustad, T., Mahajan, G., Kumar, A., Rao, K.V., Banerjee, S., Sherman, D.R. and Mande, S.C., 2016. Towards understanding the biological function of the unusual chaperonin Cpn60. 1 (GroEL1) of *Mycobacterium tuberculosis*. *Tuberculosis*, 97, pp.137-146.

Sia, J.K. and Rengarajan, J., 2019. Immunology of *Mycobacterium tuberculosis* infections. *Microbiology Spectrum*, 7(4), pp.7-4.

Silva Miranda, M., Breiman, A., Allain, S., Deknuydt, F. and Altare, F., 2012. The tuberculous granuloma: an unsuccessful host defence mechanism providing a safety shelter for the bacteria. *Clinical and Developmental Immunology*, 2012.

Sinn, H.W., Elzey, B.D., Jensen, R.J., Zhao, X., Zhao, W. and Ratliff, T.L., 2008. The fibronectin attachment protein of bacillus Calmette-Guerin (BCG) mediates antitumor activity. *Cancer Immunology, Immunotherapy*, 57(4), pp.573-579.

Si-Tahar, M., Touqui, L. and Chignard, M., 2009. Innate immunity and inflammation–two facets of the same anti-infectious reaction. *Clinical & Experimental Immunology*, 156(2), pp.194-198.

Smart, I., Goecke, T., Ramm, R., Petersen, B., Lenz, D., Haverich, A., Niemann, H. and Hilfiker, A., 2021. Dot blots of solubilized extracellular matrix allow quantification of human antibodies bound to epitopes present in decellularized porcine pulmonary heart valves. *Xenotransplantation*, 28(1), p.e12646.

Solodovnikova, V., Kumar, A.M., Hurevich, H., Sereda, Y., Auchynka, V., Katovich, D., Klimuk, D., Skrahin, A., Setkina, S., Charnysh, I. and Yedilbayev, A., 2021. Effectiveness and safety of delamanid-or bedaquiline-containing regimens among children and adolescents with multidrug resistant or extensively drug resistant tuberculosis: A nationwide study from Belarus, 2015-19. *Monaldi Archives for Chest Disease*, 91(1).

Stewart, G.R., Snewin, V.A., Walzl, G., Hussell, T., Tormay, P., O'Gaora, P., Goyal, M., Betts, J., Brown, I.N. and Young, D.B., 2001. Overexpression of heat-shock proteins reduces survival of *Mycobacterium tuberculosis* in the chronic phase of infection. *Nature Medicine*, 7(6), pp.732-737.

Stokes, R.W., Norris-Jones, R., Brooks, D.E., Beveridge, T.J., Doxsee, D. and Thorson, L.M., 2004. The glycan-rich outer layer of the cell walls of *Mycobacterium tuberculosis* acts as an antiphagocytic capsule limiting the association of the bacterium with macrophages. *Infection and Immunity*, *72*(10), pp.5676-5686.

Stokes, R.W., 2013. *Mycobacterium tuberculosis* chaperonin 60 paralogues contribute to virulence in tuberculosis. In *Moonlighting Cell Stress Proteins in Microbial Infections* (pp. 123-141). Springer, Dordrecht.

Stucki, D., Brites, D., Jeljeli, L., Coscolla, M., Liu, Q., Trauner, A., Fenner, L., Rutaihwa, L., Borrell, S., Luo, T. and Gao, Q., 2016. *Mycobacterium tuberculosis* lineage 4 comprises globally distributed and geographically restricted sublineages. *Nature Genetics*, 48(12), pp.1535-1543.

Tack, I., Dumicho, A., Ohler, L., Shigayeva, A., Bulti, A.B., White, K., Mbatha, M., Furin, J. and Isaakidis, P., 2021. Safety and effectiveness of an all-oral, bedaquiline-based, shorter treatment regimen for rifampicin-resistant tuberculosis in high human immunodeficiency virus (HIV) burden rural South Africa: A retrospective cohort analysis. *Clinical Infectious Diseases*, 73(9), pp. e3563-e3571.

Tait, D.R., Hatherill, M., Van Der Meeren, O., Ginsberg, A.M., Van Brakel, E., Salaun, B., Scriba, T.J., Akite, E.J., Ayles, H.M., Bollaerts, A. and Demoitié, M.A., 2019. Final analysis of a trial of M72/AS01E vaccine to prevent tuberculosis. *New England Journal of Medicine*, 381(25), pp.2429-2439.

Talip, B.A., Sleator, R.D., Lowery, C.J., Dooley, J.S. and Snelling, W.J., 2013. An update on global tuberculosis (TB). *Infectious Diseases: Research and Treatment*, 6, pp. IDRT-S11263.

Tameris, M.D., Hatherill, M., Landry, B.S., Scriba, T.J., Snowden, M.A., Lockhart, S., Shea, J.E., McClain, J.B., Hussey, G.D., Hanekom, W.A. and Mahomed, H., 2013. Safety and efficacy of MVA85A, a new tuberculosis vaccine, in infants previously vaccinated with BCG: a randomised, placebo-controlled phase 2b trial. *The Lancet*, 381(9871), pp.1021-1028.

Teimouri, A., Modarressi, M.H., Shojaee, S., Mohebali, M., Rezaian, M. and Keshavarz, H., 2019. Development, optimization, and validation of an in-house Dot-ELISA rapid test based on SAG1 and GRA7 proteins for serological detection of *Toxoplasma gondii* infections. *Infection and Drug Resistance*, 12, p.2657.

Telford, J.L., Barocchi, M.A., Margarit, I., Rappuoli, R. and Grandi, G., 2006. Pili in gram-positive pathogens. *Nature Reviews Microbiology*, 4(7), pp.509-519.

Theron, G., Peter, J., Richardson, M., Warren, R., Dheda, K. and Steingart, K.R., 2016. GenoType® MTBDRsl assay for resistance to second-line anti-tuberculosis drugs. *Cochrane Database of Systematic Reviews*, (9).

Thillai, M., Pollock, K., Pareek, M. and Lalvani, A., 2014. Interferon-gamma release assays for tuberculosis: current and future applications. *Expert Review of Respiratory Medicine*, 8(1), pp.67-78.

Todar, K. 2012. *Tuberculosis- Online Book of Bacteriology* [Online] Available: http://textbookofbacteriology.net/tuberculosis.html.

Trunz, B.B., Fine, P.E.M. and Dye, C., 2006. Effect of BCG vaccination on childhood tuberculous meningitis and miliary tuberculosis worldwide: a meta-analysis and assessment of cost-effectiveness. *The Lancet*, 367(9517), pp.1173-1180.

Tsara, V., Amfilochiou, A., Papagrigorakis, M. J., Georgopoulos, D., Liolios, E., Alexopoulou, C., and Vilos, G. (2009). Guidelines for diagnosing and treating sleep related breathing disorders in adults and children (Part 2: treatment). *Hippokratia*, 13(4), 247.

Tsolaki, A.G., Gagneux, S., Pym, A.S., Goguet de la Salmoniere, Y.O.L., Kreiswirth, B.N., Van Soolingen, D. and Small, P.M., 2005. Genomic deletions classify the Beijing/W strains as a distinct genetic lineage of *Mycobacterium tuberculosis*. *Journal of Clinical Microbiology*, 43(7), pp.3185-3191.

Vargas-Romero, F., Guitierrez-Najera, N., Mendoza-Hernández, G., Ortega-Bernal, D., Hernández-Pando, R. and Castañón-Arreola, M., 2016. Secretome profile analysis of hypervirulent *Mycobacterium tuberculosis* CPT31 reveals increased production of EsxB and proteins involved in adaptation to intracellular lifestyle. *FEMS Pathogens and Disease*, 74(2), p.ftv127.

Vassall, A., Siapka, M., Foster, N., Cunnama, L., Ramma, L., Fielding, K., McCarthy, K., Churchyard, G., Grant, A. and Sinanovic, E., 2017. Cost-effectiveness of Xpert MTB/RIF for tuberculosis diagnosis in South Africa: a real-world cost analysis and economic evaluation. *The Lancet Global Health*, 5(7), pp. e710-e719.

Veyron-Churlet, R., Dupres, V., Saliou, J.M., Lafont, F., Raze, D. and Locht, C., 2018. Rv0613c/MSMEG_1285 interacts with HBHA and mediates its proper cell-surface exposure in mycobacteria. *International Journal of Molecular Sciences*, 19(6), p.1673.

Voelkel, T., Andresen, C., Unger, A., Just, S., Rottbauer, W., and Linke, W. A. (2013). Lysine methyltransferase Smyd2 regulates Hsp90-mediated protection of the sarcomeric titin springs and cardiac function. Biochimica et Biophysica Acta (BBA)-*Molecular Cell Research*, 1833(4), 812-822.

Viljoen, A., Alsteens, D. and Dufrêne, Y., 2020. Mechanical forces between mycobacterial antigen 85 complex and fibronectin. *Cells*, 9(3), p.716.

Voss, G., Casimiro, D., Neyrolles, O., Williams, A., Kaufmann, S. H., McShane, H., and Fletcher, H. A. (2018). *Progress and challenges in TB vaccine Development*. *F1000Research*, 7.

Vyas, N. K., Vyas, M. N., and Quiocho, F. A. (2003). Crystal structure of *M. tuberculosis* ABC phosphate transport receptor: specificity and charge compensation dominated by ion-dipole interactions. *Structure*, 11(7), 765-774.

Wallis, R. S., Kim, P., Cole, S., Hanna, D., Andrade, B. B., Maeurer, M., ... & Zumla, A. (2013). Tuberculosis biomarkers discovery: developments, needs, and challenges. *The Lancet Infectious Diseases*, 13(4), 362-372.

Wallis, R. S., and Peppard, T. (2015). Early biomarkers and regulatory innovation in multidrug-resistant tuberculosis. *Clinical Infectious Diseases*, 61(suppl_3), S160-S163.

Wang, Z., Gerstein, M. and Snyder, M., 2009. RNA-Seq: a revolutionary tool for transcriptomics. *Nature Reviews Genetics*, 10(1), pp.57-63.

Weiss, G. and Schaible, U.E., 2015. Macrophage defense mechanisms against intracellular bacteria. *Immunological Reviews*, 264(1), pp.182-203.

Welin, A. (2011). *Survival strategies of Mycobacterium tuberculosis inside the human macrophage* (Doctoral dissertation, Linköping University Electronic Press).

Wiker, H. G., Sletten, K., Nagai, S., and Harboe, M. (1990). Evidence for three separate genes encoding the proteins of the mycobacterial antigen 85 complex. *Infection and Immunity*, 58(1), 272-274.

Wilkie, M., Satti, I., Minhinnick, A., Harris, S., Riste, M., Ramon, R.L., Sheehan, S., Thomas, Z.R.M., Wright, D., Stockdale, L. and Hamidi, A., 2020. A phase I trial evaluating the safety and immunogenicity of a candidate tuberculosis vaccination regimen, ChAdOx1 85A prime–MVA85A boost in healthy UK adults. *Vaccine*, 38(4), pp.779-789

Wilkinson, K.A., Newton, S.M., Stewart, G.R., Martineau, A.R., Patel, J., Sullivan, S.M., Herrmann, J.L., Neyrolles, O., Young, D.B. and Wilkinson, R.J., 2009. Genetic determination of the effect of post-translational modification on the innate immune response to the 19 kDa lipoprotein of *Mycobacterium tuberculosis*. *BMC Microbiology*, 9(1), pp.1-10.

Wong, G., & Gao, G. F. (2017). An mRNA-based vaccine strategy against Zika. *Cell Research*, 27(9), 1077.

World Health Organization. Global Tuberculosis control: surveillance, planning, Financing. Geneva. 2002; WHO/CDS/TB/2002.295.

World Health Organization, (2010). *World Health Statistics 2010*. World Health Organization.

World Health Organization. (2014) . Global tuberculosis report 2014. World Health Organization.

World Health Organization 2016. Global tuberculosis report 2015 [Online]. Available: https://www.who.int/tb/publications/global_report/gtbr2016_executive_summary.pdf?ua [Accessed].

World Health Organization. (2018). Global Tuberculosis Report 2018. World Health Organization.

World Health Organization, 2019. Global tuberculosis report 2018 [Online]. Available: https://www.who.int/teams/global-tuberculosis-programme/tb-reports/global-report-2019 [Accessed].

World Health Organization, 2020. Global tuberculosis report 2021. Geneva: World Health Organization; 2021. Licence: CC BY-NC-SA 3.0 IGO.

World Health Organization, Global Tuberculosis Report 2021. Geneva: World Health Organization. (2021).

Yamada, N., Ozawa, S., Kageyama, N. and Miyano, H., 2004. Detection and quantification of protein residues in food grade amino acids and nucleic acids using a Dot-Blot fluorescent staining method. *Journal of Agricultural and Food Chemistry*, 52(17), pp.5329-5333.

Yeremeev, V.V., Lyadova, I.V., Nikonenko, B.V., Apt, A.S., Abou-Zeid, C., Inwald, J. and Young, D.B., 2000. The 19-kD antigen and protective immunity in a murine model of tuberculosis. *Clinical and Experimental Immunology*, 120(2), pp.274-279.

Zumla, A., Nahid, P. and Cole, S.T., 2013. Advances in the development of new tuberculosis drugs and treatment regimens. *Nature Reviews Drug Discovery*, 12(5), pp.388-404.

CHAPTER 2: The role of specific adhesins in the regulation of other adhesin genes associated with the pathogenicity of *Mycobacterium tuberculosis*.

Mthembu, J. N*[1]*., *Senzani, S*[1] *and Pillay, M*[1]**.*

[1]Medical Microbiology, School of Laboratory Medicine and Medical Sciences, College of Health Sciences, University of KwaZulu-Natal, 1st floor, Doris Duke Medical Research Institute, Congella, Private Bag 7, Durban, 4013, South Africa.
*Corresponding author
Prof. Manormoney Pillay, Ph.D.
Medical Microbiology, School of Laboratory Medicine and Medical Sciences, College of Health Sciences, University of KwaZulu-Natal, 1st floor Doris Duke Medical Research Institute, Congella, Private Bag 7, Durban, 4013, South Africa.
Tel: +2731 260 4395
E-mail addresses: solwazikamvelase@gmail.com (Mthembu, J.N); senzanis@ukzn.ac.za (Senzani, S); pillayc@ukzn.ac.za (Pillay, M).

2.1 Abstract

Adhesins are essential for the survival of *M. tuberculosis* because they initiate and sustain host-pathogen interactions. The heparin-binding hemagglutinin adhesin (HBHA) and the *M. tuberculosis* curli pili (MTP) are well-studied adhesins. The MTP adhesin functions in the adhesion and invasion of host cells as well as the development of biofilms. The HBHA facilitates the spread of *M. tuberculosis* from the site of infection. L, D-transpeptidases (Ldts), which bind to laminin and fibronectin, are encoded by *Rv0309*. Currently, there is no existing data on the role of adhesins on regulation of other adhesins. The current study sought to determine the role of three adhesins, MTP, HBHA, and Rv0309, on the regulation of other adhesins that facilitate the binding and infection of *M. tuberculosis* in THP-1 cells. *M. tuberculosis* wild-type (WT), *Rv0309* mutant, single and double deletion of HBHA, and MTP mutants, and their respective complemented strains were used to infect the THP-1 cells. Real-time quantification PCR was used to study gene expression of intracellular *M. tuberculosis* RNA extracted from the THP-1 infected cells at 4-h and 24-h post-infection. Deletion of *mtp* gene resulted in a decrease in the expression of adhesin genes in the mutant: *Rv3763, Rv0934, Rv0350, Rv1860, Rv3804, Rv3660,* and *Rv0440* at 24-h time. Deletion of *hbhA* induced the expression of all genes in the mutant to compensate for the loss of *hbhA* gene. Double deletion of *mtp-hbhA* induced a low expression of the genes. *Rv0309* deletion resulted in the upregulation of the genes. Thus, this study demonstrated that the adhesins, MTP, HBHA and Rv0309 are important in the regulation of the expression of other adhesin genes associated with macrophage infection. The deletion of these three genes affected the genes that are associated with the virulence and survival of *M. tuberculosis.*

2.2 Introduction

The bacillus *Mycobacterium tuberculosis* (*M. tuberculosis*) is the causative agent of the disease tuberculosis (TB). Tuberculosis persists as the key cause of mortalities globally, with an estimate of 1.3 million deaths in 2020 (WHO, 2021). Globally, close to 10 million people are infected with TB (WHO, 2021). Tuberculosis persists in countries with poor resources, where over 95% of the new TB cases and deaths are reported, with the highest-burden recorded in South-East Asia and Africa (WHO, 2021). The lack of rapid diagnostics, effective vaccines, and drugs contributes to the high number of deaths recorded every year. Information relating to how the bacillus attacks and invades host cells is required to identify new biomarkers to be used in vaccine and drug development.

Mycobacterium. tuberculosis colonizes and infects host cells due to its ability to adhere to host cellular structures. This is facilitated by adhesins which are the primary point of contact between the host cell and the pathogen (Pizarro-Cerdá and Cossart, 2006; Gerlach & Hensel, 2007). This makes adhesins potentially suitable biomarkers (Kline *et al*., 2009, Kumar *et al.*, 2013). Adhesion allows *M. tuberculosis* and other pathogenic organisms to colonize the host cells, thus creating a suitable environment in which the pathogen grows, causing the release of virulence factors and toxins that result in infection (Kline *et al*., 2009). Adhesins not only facilitate host colonization, but also contribute to antibiotic resistance and reduce host clearance through biofilm formation (Stones and Krachler, 2015). In addition to this, bacterial adherence to the host not only results in a change in the signalling of bacterial cells, but also leads to a change in host signalling (Stones and Krachler, 2015). These factors promote the spread of the pathogen and evasion of host immune response (Stones and Krachler, 2015).

Mycobacterium. tuberculosis adheres to and invades host cells such as alveolar epithelial cells and macrophages (Rivas-Santiago *et.al*, 2005; Fontán *et al*., 2008). Macrophages are the main effector cells that have a defensive role against *M. tuberculosis* (Geissmann *et al*., 2010). This defence role is initiated by phagocytosis, extracellular killing, and antigen presentation to lymphocytes (Fenton and Vermeulen, 1996; Pieters, 2008). Several studies have investigated *M. tuberculosis* infection within macrophage cells (Iona *et al*., 2012; Ramsugit and Pillay, 2014; Johnson and Abramovitch, 2015; Zhang *et al*., 2017; Park *et al*., 2019; Zhang *et al*., 2021). Mehta *et al* (1996) showed that *M. tuberculosis* invaded macrophages more effectively than alveolar epithelial cells. In contrast, intracellular replication of *M. tuberculosis* was much greater in the epithelial cells compared to the macrophages (Mehta *et al*., 1996). As a result,

epithelial cells may provide a less hostile intracellular environment for pathogens than macrophages.

In order to understand the host-pathogen interaction, several *M. tuberculosis* proteins have been studied and classified as adhesins (Menozzi *et al.,* 1998; Diaz-Silvestre *et al*., 2005; Alteri *et al*., 2007, Kumar *et al.,* 2013). There is a need to understand their functional role in the pathogenesis of TB. Some adhesin molecules facilitate binding to macrophages (Squeglia *et al*., 2018). This includes the Mycobacterial 19-Kilodalton Glycolipoprotein Antigen (LpqH also known as 19-kilodalton (19-kDa) antigen) (Esparza *et.al.,* 2015), *M. tuberculosis* Phosphate-binding protein (PstS-1) (Esparza *et.al.,* 2015), Chaperone 60.2 (Cpn 60.2) (Hickey *et al*., 2010), Alanine and proline-rich antigenic glycoprotein (Apa) (Esparza *et.al*., 2015), *M. tuberculosis* curli pili (MTP) (Ramsugit and Pillay, 2014) and antigen 85 complexes (Esparza *et.al*., 2015). Alteri *et al.,* (2007) showed for the first time that *M. tuberculosis* produced two pili types i.e. type IV and curli pili.

Using *mtp* gene knockout mutant and complemented *M. tuberculosis* strains, MTP was shown to promote adhesion and invasion of macrophages (Ramsugit and Pillay, 2014) and epithelial cells (Ramsugit *et al*., 2016). The significance of the two major adhesins MTP and HBHA in promoting growth and biomass formation, as well as in adhesion and invasion of A549 epithelial cells, were demonstrated using single *mtp* and *hbhA*, as well as *mtp-hbhA* double knockout mutants (Govender, 2018). Global host transcriptomics revealed the immunomodulatory effect of MTP/HBHA in A549 pulmonary epithelial cells, THP-1 macrophages, and mouse infection models (Dlamini, 2016, Kuvar, 2016; Nyawo, 2016; Moodley, 2018; Rampersad, 2019; Balgobin 2021). Global bacterial transcriptomics identified major perturbations in central carbon metabolism, ATP synthesis, cell wall biosynthesis and processes in the absence of MTP and HBHA (Naidoo, 2021). Metabolomics elucidated the impact of MTP and HBHA in modulating both pathogen and host metabolic signatures (Reedoy *et al*., 2020, Ashokcoomar *et al*., 2020). Muniram (2018) demonstrated that L, D-transpeptidase encoded by the gene *Rv0309* contributed to biofilm formation, and cell division during bacterial growth. These findings imply that the adhesins HBHA, MTP and Rv0309 could be powerful targets for therapeutic interventions.

The use of multiple adhesins by *M. tuberculosis* in adhesion and invasion of the host cells is crucial to the global success of *M. tuberculosis*. Much progress has been made in identifying and characterizing the contribution made by the specific adhesins used by *M. tuberculosis*

during the infection of host cells. However, little is known on the ability of *M. tuberculosis*, in the absence of major adhesins, to regulate the expression of other specific adhesins as compensatory mechanisms to support adhesion and infection. This knowledge would be crucial when designing anti-adhesin compounds as adjunctive therapy or vaccine candidates. Therefore, using *in vitro* infection assays with gene knockout mutants, real-time quantitative PCR (RT-qPCR) and a western blot assay, this study aimed to elucidate the role of selected adhesins genes (*mtp, hbhA* and *Rv0309*) in regulating other adhesins during TB pathogenesis.

2.3 Materials and methods

2.3.1 Ethics Approval

The study's ethics approval was acquired from the Biomedical Research Ethics Committee (BREC), University of KwaZulu-Natal (Reference number: BREC/00001210/2020).

2.3.2 Bacterial strains and growth conditions

All experiments with *M. tuberculosis* were conducted in a Biosafety Level II Laboratory in the Discipline of Medical Microbiology, Medical School Campus, University of KwaZulu-Natal. The *M. tuberculosis* strains listed in Table 2.1 were used for *in vitro* infection assays in THP-1 cells. The *M. tuberculosis* wild-type V9124, a clinical isolate of the Fl5/LAM4/KZN (KZN) family, isolated from the Tugela Ferry (KwaZulu-Natal, South Africa) and its gene-deficient and gene-proficient strains were obtained from the culture collection of Medical Microbiology (University of KwaZulu-Natal). Briefly, gene-deficient strains were previously constructed in wild-type (WT) V9124 by specialized transduction in which the *mtp, hbhA, Rv0309* genes, were replaced with allelic exchange substrates respectively (Bardarov *et al.*, 2002). The knocked-out genes were complemented by electro transformation with pMV261 which is a non-integrating plasmid, containing the knocked-out genes, using the protocol described by Bardarov *et al.* (2002). The deletion mutant, complemented and wild-type strains were confirmed by Polymerase Chain Reaction (PCR) using hygromycin, kanamycin, and gene-specific primers respectively.

The bacterial strains were retrieved from the –80 °C freezer and thawed at (25 °C ± 5 °C). Following this, 100 µL of the suspension of each strain was cultured in 10 mL of Middlebrook 7H9 broth (Difco Laboratories, Becton, Dickinson and Company, Sparks, USA), supplemented with 10 % of a mixture of oleic acid, albumin, dextrose, catalase (OADC) (Becton, Dickinson and Company, Sparks, USA) and 0.5 % of glycerol (Sigma-Aldrich, St. Louis, MO, USA). The broth was also supplemented with 0.25 % of Tween-80 (Sigma-Aldrich, St. Louis, MO, USA). The broth cultures were incubated at 37 °C in a shaking incubator (I-26 Shaking Incubator, New Brunswick Scientific, Canada) at 1 × g for 7 days until they reached an optical density $(OD)_{600nm}$ = 1.0 (Lightwave II, Biochrom, Cambridge, UK).

Table 2.1: Bacterial strains used in this study.

***M. tuberculosis* strains**	**Source**
V9124 WT	Gandhi *et al*., 2006
Δ*mtp* mutant	Ramsugit *et al*., 2013
mtp-complemented	Ramsugit *et al*., 2013
Δ*hbhA* knockout mutant	Govender *et al.*, PhD thesis 2018
hbhA complemented	Govender *et al.*, PhD thesis 2018
Δ*mtp-hbhA* mutant	Govender *et al*., PhD thesis 2018
mtp-hbhA complemented	Muniram, 2018
Δ*Rv0309* mutant	Muniram, Masters dissertation, 2018
Rv0309 complemented	Muniram, Masters dissertation, 2018

WT: wild-type; Δ*mtp*: *mtp*-gene knockout mutant; Δ*hbhA*: *hbhA*-gene knockout mutant; Δ*mtp-hbhA*: *mtp-hbhA* gene knockout mutant.

2.3.3 The revival of frozen THP-1 cells

The THP-1 monocytic cell line (ATCC TIB-202, kindly donated by Prof Thumbi Ndung'u, HIV Pathogenesis Unit, UKZN) was used in this study. A volume of 1 mL of thawed THP-1 was added to 10 mL of R10 medium (RPMI 1640 medium with 2 mM L-glutamine, Lonza, Rockland, ME, USA) supplemented with 10 % (v/v) Fetal Bovine Serum (Biowest, Kansas City, MO, USA). The cells were revived in a 25 mL tissue culture flask (NEST Biotechnology, Shanghai, China) and incubated in a humidified 37 °C incubator with 5 % CO_2 (Shel Lab CO_2 Incubator, Cornelius, OR, USA) for 7 days. R10 media (RPMI 1640 medium with 2 mM L-glutamine, Lonza, Rockland, ME, USA) supplemented with 10 % (v/v) Fetal Bovine Serum (Biowest, Kansas City, MO, USA) was changed after 7 days, and cells were checked for viability using a microscope. The cells were then sub cultured in 250 mL flasks (NEST Biotechnology, Shanghai, China) until they reached a confluence of 80 % - 90 %.

2.3.4 Enumeration and seeding of THP-1 cells

THP-1 cells were transferred to 50 mL conical tubes (Nest Biotechnology, Jiangsu, China) and centrifuged (Mikro 200R, Hettich Zentrifugen, Tuttlingen, Germany) at 200 × *g* for 10 minutes (min). The pellets were then re-suspended in 5 mL R10 and combined into one 50 mL conical tube (Nest Biotechnology, Jiangsu, China). A cell count was determined using a haemocytometer (Neubauer 1/10 mm, Boeco, Germany) and the trypan blue (Lonza, Basel, Switzerland) exclusion assay (Strober, 1997). A coverslip was placed on the hemocytometer and an aliquot of the cell suspension (20 µL cells, 40 µL of Phosphate-buffered saline (PBS) (Sigma-Aldrich, St. Louis, MO, USA), and 60 µL trypan blue (Lonza, Walkersville, USA) was applied by capillary action. The Neubauer haemocytometer chamber (Neubauer 1/10 mm, Boeco, Germany) was placed under the microscope Nikon eclipse E200-F (Nikon instruments, USA) for the viewing of the cells over a grid. Cells in four big squares (each containing 16 small squares) were viewed and counted using the formula below. The viable cells were identified as white cells and were counted. These cells appeared white under the light microscope Nikon eclipse E200-F (Nikon instruments, USA) due to their intact cell membrane that excluded the trypan blue dye. The blue cells were considered to be dead cells. The required volume of medium, THP-1 cells and phorbol 12-myristate 13-acetate (PMA) (50 ng/mL) (Sigma-Aldrich, St. Louis, MO, USA) was calculated and added to the number of flasks required. The following formula was used to determine the THP-1 cell volume required: concentration (5×10^5) x final volume (20 mL) / THP-1 cell count. The formula to determine the amount of medium required is as follows: 20 mL – THP-1 cell volume required – 1 mL (i.e., the PMA volume required). The flasks were incubated overnight at 37 ºC in 5 % CO_2 (Shel Lab CO_2 Incubator, Cornelius, OR, USA) to enable the differentiation of monocytes into macrophage-like cells. The cell line was used between passages 6 and 7.

$$\textbf{Cells/mL} = \frac{(\text{Total number of cells} \times \text{dilution factor}(6) \times 10^{4}}{\text{Number of quadrants}}$$

2.3.5 Infection of THP-1 cells with M. tuberculosis strains

The differentiated THP-1 cells were transferred to the BSL2+ laboratory and all the infection steps were carried out in the class II safety cabinet. Bacterial cultures (OD_{600nm} = 1) were centrifuged at 2000 × *g* for 20 min (Heraeus Multifuge 3S-R Centrifuge; Thermo Scientific, Ulm, Germany). The pellets were then diluted with R10 to OD_{600nm} = 1 equivalent to l ×10^8 colony-forming units per mL (CFU mL^{-1}) (Larsen *et al*., 2007) Macrophage monolayers were infected with the bacterial suspensions at a multiplicity of infection (MOI) of 5:1 (5 bacteria/1 cell). Uninfected controls contained only macrophages with R10. The flasks (NEST Biotechnology, Shanghai, China) were incubated at 37 ºC in 5 % CO_2 (Shel Lab CO_2 Incubator, Cornelius, OR, USA) and 95 % humidity for the respective times, 4-h and 24-h. At each time point, the flasks were washed with 10 mL PBS (Sigma-Aldrich, St. Louis, MO, USA). The 4-h flasks were lysed with 10 mL of 0.1 % Triton X-100 (Sigma-Aldrich, St. Louis, MO, USA), for CFU's, pathogen RNA and bacterial protein. For the 24-h flasks, after 4-h incubation period, extracellular bacteria were removed by washing twice with PBS (Sigma-Aldrich, St. Louis, MO, USA) and a fresh 20 mL R10 media (RPMI 1640 medium with 2 mM L-glutamine, Lonza, Rockland, ME, USA) supplemented with 10 % (v/v) Fetal Bovine Serum (Biowest, Kansas City, MO, USA) was added. The flasks (NEST Biotechnology, Shanghai, China) were incubated (Shel Lab CO_2 Incubator, Cornelius, OR, USA) at 37 ˚C, 5 % CO_2 and 95 % humidity for the 24-h time points and processed the following day.

2.3.6 Determination of Colony Forming Units/mL

To determine the number of CFU mL^{-1} and to confirm the MOI, 10-fold serial dilutions of the bacterial inocula were plated onto Middlebrook 7H11 agar plates (Difco, Becton-Dickinson, Franklin Lakes, NJ, USA), supplemented with 10 % of a mixture of OADC (Becton, Dickinson and Company, Sparks, USA) and 0.5 % glycerol (Sigma-Aldrich, St. Louis, MO, USA). In order to quantify the internalised bacteria at both time points after infection, macrophages were washed with 10 mL PBS (Sigma-Aldrich, St. Louis, MO, USA). Ten mL of 0.1 % Triton X-100 (Sigma-Aldrich, St. Louis, MO, USA) were added to the flasks and incubated for 20 min to lyse the adherent macrophages. The lysed macrophages were serially diluted 10-fold in 7H9 broth and plated in triplicate onto 7H11 agar plates. All plates were incubated in an incubator (Shel Lab CO_2 Incubator, Cornelius, OR, USA) at 37 ºC for 3 weeks, after which the number of colonies were counted to determine the number of CFUs/mL.

2.3.7 Extraction of intracellular pathogen RNA from the infected THP-1 Cells (Larson et al. (2007)

At the end of incubation, media from the bacterial RNA flasks was discarded and the monolayers were washed with 20 mL PBS (Sigma-Aldrich, St. Louis, MO, USA) by gently swirling. The PBS (Sigma-Aldrich, St. Louis, MO, USA) was discarded and washing step was repeated twice for the 4-h time point and once for the 24-h interval. The cells were lysed with 10 mL of 0.1 % Triton-X 100 (Sigma-Aldrich, St. Louis, MO, USA) and incubated (I-26 Shaking Incubator, New Brunswick Scientific, Canada) horizontally at 37 °C with shaking at 1 × g for 20 min. The lysate was transferred into 15 mL centrifuge tubes (Nest Biotechnology, Jiangsu, China) and centrifuged at 2 000 × *g* for 20 min at 4 °C (Heraeus Multifuge 3S-R Centrifuge; Thermo Scientific, Ulm, Germany). The supernatant was discarded, and the pellet was resuspended in 1 mL of TriZol (Ambion, Life Technologies, USA) in O-ring tubes (Sigma-Aldrich, St. Louis, MO, USA) containing 100 µL of 0.1 µm zirconia beads (BioSpec Products, Oklahoma, USA). The tubes were placed at room temperature (25 °C ± 5 °C) for 15 min. The samples were stored at -80 °C until extraction.

Stored samples were placed on ice and thawed for 15 min. The cells were lysed in a Precellys 24 lysis and homogenisation machine (Bertin Technologies, Montigny-le-Bretonneux, France) at 6 800 rpm for 90 s at 3 cycles with 2 min pause. In between cycles, the samples were placed on ice for 2 min. After the lysis step, samples were placed at room temperature (25 °C ± 5 °C) for 5 min. Thereafter, 200 µL of chloroform (Sigma-Aldrich, St. Louis, MO, USA) was added to each sample and the 2 mL microcentrifuge tubes (Eppendorf tube, Merck) were vigorously mixed inverting by hand for 15 s.

The tubes were incubated at room temperature (25 °C ± 5 °C) for 2-3 min and centrifuged (Mikro 200R, Hettich Zentrifugen, Tuttlingen, Germany) at 26 295 × *g* for 15 min at 4 °C. The top aqueous layer was transferred into a sterile 2 mL Eppendorf tube (Merck) and 500 µL of 100 % ice-cold isopropanol (Sigma-Aldrich, St. Louis, MO, USA) was added. This was well mixed by inversion and incubated at 4 °C for 10 min. The supernatant was discarded and 1 mL of ice-cold 75 % ethanol (Sigma-Aldrich, St. Louis, MO, USA) was added and mixed by inverting. The 2 mL microcentrifuge tubes (Eppendorf tube, Merck) were centrifuged (Mikro 200R, Hettich Zentrifugen, Tuttlingen, Germany) at 7 500 × *g* at 4 °C for 5 min. The RNA wash step was repeated once. The supernatant was discarded, and the RNA pellet was air-dried at room temperature (25 °C ± 5 °C) for 15-30 min and eluted in 30 µL diethylpyrocarbonate

(DEPC)-treated water (Ambion, USA). The concentrations, purities and integrities of the RNA samples were assessed using the Nanodrop 2000 (Thermo Fisher Scientific, Massachusetts, USA).

2.3.8 Removal of genomic DNA from the RNA samples.

Traces of genomic DNA contamination were removed from 5000 ng of the extracted RNA samples using DNase-1 (Thermo Fisher Scientific, Massachusetts, USA). A volume of DEPC-treated water (Ambion, USA) was added to an RNase-free tube according to the calculation for each sample, followed by the addition of 10 X reaction buffer with $MgCl_2$ (Thermo Fisher Scientific, Massachusetts, USA) DNase 1 (Thermo Fisher Scientific, Massachusetts, USA) based on the RNA concentration of each sample. Tubes were vortexed (Thermo Fisher Scientific, Massachusetts, USA) for 2 s and incubated at 37 °C for 30 min in a heating block (Lab biotech, USA). Thereafter, 5 µL of 50 mM EDTA (Thermo Fisher Scientific, Massachusetts, USA) was added to the samples and incubated (Lab biotech, USA) at 65 °C to inhibit the action of the DNase -1 enzyme (Thermo Fisher Scientific, Massachusetts, USA).

2.3.9 Conversion of RNA to cDNA and quantitative real-time PCR (RT-qPCR)

The RNA was converted to cDNA using the Applied Biosystems™ High Capacity cDNA synthesis kit (Roche Applied Sciences, Penzberg, Germany) as per the manufacturer's instructions. In a 10 µL reaction, the master mix contained 10 X RT buffer, 25 X deoxynucleoside triphosphates (dNTP) mix, 10 x reverse transcription random primers, 1 µL multiscribe reverse transcriptase, 1 µL RNase inhibitor, and 500 ng total RNA. The cDNA synthesis thermal cycling conditions were followed as per the manufacturer's instructions. The FASTA format for each gene was obtained from MycoBrowser (Kapopoulou *et al.*, 2011) and inserted into Primer3Plus (Untergasser *et al*., 2007) to select the best primer set for each gene (Table 2.2). The primer sets were purchased from Inqaba Biotec (Inqaba Biotec, S.A). Primer efficiencies were tested for all primer sets before RT-qPCR was performed. The reverse transcription master mix included 2X SYBR green supermix (Bio-Rad Laboratories, Hercules, California, USA), 10 µM forward and reverse primers and 50 ng cDNA in a total volume of 10 µL. The RT-qPCR was conducted in a 7500 RT-qPCR Detection System (Applied Biosystems, Foster City, CA, USA). Cycling conditions were as follows; holding stage at 95 °C for 3 min, PCR stage of 40 cycles which included, 95 °C for 30 s, 60 °C for 30 s and 75 °C for 30 s. The

melt curve analysis was determined at continuous fluorescence set at 90 °C for 1 min, 60 °C for 30 s and 95 °C for 15 s. The resulting gene expression data was normalised using 16S rRNA and was analysed using the absolute quantification method.

Table 2.2: Gene and primer sequences selected for gene expression analysis using RT-qPCR. The listed primers were used to investigate gene regulation at 4 h and 24 h post-infection.

Gene	Forward Primer	Reverse Primer	Product size
PstS-1 (Rv0934)	CTACCCGCTGTTCAACCTGT	GATGTTCATCAGCCCCTTGT	187 bp
DnaK (Rv0350)	GATTGGCTGGTGGACAAGTT	AGGTTGATCGAGGTGGACTG	137 bp
19 kDa (Rv3763)	GTCTTTCCGGATGTTCAAGC	CTTACCGTCGATGACGACCT	119 bp
Cpn60.2 (Rv0440)	AATTGCGTACGACGAAGAGG	CCACTTCTTTTCCAGGACGA	118 bp
Apa (Rv1860)	AACCTGTCCGGATCGACAAC	TTGCTGAGGAGTGCTGAACC	109 bp
Ag85A Rv3804	CCGGTGCCCGACTACTACT	GTAGTCGCGGCTGTGGTC	129 bp
Type IV Pili Rv3660	GAGCAGGAGGGTGAACTGGT	GGATCGAGATCGACCAACAG	176 bp

2.3.10 Statistical analysis

All experiments were performed in independent triplicate biological experiments with triplicate technical repeats. GraphPad Prism (version 8) (GraphPad Software, La Jolla, CA, USA) was used to perform the parametric, unpaired *t*-test analysis to determine the significance values. All p-values ≤ 0.05 were considered statistically significant.

2.4 Results

2.4.1 Infection of THP-1 cells with wild-type, gene-deficient and complemented strains of M. tuberculosis

To determine whether the single deletion of *mtp, hbhA, Rv0309* genes and double deletion of *hbhA* and *mtp* in the V9124 strain of *M. tuberculosis* would result in reduced or increased adherence of *M. tuberculosis* to host cells, infection of the mutant was compared with that of the wild-type and the complemented strains in THP-1 macrophages at 4-h and 24-h post-infection. The THP-1 macrophages were infected at an MOI of 5 (5 bacteria /1 cell).

2.4.1.1 MTP mediates infection of macrophages

To determine if MTP enables infection of *M. tuberculosis* within macrophages, the average CFUs in *mtp*-deficient and *mtp*-proficient strains were compared to the wild-type at 4-h and 24-h post-infection. There was a significant difference in the number of intracellular bacteria that infected THP-1 cells (Fig 2.1) among the wild-type, Δ*mtp,* and the *mtp* complemented strains at the 4-h ($p< 0.001$) and 24-h ($p =0.001$) time points. However, the *mtp* deficient strain showed a significantly reduced capability of infecting the THP-1 cells compared to the wild-type at the 4-h ($p <0.001$) and 24-h ($p =0.002$) time points. Complementation of the *mtp* gene restored the infection capability to slightly below the wild-type level. There was no significant difference when comparing wild-type to the complemented strain at 4-h ($p =0.669$) and 24-h time points ($p =0.749$) (Fig.2.1).

2.4.1.2 Mycobacterium tuberculosis HBHA may have a role in the infection of THP-1 macrophages.

When compared to the wild-type and the complemented strain, there was a significant reduction in the number of bacteria that infected THP-1 cells by the Δ*hbhA* strain at both 4-h and 24-h time points ($p =0.049$ and $p=0.034$, respectively). Complementation of the *hbhA* gene restored the infection capability close to, but not completely to that of the wild-type strain (Fig.2.2). There was no significant difference between the *hbhA* complemented strains and the wild-type strain at the 4-h and 24-h time points ($p =0.058$ and $p =0.089$, respectively; Fig.2.2).

2.4.1.3 A double mtp-hbhA knockout mutant strain of M. tuberculosis showed reduced capability in infecting the host cells as compared to the parental and complemented strains.

There was a significant reduction in the CFU/mL of the Δ*mtp-hbhA* that infected THP-1 cells compared to the wild-type at the 4-h and 24-h time points (p =0.002 and p =0.047, respectively). There was a significant difference between the wild-type and the complemented strains at 4-h (p =0.002) and 24-h (p =0.002). No significant difference was observed between the Δ*mtp-hbhA* strain and the *mtp-hbhA* complemented strain at both time points (p =0.063 and p =0.222, respectively; Fig 2.3).

2.4.1.4 Rv0309 facilitates infection of THP-1 macrophages by M. tuberculosis.

To determine if deletion of the *Rv0309* gene has a significant effect on the infection of THP-1 cells by *M. tuberculosis*, Δ*Rv0309* was compared to the wild-type and the complemented strain at the 4-h and 24-h time points (Fig.2.4). *Rv0309* deficiency resulted in a significant reduction in infection of THP-1 cells in comparison to the wild-type strains at the 4-hour and 24-h time points (p = 0.001). Complementation did not restore infection cability to the wild-type level. There was a significant difference between the wild-type and the complemented strain at 4-h and 24-h indicated by p values of 0.000 and < 0.001, respectively. When the *Rv0309* mutant strain was compared with the complement, there was no significant difference at the 4-h time point (p =0.869). However, there was a significant difference observed at 24-h (p =0.001, Fig.2.4).

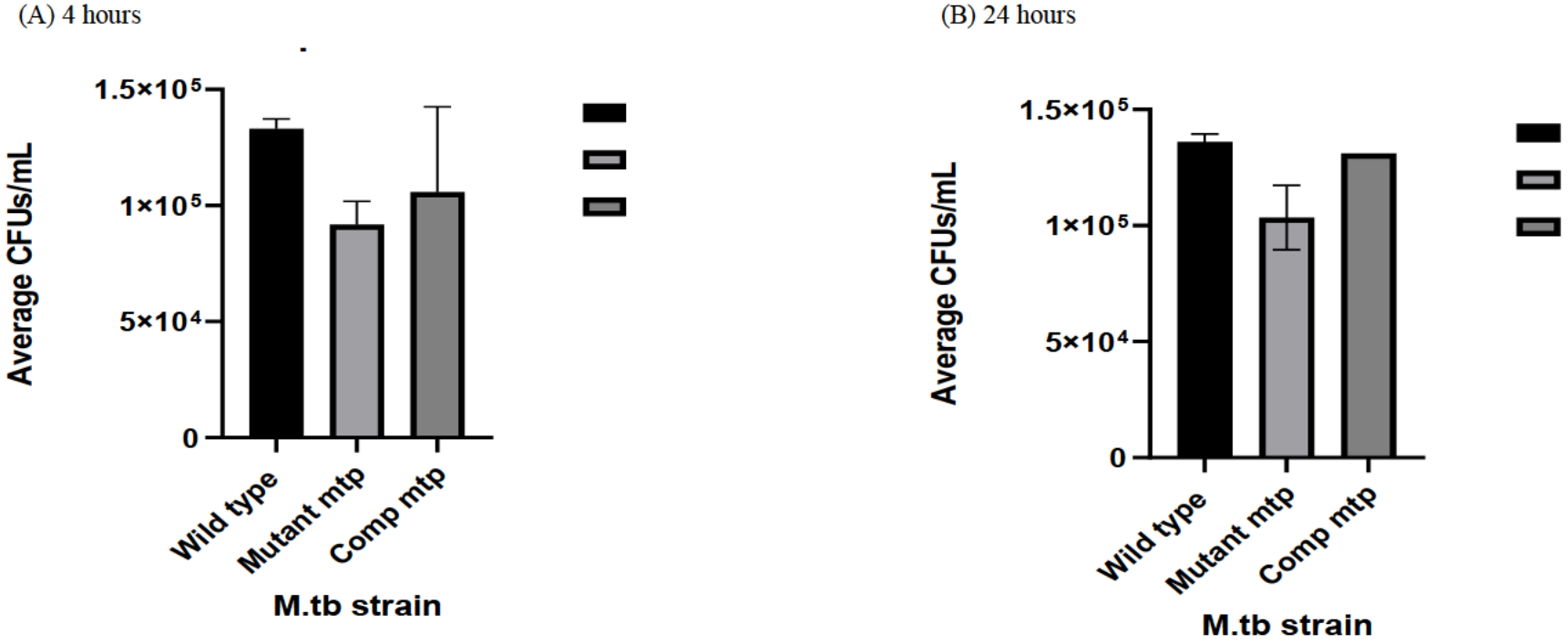

Figure 2.1 : The CFU/mL of *M. tuberculosis* wild-type, Δ*mtp*, and *mtp*-complemented strains at 4-h and 24-h time points post-infection. THP-1 macrophages were infected with each strain (MOI = 5) at 37°C. Infected differentiated THP-1 cells were washed, lysed, serially diluted and plated on 7H11 agar plates to quantitate viable CFUs in triplicate for three biological assays per strain. Results are depicted as the mean of CFUs of the mutant, complemented strain, and the wild-type as the control. The calculated ± SEM is indicated by the error bars relative to the calculated mean of 3 biological and triplicate technical repeat experiments. There was a significant difference in the ability of the strains to infect THP-1 cells among the wild-type, *Δmtp*, and the *mtp* complemented strains at the 4-h ($p < 0.001$) and 24-h ($p = 0.001$) time points. The *mtp* deficient strain showed a significantly reduced capability of infecting the THP-1 cells compared to the wild-type at the 4-h ($p < 0.001$) and 24-h ($p = 0.002$)

time points. No significant difference was observed when comparing wild-type to the complemented strain at 4-h (p =0.669) and 24-h time points (p =0.749).

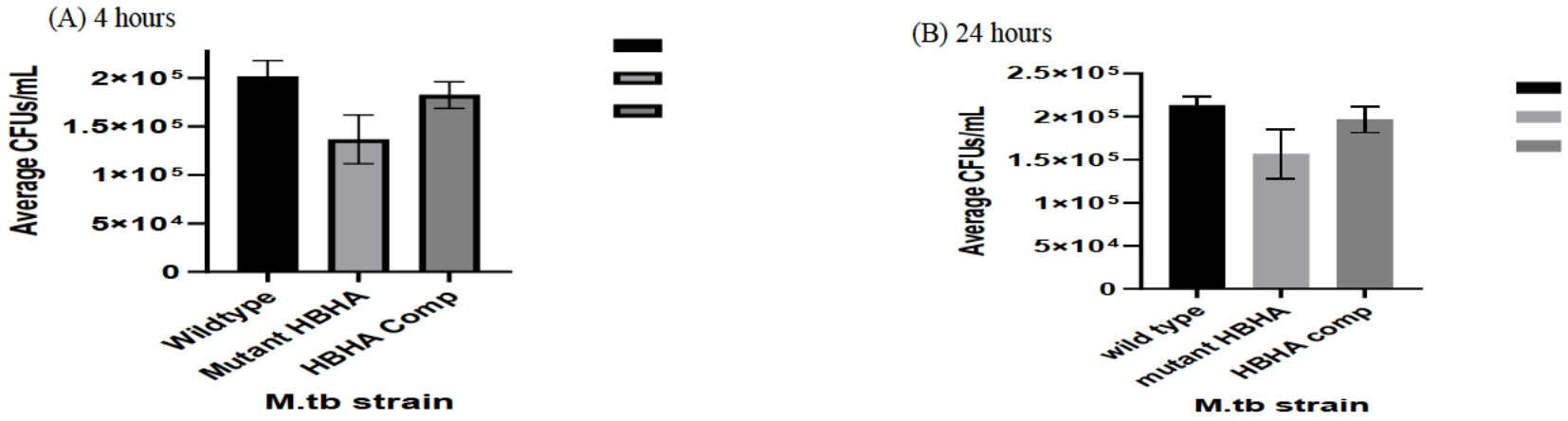

Figure 3.2 : The CFU/mL of *M. tuberculosis* wild-type, Δ*hbhA*, and *hbhA*-complemented strains at 4-h and 24-h time points post-infection. THP-1 macrophages were infected with each strain (MOI = 5) at 37°C. Infected differentiated THP-1 cells were washed, lysed, serially diluted and plated on 7H11 agar plates to quantitate viable CFUs in triplicate for three biological assays per strain. Results are depicted as the mean CFUs of the mutant, complemented strain, and the wild-type as the control. The calculated ± SEM is indicated by the error bars relative to the calculated mean of 3 biological and triplicate technical repeat experiments. There was a significant difference in ability of the ΔhbhA strain to infect THP-1 cells at both 4-h and 24-h time points indicated by the significant p values (p =0.049 and p =0.034) respectively. No significant difference was observed when comparing the hbhA complemented strains and the wild-type strain at the 4-h and 24-h time points (p =0.058 and p =0.089).

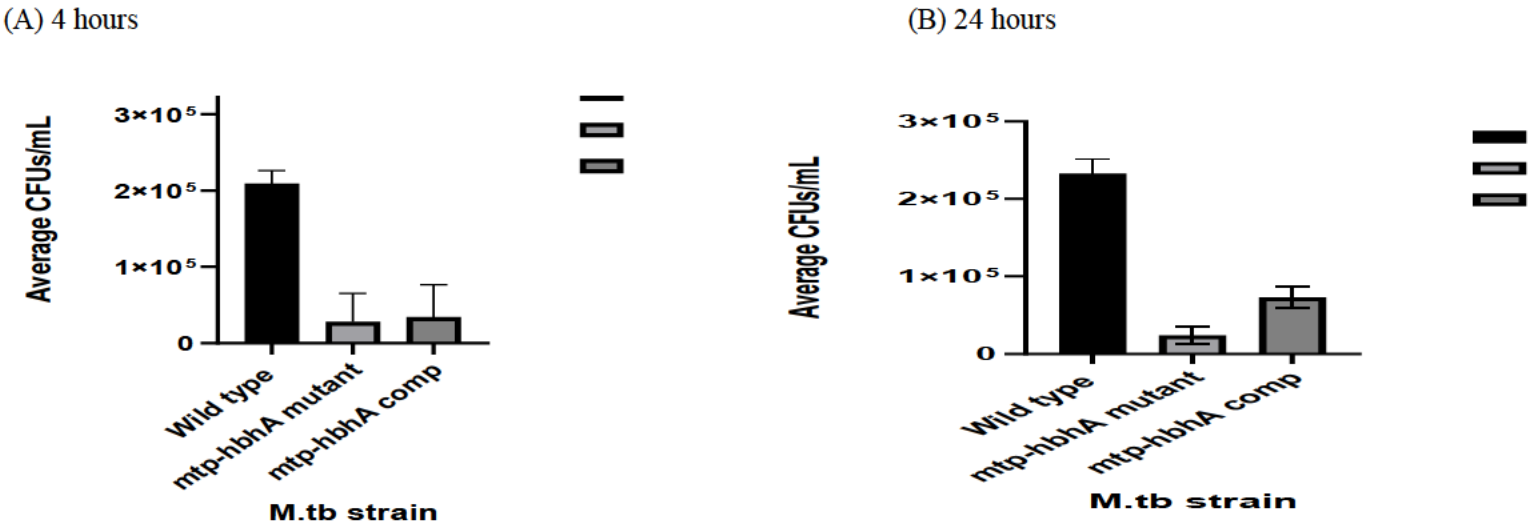

Figure 4.3: **The CFU/mL of *M. tuberculosis* wild-type, Δ*mtp-hbhA*, and *mtp-hbhA*-complemented strains at 4-h and 24-h time points post-infection.** THP-1 macrophages were infected with each strain (MOI = 5) at 37°C. Infected differentiated THP-1 cells were washed, lysed, serially diluted and plated on 7H11 agar plates to quantitate viable CFUs in triplicate for three biological assays per strain. Results are depicted as the mean of CFUs of the mutant, complemented strain, and the wild-type as the control. The calculated ± SEM is indicated by the error bars relative to the calculated mean of 3 biological and triplicate technical repeat experiments. The Δ*mtp-hbhA* that infected the THP-1 cells showed a significant reduction compared to the wild-type at the 4-h ($p = 0.002$) and 24-h ($p = 0.047$) time points. There was significant difference between the wild-type and the complemented strains at 4-h ($p = 0.002$) and 24-h ($p = 0.002$). No significant difference was observed between the Δ*mtp-hbhA* strain and the *mtp-hbhA* complemented strain at 4-h ($p = 0.063$) and 24-h ($p = 0.222$).

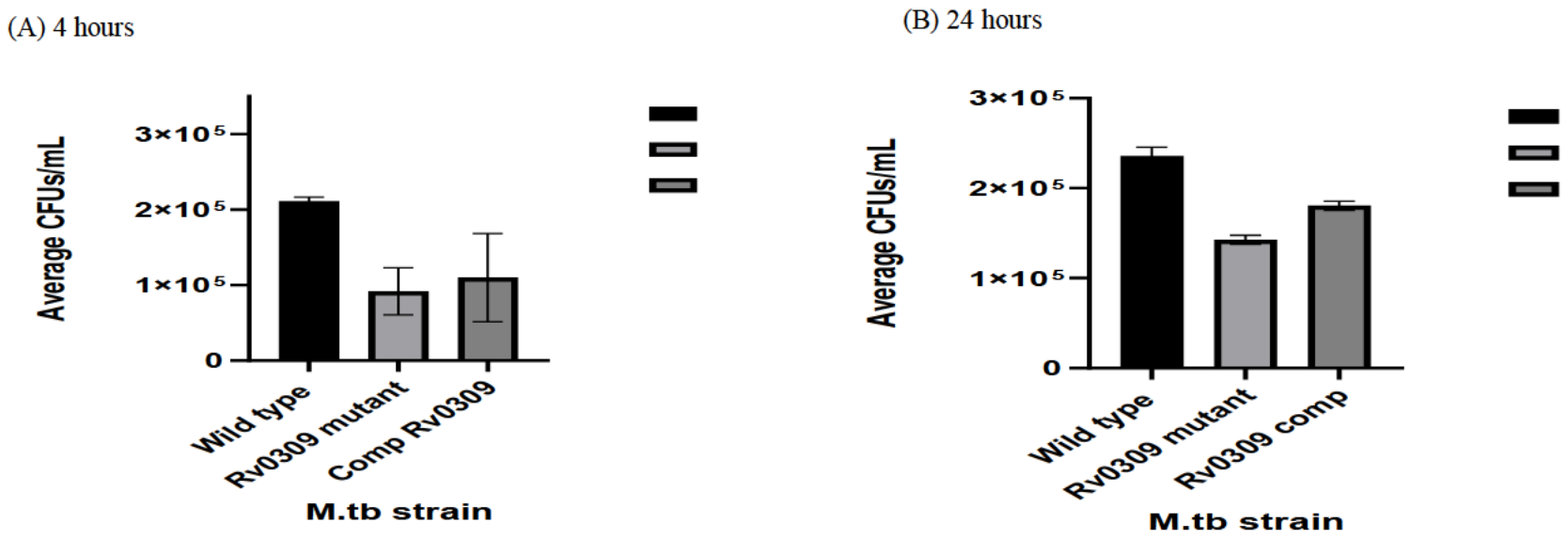

Figure 5.4: The CFU/mL of *M. tuberculosis* wild-type, Δ*Rv0309*, and *Rv0309*-complemented strains at 4-h and 24-h time points post-infection. THP-1 macrophages were infected with each strain (MOI = 5) at 37°C. Infected differentiated THP-1 cells were washed, lysed, serially diluted and plated on 7H11 agar plates to quantitate viable CFUs in triplicate for three biological assays per strain. Results are depicted as the mean of CFUs of the mutant, complemented strain, and the wild-type as the control. The calculated ± SEM is indicated by the error bars relative to the calculated mean of 3 biological and triplicate technical repeat experiments. The Δ*Rv0309* that infected the THP-1 cells showed a significant reduction compared to the wild-type at 4-h ($p=0.001$) and 24-h ($p=0.001$). There was a significant difference between the wild-type and the complemented strain at 4-h ($p=0.000$) and 24-h ($p< 0.001$). No significant difference was observed between the Δ*Rv0309* and *Rv0309*-complemented strains at 4-h ($p =0.869$), a significant difference was observed at 24-h ($p =0.001$).

2.4.2 Quantitative expression of M. tuberculosis adhesin genes using RT-qPCR.

THP-1 cells were infected with different strains of *M. tuberculosis* to study the influence of the single knockout of *mtp, hbhA, Rv0309* and the double knockout of *mtp-hbhA*- genes on the regulation of selected *M. tuberculosis* adhesin genes; *Rv0350, Rv0440, Rv0934, Rv1860, Rv3660, Rv3763* and *Rv3804* that facilitate binding to THP-1 cells (Squeglia *et al*., 2018)

2.4.2.1 The effect of Δ*mtp on adhesin gene regulation*

At 4-h post-infection, four of the seven genes, *Rv3763*, *Rv3804*, *Rv1860* and *Rv0440*, were expressed in all three strains. The expression of three of these genes, *Rv3763* (p=0.049), *Rv3804* (p=0.003) and *Rv0440* (p=0.004), was significantly increased in the Δ*mtp* compared to the wild-type strains. Of the other three genes, *Rv3660* was expressed in the Δ*mtp* but not in the wild-type (p=0.012), *Rv0934* was expressed in the wild-type, but not Δ*mtp* (p=0.006) and *Rv0350* was not expressed in both the strains (Figure 2.5). No significant difference was observed in the expression of gene *Rv1860* compared to the wild-type (p = 0.172).

At 24-h, five genes, *Rv3763*, *Rv0934*, *Rv3804, Rv1860* and *Rv0440*, were expressed in the Δ*mtp* compared to expression of all seven in the wild-type and complemented strains. In contrast to the 4-h post-infection, the expression of these five genes was significantly increased in the wild-type compared to the Δ*mtp* strain *Rv3763* (p=0.049), *Rv0934* (p=0.006), *Rv3804* (p=0.005), *Rv0350* (p=0.012) *and Rv0440* (p=0.004). *Rv0350* and *Rv3660* were not expressed in the Δ*mtp* strain (Figure 2.5).

Complementation restored function of all seven genes at 4-h and 24-h post-infection. At 4-h, the expression of seven genes *Rv3763* (p<0.001), *Rv0934* (p=0.001), *Rv3804* (p=0.000), *Rv0350* (p=0.112), *Rv3660* (p=0.001), *Rv1860* (p=0.001) and *Rv0440* (p=0.000) was significantly increased in the complemented compared to the wild-type strain (Figure 2.5). Of note, *Rv0350* (p=0.112) and *Rv3660* (p=0.001) were not expressed in the wild-type at 4-h, yet the difference was significant for the latter but not former. At 24-h, expression was significantly increased in three genes, *Rv3763* (p=0.002), *Rv3804* (p=0.025) and *Rv1860* (p=0.033) in the complemented compared to the wild-type strains, while expression of *Rv0350* (p=0.008) and *Rv3660* (p=0.022), was significantly increased in wild-type compared to complemented strains (Figure 2.5). No significant difference was observed in the expression

of *Rv0934* (p=0.212) and *Rv0440* (p=0.412) between wild-type and complemented strains (Figure 2.5).

*2.4.2.2 The effect of Δ*hbhA* on adhesin gene regulation*

At 4-h post-infection, five of the seven genes, *Rv3763*, *Rv0934*, *Rv3804*, *Rv1860* and *Rv0440*, were expressed in all three strains. The expression of *Rv3763* (p=0.001) was significantly increased in the Δ*hbhA* compared to the wild-type strains. Of the other genes, *Rv3660* (p=0.001) and *Rv0350* (p<0.001) were expressed in the Δ*hbhA* but not by the wild-type. The expression level of *Rv0934* (p=0.096), *Rv3804* (p=0.235), *Rv1860* (p=0.298) and *Rv0440* (p=0.409) was non-significant (Figure 2.6).

At 24-h, all seven genes, *Rv3763*, *Rv0934*, *Rv3804*, *Rv0350*, *Rv3660*, *Rv1860* and *Rv0440*, were expressed across all strains. In contrast to the 4-h post-infection, the expression of four of these genes was significantly increased in the wild-type compared to the Δ*hbhA* strain *Rv3763* (p=0.023), *Rv0934* (p=0.001), *Rv3804* (p=0.002), *Rv1860* (p=0.017). The expression level of *Rv3660* (0.619), *Rv0350* (p=0.241) and *Rv0440* (p=0.340) was non-significant (Figure 2.6).

Complementation restored function of all seven genes at 4-h and 24-h post-infection. At 4-h, the expression of five genes *Rv3763* (p<0.001), *Rv3804* (p=0.014), *Rv0350* (p<0.001), *Rv3660* (p=0.001) and *Rv1860* (p=0.001) was significantly increased in the complemented compared to the wild-type strain. Of note, *Rv0350* (p<0.001) and *Rv3660* (p=0.001) were not expressed in the wild-type at 4-h. At 24-h, expression was significantly increased in two genes, *Rv3804* (p=0.025) and *Rv0350* (p=0.017) in the complemented compared to the wild-type strains. No significant difference was observed in the expression of *Rv3763* (p=0.104), *Rv3804* (p=0.800), *Rv3660* (p=0.206), *Rv1860* (p=0.787) and *Rv0440* (p=0.117) between wild-type and complemented strains (Figure 2.6).

2.4.2.3 The effect of Δmtp-hbhA on adhesin gene regulation

At 4-h post-infection, five of the seven genes, *Rv3763*, *Rv0934*, *Rv3804*, *Rv1860* and *Rv0440*, were expressed in all three strains. The expression of *Rv3763* (p=0.039), *Rv0934* (p = 0.002) and *Rv3804* (p=0.000) was significantly increased in the wild-type strains compared to the Δ*mtp-hbhA*. The genes, *Rv0350* (p=0.374) and *Rv3660* (p=0.186) were expressed in the Δ*mtp-hbhA* and down regulated in the wild-type. The expression levels of the genes *Rv1860* (p=0.648) and *Rv0440* (p=0.096) was non-significant (Figure 2.7).

At 24-h, all seven genes, *Rv3763*, *Rv0934*, *Rv3804*, *Rv0350*, *Rv3660*, *Rv1860* and *Rv0440*, were expressed across all strains. Similar to the 4-h post-infection, the expression of these genes was significantly increased in the wild-type compared to the Δ*mtp-hbhA*, *Rv3763* (p=0.012), *Rv3904* (p=0.003), *Rv3804* (p=0.001), *Rv0350* (p<0.001), *Rv3660* (p=0.004) and *Rv1860* (p<0.001) and *Rv0440* (p<0.001) (Figure 2.7).

Complementation restored function of all seven genes at 4-h and 24-h post-infection. At 4-h, the expression of three genes *Rv0934* (p= 0.097), *Rv3804* (p= 0.301) and *Rv1860* (p=0.154), was restored to the wild-type level in the complemented strain. Of note, *Rv0350* (p<0.001) and *Rv3660* (p=0.004) were not expressed in the wild-type at 4-h. At 24-h, expression was significantly increased in three genes, *Rv3763* (p=0.003), *Rv3804* (p=0.028) and *Rv1860* (p=0.012) in the complemented compared to the wild-type strains, while expression of *Rv0350* (p=0.000) and *Rv3660* (p=0.004) was significantly increased in wild-type compared to complemented strains. No significant difference was observed in the expression of *Rv0934* (p=0.941) and *Rv0440* (p=0.717) between wild-type and complemented strains (Figure 2.7).

2.4.2.4 The effect of Rv0309 on adhesin gene regulation

At 4-h post-infection, five of the seven genes, *Rv3763*, *Rv0934*, *Rv3804*, *Rv1860* and *Rv0440*, were expressed in all three strains. The expression of *Rv3763* (p<0.001), *Rv0934* (p=0.000), *Rv3804* (p<0.001), *Rv1860* (p=0.000), and *Rv3660* (p=0.015) was significantly increased in the Δ*Rv0309* compared to the wild-type strains. The gene, *Rv3660* (p=0.015) was expressed in the Δ*hbhA* but not by the wild-type. The expression levels of the two genes *Rv0350* (p=0.115) and Rv*0440* (p=0.952) was non-significant (Figure 2.8).

At 24-h, all seven genes, *Rv3763*, *Rv0934*, *Rv3804*, *Rv0350*, *Rv3660*, *Rv1860* and *Rv0440*, were expressed across all strains. In contrast to the 4-h post-infection, the expression of three of these genes was significantly expressed between the wild-type and the Δ*Rv0309*: *Rv3763* (p=0.005), *Rv0934* (p=0.001) and *Rv1860* (p<0.001). The expression levels of *Rv3804* (p=0.095), *Rv0350* (p=0.0600), *Rv3660* (p=0.173) and *Rv0440* (p=0.333) were non-significant (Figure 2.8).

Complementation restored function of all seven genes at 24-h post-infection compared to at 4-h. At 4-h, five genes *Rv3763* (p=0,015), *Rv0934*(p=0.006), *Rv3804* (p<0.001), *Rv1860*

(p=0.0040) and *Rv0440* (p<0.001) were significantly expressed between the wild-type and the complemented strains. Of note, the gene *Rv3660* was not expressed in the wild-type and the *Rv0309* complement at 4-h. At 24-h, expression was significantly increased in three genes, *Rv3763* (p = 0.003*), Rv3804* (p=0.026) and *Rv1860* (p=0.007) in the complemented compared to the wild-type strains while expression of *Rv0934* (p=0.043), *Rv0350* (p=0.001) and *Rv3660* (p=0.010), was significantly increased in wild-type compared to complemented strains. No significant difference was observed in the expression of *Rv0440* (p=0.868) between wild-type and complemented strains (Figure 2.8).

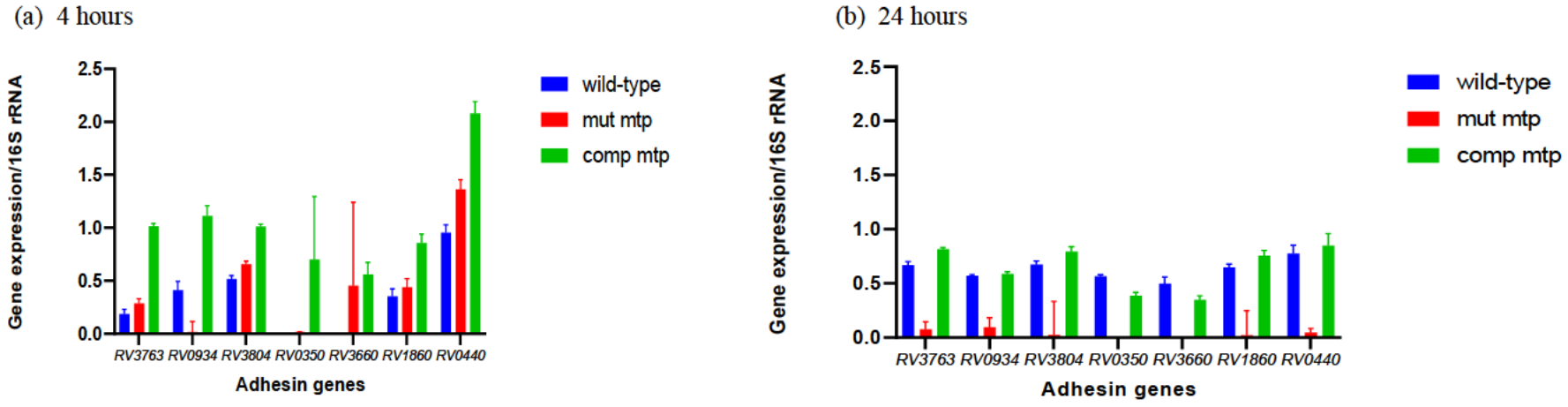

Figure 6.5: The expression of 7 genes at 4-h (a) and 24-h (b) post infection: adhesin genes (*Rv3763, Rv0934, Rv3804, Rv0350, Rv3660, Rv1860* and *Rv0440)* in the wild-type, Δ*mtp*, and *mtp*-complemented strains using real-time quantitative PCR. The absolute quantification method of interpretation was used to assess the RT-qPCR data. The gene expression levels were analysed relative to 16S rRNA for each gene of interest. Significance levels were established using an unpaired, parametric t-test for data between wild-type and Δ*mtp* strains, and for the wild-type and *mtp*-complemented strains. At 4-h post-infection, four of the seven genes, *Rv3763, Rv3804, Rv1860* and *Rv0440*, were expressed in all three strains. The expression of three of these genes, *Rv3763* (p=0.049), *Rv3804* (p=0.003) and *Rv0440* (p=0.004), was significantly increased in the Δ*mtp* compared to the wild-type strains. Of the other three genes, *Rv3660* was expressed in the Δ*mtp* but not wild-type (p=0.012), *Rv0934* was expressed in the wild-type, but not Δ*mtp* (p=0.006) and *Rv0350* was not expressed in both the strains. The gene *Rv1860* was non-significant (p = 0.172). At 24-h, five genes, *Rv3763*, *Rv0934, Rv3804, Rv1860* and *Rv0440*, were expressed in the Δ*mtp* compared to expression of all seven in the wild-type and complemented strains. In contrast to the 4-h post-infection, the expression of these five genes was significantly increased in the wild-type compared to the Δ*mtp* strain, *Rv3763* (p=0.049), *Rv0934* (p=0.006), *Rv3804* (p=0.005), *Rv0350* (p=0.012) and *Rv0440* (p=0.004). *Rv0350* and *Rv3660* were not expressed in the Δ*mtp* strain. Complementation restored function of all seven genes at 4-h and 24-h post-infection. At 4-h, the expression of seven genes *Rv3763* (p<0.001), *Rv0934* (p=0.001), *Rv3804* (p=0.000), *Rv0350* (p=0.112), *Rv3660* (p=0.001), *Rv1860* (p=0.001) and *Rv0440* (p=0.000) was significantly increased in the complemented compared to the wild-type strain. Of note, *Rv0350* (p=0.112) and *Rv3660* (p=0.001) were not expressed in the wild-type at 4-h, yet the difference was significant for the latter but not former. At 24-h, expression was significantly increased in three genes, *Rv3763* (p=0.002), *Rv3804* (p=0.025) and *Rv1860* (p=0.033) in the complemented compared to the wild-type strains, while expression of *Rv0350* (p=0.008) and *Rv3660* (p=0.022), was significantly increased in wild-type compared to complemented strains. No significant difference was observed in the expression of *Rv0934* (p=0.212) and *Rv0440* (p=0.412) between wild-type and complemented strains.

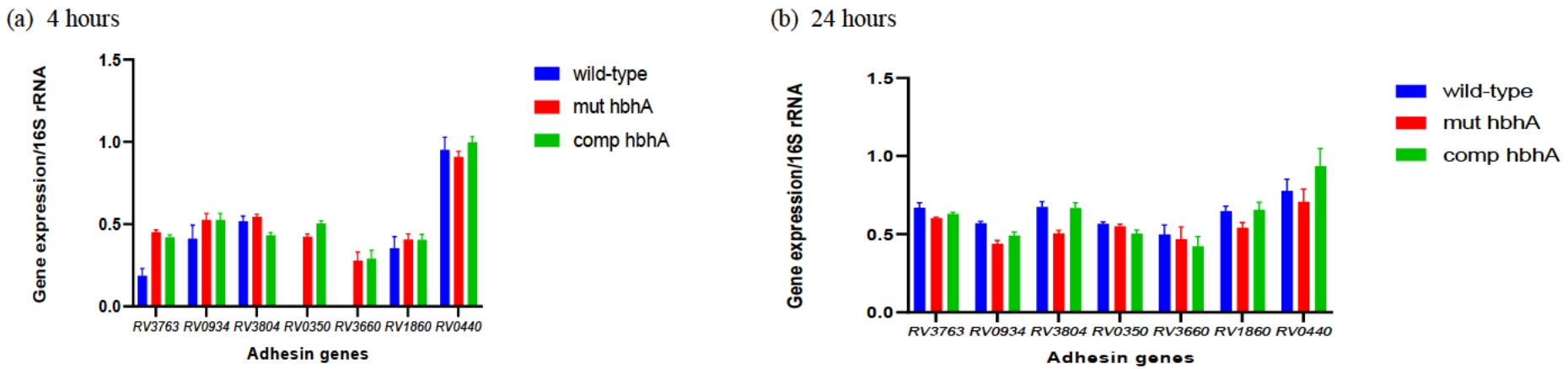

Figure 7.6 The expression of 7 genes at 4-h (a) and 24-h (b) post infection: adhesin genes (*Rv3763, Rv0934, Rv3804, Rv0350, Rv3660*, *Rv1860* and *Rv0440*) in the wild-type, Δ*hbhA* and *hbhA*-complement strains using real-time quantitative PCR. The absolute method of interpretation was used to assess the RT-qPCR data. The gene expression levels were analysed relative to 16S rRNA for each gene of interest. Significance levels were established using an unpaired, parametric t-test for data between wild-type and Δ*hbhA* strains, and the wild-type and *hbhA*-complement strains. At 4-h post-infection, five of the seven genes, *Rv3763, Rv0934, Rv3804, Rv1860* and *Rv0440*, were expressed in all three strains. The expression of *Rv3763* ($p=0.001$) was significantly increased in the Δ*hbhA* compared to the wild-type strains. Of the other genes, *Rv3660* ($p=0.001$) and *Rv0350* ($p<0.001$) were expressed in the Δ*hbhA* but not by the wild-type. The expression level of *Rv0934* ($p=0.096$), *Rv3804* ($p=0.235$), *Rv1860* ($p=0.298$) and *Rv0440* ($p=0.409$) was non-significant. At 24-h, all seven genes, *Rv3763*, *Rv0934*, *Rv3804*, *Rv0350*, *Rv3660*, *Rv1860* and *Rv0440*, were expressed across all strains. In contrast to the 4-h post-infection, the expression of four of these genes was significantly increased in the wild-type compared to the Δ*hbhA* strain: *Rv3763* ($p=0.023$), *Rv0934* ($p=0.001$), *Rv3804* ($p=0.002$), *Rv1860* ($p=0.017$). The expression level of *Rv3660* (0.619), *Rv0350* ($p=0.241$) and *Rv0440* ($p=0.340$) was non-significant. Complementation restored function of all seven genes at 4-h and 24-h post-infection. At 4-h, the expression of five genes; *Rv3763* ($p<0.001$), *Rv3804* ($p=0.014$), *Rv0350* ($p<0.001$), *Rv3660* ($p=0.001$) and *Rv1860* ($p=0.001$) was significantly increased in the complemented compared to the wild-type strain. Of note, *Rv0350* ($p<0.001$) and *Rv3660* ($p=0.001$) were not expressed in the wild-type at 4-h. At 24-h, expression was significantly increased in two genes, *Rv3804* ($p=0.025$) and *Rv0350* ($p=0.017$) in the complemented compared to the wild-type strains. No significant difference was observed in the expression of *Rv3763* ($p=0.104$), *Rv3804* ($p=0.801$), *Rv3660* ($p=0.206$), *Rv1860* ($p=0.787$) and *Rv0440* ($p=0.117$) between wild-type and complemented strains.

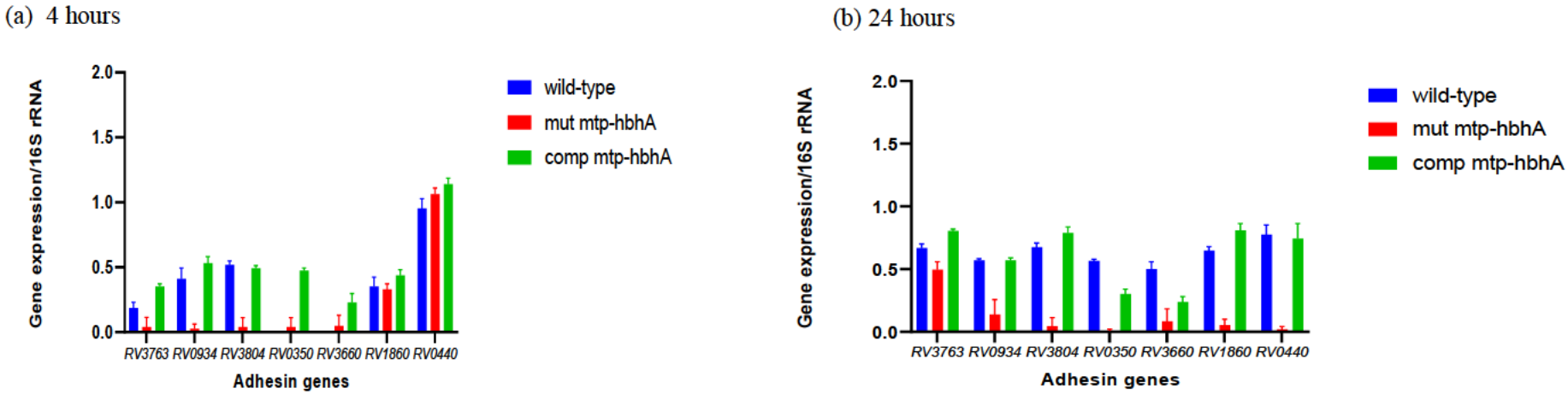

Figure 8.7. **The expression of 7 genes at 4-h (a) and 24-h (b) post infection: adhesin genes (*Rv3763, Rv0934, Rv3804, Rv0350, Rv3660, Rv1860* and *Rv0440*) in the wild-type, Δ*mtp-hbhA* and *mtp-hbhA* complement strains using real-time quantitative PCR.** The absolute quantification method of interpretation was used to assess the RT-qPCR data. The gene expression levels were analysed relative to 16S rRNA for each gene of interest. Significance levels were established using an unpaired, parametric t-test for data between wild-type and Δ*mtp-hbhA* strains, and the wild-type and *mtp-hbhA* complement strains. At 4-h post-infection, five of the seven genes, *Rv3763, Rv0934, Rv3804*, *Rv1860* and *Rv0440*, were expressed in all three strains. The expression of *Rv3763* (p=0.039), *Rv0934* (p = 0.002) and *Rv3804* (p=0.000) was significantly increased in the wild-type strains compared to the Δ*mtp-hbhA*. The genes, *Rv0350* (p=0.374) and *Rv3660* (p=0.186) were expressed in the Δ*mtp-hbhA* but down regulated in the wild-type. The expression levels of the four genes, *Rv0350* (p=0.374), *Rv3660* (p=0.186), *Rv1860* (p=0.648) and *Rv0440* (p=0.096) was non-significant. At 24-h, all seven genes, *Rv3763*, *Rv0934*, *Rv3804, Rv0350*, *Rv3660*, *Rv1860* and *Rv0440*, were expressed across all strains. Unlike the 4-h post-infection, the expression of all seven genes was significantly increased in the wild-type compared to the Δ*mtp-hbhA*: *Rv3763* (p=0.014), *Rv0934* (p=0.003), *Rv3804* (p=0.000), *Rv0350* (p<0.001), *Rv3660* (p=0.004) and *Rv1860* (p<0.001) and *Rv0440* (p<0.001). Complementation restored function of all seven genes at 4-h and 24-h post-infection. At 4-h, the expression of three genes *Rv0934* (p= 0.097), *Rv3804* (p= 0.301) and *Rv1860* (p=0.154), was restored to the wild-type level in the complemented strain. Of note, *Rv0350* (p<0.001) and *Rv3660* (p=0.004) were not expressed in the wild-type at 4-h. *Rv3663* (p=0.004) and *Rv0440* (p=0.022) were significantly expressed in the complemented strains compared to the wild-type at 4-h. At 24-h, expression was significantly increased in three genes, *Rv3763* (p=0.003), *Rv3804* (p=0.028) and *Rv1860* (p=0.012) in the complemented compared to the wild-type strains, while expression of *Rv0350* (p=0.000) and *Rv3660* (p=0.004) was significantly increased in wild-type compared to complemented strains. No significant difference was observed in the expression of *Rv0934* (p=0.941) and *Rv0440* (p=0.717) between wild-type and complemented strains.

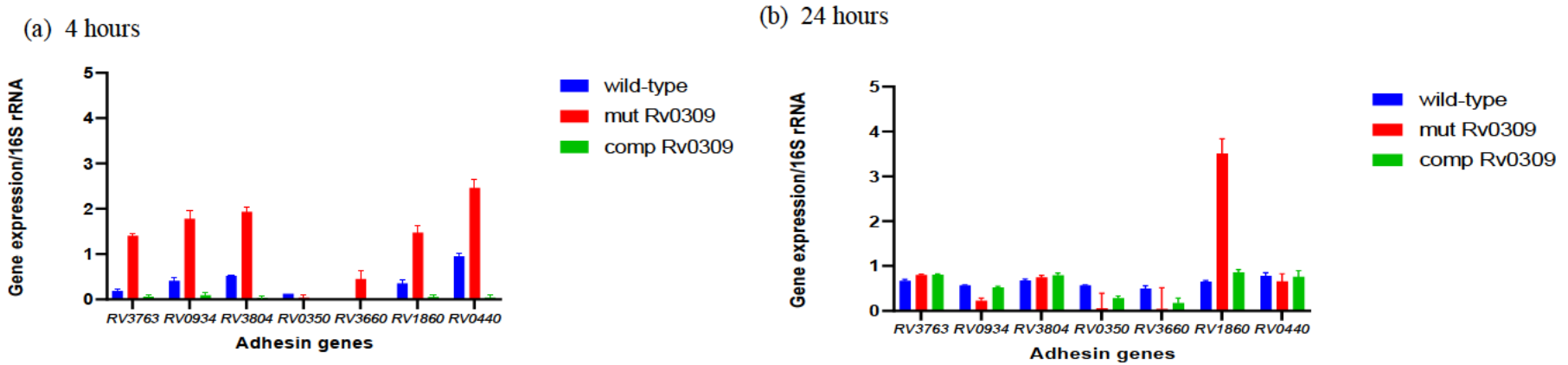

Figure 9.8 The expression of 7 genes at 4-h (a) and 24-h (b) post infection: adhesin genes (*Rv3763, Rv0934, Rv3804, Rv0350, Rv3660, Rv1860* and *Rv0440*) in the wild-type, Δ*Rv0309* and *Rv0309*-complement strains using real-time quantitative PCR. The absolute quantification method of interpretation was used to assess the RT-qPCR data. The gene expression levels were analysed relative to 16S rRNA for each gene of interest. Significance levels were established using an unpaired, parametric t-test for data between wild-type and Δ*Rv0309* strains, and the wild-type and *Rv0309*-complement strains. At 4-h post-infection, five of the seven genes, *Rv3763, Rv0934, Rv3804, Rv1860* and *Rv0440*, were expressed in all three strains. The expression of *Rv3763* ($p<0.001$), *Rv0934* ($p=0.000$), *Rv3804* ($p<0.001$), *Rv1860* ($p=0.000$), and *Rv0440* ($p=0.001$) was significantly increased in the Δ*Rv0309* compared to the wild-type strains. The gene, *Rv3660* ($p=0.015$) was expressed in the Δ*Rv0309* but not by the wild-type. The expression levels of the gene *Rv0350* ($p=0.115$) was non-significant. At 24-h, all seven genes, *Rv3763*, *Rv0934*, *Rv3804, Rv0350, Rv3660, Rv1860* and *Rv0440*, were expressed across all strains. In contrast to the 4-h post-infection, the expression of three of these genes was significantly expressed between the wild-type and the Δ*Rv0309*: Two of the genes *Rv3763* ($p=0.005$) and *Rv1860* ($p<0.001$) were increased in mutant and one of the genes *Rv0934* ($p=0.001$) was increased in wild-type. The expression levels of *Rv3804* (0.095), *Rv0350* ($p=0.060$), *Rv3660* ($p=0.173$) and *Rv0440* ($p=0.333$) were non-significant. Complementation restored function of all seven genes at 24-h post-infection compared to at 4-h. At 4-h, the expression of five genes *Rv3763* ($p=0.015$), *Rv0934* ($p=0.006$), *Rv3804* ($p<0.001$), *Rv1860* ($p=0.004$) and *Rv0440* ($p<0.001$) was significantly expressed between the wild-type strain and the complemented. Of note, the gene *Rv3660* was not expressed in the wild-type and the complement at 4-h. At 24-h, expression was significantly increased in three genes, *Rv3763* ($p = 0.003$), *Rv3804* ($p=0.026$) and *Rv1860* ($p=0.007$) in the complemented compared to the wild-type strains while expression of *Rv0934* ($p=0.043$), *Rv0350* ($p=0.001$) and *Rv3660* ($p=0.010$), was significantly increased in wild-type compared to complemented strains. No significant difference was observed in the expression of *Rv0440* ($p=0.868$) between wild-type and complemented strains

2.5 Discussion

This study aimed to investigate the role of the selected adhesin genes, MTP, HBHA and Rv0309, in the regulation of other adhesin genes involved in the pathogenicity of *M. tuberculosis* in the THP-1 infection model. Adhesins on the bacterial surfaces are important for the survival of the pathogenic bacteria since these molecules are essential to initiate and maintain host-pathogen interaction (Kline *et al*., 2009). Infection of host cells by *M. tuberculosis* is regulated by several factors. This involves interactions between the host's immune system and the bacillus, which is facilitated by adhesins. The identification and characterization of key adhesin molecules involved in the interaction of the pathogen with the host cells could offer new targets for drug development and possible new vaccine strategies capable of effectively disrupting early interactions between host pathogens (Govender, 2018). This makes adhesins attractive therapeutic targets (Kline *et al*., 2009). This study identified the impact triggered by three important adhesins, MTP, HBHA, and Rv0309, on regulation of other adhesins, as well as infection, of macrophages by *M. tuberculosis* during early stages of the life cycle.

2.5.1.1 Mycobacterium tuberculosis curli pili facilitates infection of macrophages in M. tuberculosis V9124 strain

In a post-antibiotic era, anti-adhesion therapy could be a promising treatment and prevention option for TB. *Mycobacterium tuberculosis* curli pili (MTP) are small adhesion molecules that belong to the pili or curli family of bacterial amyloids (Alteri *et al*., 2007). *Mycobacterium tuberculosis* curli pili has shown adhesion capabilities that allow binding with laminin found in the host cell's extracellular matrix (ECM) (Alteri *et al*., 2007). In the current study, the average intracellular bacterial count obtained during the *in vitro* infection assay, demonstrated that the MTP deficient strain was unable to infect THP-1 macrophages to the same extent as the wild-type in the presence of the adhesin. This supported the findings of Ramsugit and Pillay, (2014), thus, confirming the adhesion property of MTP. The current finding also correlates with the results of another study by Moodley, (2018, unpublished) in which *Δmtp* displayed a reduced capability in infecting THP-1 cells (Moodley, 2018, unpublished). The restoration of *mtp* gene function using complementation suggests that MTP in the F15/LAM4/KZN V9124 strain is an invasin of THP-1 macrophages.

2.5.1.2 Infection of THP-1 cells with ΔhbhA M. tuberculosis strains may indicate the role of HBHA in binding to THP-1 cells.

To evaluate if HBHA participates in the infection of THP-1 macrophages with *M. tuberculosis*, HBHA gene-deficient and gene-proficient strains were used in comparison to the wild-type strain. The HBHA mutant and the complemented strains demonstrated the capability of *M. tuberculosis* to infect macrophages. In comparison to the wild-type strain, the mutant *hbhA* showed a decrease in the ability to infect THP-1 cells at both 4-h ($p = 0.049$) and 24-h ($p = 0.034$) time points. This was similar to the findings of Moodley, (2018, unpublished) that demonstrated the role of HBHA in macrophage invasion using a *hbhA* gene deficient *M. tuberculosis*. In contrast, Pethe *et al*., (2001) demonstrated that HBHA has no impact on adhesion and invasion of macrophages. This could be explained by the different strain (*Mycobacterium bovis* Bacille Calmette–Guérin) and the type of macrophages (bone marrow-derived macrophages) used by Pethe *et al*., (2001). Heparin binding haemagglutin adhesin has been shown to bind to complement component C3 and recombinant HBHA has been discovered to facilitate the attachment of latex beads to murine macrophage-like cells in both C3-dependent and -independent ways (Mueller-Ortiz *et al.,* 2001). *Mycobacterium tuberculosis* has been reported to bind to complement receptors and can be delivered into phagocytic cells (Schlesinger *et al*., 1990). This further supports that HBHA can be an adhesin and invasin of macrophages.

2.5.1.3 Double Knockout Δmtp-hbhA mutant strain showed a reduced capability in infecting THP-1 macrophages as compared to the parental and complemented strains.

The double knockout mutant strain demonstrated a reduced capability to infect the THP-1 macrophages. This reduction in the infection capability was significantly more when compared to the single deletion of *mtp* and *hbhA* strains. A recent study by Ashokcoomar *et al*., (2020) found that the deletion of the *mtp* gene resulted in the elevated relative concentration of D-galactose, D-mannose, and D-glucose metabolites in the mutant strain compared to the wild-type strain. Furthermore, Ashokcoomar *et al*., (2020) explained the importance of these metabolites in cell wall synthesis. The deletion of *mtp* gene resulted in the mutant strain not having the ability to utilize these metabolites for cell wall synthesis (Ashokcoomar *et al*., 2020).

This further suggests the role of the MTP in cell wall synthesis and significance as an adhesin and invasin of *M. tuberculosis* to host cells. The impairment of the double knockout strain to adhere to and infect the THP-1 cells might have been caused by the deletion of the *mtp* gene most likely leading to a compromised mycobacterial cell envelope during the infection process. Naidoo, (2021) found that the differentially expressed up- and down-regulated genes, respectively induced by the deletion mutants relative to the wild-type strain, varied: Δ*mtp*, 45 and 16; Δ*hbhA*, 23 and 20; and Δ*mtp-hbhA*, 15 and 16. Moreover, Naidoo (2021) found that deletion of *mtp* and *hbhA* had an impact in central carbon metabolism. Deletion of *hbhA* caused a down-regulation of virulence associated proteins (VapBC), involved in maintenance of virulence factors and chaperonin proteins that prevent misfolding and promote refolding (Naidoo, 2021) which could also explain the observed impairment of the double knock out of *mtp-hbhA* to infect THP-1 cells.

THP-1 cells are the first line of defense and are regarded as the key component of the innate immune system encountered by *M. tuberculosis* (Pieters, 2008). As part of the host immune response, macrophages have been involved in the clearing of *M. tuberculosis*. It is also plausible that the double knockout mutant of *mtp-hbhA* strain is particularly susceptible to anti-mycobacterial host defences that characterize the chronic phase of infection. The results of the present study are similar to a study by Saikolappan *et al*., (2012) that showed that a double knockout mutant of *fbpA-sapM* resulted in an attenuation of the strain in mouse macrophages and PMA activated human THP-1 macrophages. Another study by Russell-Goldman *et al*., (2008) demonstrated that a double knockout of *Rpf* resulted in the attenuation of the strain in macrophages. In addition to this, Russell-Goldman *et al*., (2008) suggested that the double knockout of *Rpf* genes could result in *M. tuberculosis* being more prone to host antimicrobial defence mechanisms. This may also apply to the double knockout mutant of the *mtp-hbhA* strain in the current study. It would be valuable to explore the antimicrobial defence mechanisms employed by macrophages and the ability of the double Δ*mtp-hbhA* and the single mutant strains to survive in such harsh conditions.

Gene function was not restored by complementation of Δ*mtp-hbhA* mutant, as observed by the similar infection rate as that of the double mutant, in contrast to that of the wild-type. This defect of the double complemented strain in attaining the same infectivity capability as the wild-type, may in part be explained by the fact that complementation was effected by an episomal rather than an integrative plasmid, and this may have imposed a fitness cost to the complemented strain, unlike the single complemented strains. Collectively, these findings

suggest that in the F15/LAM4/KZN susceptible strain, MTP and HBHA in combination, significantly influence the virulence of the strain.

2.5.1.4 Mycobacterium tuberculosis Rv0309 facilitates infection of THP-1 macrophages

In the present study, *in vitro* infection assays demonstrated a reduced capability of the *Rv0309* mutant strain in infecting the macrophages in comparison to the wild-type strain at both time points. During the 4-h time point, restoration was significantly lower than the wild-type. This may indicate that at the 4-h time point, the mutant and the complemented strains may behave in a similar way. In addition to this, complementation of the *Rv0309* gene restored gene function partially to the wild-type strain at the 24-h time point signifying that the reduced capability of the mutant in infecting the THP-1 macrophages was due to the absence of Ldt. Partial restoration of adhering capacity indicates that *Rv0309* is required for infection of *M. tuberculosis* within the host cells. This is similar to the study by Peng *et al*., (2022) which demonstrated that the expression of *Rv0309* enhanced the intracellular survival of *M. smegmatis* and BCG *in vivo* and *in vitro.* In addition to this, Peng *et al*., (2022) found that at 2-h post-infection, more Ms_*rv0309* cells than Ms_Vec cells (control) survived in macrophages. Further experiments in mice demonstrated that the lung bacterial load of mice infected with the *Rv0309* mutant strain was significantly lower than that of mice infected with wild-type at an 8-h time point (Peng *et al*., 2022). Moreover, Peng *et al*., (2022) deduced that their experimental findings could be due in part to the YkuD-like superfamily domain's L, D-transpeptidase catalytic site, which reduces cell wall permeability, increasing mycobacterial resistance to external stressors and thus intracellular survival. The results obtained by Peng *et al*., (2022) provided evidence that *Rv0309* is required for intracellular survival of *M. tuberculosis*. The present study showed reduced infection levels of the *Rv0309* deficient compared to the wild-type strain in THP-1 macrophages, thus supporting the findings by Peng *et al.,* (2022).

In response to various microbial infections, macrophages can be functionally polarized into M1 or M2 phenotypes, according to prior findings. In the study by Peng *et al*., (2022), the Rv0309 protein suppressed the production of M1-related cytokines (IL-1 and TNF-) resulting in bacterial survival in an *in vitro* experiment. It has been reported that TNF-α may inhibit and/or kill *M. tuberculosis* in the host cells (Shiloh *et al*., 2000; Yao *et al.,* 2018), induce autophagy, and enhance the fusion of *M. tuberculosis* phagosomes with auto phagosomes, allowing the

bacilli to be cleared from autophagolysosomes (Gutierrez *et al.*, 2004; Harris *et al*., 2009). The current study did not explore the host response mechanism and the response brought by TNF-α. From the present results, it can be hypothesized that *Rv0309* in the *M. tuberculosis* V9124 strain may have some inhibitory effect on the host response mechanism likely to contribute to intracellular *M. tuberculosis* survival.

2.5.2.1 Infection of macrophages with the mtp deficient strain influences gene expression.

Since the original study establishing the existence of pili in *M. tuberculosis* (Alteri *et al*., 2007), interest in further characterizing this pathogen's curli pili (MTP) has grown rapidly with the aim of investigating its potential as a biomarker for rapid diagnostics and treatments (Govender *et al*., 2014; Naidoo *et al*., 2014; Ramsugit and Pillay, 2015, Govender 2018, Ashokcoomar *et al*., 2020).

In this study, RT-qPCR was used to investigate the regulatory mechanism of the infecting *M. tuberculosis* on other adhesin genes from infected THP-1 cells to elucidate the *in vitro* role of MTP in gene regulation using a *mtp* gene mutant strain of *M. tuberculosis*. The number of infecting bacteria in THP-1 cells infected with the Δ*mtp* mutant strain was significantly lower than with the wild-type strain at both 4-h and 24-h. Concomitantly, the number of highly expressed genes induced during infection with Δ*mtp* strain at 24-h was decreased, suggesting that MTP influences gene expression in *M. tuberculosis*. The expression level of *Rv3763* and *Rv0934* in the mutant *mtp* was low at the 4-h time point relative to the complemented strain. The expression of *Rv3763*, *Rv3804*, *Rv1860* and *Rv0440* was higher in the mutant than the wild-type at 4-h. It may be possible that in the absence of *mtp* at 4-h, *M. tuberculosis* expresses these genes to compensate for the loss of *mtp* which at the later stage are being down regulated. Moreover, infection of THP-1 cells with Δ*mtp* induced a low expression of the genes *Rv3763*, *Rv0934*, *Rv3804*, *Rv1860* and *Rv0440* at 24-h time points. These findings suggest that the decrease in the gene expression levels is attributable to the significant decrease in the bacterial count due to the deletion of the *mtp* gene.

Differences in the number of expressed genes as well as the biological functions they are associated with, are most likely attributed to the different infecting pathogen strains. Schnappinger *et al*., (2003) compared the transcriptional profile of *M. tuberculosis* clinical isolate 1254 infecting the murine bone marrow macrophages to the actively growing strain in broth, using microarray technology and further confirmed the genes with RT-qPCR. A

comparison of the 4, 24, and 48-h post-infection periods revealed substantial changes in *M. tuberculosis* gene expression between 4-h and 24-h (Schnappinger *et al*., 2003). The *M. tuberculosis* expression patterns at 24-h and 48-h after infection, on the other hand, were quite comparable (Schnappinger *et al*., 2003). Moreover, Schnappinger *et al.,* (2003) found that after a 24-h time point, 454 of the *M. tuberculosis* genes were induced and 147 repressed. Upregulated genes were associated with transcriptional regulation, intermediary metabolism, lipid metabolism, iron acquisition, and stress response (Schnappinger *et al*., 2003). Their findings suggested that *M. tuberculosis* is most likely to alter its gene expression upon infection of the host cells.

In the present study, *in vitro* infection of the THP-1 cells by the Δ*mtp* strain resulted in a low expression of (*Rv0934*) *pstS-1* at 24-h. This gene encodes a mycobacterial cell wall adhesin that has been demonstrated to promote phagocytosis of mycobacteria via binding to the mannose receptor (Esparza *et al*., 2015). *Mycobacterium tuberculosis* PstS-1 is a major adhesin that facilitates binding to macrophages (Esparza *et al*., 2015). Peirs *et al*., (2005) showed that deletion of PstS-1 in *M. tuberculosis* impaired virulence. Low expression of PstS-1 by the Δ*mtp* strain may contribute to the reduced capability of *M. tuberculosis* to infect the host cells. In addition to this, the Δ*mtp* strain induced the expression of *Rv3763* (LpqH), another important *M. tuberculosis* virulence factor at the 4-h time point, and at the 24-h time point, the expression level of *Rv3763* was reduced compared to the wild-type. In contrast to *Rv3763* expression, the Δ*mtp* strain at the 4-h time point did not induce the expression of *Rv0934* compared to 24-h where *Rv0934* expression was also reduced compared to the wild-type. This could be explained by the fact that at first, gene expression occurs in a temporal fashion such that cell wall proteins and surface adhesins are expressed earlier, during the colonization phases of infection, whereas toxins and secreted proteins are expressed later, during the tissue-damaging phase of illness (Oscarsson *et al*., 2005; Oscarsson *et al.,* 2006; Xiong *et al*., 2006).

Phosphate-specific transporters may contribute to *M. tuberculosis* survival and appear to be involved in phosphate uptake from media with low phosphate concentrations (Peirs *et al*., 2005). The reduced expression of *Rv0934* in the mutant found in the current study may be explained by the presence of phosphate and other nutrients in the media. Also, the deletion of *mtp* gene from the mutant might have affected the pathways that utilize the phosphate leading to the phosphate not being used by the Δ*mtp* strain to the same extent as the wild-type. As the infection progressed to 24-h, the expression of *Rv0934* was slightly increased in the mutant indicating that there may have been a potential reduction in phosphate level in the media. In

the presence of the *mtp* gene in both the wild-type and the complemented strains, the level of *Rv0934* expression was high. This may indicate that the pathways that are involved in phosphate uptake were not affected and that the *Rv0934* gene was stimulated resulting in the uptake of phosphate which led to the increased expression of the gene.

The *Rv3763* gene encoding the 19 kDa antigen, a lipoprotein (lpqH) that is both cell wall-associated and released, has been extensively researched as a potential virulence factor. This protein interacts with TLR-2, inducing the production of IL-12 p40 when added to macrophages (Brightbill *et al*., 1999). The prolonged exposure of cells to 19 kDa has negative effects (Pennini *et al*., 2006). In the current study, the Δ*mtp* strain induced the expression of *Rv3763* at both time points, albeit reduced at 24-h in comparison to the wild type, as well as compared to the 4-h time point. The deletion of the *mtp* gene in the mutant strain might have affected the pathways that are involved in cell wall synthesis.

Ashokcoomar *et al*., (2020) compared the Δ*mtp* and wild-type strains and found a total of 27 metabolites to be biologically significant, which explained the reduced cell wall biogenesis, fatty acid metabolism, amino acid metabolism, protein synthesis, and peptidoglycan synthesis exhibited in the Δ*mtp* strain in that study. Furthermore, when the Δ*mtp* strain was compared to the wild-type strain, Ashokcoomar *et al.*, (2020) found seven significant metabolites, all of which were associated with cell envelope functionality. The results from the study by Ashokcoomar *et al.*, (2020) indicated the significance of the *mtp* gene in cell wall activities. In the current study, the deletion of the *mtp* gene in the mutant strain might have affected the acylation and *O*-glycosylation processes which are required for the protein to remain in the cell wall. Inhibiting acylation or glycosylation leads to decreased proliferation and pathogenicity in *M. tuberculosis* (Becker *et al*., 2017). The conservation of lipoprotein glycosylation in *M. tuberculosis* and *M. abscessus* suggests the presence of an O-glycosylation motif or other regulatory mechanisms governing this post-translational modification. The deletion of the *pmt* gene in the *M. abscessus* increased the cell wall permeability and caused the reduced capability of the mutant to establish infection and to survive inside the macrophages (Becker *et al*., 2017).

Similarly, the current *in vitro* infection results demonstrated a reduced capability of the Δ*mtp* strain to initiate infection in the macrophages. The deletion of the *mtp* gene is most likely to affect the expression of the *Rv3763* gene. In addition to this, the 19 kDa protein is acylated and glycosylated (Wilkinson *et al*., 2009). The current RT-qPCR data suggested that the absence of *mtp* gene is associated with the downregulation of major adhesins that are associated with

cell wall functioning. In addition to this, the decrease in the expression of *Rv3763* by the mutant strain may indicate the inability of the mutant to utilize the metabolites that are associated with the cell wall synthesis.

It is well recognized that the specific lipid components of mycobacteria contribute to the pathogen's effectiveness, and as a result, this has been pharmacologically important (Barry *et al*., 1998; Kinsella *et al.,* 2003). Ashokcoomar *et al.,* (2020) detected several lipid metabolites that were involved in the production of fatty acids necessary for cell envelope biogenesis. Furthermore, Ashokcoomar *et al.,* (2020) found that the Δ*mtp*-infected cells exhibited relatively lower concentrations of lipid metabolites compared to the wild-type-infected cells, most likely leading to a compromised mycobacterial cell envelope during the infection process. The expression of cell wall lipids may be further reduced in the mutant, jeopardizing the *M. tuberculosis* cell envelope's overall integrity and permeability.

Lipoproteins are post-translationally modified with lipid- and glycosyl-residues, and interfering with acylation or glycosylation causes decreased growth and pathogenicity in *M. tuberculosis* (Becker *et al*., 2017). The deletion of the *mtp* gene in the mutant might have resulted in the reduction of lipid metabolites that are necessary for *M. tuberculosis* cell wall integrity. This may be seen by the decreased expression of *Rv3763* by the Δ*mtp* strain. In addition to this, the deletion of the *mtp* gene might have resulted in conditions that caused the downregulation of biosynthesis of cell wall lipids. These findings indicate the significance of *mtp* as an adhesin molecule and that the deletion in the *mtp* gene results in altered cell wall activities.

Rv0440 encodes Cpn60.2 also known as groeL2. The Cpn60.2 and DnaK are two mycobacterial conserved chaperones from the heat shock protein (HSP) family (Cehovin *et al.,* 2010) that have been discovered as CD43 ligands (Wilkinson *et al.,* 2009). The CD43 is a heavily glycosylated and sialic transmembrane type 1 protein that regulates the first contact of a cell (Howell *et al*., 1994). In the current study, the expression *Rv0440* was high in the Δ*mtp* strain at 4-h compared to the wild-type. Also, the expression of *Rv0440* at 24-h was reduced indicating a downregulation by the Δ*mtp* strain, suggesting a potential disturbance in CD43 ligand. This may be due to altered cell wall activities which are caused by the inability of the Δ*mtp* strain to utilize the metabolites that are associated with cell wall biogenesis. The *Rv0440* expression was be high in the the *mtp* complemented strain, indicating that gene expression was restored to that of the wildtype, suggestive of the significance of the *mtp* gene in the

expression of *Rv0440*. The overexpression of the gene in the complement may be due to the complementation being done via an episomal plasmid.

Rv0440 has been known to be expressed under stressful conditions (Henderson *et al*., 2010). In this study, the deletion of the *mtp* gene in the mutant strain might have altered the activity of *M. tuberculosis* resulting in a reduced stress response. It is known that upon infection, host cells respond to the invading pathogen by secreting cytokines that regulate the host response thus creating some intracellular stress on the pathogen. *Mycobacterium tuberculosis* alters its cell wall architecture in response to *in vitro* stressors that are thought to be related to infection including cell wall thickening and changes in surface lipid and protein content (Cunningham and Spreadbury, 1998; Singh *et al*., 2009). When Singh *et al*. (2009) discovered that the *M. tuberculosis* WhiB3 transcription factor responds to fluctuations in the intracellular redox environment by directing the synthesis of virulence lipids that may act as a reductant sink, such changes in the cell surface were linked to resistance to host stress. Similarly, the deletion of *mtp* gene may have affected the pathways that are involved with cell wall thickening and protein synthesis, thus resulting in the altered cell wall phenotype which may have further reduced the ability of the mutant to withstand host stress.

It was deduced that the deletion of the *mtp* gene in the mutant might have resulted in the low expression of *Rv0440* as a result of the low-stress level induced by the host cell as a response to the pathogen invasion. Also, silencing the expression of *Rv0440* is fatal to mycobacteria, proving that it is required for mycobacterial survival (Hu *et al.*, 2008; Cehovin *et al.*, 2010;). However, the current study did not explore the deletion of *Rv0440* in *M. tuberculosis.* We showed that the deletion of the *mtp* gene in the mutant strain alters the expression of the *R0440* gene at 24-h time point. This demonstrates the importance of *mtp* as a candidate biomarker for vaccine and drug development.

The macrophage phagosome harbouring *M. tuberculosis* is known to be nutrition and iron limiting (Schnappinger *et al.*, 2003; Podinovskaia *et al*., 2013). Depending on the organism and the intracellular target of microbial effector molecules, bacterial pathogens can manipulate host cellular processes in a variety of ways (Knodler *et al.*, 2003). When *M. tuberculosis's* intra-phagosomal expression profile is compared to that of *Escherichia coli* (Staudinger *et al*., 2002) and *Salmonella enterica* (Eriksson *et al.*, 2003), it is clear that the conditions these microorganisms experience within the host cells differ. In response to heat, the increased production of heat shock proteins which include molecular chaperones essential for the proper

folding of freshly produced and denatured proteins occurs when the heat shock response is induced (Hendrick and Hartl, 1993). In this study, infection with the wild-type and the mutant *mtp* strain at the 4-h time resulted in no expression of the *Rv0350*. The *Rv3050* gene encoding DnaK is expressed in response to heat shock. Hu *et al*., (2000) found the mRNA identified by RT-PCR to be persistent in bacteria at 37 °C, and at a temperature of 45°C, mRNA encoding DnaK level was increased. Stewart *et al*., (2002) found that mRNA encoding DnaK identified using DNA microarray technology was upregulated in high temperatures and was possibly down-regulated by the presence of *Rv0353* and *Rv2374c*. In this study, *in vitro* infection assays were performed at 37 °C, a temperature that mimics the human body temperature. The lack of expression observed in the wild-type and the mutant strains could be explained by the temperature that was used in the *in vitro* infection assays. In addition to this, the presence of the *mtp* gene in the wild-type might not have affected the expression of *Rv0350* at 4-h time point. At 24-h time point the wild-type induced the expression of *Rv0350* which is also involved in folding of newly synthesised proteins (Hesterkamp and Bukau, 1998). Expression of *Rv0350* by the wild-type and the complemented strains at 24-h time could have been due to the new proteins being synthesized as the infection progressed from 4-h to 24-h. Moreover, complementation of the *mtp* gene induced the expression of *Rv0350* at both time-points. This pattern of expression seen in the *mtp* complement may be due to the overexpression of *mtp* gene by the complementing episomal vector.

Mycobacterium tuberculosis has been shown to bind laminin and fibronectin. Among the *M. tuberculosis* proteins that binds to fibronectins are Antigen 85 complex denoted by 85A, 85B, and 85C, which are encoded by three genes located at different sites in the mycobacterial genome (Wiker and Harboe,1992). Antigen 85 complex may aid in the adhesion, invasion, and dissemination of organisms in host tissue since Fn-binding proteins are thought to be key virulence factors in *Mycobacterium spp*. In the current study, deletion of the *mtp* gene induced the expression of *Rv3804* at an early time point. *Rv3804* encodes Ag85c which is involved in cell wall mycoloylation. In addition to this, *Rv3804* has a mycolyl-transferase activity that is essential for the synthesis of trehalose dimycolate (cord factor), a major structure that keeps cell walls intact (Viljoen *et al*., 2018). In *M. tuberculosis*, loss of Ag85C causes cell wall-linked mycolates to be depleted, but ag85A and ag85B mutants have normal cell wall-associated mycolate levels (Backus *et al*., 2014). However, the present study did not test deletion of the Ag85C protein, but demonstrated that deletion of the *mtp* gene in the mutant might have

induced the expression of *Rv3804* to compensate for the loss of function of the *mtp* gene which is associated with cell wall and cell wall processes.

2.5.2.2 Infection with ΔhbhA induced high expression of all the genes at a 24-h time point compared to other strains.

The heparin-binding hemagglutinin antigen is a surface-associated as well as secreted protein (Pethe *et al*., 2001). *Mycobacterium tuberculosis* HBHA has been reported to be essential for TB bacilli to spread from the lungs to other tissues and is involved in the binding of *M. tuberculosis* to type II pneumocytes, but not to professional phagocytes like macrophages (Pethe *et al.,* 2001). Its impact on macrophages has received comparatively little research in this regard. However, it was recently discovered that HBHA can bind to complement component C3 and that recombinant HBHA can mediate the attachment of latex beads to murine macrophage-like cells in both C3-dependent and C3-independent ways (Mueller-Ortiz *et al*., 2001). These findings point to the possibility of HBHA and macrophage interaction during mycobacterial infection.

When the Δ*hbhA* strain was used to infect THP-1 cells, more genes were expressed at the 4-h time point compared to the other strains used in this study. The wild-type strain did not induce the expression of *Rv3660* and *Rv0350* genes at the 4-h time point. In *M. tuberculosis, Rv3660* has been reported to encode a septum determining factor (*ssd*) that has been shown to play an important role in cell division (England *et al*., 2011). When gene expression in the *M. tuberculosis ssd* merodiploid strain was examined, it was discovered that there was a Dos-like response characterized by upregulation of genes involved in fatty acid degradation, anaerobic respiration, electron transport or redox potential, and downregulation of ribosomal proteins and protein synthesis in conjunction with induction of the *dosR* regulon (England *et al*., 2011). The current findings suggest that deletion of the *hbhA* gene in the mutant induced the expression of *Rv3660* which in turn may likely induce the expression of the genes that regulate stress. England *et al*., (2011) found that increased *ssd* expression induced a novel response in *M. tuberculosis*, including the dormancy regulon and alternative sigma factors, which are considered to have a role in adaptive metabolism, according to transcriptional mapping. The deletion of the *hbhA* gene in the mutant might have increased stress at the earlier time point. The expression of the *hbhA* gene at 4-h in the wild-type might have repressed the expression of the *Rv0350* gene. This may imply that *Rv0350* is more expressed by all strains at the later

stage of infection regardless of the presence or the absence of the *hbhA* gene. The activity of *Rv0350* is repressed by the presence of other genes (Kapopoulou *et al.*, 2011) . However, complementation of the *hbhA* gene in this study restored the expression of *Rv0350* at the early time point, possibly due to the overexpressing episomal vector.

In response to infection, host cells try to reduce the number of nutrients available to the intracellular bacteria (Zhang and Rubin, 2013), thus creating the intracellular stress for the infecting pathogen. In addition to this, the presence of particular conditions *in vitro*, including hypoxia, nutrient starvation, nitric oxide (NO) exposure and acidic pH causes *M. tuberculosis* to alter its transcriptional profile (Sherman *et al*., 2001; Betts *et al*., 2002). Expression of the genes *Rv3763, Rv0934, Rv3804, Rv0350* and *Rv0440* could contribute to the *M. tuberculosis*-host interaction. The deletion of the *hbhA* gene in the mutant resulted in the high expression of *Rv3763, Rv0934* and *Rv3804* at 4-h compared to the wild-type strain. These genes were reported to contribute to the binding of *M. tuberculosis* to THP- cells. The 19 kDa and PstS-1 proteins have been identified as important virulence factors for *M. tuberculosis*. In addition to this, both PstS-1 (Sanchez *et al*., 2009) and LpqH (Ciaramella *et al*., 2000; López *et al*., 2003) have been associated with apoptosis of macrophages. Moreover, the HBHA antigen has been associated with apoptosis of macrophages (Choi *et al*., 2013). Choi *et al*., (2013) revealed that HBHA activation generates reactive oxygen species (ROS) by disrupting intracellular Ca^{2+} homeostasis and that ROS increases the overproduction of pro-inflammatory cytokines, resulting in endoplasmic reticulum (ER) stress-mediated death in macrophages. However, the present study did not focus on the apoptotic pathways induced by HBHA protein, but showed that *M. tuberculosis* most likely compensated for the loss of *hbhA* gene by upregulation of the genes. The expression of all genes in the Δ*hbhA* might have increased the virulence of the *hbhA* in deletion mutant thus contributing to cell death. These findings suggest that HBHA can have a detrimental effect on macrophages.

The expression of adhesion genes in this study by different strains might indicate that HBHA is most likely to participate in the pathogenicity of *M. tuberculosis*. In this study, deletion of the *hbhA* gene did not affect the expression of three major adhesins that facilitate the binding of *M. tuberculosis* to THP-1 cells i.e. *Rv3763, Rv0934* and *Rv0440*. This was observed in the wild-type and the complemented strains. Such expression is due to the deletion of *hbhA* in the mutant.

2.5.2.3 The deletion of mtp and hbhA in M. tuberculosis V9124 influences gene expression of the strain during infection of THP-1 macrophages.

The present study supports a role for MTP and HBHA in the regulation of adhesins that facilitates the translocation of *M. tuberculosis* into macrophages. The ability of the double knockout mutant strain to infect macrophages was more impaired compared to the single knockout of individual genes. In the current study, the combined *mtp* deletion caused decreased expression of the major adhesins that facilitate binding to THP-1 cells. Overall, the results indicate an extreme defect in ability of the *Δmtp-hbhA* strain to induce expression of *Rv3763, Rv0934, Rv3804, Rv0350* and *Rv3660* at 4-h. This in turn may possibly retard the ability of the *Δmtp-hbhA* to infect the macrophages. This is supported by the observation that the *Δmtp-hbhA* strain displayed low capability to infect THP-1 cells as evidenced by their low colony counts. Involvement of the *mtp-hbhA* regulatory system during the infection of THP-1 macrophages with *M. tuberculosis* was also evident as demonstrated by the upregulation of studied genes in the wild-type and the complemented strains. However, only two genes were not expressed by the wild-type at 4-h (*Rv0350* and *Rv3660*) compared to the 24-h. As discussed above, *hbhA* is most likely to induce apoptosis in macrophages. As a result, it can be surmised that *hbhA* complement over-expression of HBHA may have induced macrophage cell death at a higher rate than MTP strains, resulting in a decrease in the number of bacteria in the macrophages. In addition to this, it is most likely that the observed expression of genes in the double knockout may be attributed to the deletion of the *mtp* gene. This is because the deletion of the *mtp* gene alone resulted in the decreased expression of the genes in a similar pattern as observed in a double knockout mutant strain. Taken together, these findings suggest that MTP independently plays a larger role in the infection of macrophages than HBHA.

2.5.2.4 ΔRv0309 induced the highest expression of Rv3763, Rv0934, Rv3804, Rv3660, Rv1860 and Rv0440 at the 4-h time point

In this study, the *in vitro* role of the *Rv0309* gene was evaluated by infecting the THP-1 cells with the wild-type, Δ*Rv0309* strain and with the *Rv0309* complemented strain. The Δ*Rv0309 M. tuberculosis* strain induced high expression of the gene *Rv3763* in the mutant compared to the wild-type at both time points. The induced expression of *Rv3763* by the mutant is most likely attributable to the impact of *Rv0309* on cell wall permeability. *Rv0309* has been shown to promote the intracellular survival of *M. tuberculosis* (Peng *et al.,* 2022). The removal of *Rv0309* in the mutant strain induced high expression of the genes that are essential for the survival of *M. tuberculosis* under stressful conditions. *Rv0934* was one of the genes that was highly expressed at the 4-h time point. Under phosphate deprivation, the *Rv0934* gene is most likely to be expressed to contribute to the survival of *M. tuberculosis*. This may indicate the importance of the *Rv0309* gene in controlling cell wall permeability. The current findings suggest increased virulence in mycobacteria subjected to deletion of the *Rv0309* gene at an early time point. This is also supported by the expression of important virulence factors of *M. tuberculosis* such as *Rv3763*, *Rv0934* and *Rv1860* which may support that the *Rv0309* protein may be conducive to the intracellular survival of mycobacteria at the early stage of infection.

There is a great deal of knowledge concerning the role that membrane proteins of *M. tuberculosis* and other microorganisms may play in TB pathogenesis (Målen *et al*., 2008). *Mycobacterium tuberculosis* membrane proteins may also harm host cell function. In this study, deletion of the *Rv0309* gene in the mutant strain resulted in the expression of other membrane proteins that are involved in TB pathogenesis. The Apa antigen encoded by *Rv1860* is important for *M. tuberculosis* virulence because it acts as a mycolyl-transferase, catalysing the attachment of mycolic acids to arabinogalactan and synthesis of cord factor, a very active virulence factor (Babaki *et al*., 2017). Infection of THP-1 cells with the Δ*Rv0309* strain elevated the levels of *Rv1860* at both time points, suggesting its role as an important adhesin in the binding to THP-1 cells.

The *Rv3660* gene encodes type-IV pili which mediate different functions in Gram-positive and Gram-negative bacteria including biofilm formation, DNA uptake, adhesion to host cells, and mortality (Reguera *et al*., 2002, Piepenbrink and Sundberg, 2016). *Mycobacterium tuberculosis* expresses type-IV pili, which appear as rope-like bundles on the cell surface under electron

microscopy (Kolbe *et al.*, 2019). The mature type-IV pili are encoded by a seven-gene operon, the expression of which is increased when A549 epithelial cells and macrophages come into contact (Hosseini *et al*., 2014, Kolbe *et al*., 2019). However, the significance of type-IV pili in *M. tuberculosis* pathogenicity has hitherto not been investigated. Expression of *Rv3660* by the Δ*Rv0309* strain at 4-h followed the same pattern of expression as seen in the Δ*mtp* strain. In the wild-type strains at an early stage of infection, expression of the *Rv3660* gene was silenced. Moreover, *Rv0309* has been associated with the cell wall and cell processes. The expression of *Rv3660* by the mutant strain could most likely be attributed to the absence of *Rv0309* which may have upregulated *Rv3660* to try to compensate for the loss of function of *Rv0309*. The *Rv3660* gene has been shown to be involved in the cellular differentiation process (Kapopoulou *et al.*, 2011). The deletion of *Rv0309* in the mutant also induced high expression of *Rv3804* in the mutants at both time points. Moreover, *Rv3804* expression was much higher at the 4-h time point than at 24-h where the expression was also high. *Rv3804* is responsible for the high affinity of mycobacteria to bind to fibronectin and laminin (Kumar *et al.*, 2013). Moreover, *Rv3804* has a mycolyl-transferase activity that is critical for the synthesis of trehalose dimycolate (cord factor), a prominent structure important for preserving cell wall integrity (Ronning *et al*., 2000). *Rv0309* is also a fibronectin binding adhesin (Kumar *et al*., 2013). The high expression of the *Rv3804* in both time points could also be attributed to deletion of the *Rv0309* gene which functions in cell wall processes. Deletion of the *Rv0309* gene might have caused upregulation of the *Rv3804* gene to try to compensate for the loss of function of *Rv0309*.

The deletion of *Rv0309* in the mutant resulted in a high expression of Apa gene encoded by *Rv1860*. Alanine- and proline-rich antigen is heavily glycosylated with O-mannosylation occurring in the threonine residues (Dobos *et al*., 1996). The substantial O-mannosylation is the fundamental characteristic that determines Apa protein recognition by host cell receptors. Pulmonary surfactant protein and C-type lectin receptors such as DC-SIGN and macrophage mannose receptors bind to Apa (Ragas *et al*., 2007). The Apa has also been implicated in cell walls and cell processes. The deletion of the *Rv0309* gene might have affected the cell wall processes which may have resulted in the upregulation of *Rv1860* to compensate for the loss of function of the *Rv0309* gene in the mutant. *Rv1860* expression was elevated at 4-h and doubled at 24-h of infection. This may also indicate that deletion of *Rv0309* results in altered activity of cell wall process which further stimulates the activity of other genes to compensate for the loss of the *Rv0309* gene in the deletion mutants.

The results from this study demonstrated that HBHA and MTP independently play a role in the regulatory mechanism of *M. tuberculosis.* In the absence of both genes, the *M. tuberculosis* resulted in reduced capability to infect the THP-1 cells due to the altered expression of the adhesion genes. The deletion of *mtp* implied a decline in pathogenicity as a result of the decrease in genes associated with the virulence of the strain. The absence of the individual genes *Rv0309* and *hbhA*, induced the high expression of the genes that are important in the virulence of *M. tuberculosis* as a compensatory mechanism for the loss of these genes. This study revealed the impact of MTP, HBHA and Rv0309 on the regulation of other adhesin that are associated with *M. tuberculosis* pathogenicity.

The study investigated the role of specific adhesins genes on the regulation of other adhesins genes using RT-qPCR. Only the selected adhesins that facilitate binding of *M. tuberculosis* to macrophages were studied. In addition, only one clinical strain of *M. tuberculosis* was used, and the results obtained in this study cannot be extrapolated to other clinical strains of the same family. Confirmation of phenotypic expression of the proteins failed using the western blot assays (see Chapter 3).

It would be useful for future studies to include different clinical strains from the same family of *M. tuberculosis.* Also, future experiments should also investigate the regulation role on the time points outside 24-h. Phenotypic expression of the studied genes need to be conducted using validated antibodies. Moreover, the volume of the infecting bacteria needs to be up scaled in order to obtain sufficient number of intracellular pathogen to increase protein concentration for phenotypic expression studies.

2.6 References

Alteri, C.J., Xicohténcatl-Cortes, J., Hess, S., Caballero-Olín, G., Girón, J.A. and Friedman, R.L., 2007. *Mycobacterium tuberculosis* produces pili during human infection. *Proceedings of the National Academy of Sciences*, 104(12), pp.5145-5150.

Ashokcoomar, S., Reedoy, K.S., Senzani, S., Loots, D.T., Beukes, D., Van Reenen, M., Pillay, B. and Pillay, M., 2020. *Mycobacterium tuberculosis* curli pili (MTP) deficiency is associated with alterations in cell wall biogenesis, fatty acid metabolism and amino acid synthesis. *Metabolomics*, 16(9), pp.1-15.

Babaki, M.K.Z., Soleimanpour, S. and Rezaee, S.A., 2017. Antigen 85 complex as a powerful *Mycobacterium tuberculosis* immunogene: Biology, immune-pathogenicity, applications in diagnosis, and vaccine design. *Microbial Pathogenesis*, 112, pp.20-29.

Backus, K.M., Dolan, M.A., Barry, C.S., Joe, M., McPhie, P., Boshoff, H.I., Lowary, T.L., Davis, B.G. and Barry, C.E., 2014. The three *Mycobacterium tuberculosis* antigen 85 isoforms have unique substrates and activities determined by non-active site regions. *Journal of Biological Chemistry*, 289(36), pp.25041-25053.

Balgobin (2018) Whole genome transcript analysis to elucidate the role of the *Mycobacterium tuberculosis* pili (MTP) in gene regulation of THP-1 macrophages. Masters dissertation in preparation.

Bardarov, S., Bardarov Jr, S., Pavelka Jr, M. S., Sambandamurthy, V., Larsen, M., Tufariello, J., Chan, J., Hatfull, G. and Jacobs Jr, W. R. 2002. Specialized transduction: An efficient method for generating marked and unmarked targeted gene disruptions in *Mycobacterium tuberculosis*, *M. bovis* BCG and *M. smegmatis*. *Microbiology*, 148, 3007-3017.

Barry III, C.E., Lee, R.E., Mdluli, K., Sampson, A.E., Schroeder, B.G., Slayden, R.A. and Yuan, Y., 1998. Mycolic acids: structure, biosynthesis and physiological functions. *Progress in lipid Research*, 37(2-3), pp.143-179.

Becker, K., Haldimann, K., Selchow, P., Reinau, L.M., Dal Molin, M. and Sander, P., 2017. Lipoprotein glycosylation by protein-O-mannosyltransferase (MAB_1122c) contributes to low cell envelope permeability and antibiotic resistance of *Mycobacterium abscessus*. *Frontiers in Microbiology*, 8, p.2123.

Betts, J.C., Lukey, P.T., Robb, L.C., McAdam, R.A. and Duncan, K., 2002. Evaluation of a nutrient starvation model of *Mycobacterium tuberculosis* persistence by gene and protein expression profiling. *Molecular Microbiology*, 43(3), pp.717-731.

Brightbill, H.D., Libraty, D.H., Krutzik, S.R., Yang, R.B., Belisle, J.T., Bleharski, J.R., Maitland, M., Norgard, M.V., Plevy, S.E., Smale, S.T. and Brennan, P.J., 1999. Host defense mechanisms triggered by microbial lipoproteins through toll-like receptors. *Science*, 285(5428), pp.732-736.

Cehovin, A., Coates, A.R., Hu, Y., Riffo-Vasquez, Y., Tormay, P., Botanch, C., Altare, F. and Henderson, B., 2010. Comparison of the moonlighting actions of the two highly homologous chaperonin 60 proteins of *Mycobacterium tuberculosis*. *Infection and Immunity*, 78(7), pp.3196-3206.

Choi, J.A., Lim, Y.J., Cho, S.N., Lee, J.H., Jeong, J.A., Kim, E.J., Park, J.B., Kim, S.H., Park, H.S., Kim, H.J. and Song, C.H., 2013. Mycobacterial HBHA induces endoplasmic reticulum stress-mediated apoptosis through the generation of reactive oxygen species and cytosolic Ca2+ in murine macrophage RAW 264.7 cells. *Cell Death & Disease*, 4(12), pp.e957-e957.

Ciaramella A, Martino A, Cicconi R, Colizzi V and Fraziano M. Mycobacterial 19-kDa lipoprotein mediates *Mycobacteriumtuberculosis*-induced apoptosis in monocytes/macrophages at early stages of infection. *Cell Death and Differentiation*. 2000;7(12):1270–1272.

Cunningham, A.F. and Spreadbury, C.L., 1998. Mycobacterial stationary phase induced by low oxygen tension: cell wall thickening and localization of the 16-kilodalton α-crystallin homolog. *Journal of Bacteriology*, 180(4), pp.801-808.

Diaz-Silvestre, H., Espinosa-Cueto, P., Sanchez-Gonzalez, A., Esparza-Ceron, M.A., Pereira-Suarez, A.L., Bernal-Fernandez, G., Espitia, C. and Mancilla, R., 2005. The 19-kDa antigen of *Mycobacterium tuberculosis* is a major adhesin that binds the mannose receptor of THP-1 monocytic cells and promotes phagocytosis of mycobacteria. *Microbial Pathogenesis*, 39(3), pp.97-107.

Dlamini MT (2016) Whole transcriptome analysis to elucidate the role of MTP in gene regulation of pulmonary epithelial cells infected with *Mycobacterium tuberculosis*. Masters Dissertation, University of KwaZulu-Natal.

Dobos, K.M., Khoo, K.H., Swiderek, K.M., Brennan, P.J. and Belisle, J.T., 1996. Definition of the full extent of glycosylation of the 45-kilodalton glycoprotein of *Mycobacterium tuberculosis*. *Journal of Bacteriology*, 178(9), pp.2498-2506.

England, K., Crew, R. and Slayden, R.A., 2011. *Mycobacterium tuberculosis* septum site determining protein, Ssd encoded by rv3660c, promotes filamentation and elicits an alternative metabolic and dormancy stress response. *BMC Microbiology*, 11(1), pp.1-12.

Eriksson, S., Lucchini, S., Thompson, A., Rhen, M. and Hinton, J.C., 2003. Unravelling the biology of macrophage infection by gene expression profiling of intracellular *Salmonella enterica*. *Molecular Microbiology*, 47(1), pp.103-118.

Esparza, M., Palomares, B., García, T., Espinosa, P., Zenteno, E. and Mancilla, R., 2015. PstS-1, the 38-kDa *Mycobacterium tuberculosis* Glycoprotein, is an Adhesin, Which Binds the Macrophage Mannose Receptor and Promotes Phagocytosis. *Scandinavian journal of Immunology*, 81(1), pp.46-55.

Fenton, M.J. and Vermeulen, M.W., 1996. Immunopathology of tuberculosis: roles of macrophages and monocytes. *Infection and Immunity*, 64(3), p.683.

Fontán, P., Aris, V., Ghanny, S., Soteropoulos, P. and Smith, I., 2008. Global transcriptional profile of *Mycobacterium tuberculosis* during THP-1 human macrophage infection. *Infection and Immunity*, 76(2), pp.717-725.

Gandhi, N. R., Moll, A., Sturm, A. W., Pawinski, R., Govender, T., Lalloo, U., Zeller, K., Andrews, J. & Friedland, G. 2006. Extensively drug-resistant tuberculosis as a cause of death in patients co-infected with tuberculosis and HIV in a rural area of South Africa. *The Lancet*, 368, 1575-1580.

Geissmann, F., Manz, M.G., Jung, S., Sieweke, M.H., Merad, M. and Ley, K., 2010. Development of monocytes, macrophages, and dendritic cells. *Science*, 327(5966), pp.656-661.

Gerlach, R.G. and Hensel, M., 2007. Protein secretion systems and adhesins: the molecular armory of Gram-negative pathogens. *International Journal of Medical Microbiology*, 297(6), pp.401-415.

Govender, V. S., Ramsugit, S. and Pillay, M. 2014. *Mycobacterium tuberculosis* adhesins: potential biomarkers as anti-tuberculosis therapeutic and diagnostic targets. Microbiology, 160, 1821-1831.

Govender, V.S., 2018. Investigating the *in vitro* roles played by the major adhesins HBHA and MTP in the pathogenesis of *M. tuberculosis,* in a novel double gene knock-out mutant strain (Doctoral thesis).

Gutierrez, M.G., Master, S.S., Singh, S.B., Taylor, G.A., Colombo, M.I. and Deretic, V., 2004. Autophagy is a defense mechanism inhibiting BCG and *Mycobacterium tuberculosis* survival in infected macrophages. *Cell*, 119(6), pp.753-766.

Harris, J., Hope, J.C. and Lavelle, E.C., 2009. Autophagy and the immune response to TB. *Transboundary and emerging diseases*, 56(6-7), pp.248-254.

Henderson, B., Lund, P.A. and Coates, A.R., 2010. Multiple moonlighting functions of mycobacterial molecular chaperones. *Tuberculosis*, 90(2), pp.119-124.

Hendrick, J.P. and Hartl, F.U., 1993. Molecular chaperone functions of heat-shock proteins. *Annual Review of Biochemistry*, 62(1), pp.349-384.

Hesterkamp, T. and Bukau, B., 1998. Role of the *DnaK* and *HscA* homologs of Hsp70 chaperones in protein folding in *E. coli*. *The EMBO Journal*, 17(16), pp.4818-4828.

Hickey, T.B., Thorson, L.M., Speert, D.P., Daffé, M. and Stokes, R.W., 2009. *Mycobacterium tuberculosis* Cpn60. 2 and DnaK are located on the bacterial surface, where Cpn60. 2 facilitates efficient bacterial association with macrophages. *Infection and Immunity*, 77(8), pp.3389-3401.

Hickey, T.B., Thorson, L.M., Speert, D.P., Daffé, M. and Stokes, R.W., 2009. *Mycobacterium tuberculosis* Cpn60. 2 and DnaK are located on the bacterial surface, where Cpn60. 2 facilitates efficient bacterial association with macrophages. *Infection and Immunity*, 77(8), pp.3389-3401.

Hosseini, H., Fooladi, A.A.I., Arjomandzadegan, M., Emami, N. and Bornasi, H., 2014. Genetics study and transmission electron microscopy of pili in susceptible and resistant clinical isolates of *Mycobacterium tuberculosis*. Asian Pacific Journal of Tropical Medicine, 7, pp.S199-S203.

Howell, D.N., Ahuja, V., Jones, L., Blow, O. and Sanfilippo, F.P., 1994. Differential expression of CD43 (leukosialin, sialophorin) by mononuclear phagocyte populations. *Journal of leukocyte Biology*, 55(4), pp.536-544.

Hu, Y., Mangan, J.A., Dhillon, J., Sole, K.M., Mitchison, D.A., Butcher, P.D. and Coates, A.R., 2000. Detection of mRNA transcripts and active transcription in persistent *Mycobacterium tuberculosis* induced by exposure to rifampin or pyrazinamide. *Journal of Bacteriology*, 182(22), pp.6358-6365.

Hu, Y., Henderson, B., Lund, P.A., Tormay, P., Ahmed, M.T., Gurcha, S.S., Besra, G.S. and Coates, A.R., 2008. A *Mycobacterium tuberculosis* mutant lacking the groEL homologue cpn60. 1 is viable but fails to induce an inflammatory response in animal models of infection. *Infection and Immunity*, 76(4), pp.1535-1546.

Hummon, A.B., Lim, S.R., Difilippantonio, M.J. and Ried, T., 2007. Isolation and solubilization of proteins after TRIzol® extraction of RNA and DNA from patient material following prolonged storage. *Biotechniques*, 42(4), pp.467-472.

Iona, E., Pardini, M., Gagliardi, M.C., Colone, M., Stringaro, A.R., Teloni, R., Brunori, L., Nisini, R., Fattorini, L. and Giannoni, F., 2012. Infection of human THP-1 cells with dormant *Mycobacterium tuberculosis*. *Microbes and Infection*, 14(11), pp.959-967.

Johnson, B.K. and Abramovitch, R.B., 2015. Macrophage infection models for *Mycobacterium tuberculosis*. In *Mycobacteria Protocols* (pp. 329-341). Humana Press, New York, NY.

Kapopoulou, A., Lew, J. M. and Cole, S. T. 2011. The MycoBrowser portal: A comprehensive and manually annotated resource for mycobacterial genomes. *Tuberculosis*, 91, 8-13.

Kinsella, R.J., Fitzpatrick, D.A., Creevey, C.J. and McInerney, J.O., 2003. Fatty acid biosynthesis in *Mycobacterium tuberculosis*: lateral gene transfer, adaptive evolution, and gene duplication. *Proceedings of the National Academy of Sciences*, 100(18), pp.10320-10325.

Kline, K.A., Fälker, S., Dahlberg, S., Normark, S. and Henriques-Normark, B., 2009. Bacterial adhesins in host-microbe interactions. *Cell Host & Microbe*, 5(6), pp.580-592.

Knodler, L.A., Celli, J. and Finlay, B.B., 2001. Pathogenic trickery: deception of host cell processes. *Nature Reviews Molecular Cell Biology*, 2(8), pp.578-588.

Kolbe, K., Veleti, S.K., Reiling, N. and Lindhorst, T.K., 2019. Lectins of *Mycobacterium tuberculosis*–rarely studied proteins. Beilstein Journal of Organic Chemistry, 15(1), pp.1-15.

Kumar, S., Puniya, B.L., Parween, S., Nahar, P. and Ramachandran, S., 2013. Identification of novel adhesins of *M. tuberculosis* H37Rv using integrated approach of multiple computational algorithms and experimental analysis. *PLoS One*, 8(7), p.e69790

Kuvar S (2016) The role of *hbhA* in gene regulation *in vivo* using a *hbhA* knockout mutant of *M. tuberculosis*. Masters Dissertation, University of KwaZulu-Natal.

Larsen, M. H., Biermann, K., Tandberg, S., Hsu, T., and Jacobs Jr, W. R. (2007). Genetic manipulation of *Mycobacterium tuberculosis*. *Current Protocols in Microbiology*, 6(1), 10A-2.

López, M., Sly, L.M., Luu, Y., Young, D., Cooper, H. and Reiner, N.E., 2003. The 19-kDa *Mycobacterium tuberculosis* protein induces macrophage apoptosis through Toll-like receptor-2. *The Journal of Immunology*, 170(5), pp.2409-2416.

Målen, H., Berven, F.S., Søfteland, T., Arntzen, M.Ø., D'Santos, C.S., De Souza, G.A. and Wiker, H.G., 2008. Membrane and membrane-associated proteins in Triton X-114 extracts of *Mycobacterium bovis* BCG identified using a combination of gel-based and gel-free fractionation strategies. *Proteomics*, 8(9), pp.1859-1870.

Mehta, P.K., King, C.H., White, E.H., Murtagh, J.J. and Quinn, F.D., 1996. Comparison of *in vitro* models for the study of *Mycobacterium tuberculosis* invasion and intracellular replication. *Infection and Immunity*, 64(7), pp.2673-2679.

Menozzi FD, Bischoff R, Fort E, Brennan MJ, Locht C (1998) Molecular characterization of the mycobacterial heparin-binding hemagglutinin, a mycobacterial adhesin. *Proc Natl Acad Sci U S A 95*: 12625–12630.

Moodley, S. 2018. "The role of heparin binding haemaggluttin adhesin and curli pili on the pathogenicity of *Mycobacterium tuberculosis*.' Unpublished PhD thesis, University of Kwa-Zulu- Natal, Durban, South Africa.

Mueller-Ortiz, S.L., Wanger, A.R. and Norris, S.J., 2001. Mycobacterial protein HBHA binds human complement component C3. *Infection and Immunity*, 69(12), pp.7501-7511.

Muniram S. (2018). *Mycobacterium Tuberculosis* L, D-Transpeptidase Promotes *In-Vitro* Growth, Biofilm Production and Septum Formation During Cell Division (Masters dissertation). University of KwaZulu-Natal, Durban, South Africa.

Naidoo, N., Ramsugit, S. and Pillay, M. 2014. *Mycobacterium tuberculosis* pili (MTP), a putative biomarker for a tuberculosis diagnostic test. Tuberculosis, 94, 338-345.

Naidoo, T.J., 2021. The role of *Mycobacterium tuberculosis* curli pili (MTP) and heparin-binding hemagglutinin adhesin (HBHA) on global *in vitro* bacterial transcriptomics (Masters dissertation).

Nyawo GN (2016) The role of *Mycobacterium tuberculosis* pili in pathogenesis: Growth and survival kinetics, gene regulation and host immune response, and *in vitro* growth kinetics. Masters Dissertation, University of KwaZulu-Natal.

Oscarsson, J., Harlos, C. and Arvidson, S., 2005. Regulatory role of proteins binding to the spa (protein A) and *sarS* (*staphylococcal* accessory regulator) promoter regions in *Staphylococcus aureus* NTCC 8325-4. *International Journal of Medical Microbiology*, 295(4), pp.253-266.

Oscarsson, J., Tegmark-Wisell, K. and Arvidson, S., 2006. Coordinated and differential control of aureolysin (aur) and serine protease (sspA) transcription in *Staphylococcus aureus* by *sarA*, *rot* and *agr* (RNAIII). *International Journal of Medical Microbiology*, 296(6), pp.365-380.

Park, H.S., Back, Y.W., Shin, K.W., Bae, H.S., Lee, K.I., Choi, H.G., Choi, S., Lee, H.H., Choi, C.H., Park, J.K. and Kim, H.J., 2019. *Mycobacterium tuberculosis* Rv3463 induces mycobactericidal activity in macrophages by enhancing phagolysosomal fusion and exhibits therapeutic potential. *Scientific Reports*, *9*(1), pp.1-16.

Peirs, P., Lefevre, P., Boarbi, S., Wang, X.M., Denis, O., Braibant, M., Pethe, K., Locht, C., Huygen, K. and Content, J., 2005. *Mycobacterium tuberculosis* with disruption in genes encoding the phosphate binding proteins PstS1 and PstS2 is deficient in phosphate uptake and demonstrates reduced *in vivo* virulence. *Infection and Immunity*, 73(3), pp.1898-1902.

Peng, Y., Zhu, X., Gao, L., Wang, J., Liu, H., Zhu, T., Zhu, Y., Tang, X., Hu, C., Chen, X. and Chen, H., 2022. *Mycobacterium tuberculosis* Rv0309 Dampens the Inflammatory Response and Enhances Mycobacterial Survival. *Frontiers in Immunology*, 13, pp.829410-829410.

Pennini, M.E., Pai, R.K., Schultz, D.C., Boom, W.H. and Harding, C.V., 2006. *Mycobacterium tuberculosis* 19-kDa lipoprotein inhibits IFN-γ-induced chromatin remodeling of MHC2TA by TLR2 and MAPK signaling. *The Journal of Immunology*, 176(7), pp.4323-4330.

Pethe, K., Alonso, S., Biet, F., Delogu, G., Brennan, M.J., Locht, C. and Menozzi, F.D., 2001. The heparin-binding haemagglutinin of *M. tuberculosis* is required for extrapulmonary dissemination. *Nature*, 412(6843), p.190.

Piepenbrink, K.H. and Sundberg, E.J., 2016. Motility and adhesion through type IV pili in Gram-positive bacteria. *Biochemical Society Transactions*, 44(6), pp.1659-1666.

Pieters, J., 2008. *Mycobacterium tuberculosis* and the macrophage: maintaining a balance. *Cell Host & Microbe*, 3(6), pp.399-407.

Pizarro-Cerdá, J. and Cossart, P., 2006. Bacterial adhesion and entry into host cells. *Cell*, 124(4), pp.715-727.

Podinovskaia, M., Lee, W., Caldwell, S. and Russell, D.G., 2013.Infection of macrophages with *Mycobacterium tuberculosis* induces global modifications to phagosomal function. *Cellular Microbiology*, 15(6), pp.843-859.

Ragas, A., Roussel, L., Puzo, G. and Riviere, M., 2007. The *Mycobacterium tuberculosis* cell-surface glycoprotein apa as a potential adhesin to colonize target cells via the innate immune system pulmonary C-type lectin surfactant protein A. *Journal of Biological Chemistry*, 282(8), pp.5133-5142.

Rampersad (2018) Whole genome transcript analysis to elucidate the role of *Mycobacterium tuberculosis* HBHA in host response of THP-1 macrophages. Masters dissertation. University of KwaZulu-Natal.

Ramsugit, S., Guma, S., Pillay, B., Jain, P., Larsen, M. H., Danaviah, S. and Pillay, M. 2013. Pili contribute to biofilm formation *in vitro* in *Mycobacterium tuberculosi*s. *Antonie Van Leeuwenhoek*, 104, 725-735.

Ramsugit, S. and Pillay, M. 2014. *Mycobacterium tuberculosis* pili promote adhesion to and invasion of THP-1 macrophages. *Japanese Journal of Infectious Diseases*, 67, 476-478.

Ramsugit, S., Pillay, B. and Pillay, M. 2016. Evaluation of the role of *Mycobacterium tuberculosis* pili (MTP) as an adhesin, invasin, and cytokine inducer of epithelial cells. *The Brazilian Journal of Infectious Diseases*, 20, 160-165

Reedoy, K.S., 2020. *Mycobacterium tuberculosis* pili (MTP) modulates pathogen and host metabolomic changes in an A549 epithelial cell model of infection (Masters dissertation, University of KwaZulu-Natal).

Reguera, G., McCarthy, K.D., Mehta, T., Nicoll, J.S., Tuominen, M.T. and Lovley, D.R., 2005. Extracellular electron transfers via microbial nanowires. *Nature*, 435(7045), pp.1098-1101.

Rivas-Santiago, B., Schwander, S.K., Sarabia, C., Diamond, G., Klein-Patel, M.E., Hernandez-Pando, R., Ellner, J.J. and Sada, E., 2005. Human β-defensin 2 is expressed and associated with *Mycobacterium tuberculosis* during infection of human alveolar epithelial cells. *Infection and Immunity*, 73(8), pp.4505-4511.

Ronning, D.R., Klabunde, T., Besra, G.S., Vissa, V.D., Belisle, J.T. and Sacchettini, J.C., 2000. Crystal structure of the secreted form of antigen 85C reveals potential targets for mycobacterial drugs and vaccines. *Nature Structural Biology*, 7(2), pp.141-146.

Russell-Goldman, E., Xu, J., Wang, X., Chan, J. and Tufariello, J.M., 2008. A *Mycobacterium tuberculosis Rpf* double-knockout strain exhibits profound defects in reactivation from chronic tuberculosis and innate immunity phenotypes. *Infection and Immunity*, 76(9), pp.4269-4281.

Saikolappan, S., Estrella, J., Sasindran, S.J., Khan, A., Armitige, L.Y., Jagannath, C. and Dhandayuthapani, S., 2012. The *fbpA*/*sapM* double knock out strain of *Mycobacterium tuberculosis* is highly attenuated and immunogenic in macrophages. *PloS One*, 7(5), p.e36198.

Sanchez, A., Espinosa, P., Esparza, M.A., Colon, M., Bernal, G. and Mancilla, R., 2009. *Mycobacterium tuberculosis* 38-kDa lipoprotein is apoptogenic for human monocyte-derived macrophages. *Scandinavian Journal of Immunology*, 69(1), pp.20-28.

Schlesinger, L.S., Bellinger-Kawahara, C.G., Payne, N.R. and Horwitz, M.A., 1990. Phagocytosis of *Mycobacterium tuberculosis* is mediated by human monocyte complement receptors and complement component C3. *The Journal of Immunology*, 144(7), pp.2771-2780.

Schnappinger, D., Ehrt, S., Voskuil, M.I., Liu, Y., Mangan, J.A., Monahan, I.M., Dolganov, G., Efron, B., Butcher, P.D., Nathan, C. and Schoolnik, G.K., 2003. Transcriptional adaptation of *Mycobacterium tuberculosis* within macrophages: insights into the phagosomal environment. *The Journal of Experimental Medicine*, 198(5), pp.693-704.

Sherman, D.R., Voskuil, M., Schnappinger, D., Liao, R., Harrell, M.I. and Schoolnik, G.K., 2001. Regulation of the *Mycobacterium tuberculosis* hypoxic response gene encoding α-crystallin. *Proceedings of the National Academy of Sciences*, 98(13), pp.7534-7539.

Shiloh, M.U. and Nathan, C.F., 2000. Reactive nitrogen intermediates and the pathogenesis of Salmonella and mycobacteria. *Current Opinion in Microbiology*, 3(1), pp.35-42.

Singh, A., Crossman, D.K., Mai, D., Guidry, L., Voskuil, M.I., Renfrow, M.B. and Steyn, A.J., 2009. *Mycobacterium tuberculosis* WhiB3 maintains redox homeostasis by regulating virulence lipid anabolism to modulate macrophage response. *PLoS Pathogens*, *5*(8), p.e1000545.

Squeglia, F., Ruggiero, A., De Simone, A. and Berisio, R., 2018. A structural overview of mycobacterial adhesins: Key biomarkers for diagnostics and therapeutics. *Protein Science*, 27(2), pp.369-380.

Staudinger, B.J., Oberdoerster, M.A., Lewis, P.J. and Rosen, H., 2002. mRNA expression profiles for *Escherichia coli* ingested by normal and phagocyte oxidase-deficient human neutrophils. *The Journal of Clinical Investigation*, 110(8), pp.1151-1163.

Stewart, G.R., Wernisch, L., Stabler, R., Mangan, J.A., Hinds, J., Laing, K.G., Young, D.B. and Butcher, P.D., 2002. Dissection of the heat-shock response in *Mycobacterium tuberculosis* using mutants and microarraysaaA list of the 100 ORFs most highly induced by heat shock is provided as supplementary data with the online version of this paper (http://mic. sgmjournals. org). *Microbiology*, 148(10), pp.3129-3138.

Stones, D.H. and Krachler, A.M., 2015. Fatal attraction: how bacterial adhesins affect host signaling and what we can learn from them. *International Journal of Molecular Sciences*, 16(2), pp.2626-2640.

Untergasser, A., Nijveen, H., Rao, X., Bisseling, T., Geurts, R. & Leunissen, J. A. 2007. Primer3Plus, an enhanced web interface to Primer3. Nucleic Acids Research, 35, W71- W74.

Viljoen, A., Richard, M., Nguyen, P.C., Fourquet, P., Camoin, L., Paudal, R.R., Gnawali, G.R., Spilling, C.D., Cavalier, J.F., Canaan, S. and Blaise, M., 2018. Cyclipostins and cyclophostin analogs inhibit the antigen 85C from *Mycobacterium tuberculosis* both *in vitro* and *in vivo*. *Journal of Biological Chemistry*, 293(8), pp.2755-2769.

Wiker, H.G. and Harboe, M., 1992. The antigen 85 complex: a major secretion product of *Mycobacterium tuberculosis*. *Microbiological Reviews*, 56(4), pp.648-661.

Wilkinson, K.A., Newton, S.M., Stewart, G.R., Martineau, A.R., Patel, J., Sullivan, S.M., Herrmann, J.L., Neyrolles, O., Young, D.B. and Wilkinson, R.J., 2009. Genetic determination of the effect of post-translational modification on the innate immune response to the 19 kDa lipoprotein of *Mycobacterium tuberculosis*. *BMC Microbiology*, 9(1), pp.1-10.

World Health Organization, Global Tuberculosis Report 2021. Geneva: World Health Organization. (2021).

Xiong, Y.Q., Willard, J., Yeaman, M.R., Cheung, A.L. and Bayer, A.S., 2006. Regulation of Staphylococcus aureus α-toxin gene (hla) expression by agr, sarA and sae *in vitro* and in experimental infective endocarditis. *The Journal of Infectious Diseases*, 194(9), pp.1267-1275

Yao, J., Du, X., Chen, S., Shao, Y., Deng, K., Jiang, M., Liu, J., Shen, Z., Chen, X. and Feng, G., 2018. Rv2346c enhances mycobacterial survival within macrophages by inhibiting TNF-α and IL-6 production via the p38/miRNA/NF-κB pathway. *Emerging microbes & infections*, 7(1), pp.1-16.

Zhang, Y.J. and Rubin, E.J., 2013. Feast or famine: the host–pathogen battle over amino acids. *Cellular Microbiology*, 15(7), pp.1079-1087.

Zhang, Q., Sun, J., Wang, Y., He, W., Wang, L., Zheng, Y., Wu, J., Zhang, Y. and Jiang, X., 2017. Antimycobacterial and anti-inflammatory mechanisms of baicalin via induced autophagy in macrophages infected with *Mycobacterium tuberculosis*. *Frontiers in Microbiology*, *8*, p.2142.

Zhang, W., Ellingson, L., Frascoli, F. and Heffernan, J., 2021. An investigation of tuberculosis progression revealing the role of macrophages apoptosis via sensitivity and bifurcation analysis. *Journal of Mathematical Biology*, *83*(3), pp.1-32.

Chapter 3. Confirmation of phenotypic expression of genes in study using western blot and dot blot analysis.

3.1 Introduction

To confirm phenotypic expression of the studied genes, western blot and dot blot analysis were attempted on intracellular *M. tuberculosis* protein samples extracted from the infected THP-1 cells at 4-h and 24-h time points. The antibodies for Cpn60.2 (sc-58170, Santa Cruz, USA) and PstS-1 (sc-52102 Santa Cruz, USA) were used in this study. The two antibodies were selected because the genes Cpn60.2 (Hickey *et al*., 2009) and PstS-1(Esparza *et al*., 2015) are always expressed by *M. tuberculosis* during infection of macrophages.

3.2 Methodology

3.2.1 Total protein extraction and quantification

Proteins were isolated from intracellular bacteria using the TriZol method (Hummon *et al.*, 2007). In addition, proteins were also extracted from wild-type, Δ *hbhA* and complemented *hbhA* strains from the 7H9 broth. The bacterial strains were cultured in 10 mL of Middlebrook 7H9 broth (Difco Laboratories, Becton, Dickinson and Company, Sparks, USA), supplemented with 10 % oleic acid, albumin, dextrose, catalase (OADC) (Becton, Dickinson and Company, Sparks, USA) and 0.5 % of glycerol (Sigma-Aldrich, St. Louis, MO, USA). The broth was also supplemented with 0.25 % of Tween-80 (Sigma-Aldrich, St. Louis, MO, USA). The broth cultures were incubated at 37 °C in a shaking incubator (I-26 Shaking Incubator, New Brunswick Scientific, Canada) at 1 × g for 7 days until they reached an optimal density $(OD)_{600\ nm}$ = 1.0 (Light wave II, Biochrom, Cambridge, UK).

Briefly, the TriZol method involved adding 200 µL of chloroform (Sigma-Aldrich, Missouri, USA) on bacterial cell lysate obtained from the broth and the infected cells that was stored in 1 mL of TriZol reagent (Ambion, Life Technologies, California, USA), mixed vigorously, and centrifuged (Mikro 200R, Hettich Zentrifugen, Tuttlingen, Germany) at 26 295× *g* for 15 min at 4 °C. The upper aqueous phase was removed and used for RNA isolation. Thereafter, 300 µL of 100 % ethanol (Sigma-Aldrich, St. Louis, MO, USA) was added to the remaining phase and incubated at room temperature for 3 min before centrifugation (Mikro 200R, Hettich

Zentrifugen, Tuttlingen, Germany) at 2,000 x g for 15 min at 4 ℃. A volume of 1.5 mL of isopropanol (Sigma-Aldrich, St. Louis, MO, USA) was added to the supernatant. The samples were incubated for 10 min at room temperature (25 ℃ ± 5 ℃) and centrifuged (Mikro 200R, Hettich Zentrifugen, Tuttlingen, Germany) at at 12 000 × g at 4 ℃ for 10 min and the supernatant discarded. The protein pellet was thoroughly first washed thrice with 0.3 M Guanidium- Hydrochloric acid (Sigma-Aldrich, Missouri, USA) in 95 % ethanol (Sigma-Aldrich, St. Louis, MO, USA) and then two times with 99 % ethanol (Sigma-Aldrich, St. Louis, MO, USA). The proteins were centrifuged (Mikro 200R, Hettich Zentrifugen, Tuttlingen, Germany) at at 12 000 × g at 4 ℃ for 5 min and the supernatant was discarded. The protein pellets were air dried for 5 -10 min, dissolved in 150 µL of 1 % sodium dodecyl sulfate (SDS) (Sigma-Aldrich, Missouri, USA) and centrifuged (Mikro 200R, Hettich Zentrifugen, Tuttlingen, Germany) at 10 000 × g at 4 ℃ for 10 min. Thereafter, total proteins from the intracellular bacteria and the bacterial broth culture were quantified by the Nanodrop 2000 (Thermo Fisher Scientific, Massachusetts, USA).

3.2.2 Sodium dodecyl sulfate–polyacrylamide gel electrophoresis (SDS-PAGE) and Western blot.

Protein samples were standardised and mixed with 5 µL of 5 X Laemmle loading dye (Catalog #161-0747, Bio-Rad). Thereafter, proteins were boiled at 100 ℃ for 10 min on a heating block (Lab biotech, USA). Total proteins were separated in a 10 % Sodium dodecyl sulfate (Sigma-Aldrich, Missouri, USA)–polyacrylamide gel electrophoresis (SDS-PAGE) for approximately 3-h at 90 V in running buffer (25 mM Tris base (Sigma-Aldrich, Missouri, USA), 192 mM glycine (Sigma-Aldrich, Missouri, USA), 1 % SDS (Sigma-Aldrich, Missouri, USA), pH 8.3). The gel was stained with Coomassie brilliant blue (Sigma-Aldrich, Missouri, USA) for 1-h with shaking in a shaker at 80 revolutions per minute (rpm) (Stuart Orbital shaker SSL1, USA) and de-stained with de-staining solution (containing water, methanol Sigma-Aldrich, Missouri, USA, glacial acetic acid Sigma-Aldrich, Missouri, USA) at a ratio of 3:2:1) for 4-h. A second, identical gel was electrophoresed (Bio-Rad) concurrently in order to perform a western blot. Proteins were transferred from the electrophoreses second gel to nitrocellulose membranes (CatLog: 170–4159, Bio-Rad) using the Bio-Rad Trans-Blot Turbo Transfer System for 7 min. Membranes were blocked for 1-h in blocking buffer containing phosphate-buffered saline (containing 0.05 % Tween-20, pH 7.4) (PBS-T) (Sigma-Aldrich, St. Louis, MO, USA) with 5 % non-fat milk. Thereafter, the membranes were treated separately with primary antibodies for Cpn60.2 (1:500) (sc-58170, Santa Cruz, USA) and PstS-1(1:500) (sc-52102, Santa Cruz, USA)

prepared in PBS-T (Sigma-Aldrich, St. Louis, MO, USA) with 5 % non-fat milk overnight at 4 °C. Excess primary antibody was removed by washing the membranes four times in PBS-T (Sigma-Aldrich, St. Louis, MO, USA) for 15 min each. The Goat anti-Mouse IgG (H+L) secondary antibody HRP conjugate (1:10000), was incubated with the membrane for 1-h at room temperature (25 °C ± 5 °C) in PBS-T (Sigma-Aldrich, St. Louis, MO, USA) with 5 % non-fat dry milk. The membranes were washed four times in PBS-T (Sigma-Aldrich, St. Louis, MO, USA) for 15 min each to eliminate any extra secondary antibody. To develop colour, western blot 3,3',5,5'-Tetramethylbenzidine (TMB) (Thermo Fisher Scientific, Massachusetts, USA) was added to the membrane and left in the dark for 15-20 min.

3.2.3 Dot Blot: (Abcam protocol- Dot Blot)

Nitrocellulose membrane (CatLog: 170–4159, Bio-Rad) was cut into pieces of 2 x 2 centimetres (cm). Protein samples (1 µg; 2 µg; 4 µg; 8 µg; 16 µg; 32 µg; 50 µg; 70 µg; 90 µg; 110 µg) were spotted onto the nitrocellulose membrane (CatLog: 170–4159, Bio-Rad) at the centre of the grid. The area that the solution penetrates was minimized (usually 3-4 mm) by applying it slowly. The membrane was allowed to dry, and soaked in 3 mL of skimmed milk for 30 min at room temperature (25 °C ± 5 °C). The membrane was incubated with 3 mL primary antibody (1:100; 1:200; 1:500; 1:1000; 1:10 000) in PBS-T (Sigma-Aldrich, St. Louis, MO, USA) with 5 % non-fat dry milk for 30 min at room temperature (25 °C ± 5 °C). After washing three times with 3 mL PBS-T (Sigma-Aldrich, St. Louis, MO, USA) (3 x 5 min), the membrane was incubated separately with 3 mL previously purchased secondary Goat anti-Mouse IgG Fc horse peroxidase (HRP) conjugated secondary antibody (Product # A16084) (1:5 000) for 30 min at room temperature (25 °C ± 5 °C) and a new, recently purchased secondary antibody Goat anti-Mouse IgG (H+L) secondary Antibody- HRP conjugate (Product # 62-6520) (1:10 000). Thereafter, the membranes were washed three times with 3 mL PBS-T (Sigma-Aldrich, St. Louis, MO, USA) (15 min each), then once with 3 mL PBS (Sigma-Aldrich, St. Louis, MO, USA) (5 min). To assess reactivity by colour development, TMB (Thermo Fisher Scientific, Massachusetts, USA) was added to the blot and left in the dark for 15-20 min. Thereafter, distilled water was added to stop the reaction.

3.3 Results

3.3.1 Determination of protein concentration from broth culture of the wild-type V9124

The concentration of proteins was established using the Nanodrop (Thermo Fisher Scientific, Massachusetts, USA). The concentrations were standardized and the amount of protein sample to be loaded on the SDS-PAGE was calculated (Figure 3.2). The proteins were resolved in SDS-PAGE at 90 V for 3-h.

3.3.2 SDS-PAGE and western blot analysis

The SDS-PAGE revealed the presence of faint bands, suggestive of the low yield of proteins in the four intracellular bacterial samples: wild-type at 24 hr, and wild-type, Δ *hbhA* and comp *hbhA* at 4-h post-infection (Figure 3.1). In contrast, dark bands indicating high quantities of protein with good band separation were obtained from the broth culture of *M. tuberculosis* wild-type V9124 (Figure 3.2). The protein ladder was not included on the gels since the main purpose was to check for the presence of the proteins and protein integrity (Figure 3.1 and Figure 3.2).

Western blot analysis did not show any bands with the exception of the ladder (Figure E1.1, Appendix E). Since low protein yields were obtained from the intracellular *M. tuberculosis* post infection, it was decided to discontinue the SDS-PAGE/western blot, in order to avoid depletion of the remainder of the protein samples.

A dot blot was thereafter used to analyse the protein expression, and to determine whether the primary and secondary antibody dilutions and the low protein concentrations were responsible for the lack of signals obtained in the western blot.

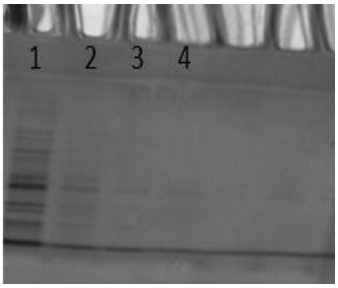

Figure 3.1: Total *M. tuberculosis* proteins extracted from the infected cells at 24-h (Lane 1-wild-type infected cells) and 4-h (Lane 2-wild-type, Lane 3- ΔhbhA and Lane 4- hbhA complement) post-infection using the TriZol method. Proteins were resolved in SDS – PAGE at 90V for 3-h.

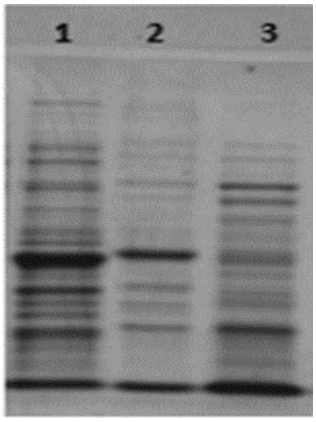

Figure 3.2: Total *M. tuberculosis* proteins extracted from the broth culture after standardisation (Lane 1- wild-type, Lane 2- Δ*hbhA*, Lane 3- *hbhA* complement) using TriZol method. Proteins were resolved in SDS –PAGE at 90V for 3-h.

3.3.3 Determination of antibody working dilution using the dot blot assay

3.3.3.1 Testing of the secondary antibodies

The recombinant protein (*Rv0309*) sample with a concentration of 30 µg was used as a positive control using the anti-GST tag as primary antibody. Two secondary antibodies were tested in parallel i.e. a previously purchased and stored Goat anti-Mouse IgG Fc HRP conjugated secondary antibody (Product # A16084) (i) (Figure 3.3) and a newly purchased Goat anti-Mouse IgG (H+L) secondary Antibody, HRP conjugate (ii) (Figure 3.3). Two different dilutions were tested for the secondary antibodies: 1:5000 for a previously purchased and stored secondary antibody, and 1:10 000 for a newly purchased secondary antibody. Positive signals were obtained for both sets of secondary antibodies (Fig. 3.3), suggesting that these reagents retained their functionality.

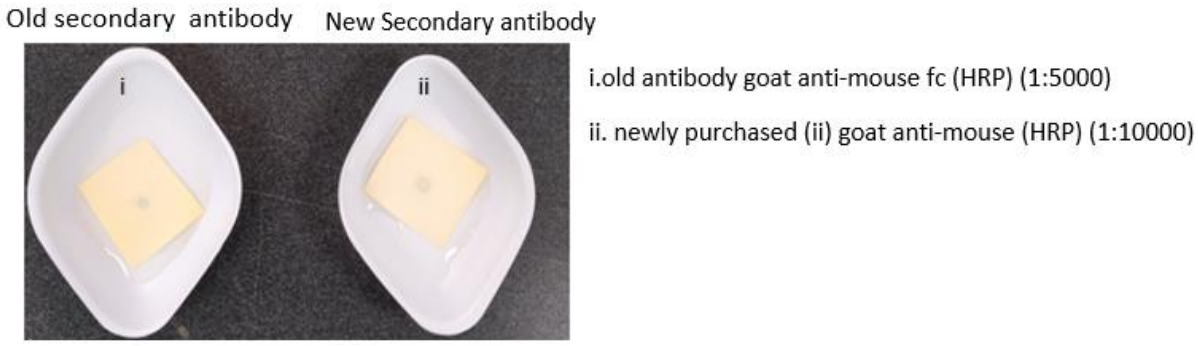

Figure 3.3: Dot blot testing positive control sample and anti-GST tag primary antibody using two secondary antibodies (i) Goat anti-Mouse IgG Fc HRP conjugated secondary antibody (1:5000) and the newly purchased (ii) Goat anti-Mouse IgG (H+L), HRP conjugate (1:10000). The faint blue colour indicates a positive result.

3.3.3.2 Testing anti-Cpn 60.2 and anti-PstS1 and different concentrations of protein samples

A dot blot assay was performed to test different dilutions (1:100; 1:200; 1:500; 1:1000; 1:10 000) of the commercial anti-Cpn 60.2 and anti-PstS-1 antibodies against different concentrations (1 µg; 2 µg; 4 µg; 8 µg; 16 µg; 32 µg; 50 µg; 70 µg; 90 µg; 110 µg) of protein extracted from *M. tuberculosis* cultured in broth (Figures 3.4 to 3. 13). The new secondary antibody, Goat anti-Mouse IgG (H+L), HRP conjugate was used in test samples I to X. The positive control included Rv0309 recombinant protein and the anti-GST tag as the primary antibody with the old (A) and new (B) secondary antibodies.

Only the positive control protein samples came up positive for both secondary antibodies. This demonstrated the technique was correct and the reagents were functional, and experimental design was successful. However, no signal was obtained for the test proteins when detected with the anti-Cpn 60.2 and PstS1 antibodies. This strongly suggests that the commercial antibodies that were purchased, did not work (Figures 3.4 to 3.13), i.e. they were non-functional.

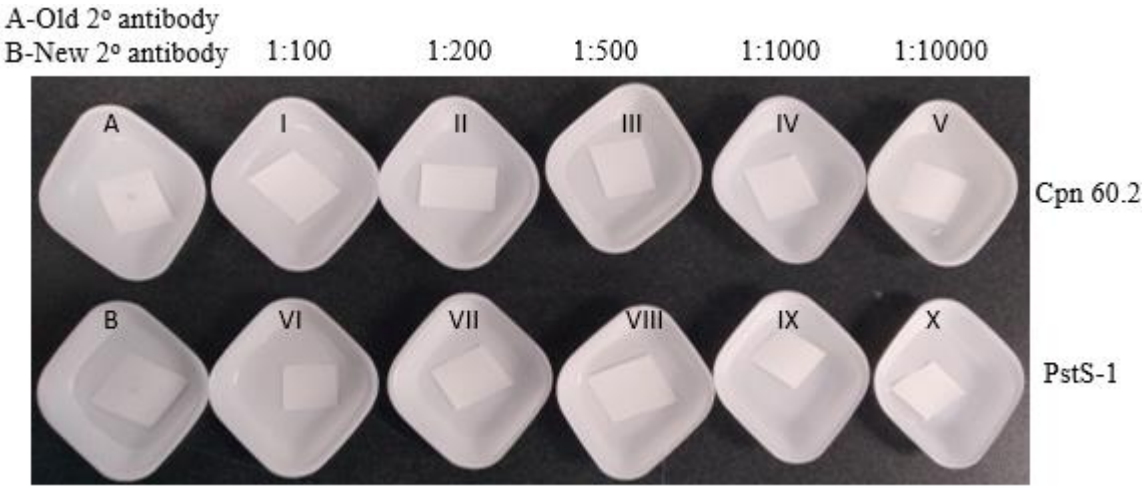

Figure 3.4: Dot blot testing Cpn60.2 (I-V) and PstS-1 (VI-X) antibodies in different dilutions i.e. 1:100; 1:200; 1:500, 1:1000, and 1:10000 respectively, using 1 µg of wild-type total proteins extracted from the broth culture of *M. tuberculosis*.

A newly purchased goat anti-mouse secondary antibody was used for both Cpn 60.2 and PstS-1 primary antibodies at a dilution of 1:10000 (I to X). A positive control Rv0309 protein sample and the primary antibody (anti-GST-tag 1:1000) were used with an old secondary antibody Goat anti-Mouse Fc HRP (1:5000) (A) and with a new secondary antibody Goat anti-Mouse IgG (H+L), HRP conjugate (1:10000) (B). Colour development only occurred in the positive controls. The tested antibodies did not work as demonstrated by the lack of colour development.

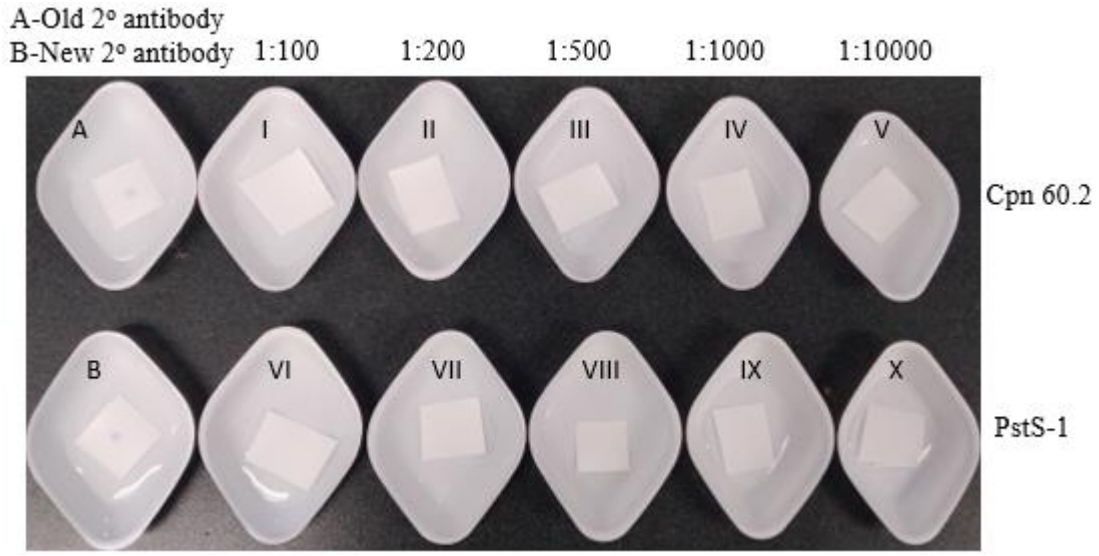

Figure 3.5: Dot blot testing Cpn60.2 (I-V) and PstS-1(VI-X) antibodies in different dilutions i.e. 1:100; 1:200; 1:500, 1:1000, and 10000 respectively using 2 µg of wild-type total proteins extracted from the broth culture of *M. tuberculosis*.

A newly purchased goat anti-mouse secondary antibody was used for both Cpn 60.2 and PstS-1 primary antibodies at a dilution of 1:10000 (I to X). A positive control protein sample and the primary antibody (anti-GST-tag 1:1000) were used with an old secondary antibody Goat anti-Mouse Fc HRP (1:5000) (A) and with a new secondary antibody Goat anti-Mouse IgG (H+L), HRP conjugate (1:10000) (B). Colour development only occurred in the positive control. The tested antibodies did not work, as demonstrated by the lack of colour development.

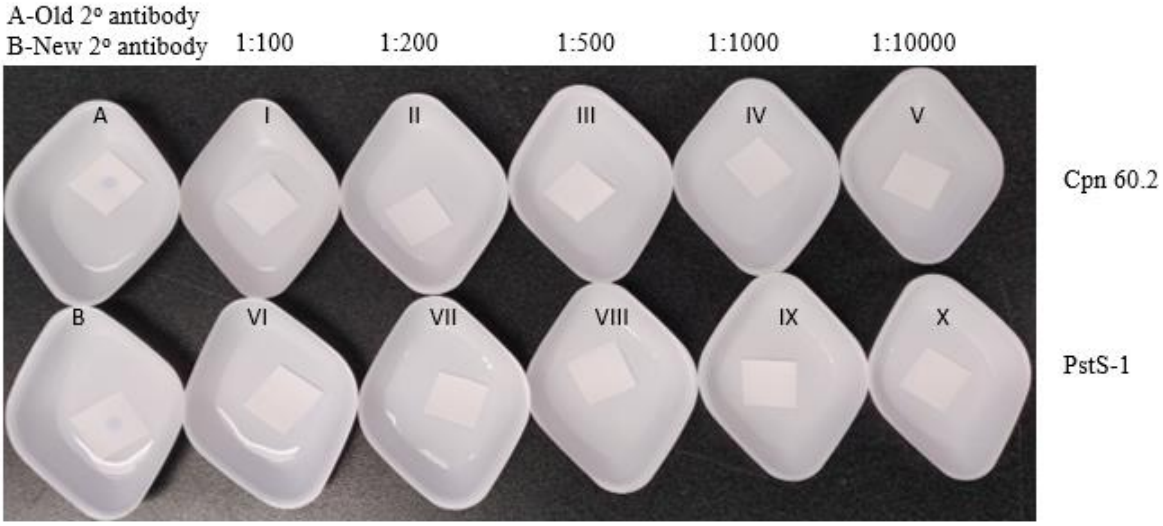

Figure 3.6: Dot plot testing Cpn60.2 (I-V) and PstS-1(VI-X) antibodies in different dilutions i.e. 1:100;1:200; 1:500, 1:1000, and 10000 respectively using 4 µg of wild-type total proteins extracted from the broth culture of *M. tuberculosis*.

A newly purchased goat anti-mouse secondary antibody was used for both Cpn 60.2 and PstS-1 primary antibodies at a dilution of 1:10000 (I to X). A positive control protein sample and the primary antibody (anti-GST-tag 1:1000) were used with an old secondary antibody Goat anti-Mouse Fc HRP (1:5000) (A) and with a new secondary antibody Goat anti-Mouse IgG (H+L), HRP conjugate (1:10000) (B). Colour development only occurred in the positive control. The tested antibodies did not work, as demonstrated by the lack of colour development.

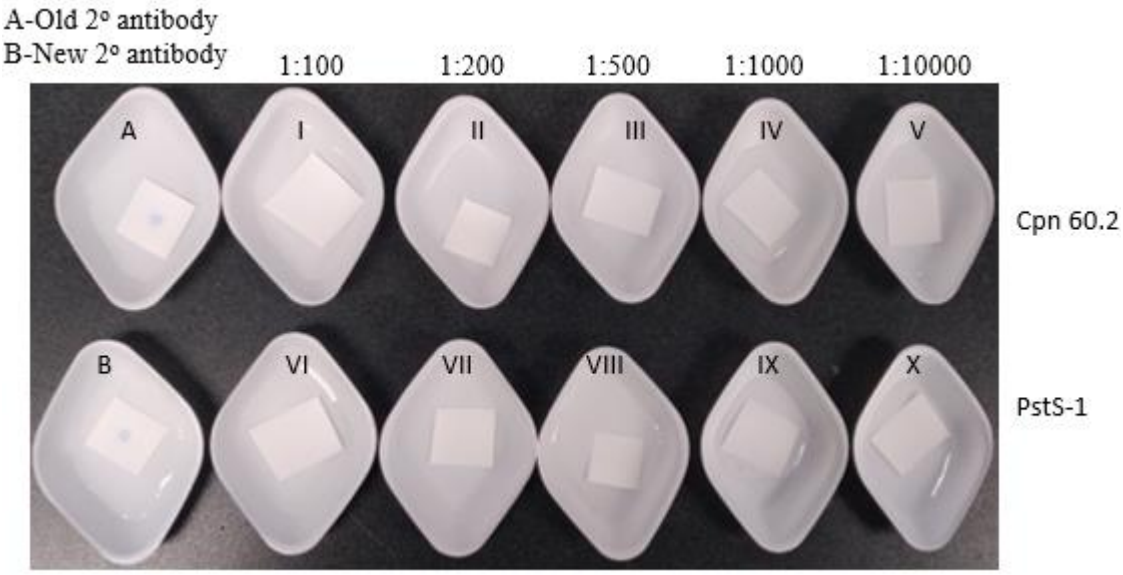

Figure 3.7: Dot plot testing Cpn60.2 (I-V) and PstS-1(VI-X) antibodies in different dilutions i.e. 1:100;1:200; 1:500, 1:1000, and 10000 respectively using 8 µg of wild-type total proteins extracted from the broth culture of *M. tuberculosis*.

A newly purchased goat anti-mouse secondary antibody was used for both Cpn 60.2 and PstS-1 primary antibodies at a dilution of 1:10000 (I to X). A positive control protein sample and the primary antibody (anti-GST-tag 1:1000) were used with an old secondary antibody Goat anti-Mouse Fc HRP (1:5000) (A) and with a new secondary antibody Goat anti-Mouse IgG (H+L), HRP conjugate (1:10000) (B). Colour development only occurred in the positive control. The tested antibodies did not work, as demonstrated by the lack of colour development.

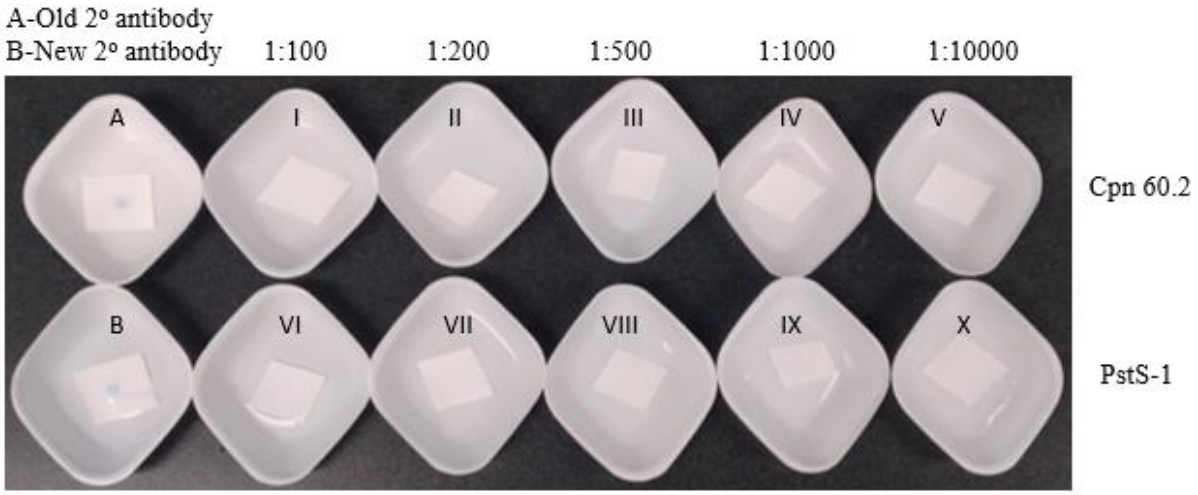

Figure 3.8: Dot plot testing Cpn60.2 (I-V) and PstS-1(VI-X) antibodies in different dilutions i.e. 1:100; 1:200; 1:500, 1:1000, and 10000 respectively using 16 µg of wild-type total proteins extracted from the broth culture of *M. tuberculosis*.

A newly purchased goat anti-mouse secondary antibody was used for both Cpn 60.2 and PstS-1 primary antibodies at a dilution of 1:10000 (I to X). A positive control protein sample and the primary antibody (anti-GST-tag 1:1000) were used with an old secondary antibody Goat anti-Mouse Fc HRP (1:5000) (A) and with a new secondary antibody Goat anti-Mouse IgG (H+L), HRP conjugate (1:10000) (B). Colour development only occurred in the positive control. The tested antibodies did not work, as demonstrated by the lack of colour development.

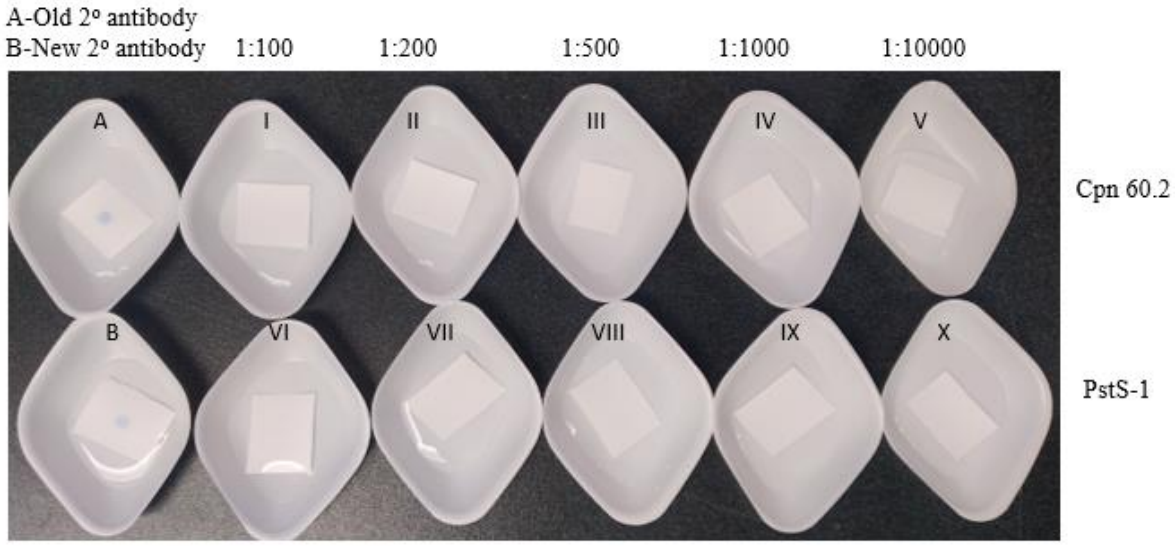

Figure 3.9: Dot plot testing Cpn60.2 (I-V) and PstS-1(VI-X) antibodies in different dilutions i.e. 1:100;1:200; 1:500, 1:1000, and 10000 respectively using 32 µg of wild-type total proteins extracted from the broth culture of *M. tuberculosis*.

A newly purchased goat anti-mouse secondary antibody was used for both Cpn 60.2 and PstS-1 primary antibodies at a dilution of 1:10000 (I to X). A positive control protein sample and the primary antibody (anti-GST-tag 1:1000) were used with an old secondary antibody Goat anti-Mouse Fc HRP (1:5000) (A) and with a new secondary antibody Goat anti-Mouse IgG (H+L), HRP conjugate (1:10000) (B). Colour development only occurred in the positive control. The tested antibodies did not work, as demonstrated by the lack of colour development.

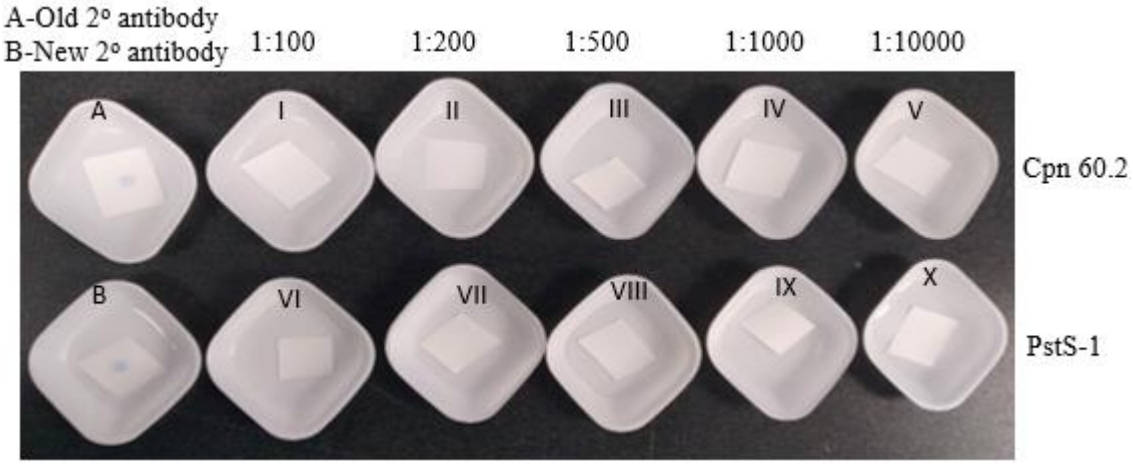

Figure 3.10: Dot plot testing Cpn60.2 (I-V) and PstS-1(VI-X) antibodies in different dilutions i.e. 1:100; 1:200; 1:500, 1:1000, and 10000 respectively using 50 µg of wild-type total proteins extracted from the broth culture of *M. tuberculosis*.

A newly purchased goat anti-mouse secondary antibody was used for both Cpn 60.2 and PstS-1 primary antibodies at a dilution of 1:10000 (I to X). A positive control protein sample and the primary antibody (anti-GST-tag 1:1000) were used with an old secondary antibody Goat anti-Mouse Fc HRP (1:5000) (A) and with a new secondary antibody Goat anti-Mouse IgG (H+L), HRP conjugate (1:10000) (B). Colour development only occurred in the positive control. The tested antibodies did not work, as demonstrated by the lack of colour development.

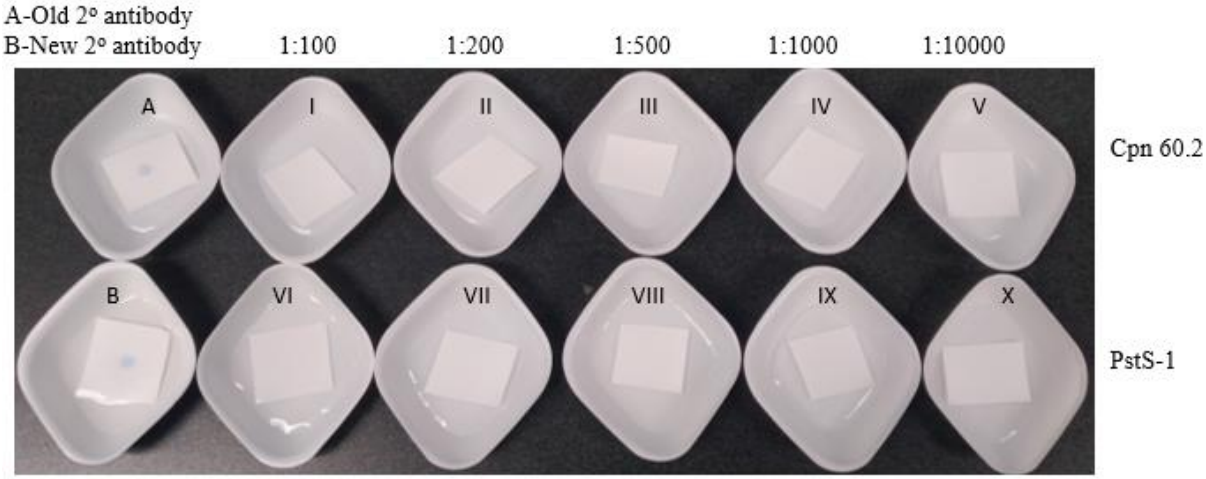

Figure 3.11: Dot plot testing Cpn60.2 (I-V) and PstS-1(VI-X) antibodies in different dilutions i.e. 1:100; 1:200; 1:500, 1:1000, and 10000 respectively using 70 µg of wild-type total proteins extracted from the broth culture of *M. tuberculosis*.

A newly purchased goat anti-mouse secondary antibody was used for both Cpn 60.2 and PstS-1 primary antibodies at a dilution of 1:10000 (I to X). A positive control protein sample and the primary antibody (anti-GST-tag 1:1000) were used with an old secondary antibody Goat anti-Mouse Fc HRP (1:5000) (A) and with a new secondary antibody Goat anti-Mouse IgG (H+L), HRP conjugate (1:10000) (B). Colour development only occurred in the positive control. The tested antibodies did not work, as demonstrated by the lack of colour development.

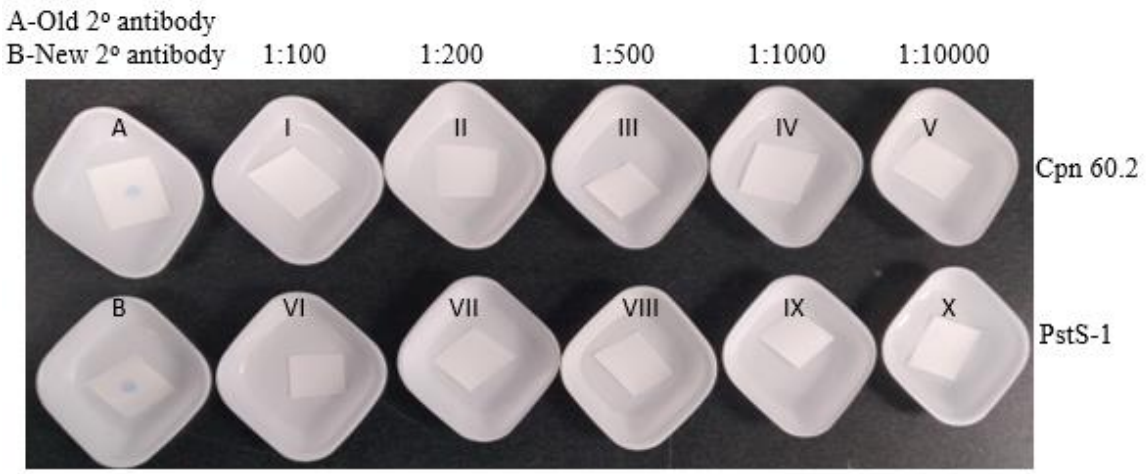

Figure 3.12: Dot plot testing Cpn60.2 (I-V) and PstS-1(VI-X) antibodies in different dilutions i.e. 1:100; 1:200; 1:500, 1:1000, and 10000 respectively using 90 µg of wild-type total proteins extracted from the broth culture of *M. tuberculosis*.

A newly purchased goat anti-mouse secondary antibody was used for both Cpn 60.2 and PstS-1 primary antibodies at a dilution of 1:10000 (I to X). A positive control protein sample and the primary antibody (anti-GST-tag 1:1000) were used with an old secondary antibody Goat anti-Mouse Fc HRP (1:5000) (A) and with a new secondary antibody Goat anti-Mouse IgG (H+L), HRP conjugate (1:10000) (B). Colour development only occurred in the positive control. The tested antibodies did not work, as demonstrated by the lack of colour development.

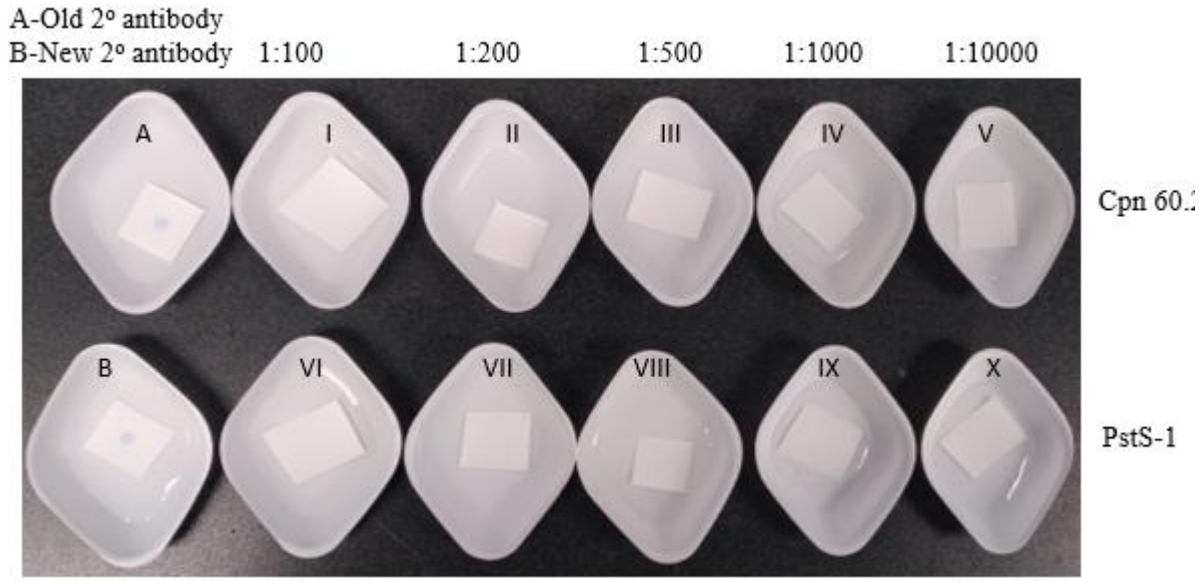

Figure 3.13: Dot plot testing Cpn60.2 (I-V) and PstS-1(VI-X) antibodies in different dilutions i.e. 1:100; 1:200; 1:500, 1:1000, and 10000 respectively using 110 µg of wild-type total proteins extracted from the broth culture of *M. tuberculosis*.

A newly purchased goat anti-mouse secondary antibody was used for both Cpn 60.2 and PstS-1 primary antibodies at a dilution of 1:10000 (I to X). A positive control protein sample and the primary antibody (anti-GST-tag 1:1000) were used with an old secondary antibody Goat anti-Mouse Fc HRP (1:5000) (A) and with a new secondary antibody Goat anti-Mouse IgG (H+L), HRP conjugate (1:10000) (B). Colour development only occurred in the positive control. The tested antibodies did not work, as demonstrated by the lack of colour development.

3.4 Discussion

In this study, western blot was attempted to confirm phenotypic expression of the genes investigated, following RT-qPCR. However, no colour development occurred (results not shown). Troubleshooting was performed on various aspects including procedure, reagents, protein concentration, and antibody concentration using a dot blot assay. These efforts were not successful. To identify the responsible factor/s for this lack of success, a dot blot assay was then attempted, using 2 different secondary antibodies, different dilutions of the primary antibodies, with a range of protein concentrations tested along with a positive control sample.

The western blot has become more accessible to many laboratories and more antibodies are increasingly becoming available and purchased (Gilda *et al*., 2015). This is due to the decrease in the cost of the western blot. Although it is now relatively simple to produce antibodies, it is time consuming and expensive to assess each antibody's usefulness in different applications. This further results in the science community experiencing problems because of the antibodies that are sold with little or no validation (Gilda *et al*., 2015). A study done by Berglund *et al*., 2008 revealed that less than 50% of around 6,000 commonly used commercial antibodies recognized their specific targets. While some of the inaccuracy is most likely due to experimental error, a large portion is attributable to poor quality antibodies (Gilda *et al*., 2015).

In the present study, experimental error as a cause of the unsuccessful outcome, was investigated with the use of a dot blot assay along with the positive control. The positive control resulted in colour development upon the addition of the TMB substrate. This showed that all the experimental procedures were followed with accuracy. Factors such as the amount of protein loaded, the use of un-optimized buffers and lack of positive control that affect reproducibility in western blot were taken into consideration in the experimental design. In this study, protein concentration of the test sample was determined and the amount of protein that was used in a dot blot assay was calculated. Moreover, a positive control was used and the buffers including the running buffer used in the SDS-PAGE, the transfer buffer, wash buffers and the blocking buffer were prepared and tested before being used in the actual experiment. In addition, a range of protein concentrations was used (1 µg; 2 µg; 4 µg; 8 µg; 16 µg; 32 µg; 50 µg; 70 µg; 90 µg; 110 µg) with different primary antibody dilutions from (1:100; 1:200; 1:500; 1:1000; 1:10000). The positive controls produced a colour reaction. However, none of

the test samples at the different protein concentrations and primary antibody dilutions resulted in colour development.

A limitation in this study, was the difficulty to source the antibodies for the studied genes. Adhesin research is still in its infancy, and there are a limited number of studies that have utilized anti- PstS-1 and Cpn60.2 antibodies. No published papers on the anti- PstS-1 antibody were available from the supplier website and through the web search, to assist with the trouble shooting. Moreover, the manufacturers had not determined the preferred secondary antibody for both Cpn60.2 and PstS-1. However, the goat anti-mouse antibody was suggested by the supplier, but had not been validated. For Cpn60.2, only four published papers had used this antibody for studies on *M. smegmatis* (Bai *et al*., 2020; Ko and Oh, 2020; Oh *et al*., 2020; Zhou *et al*., 2020), but not on *M. tuberculosis.*

It can be concluded from the findings of the dot blot assay that the commercial primary antibodies used in this study, could not detect the proteins of interest, resulting in the inability to confirm genotypic expression of the genes investigated. It is possible that the antibodies were not validated for the detection of *M. tuberculosis* proteins by the supplier prior to sale. Therefore, it is recommended that these antibodies be validated on *M. tuberculosis* samples before use in other studies.

3.5 References

Bai, L., Parkin, L.A., Zhang, H., Shum, R., Previti, M.L. and Seeliger, J.C., 2020. Dimethylaminophenyl hydrazides as inhibitors of the lipid transport protein LprG in mycobacteria. *ACS Infectious Diseases*, 6(4), pp.637-648.

Berglund, L., Björling, E., Oksvold, P., Fagerberg, L., Asplund, A., Szigyarto, C.A.K., Persson, A., Ottosson, J., Wernerus, H., Nilsson, P. and Lundberg, E., 2008. A gene-centric Human Protein Atlas for expression profiles based on antibodies. *Molecular and Cellular Proteomics*, 7(10), pp.2019-2027.

Esparza, M., Palomares, B., García, T., Espinosa, P., Zenteno, E. and Mancilla, R., 2015. PstS-1, the 38-kDa *Mycobacterium tuberculosis* Glycoprotein, is an Adhesin, Which Binds the Macrophage Mannose Receptor and Promotes Phagocytosis. *Scandinavian Journal of Immunology*, 81(1), pp.46-55.

Gilda, J.E., Ghosh, R., Cheah, J.X., West, T.M., Bodine, S.C. and Gomes, A.V., 2015. Western blotting inaccuracies with unverified antibodies: need for a Western blotting minimal reporting standard (WBMRS). *PloS One*, 10(8), p. e 0135392.

Hickey, T.B., Thorson, L.M., Speert, D.P., Daffé, M. and Stokes, R.W., 2009. *Mycobacterium tuberculosis* Cpn60. 2 and DnaK are located on the bacterial surface, where Cpn60. 2 facilitates efficient bacterial association with macrophages. *Infection and Immunity*, 77(8), pp.3389-3401.

Hummon, A.B., Lim, S.R., Difilippantonio, M.J. and Ried, T., 2007. Isolation and solubilization of proteins after TRIzol® extraction of RNA and DNA from patient material following prolonged storage. *Biotechniques*, 42(4), pp.467-472.

Ko, E.M. and Oh, J.I., 2020. Induction of the cydAB operon encoding the bd quinol oxidase under respiration-inhibitory conditions by the major cAMP receptor protein MSMEG_6189 in *Mycobacterium smegmatis*. *Frontiers in Microbiology*, 11, p.608624.

Oh, Y., Song, S.Y., Kim, H.J., Han, G., Hwang, J., Kang, H.Y. and Oh, J.I., 2020. The partner switching system of the SigF sigma factor in *Mycobacterium smegmatis* and induction of the SigF regulon under respiration-inhibitory conditions. *Frontiers in Microbiology*, 11, p.588487.

Zhou, Y., Wei, W., Fleming, J., Ye, C., Zheng, S., Liu, F., Zhou, L., Bi, L. and Liu, W., 2020. *Mycobacterium smegmatis* MSMEG_0129 is a nutrition-associated regulator that interacts with CarD and ClpP2. *The International Journal of Biochemistry and Cell Biology*, 124, p.105763.

Chapter 4: Synthesis of research findings, conclusions and recommendations

Tuberculosis (TB), caused by *Mycobacterium tuberculosis*, is still the leading cause of death from a single infectious pathogen World Health Organization (WHO, 2021). There should be more focus placed on early detection and prevention of TB given the persistent challenges including the increasing drug resistance, the expanding human immunodeficiency virus (HIV) epidemic (Karim *et al*., 2009), the lack of efficient point-of-care (POC) test, efficient drugs and efficient vaccines (Andersen and Doherty, 2005). Innovative research elucidating the pathogenicity of *M. tuberculosis* to identify novel biomarkers for this purpose is required to develop new rapid TB diagnostic tools and effective treatment alternatives. Since adhesins can be externally located or secreted by the pathogen and due to their immunogenic properties, these molecules are promising targets for drug and vaccine development (Stones and Krachler, 2015). Studies have demonstrated that the *M. tuberculosis* curli pili (*Rv3312A*) (MTP), heparin-binding hemagglutinin adhesin (*Rv0475*) (HBHA) and L, D-transpeptidase (Ldt) (*Rv0309)* offer tremendous promise as biomarkers and vaccine candidates.

Several studies have previously shown that MTP plays a key role in the host-pathogen interaction (Ramsugit and Pillay, 2014; Ramsugit *et al*., 2016; Dlamini, 2016 and Govender, 2018). The MTP adhesin binds to laminin and interacts with immunoglobulin (IgG) antibodies in the patient's serum (Alteri *et al.,* 2007). The MTP has features similar to curli amyloid fibers, and it was discovered that *M. tuberculosis* H37Rv was able to attach *in vitro* to an extracellular matrix protein and laminin, indicating its adhesive capabilities (Alteri *et al*., 2007). Moreover, MTP functions in the formation of biofilm (Ramsugit *et al.,* 2013) and is unique to *Mycobacterium tuberculosis* complex (MTBC) members (Naidoo *et al*., 2014). The *in vitro* infection studies using THP-1 macrophages (Ramsugit and Pillay, 2014) and A549 epithelial cells (Ramsugit *et al*., 2016) shed light on MTP's role in adhesion and invasion. As a survival mechanism, the MTP adhesin may modulate chemokine or cytokine production in A549 epithelial cells (Ramsugit *et al*., 2016). Global transcriptomics in the mouse model (Nyawo, 2016) and epithelial cells (Dlamini, 2016) demonstrated additional evidence of MTP's participation in triggering important host immune response genes, pathways, and networks. In serum samples from patients, including HIV-uninfected as well as TB-HIV co-infected patients, a synthetic MTP peptide showed 97 % accuracy in detecting anti-MTP IgG antibodies (Naidoo *et al.,* 2018). Using MTP-proficient and MTP-deficient strains of *M. tuberculosis* V9124 in a metabolomics study, Ashokcoomar *et al*., (2020) found that a total of 28 metabolites

related to cell wall biogenesis, decreased amino acid synthesis, and fatty acids hydrolysis were substantially different in the MTP-deficient strain compared to the wild-type.

Heparin-binding hemagglutinin adhesin is a virulence factor found in the early stages of TB infection (Pethe *et al*., 2001). In a mouse infection model, Kuvar (2016) showed that HBHA regulates host-pathogen interactions and immune responses causing differential gene expression (unpublished). The *in vitro* infection studies using A549 pneumocytes revealed that the HBHA-deficient strain of *M. tuberculosis* significantly decreased adhesion and invasion compared to the wild-type strain (Govender, 2018). Moodley (2018, unpublished) demonstrated that single deletion of HBHA in *M. tuberculosis* V9124 strain induced a 22.78 % and 22.29 % decrease in percentage adhesion and invasion respectively compared to wild-type in macrophages. The results suggested that HBHA plays a minimal role in the adhesion and invasion of macrophages (Moodley 2018, unpublished).

The *Rv0309* is a conserved fibronectin-binding adhesin encoding a putative region of difference 8 (RD8) protein localized in the cell wall (Song *et al*., 2008; Kumar *et al*., 2013). Peng *et al*., (2022) identified a new putative cell wall protein, *Rv0309/BCG RS01790*, which can influence the *Mycobacterium* colony morphology, lessen the permeability of the bacterial cell wall, promote bacterial survival in host cells, and most importantly, suppress the production of pro-inflammatory cytokines by activating the signalling pathways. Muniram (2018, unpublished), showed reduced growth of the *Rv0309* mutant compared to the wild-type strain during two different growth phases *in vitro*. Biofilm forming ability was significantly lower in the *Rv0309* mutant with a 55.75 % reduction compared to the V9124 wild-type strain.

Despite the research elucidating the influence of MTP, HBHA and Rv0309 in *M. tuberculosis* pathogenesis, little is known about the ability of *M. tuberculosis*, in the absence of these adhesins, to regulate the expression of other specific adhesins as compensatory mechanisms to support adhesion and infection. In the current study, the role of selected adhesin genes (*mtp, hbhA,* and *Rv0309*) in regulating other adhesins during TB pathogenesis was investigated using *in vitro* infection assays with gene knockout mutants, real-time quantitative PCR (RT-qPCR), and a dot blot assay.

4.1 *Mycobacterium tuberculosis pili facilitates infection of macrophages in M. tuberculosis V9124 strain*

In the current study, the average intracellular bacterial count obtained during the *in vitro* infection assay revealed that the MTP deficient strain was unable to infect THP-1 macrophages to the same extent as the wild-type. This suggests that the *mtp* gene is required for virulence of *M. tuberculosis* V9124 strain.

4.2 The HBHA in M. tuberculosis V9124 strain participates in the infection of THP-1 macrophages

HBHA gene-deficient and gene-proficient strains were used in comparison to the wild-type strain to infect THP-1 cells. The mutant *hbhA* strain showed a decrease in the ability to infect THP-1 cells at both 4-h ($p = 0.049$) and 24-h ($p = 0.034$) time points suggesting that *hbhA* gene plays a role in the infection of macrophages.

4.3 Double Knockout mutant strain of mtp and hbhA shows a reduced capability in infecting the host cells as compared to the parental strain and complemented strain.

In the present study, deletion of both *mtp* and *hbhA* genes in the *M. tuberculosis* V9124 strain resulted in the great impairment of the strain to initiate infection in THP-1 macrophages. This suggests that MTP and HBHA play an essential role in the initial stages of infection of macrophages. Deletion of both *mtp* and *hbhA* genes in this strain might have interfered with the pathways that are associated with these genes such as central carbon metabolism, Adenosine triphosphate (ATP) synthesis, cell wall biosynthesis, and lipid metabolism (Naidoo, 2021). In addition to this, double deletion of *mtp* and *hbhA* may also have down-regulated genes that are required for *M. tuberculosis* to survive host stress or other virulence factors that were not part of this study, resulting in the susceptibility of the double knockout mutant strain.

4.4 Rv0309 facilitates infection of THP-1 macrophages

The deletion of the *Rv0309* gene in the *M. tuberculosis* V9124 strain resulted in a reduced capability of the *Rv0309* mutant strain in initiating infection on the macrophages in comparison to the wild-type strain. Complementation of the *Rv0309* gene restored gene function to a level below the wild-type strain. This indicated that *Rv0309* is required by *M. tuberculosis* to induce infection in macrophages.

4.5 The effect of mtp and hbhA on gene regulation

Infection of THP-1 cells with Δ*mtp* induced a low expression of the genes facilitating adhesion of *M. tuberculosis* to macrophages; *Rv3763, Rv0934, Rv0350, Rv3660, Rv1860,* and *Rv0440* at 24-h time points compared to the 4-h time point. Deletion of *mtp* in the mutant caused a low expression of the genes Rv*3763, Rv0934,* and *Rv1860* which are important cell wall components and important virulence factors of *M. tuberculosis*. Down-regulation of these genes observed in the Δ*mtp* deletion mutant, suggests the lack of the MTP adhesin may result in altered cell wall activities, therefore, reducing the virulence of the strain. In addition to this, the deletion of *mtp* gene in the mutant might have altered the activity of *M. tuberculosis* resulting in a reduced stress response, thereby down-regulating the genes encoding chaperone proteins i.e *Rv0350* and *Rv0440*. Furthermore, the expression of the gene (*Rv3660*) which regulate cell division and morphology, was reduced, thus emphasizing the alterations in cell wall biosynthesis leading to an increased susceptibility of the pathogen to killing.

When the Δ*hbhA* strain was used to infect THP-1 cells, more genes were expressed at the 4-h time point compared to the other strains used in this study. The wild-type strain did not induce the expression of *Rv3660* and *Rv0350* genes at the 4-h time point. Deletion of the *hbhA* gene in the mutant might have induced the expression of *Rv3660* which is most likely to induce the expression of *Rv0350*. *Rv3660* expression may have caused the strain to proliferate and new proteins to be synthesized which further induced *Rv0350*. *Rv0350* is important for cell growth and proper folding of newly synthesized proteins and is stimulated under heat response. Moreover, the deletion of the *hbhA* gene in the mutant resulted in the high expression of *Rv3763, Rv0934* and *Rv3804* at 4-h compared to the wild-type strain. In an absence of *hbhA* in the mutant at the 24-h time point, there was an expression of all the genes that are associated with the virulence of *M. tuberculosis* as a compensatory mechanism. There was a reduced

expression in the genes that are expressed under stress conditions; *Rv0350* and *Rv0440* at 24-h in the double knockout mutant strain. This indicates the ability of the pathogen to alter its gene expression in the cell wall to increase its virulence as a compensatory mechanism. This suggests that other adhesins (*Rv3763, Rv0934, Rv3804, Rv0440,* and *Rv1860*), in addition to these 2, may use pattern recognition receptors during early infection.

4.6 ∆Rv0309 induced the highest expression of Rv3763, Rv0934, Rv3804, Rv3660, Rv1860 and Rv0440

The deletion of *Rv0309* in the mutant strain induced high expression of the genes that are associated with different functions in *M. tuberculosis*. Infection of THP-1 cells with the ∆*Rv0309* strain elevated the levels of *Rv1860* at both time points suggesting its role as an important adhesin in the binding to THP-1 cells. The Apa antigen encoded by *Rv1860* is important for *M. tuberculosis* virulence because it acts as a mycolyl-transferase, catalyzing the attachment of mycolic acids to arabinogalactan and synthesis of cord factor, a very active virulence factor (Babaki *et al*., 2017). Upregulation of genes in the mutant that are important for the survival of *M. tuberculosis* inside the macrophages indicates the importance of the *Rv0309* gene in the infection process.

4.7 Phenotypic confirmation of gene expression was unsuccessful

Western blot was attempted using anti-Cpn60.2 (*Rv0440)* and anti-PstS-1 (*Rv0934)* antibodies. However, no protein detection was observed. Trouble-shooting was carried out on experimental procedure with a positive control different antibody dilutions and different concentration of proteins using a dot blot assay. The anti-GST tag primary antibody with the newly purchased secondary antibody were tested in parallel with the old secondary antibody on the purified protein as the positive control. The colour development in the positive control demonstrated that the experimental procedure was performed well and that the reagents were in a good condition. Moreover, when the total extracted *M. tuberculosis* proteins were tested using antibodies for anti-Cpn60.2 and anti-PstS-1 together with the newly purchased secondary antibody, no colour development occurred in contrast to the positive control. Therefore, it was concluded that the purchased antibodies did not work.

4.8 Conclusion

This study revealed that HBHA and MTP independently play a role in the regulatory mechanism of *M. tuberculosis*. The absence of both MTP and HBHA, resulted in the impairment of the *M. tuberculosis* strain to infect THP-1 cells as a result of an altered expression of specific genes which might have led to perturbations in the regulatory pathways of the genes involved. The deletion of *mtp* implied a decline in pathogenicity as a result of the decrease in genes associated with the virulence of the strain. The absence of the individual genes *Rv0309* and *hbhA*, induced the high expression of the genes that are important in the virulence of *M. tuberculosis* as a compensatory mechanism for the loss of these genes. This resulted in a slight decrease in the virulence of the strain.

4.9 Limitations

The study investigated the role of specific adhesins genes on the regulation of other adhesins genes using RT-qPCR. Only adhesins that facilitate the binding of *M. tuberculosis* to THP-1 cells were selected. The results of this study cannot be extrapolated to other clinical strains of the same family or other strain families of *M. tuberculosis* because only a single representative of the F15/LAM4/KZN strain was employed. Phenotypic confirmation of expression of proteins using western blot failed. Several attempts were made to optimize the working primary antibodies concentration. However, no detection was obtained. Positive controls to test the secondary antibodies, and the use of a relevant protein sample and corresponding antibodies to test the experimental design did work. This strongly suggested that the commercial antibodies that were purchased, did not work. Because this was the first study that tried to confirm the expression of the studied adhesins, it was difficult to find the supplier of antibodies at first, and not all genes studied, had available antibodies. Considering the cost of antibodies, we could not afford to purchase new antibodies. Future studies investigating the regulatory mechanism of intracellular bacteria need to upscale the volume of infecting bacteria to obtain sufficient bacterial proteins. Despite these drawbacks, this innovative study added to our understanding of the roles played by three adhesins in the pathogenesis of TB.

4.10 Recommendations for future research

The current study failed to detect the proteins using the western blot due to the purchased antibodies. It would be useful for future studies to use antibodies that have been used in many publications and which have been validated and known to have worked. Also, to obtain a sufficient amount of intracellular protein from the infected cells, future studies need to increase the intracellular bacterial yield by upscaling the volume of media used for the infection. Since the research on the studied genes is still in its infancy, *in vivo* infection model can be used to ascertain whether what happens *in vitro* also happens *in vivo* in these genes. Studies also utilizing different other clinical strains need to be conducted.

4.11 References

Alteri, C. J., Xicohténcatl-Cortes, J., Hess, S., Caballero-Olín, G., Girón, J. A. and Friedman, R. L. 2007. *Mycobacterium tuberculosis* produces pili during human infection. *Proceedings of the National Academy of Sciences,* 104, 5145-5150

Andersen, P. and Doherty, T. M. 2005. The success and failure of BCG—implications for a novel tuberculosis vaccine. *Nature Reviews Microbiology,* 3**,** 656-662.

Ashokcoomar, S., Reedoy, K.S., Senzani, S., Loots, D.T., Beukes, D., Van Reenen, M., Pillay, B. and Pillay, M., 2020. *Mycobacterium tuberculosis* curli pili (MTP) deficiency is associated with alterations in cell wall biogenesis, fatty acid metabolism and amino acid synthesis. *Metabolomics*, 16(9), pp.1-15.

Babaki, M.K.Z., Soleimanpour, S. and Rezaee, S.A., 2017. Antigen 85 complex as a powerful *Mycobacterium tuberculosis* immunogene: Biology, immune-pathogenicity, applications in diagnosis, and vaccine design. *Microbial Pathogenesis*, 112, pp.20-29.

Dlamini MT (2016) Whole transcriptome analysis to elucidate the role of MTP in gene regulation of pulmonary epithelial cells infected with *Mycobacterium tuberculosis*. Masters Dissertation, University of KwaZulu-Natal.

Govender, V.S., 2018. Investigating the *in vitro* roles played by the major adhesins HBHA and MTP in the pathogenesis of *M. tuberculosis*, in a novel double gene knock-out mutant strain (Doctoral dissertation).

Karim, S. S. A., Churchyard, G. J., Karim, Q. A. & Lawn, S. D. 2009. HIV infection and tuberculosis in South Africa: an urgent need to escalate the public health response. *The Lancet,* 374**,** 921-933.

Kumar, S., Puniya, B.L., Parween, S., Nahar, P. and Ramachandran, S., 2013. Identification of novel adhesins of *M. tuberculosis* H37Rv using integrated approach of multiple computational algorithms and experimental analysis. *PLoS One*, 8(7), p. e69790

Kuvar S (2016) The role of *hbhA* in gene regulation *in vivo* using a *hbhA* knockout mutant of *M. tuberculosis*. Masters Dissertation, University of KwaZulu-Natal.

Moodley, S. 2018. "The role of heparin binding haemagglutin adhesin and curli pili on the pathogenicity of *Mycobacterium tuberculosis*.' Unpublished PhD thesis, University of Kwa-Zulu-Natal, Durban, South Africa.

Muniram S. (2018). *Mycobacterium Tuberculosis* L, D-Transpeptidase Promotes *In-Vitro* Growth, Biofilm Production and Septum Formation During Cell Division (Masters dissertation). University of KwaZulu-Natal, Durban, South Africa.

Naidoo, N., Ramsugit, S. and Pillay, M. 2014. *Mycobacterium tuberculosis pili* (MTP), a putative biomarker for a tuberculosis diagnostic test. *Tuberculosis,* 94**,** 338-345.

Naidoo, N., Pillay, B., Bubb, M., Pym, A., Chiliza, T., Naidoo, K., Ndung'u, T., Kasprowicz, V. O. and Pillay, M. 2018. Evaluation of a synthetic peptide for the detection of anti-*Mycobacterium tuberculosis* curli pili IgG antibodies in patients with pulmonary tuberculosis. *Tuberculosis,* 109**,** 80-84.

Nyawo GN (2016) The role of *Mycobacterium tuberculosis* pili in pathogenesis: Growth and survival kinetics, gene regulation and host immune response, and *in vitro* growth kinetics. Masters Dissertation, University of KwaZulu-Natal.

Peng, Y., Zhu, X., Gao, L., Wang, J., Liu, H., Zhu, T., Zhu, Y., Tang, X., Hu, C., Chen, X. and Chen, H., 2022. Mycobacterium tuberculosis Rv0309 Dampens the Inflammatory Response and Enhances Mycobacterial Survival. *Frontiers in Immunology*, 13, pp.829410-829410.

Pethe, K., Alonso, S., Biet, F., Delogu, G., Brennan, M. J., Locht, C. and Menozzi, F. D. 2001. The heparin-binding hemagglutinin of *M. tuberculosis* is required for extrapulmonary dissemination. *Nature,* 412**,** 190-194.

Ramsugit, S., Guma, S., Pillay, B., Jain, P., Larsen, M. H., Danaviah, S. & Pillay, M. 2013. Pili contribute to biofilm formation in vitro in *Mycobacterium tuberculosis*. *Antonie Van Leeuwenhoek,* 104**,** 725-735.

Ramsugit, S. and Pillay, M. 2014. *Mycobacterium tuberculosis* pili promote adhesion to and invasion of THP-1 macrophages. *Japanese Journal of Infectious Diseases,* 67**,** 476-478

Ramsugit, S., Pillay, B. and Pillay, M. 2016. Evaluation of the role of *Mycobacterium tuberculosis* pili (MTP) as an adhesin, invasin, and cytokine inducer of epithelial cells. *The Brazilian Journal of Infectious Diseases,* 20**,** 160-165.

Song, H., Sandie, R., Wang, Y., Andrade-Navarro, M.A. and Niederweis, M., 2008. Identification of outer membrane proteins of *Mycobacterium tuberculosis. Tuberculosis,* 88(6), pp.526-544.

Stones, D. H. and Krachler, A.-M. 2015. Fatal attraction: how bacterial adhesins affect host signaling and what we can learn from them. *International Journal of Molecular Sciences,* 16**,** 2626-2640.

World Health Organization, Global Tuberculosis Report 2021. Geneva: World Health Organization. (2021).

APPENDICES

Appendix A: BREC Approval

UNIVERSITY OF KWAZULU-NATAL
INYUVESI YAKWAZULU-NATALI

11 July 2022

Mr Johannes Nkanyiso Thandabantu Mthembu (214539650)
School of Laboratory Medicine & Medical Science
Medical School

Dear Mr Mthembu

Protocol reference number: BREC/00001210/2020
Project title: The role of specific adhesins on the regulation of other adhesin genes associated with Mycobacterium tuberculosis pathogenicity.
Degree Purposes: Masters

RECERTIFICATION APPLICATION APPROVAL NOTICE

Approved: 23 April 2022
Expiration of Ethical Approval: 22 April 2023

I wish to advise you that your application for recertification received on 05 July 2022 for the above study has been noted and approved by a subcommittee of the Biomedical Research Ethics Committee (BREC). The start and end dates of this period are indicated above.

Please note: It is not clear from the list of amendments described whether these have been approved by BREC. All amendments must be BREC approved via a separate BREC application process and may not be implemented until approved by BREC.

If any modifications or adverse events occur in the project before your next scheduled review, you must submit them to BREC for review. Except in emergency situations, no change to the protocol may be implemented until you have received written BREC approval for the change.

The committee will be notified of the above approval at its next meeting to be held on 16 August 2022.

Yours sincerely

.....
Ms A Marimuthu
(for) Prof D Wassenaar
Chair: Biomedical Research Ethics Committee

Appendix B: Media, solutions and reagents

Middlebrook 7H9 broth (1L)

- 900 mL distilled water
- 4.71 g Middlebrook 7H9 powder (Difco, Becton, Dickinson and Company, South Africa)
- 100 mL oleic acid-albumin-dextrose-catalase (Becton, Dickinson and Company, South Africa)
- 10 mL of 50 % (w/v) glycerol
- 2.5 mL 20 % Tween-80 (Sigma, Capital lab supplies, South Africa

1. Dissolved 4.71 g of Middlebrook 7H9 powder (Difco, Becton, Dickinson and Company, South Africa in 900 mL of distilled water

2. Autoclaved at 121 ºC for 15 min and cooled.

3. Added 10 mL of 50 % (w/v) glycerol, 2.5 mL of 20 % Tween-80 (Sigma, Capital lab supplies, South Africa) and 100 mL of oleic acid-albumin-dextrose-catalase (Becton, Dickinson and Company, South Africa).

4. Stored at 4 °C until further use.

Middlebrook 7H11 Agar (1L)

- 21 g Middlebrook 7H11 powder (Difco, Becton, Dickinson and Company, South Africa)
- 900 mL distilled water
- 100 mL oleic acid-albumin-dextrose-catalase (Becton, Dickinson and Company, South Africa)
- 10 mL of 50 % (w/v) glycerol (Merck, South Africa)

1. Dissolved 21 g of Middlebrook 7H11 powder (Difco, Becton, Dickinson and Company, South Africa) in 900 mL of distilled water.

2. Autoclaved at 121 ºC for 15 mins and cooled.

3. Added 10 mL of 50 % (w/v) glycerol (Merck, South Africa) and 100 mL of oleic acid-albumin-dextrose-catalase (Becton, Dickinson and Company, South Africa) were added after

4. Dispensed approximately 12.5 mL was aliquoted into 65 mm petri dishes, and

5. Stored at 4 °C until further use.

Phosphate buffered saline (PBS)

- PBS tablets (Oxoid, Quantum Biotechnologies, South Africa)
- 1000 mL distilled water

1. Dissolved 2 PBS tablets in 1000 mL autoclaved distilled water.
2. Autoclaved at 121 °C for 15 mins.
3. Added 2.5 mL 20 % Tween 80 for serial dilutions (omitted for PBS used in wash steps).
4. Stored at 4 °C until further use.

Diethylpyrocarbonate (DEPC-treated) water (1L)

- 1 mL 0.1 % DEPC (Sigma, Capital lab supplies, South Africa)
- 1 L autoclaved distilled water

1. Added 1 mL of 0.1 % DEPC (Sigma, Capital lab supplies, South Africa) to 1 L of autoclaved distilled water.
2. Left at room temperature (25 °C ± 5 °C) for overnight.
3. Autoclaved at 121 °C for 15 mins.
4. Stored at room temperature (25 °C ± 5 °C) until further use.

MOPS Buffer (1L)

- 41.9 g MOPs (Sigma, Capital lab supplies, South Africa)
- 8.2 g Sodium acetate.3H2O (Sigma, Capital lab supplies, South Africa)
- 3.72 g Ethylenediaminetetraacetic acid (EDTA) (Sigma, Capital lab supplies, South Africa)

1. Dissolved MOPs in 1000 mL of DEPC-treated water.
2. Autoclaved at 121 °C for 15 mins.
3. Stored at room temperature (25 °C ± 5 °C) in darkroom until further use.

Appendix C: Chapter 2 Supplementary Material

C1. PCR confirmation of bacterial strains

InstaGene Matrix (BioRad) was used to perform total DNA extraction for all strains. This method was selected based on standardizing the DNA extraction for the inclusion of both genomic and plasmid DNA given how the mutant and complemented strains were constructed. The crude DNA from each strain was used to perform conventional PCR reactions using the specific primers and their respective annealing temperatures reported in Table C1. The expected PCR product of 824 bp was observed in Figure C1.1 for the wild-type (Lane 2), *mtp*-complement (Lane 4), *mtp-hbhA*-complement (Lane 6 and 7) samples indicate the presence of the *mtp* gene which is absent Δ*mtp* (Lane e 3) and Δ*mtp-hbhA* (Lane 5). The expected PCR product of 624 bp was observed in Figure C1.2 for the wild-type (Lane 3 and 7), *hbhA*-complement (Lane 5), *mtp-hbhA*-complement (Lane 9) samples indicate the presence of the *hbhA* gene which is absent Δ*hbhA* (Lane 4), Δ*mtp-hbhA* (Lane 8) and a negative control (Lane 2 and 6). The expected PCR product of 700 bp was observed in Figure C1.3 for the wild-type (Lane 4), *Rv0309* complement (Lane 5), Δ*Rv0309* (Lane 3), Negative control (Lane 2,6 and 7).

Table C1.1 PCR target and primer sequences used for confirmation of three strains

PCR target	Primers	Annealing temperature (°C)
Rv0309 gene	F: 5'- TTTTTTAAGCTTATGAGCCGACTCCTAGCTTT -3' R: 5'- TTTTTTGAA TTCTTACTTGGCGATCGCGATCA -3'	55
mtp gene	Mtp-F: 5' CTCATGGGTCACAGCGAGTA 3' Mtp-R: 5' ATGACAGGTTCCCTTCAAGC 3'	60
hbhA gene	HbhA-F: 5' TTTTTTGAATTCATGGCTGAAAACTCGAACAT 3' HbhA -R: 5' TTTTTTAAGCTTCTACTTCTGGGTGACCTTCT 3'	65

Rv0309 encoding L, D-transpeptidase, *mtp*: gene encoding MTP; *hbhA*: gene encoding HBHA (Govender, 2018)

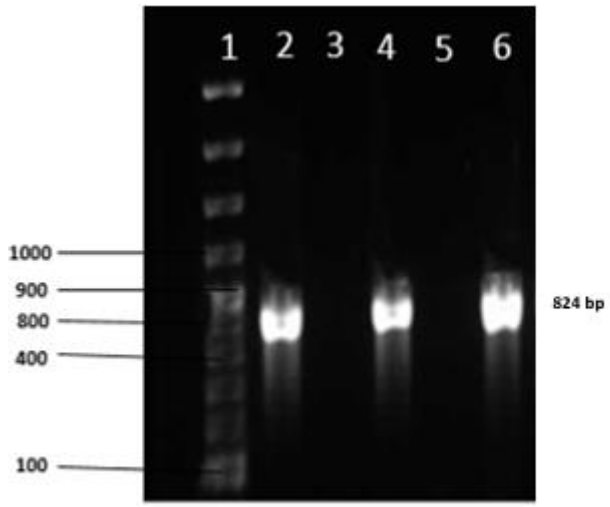

Figure C1.1 Gel electrophoresis images of PCR products confirming bacterial strains run at 70V for 3 hours on a 1.5% agarose gel using 100 bp (BioLabs) marker. (a) PCR targeting the *mtp* gene. (Lane 1) Molecular weight marker, (Lane 2) wild-type (V9124), (Lane 3) Δ*mtp*, (Lane 4) *mtp*-complement, (Lane 5) Δ*mtp-hbhA*, (Lane 6) *mtp-hbhA*-complement.

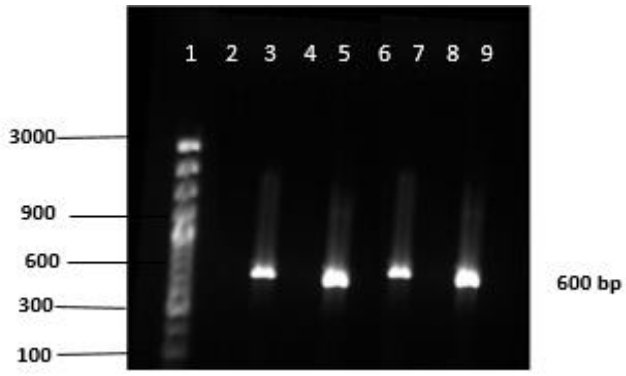

Figure C1.2 Gel electrophoresis images of PCR products confirming bacterial strains run at 70V for 3 hours on a 1.5% agarose gel using 100 bp (BioLabs) marker. (a) PCR targeting the *hbhA* gene. (Lane 1) Molecular weight marker, (Lane 2) Negative control, (Lane 3) wild-type (V9124), (Lane 4) Δ*hbhA*, (Lane 5) *hbhA*-complement, (Lane 6) Negative control, (Lane7) wild-type (V9124), (Lane 8) Δ*mtp-hbhA*, (Lane 9) *mtp-hbhA*-complement.

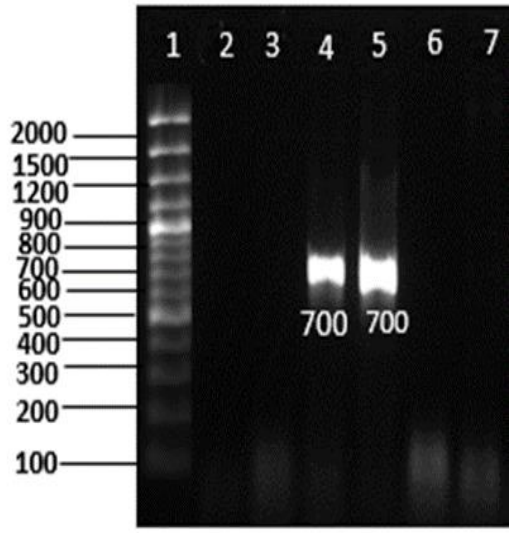

Figure C1.2 Gel electrophoresis images of PCR products confirming bacterial strains run at 70V for 3 hours on a 1.5% agarose gel using 100 bp (BioLabs) marker. (a) PCR targeting the *Rv0309 gene*. (Lane 1) Molecular weight marker, (Lane 2) Negative control, (Lane 3) Δ*Rv0309*, (Lane 4) wild-type (V9124), (Lane 5) *Rv0309*-complement, (Lane 6) Negative control, (Lane7) Negative control.

Bacterial CFU counts

Broth cultures were revived and grown to an OD600nm of 1 and plated to confirm that the *M. tuberculosis* cultures at this optical density were equivalent to approximately 1 X 10^8 CFU/mL (Larsen *et al*., 2007). The cultures were 10-fold serially diluted to determine CFU/mL for each strain (Table C1.2). Dilutions were made in Eppendorf tubes (Merck) by mixing 900 µL of 7H9 broth with 100 µL of OD600nm 1 bacterial culture. On 7H11 agar plates, a volume of 100 µL was plated. Colonies were enumerated after 3 weeks of incubation at 37 °C with plates enclosed in CO_2 permeable plastic bags. Using non-parametric, unpaired Mann Whitney testing, the significance levels across combinations of the strains were evaluated using GraphPad Prism version 8 software (GraphPad Software, La Jolla, CA, USA) (Table C1.2). Since all of the p-values were higher than 0.05, the differences in CFU/mL values were not statistically significant. This demonstrates that any anomalies found in the experimental data will be ascribed to the deletion of the genes under investigation and not to any other difference in the experimental setup.

Table C1.2: Level of significance in inoculum used for different *M. tuberculosis* strains.

Strain comparison	**p-value**	**significance**
WT and Δ*mtp*	0.700	None
Δ*mtp* and *mtp*-complement	0.850	None
WT and *mtp*-complement	0.869	None
WT and Δ*hbhA*	0.849	None
ΔhbhA and *hbhA*-complement	0.860	None
WT and *hbhA*-complement	0.958	None
WT and Δ*Rv0309*	0.801	None
Δ*Rv0309* and *Rv0309* complement	0.869	None
Wand *Rv0309* complement	0.801	None
WT and Δ*mtp-hbhA*	0.702	None
Δ*hbhA* and *mtp-hbhA* complement	0.663	None
WT and *mtp-hbhA* complement	0.902	None

Table C2.1: THP-1 cell count and MOI calculations for MTP biological assay 1

Wild type	**Mutant mtp**	**Mtp comp**
Alive cells: 13+12+09+13	**Alive cells**: 14+12+16+14	**Alive cells:** 14+12+16+14
Cells/mL = $\frac{(\text{Total number of cells} \times \text{dilution factor}(6) \times 104}{\text{Number of quadrants}}$ $= \frac{(47 \times 6 \times 104)}{4}$ $= 7.05 \times 10^5$ Total cell= $7.05 \times 10^5 \times 20$ mL MOI $= \frac{\text{Total number of bacterial cells}}{\text{Total number of THP}-1 \text{ cells}}$ $5 = \frac{(1x10^8 \text{ cells/mL})\,(x)}{(7.05x10^5 \text{ cells/mL})\,(20 \text{ mL})}$ Therefore: $x = \frac{(5)(7.05x10^5 \text{ cells/mL})\,(20 \text{ mL})}{(1x10^8 \text{ cells/mL})}$ x = 0.7 mL =700 µL	**Cells/mL** = $\frac{(\text{Total number of cells} \times \text{dilution factor}(6) \times 104}{\text{Number of quadrants}}$ $= \frac{(56 \times 6 \times 104)}{4}$ $= 8.40 \times 10^5$ Total cell= $8.40 \times 10^5 \times 20$ mL MOI $= \frac{\text{Total number of bacterial cells}}{\text{Total number of THP}-1 \text{ cells}}$ $5 = \frac{(1x10^8 \text{ cells/mL})\,(x)}{(8.40x10^5 \text{ cells/mL})\,(20 \text{ mL})}$ Therefore: $x = \frac{(5)(8.40x10^5 \text{ cells/mL})\,(20 \text{ mL})}{(1x10^8 \text{ cells/mL})}$ x = 0.84 mL =840 µL	**Cells/mL** = $\frac{(\text{Total number of cells} \times \text{dilution factor}(6) \times 104}{\text{Number of quadrants}}$ $= \frac{(56 \times 6 \times 104)}{4}$ $= 8.40 \times 10^5$ Total cell= $8.40 \times 10^5 \times 20$ mL MOI $= \frac{\text{Total number of bacterial cells}}{\text{Total number of THP}-1 \text{ cells}}$ $5 = \frac{(1x10^8 \text{ cells/mL})\,(x)}{(8.40x10^5 \text{ cells/mL})\,(20 \text{ mL})}$ Therefore: $x = \frac{(5)(8.40x10^5 \text{ cells/mL})\,(20 \text{ mL})}{(1x10^8 \text{ cells/mL})}$ x = 0.84 mL =840 µL

Table C2.2: Confirmation of MOI MTP biological assay 1

Wild-type	Mutant mtp	mtp comp
Selected dilution: 10^{-5} Average number of colonies = $\frac{(85+83+97)}{3}$ = 8.83 x 10^1 = 88 colonies CFU/mL = $\frac{\textbf{(average number of colonies} \times \textbf{dilution factor)}}{\textbf{volume plated out in mL}}$ = $\frac{(88)(10^5)}{(0.1)\text{mL}}$ = 9.7 ×10^7 CFU/mL MOI = $\frac{(\text{bacterial cells/mL of} \times \text{total volume of inoculum})}{(\text{THP}-1\ \text{cells/mL} \times \text{total volume})}$ $= \frac{(9.7\times 10^7\ \text{cells/mL})(0.700\ \text{mL})}{(7.05\times 10^5\ \text{cells/mL})\times(20\ \text{mL})}$ $= 4.81$	**Selected dilution: 10^{-5}** Average number of colonies = $\frac{(65+63+69)}{3}$ = 6.6 x 10^1 = 7x10^1 colonies CFU/mL = $\frac{\textbf{(average number of colonies} \times \textbf{dilution factor)}}{\textbf{volume plated out in mL}}$ = $\frac{(7x10^1)(10^5)}{(0.1)\text{mL}}$ = 7 ×10^7 CFU/mL MOI = $\frac{(\text{bacterial cells/mL of} \times \text{total volume of inoculum})}{(\text{THP}-1\ \text{cells/mL} \times \text{total volume})}$ $= \frac{(7\times 10^7\ \text{cells/mL})(0.840\ \text{mL})}{(8.40\times 10^5\ \text{cells/mL})\times(20\ \text{mL})}$ = 3.5	**Selected dilution: 10^{-5}** Average number of colonies = $\frac{(79+69+80)}{3}$ = 7.60 x 10^1 colonies CFU/mL = $\frac{\textbf{(average number of colonies} \times \textbf{dilution factor)}}{\textbf{volume plated out in mL}}$ = $\frac{(7.60x10^1)(10^5)}{(0.1)\text{mL}}$ = 7.60 ×10^7 CFU/mL MOI = $\frac{(\text{bacterial cells/mL of} \times \text{total volume of inoculum})}{(\text{THP}-1\ \text{cells/mL} \times \text{total volume})}$ $= \frac{(7.60\times 10^7\ \text{cells/mL})(0.840\ \text{mL})}{(8.40\times 10^5\ \text{cells/mL})\times(20\ \text{mL})}$ = 3.8

Table C2.3: CFU's for inoculum, 4-h and 24-h time done in triplicates for biological assay 1

	Dilution factor	Biological Assay 1										
		V9124 Wild-type (colonies count)			CFU/mL & MOI	*Mutant mtp* (colonies count)			CFU/mL calculation	*Mtp comp* (colonies count)			CFU/mL calculation
		Rep 1	Rep 2	Rep 3		Rep 1	Rep 2	Rep 3		Rep 1	Rep 2	Rep 3	
Inoculum	$x10^{-1}$	lawn	lawn	lawn		lawn	lawn	lawn		lawn	lawn	lawn	
	$x10^{-2}$	lawn	lawn	lawn		lawn	lawn	lawn		lawn	lawn		
	$x10^{-3}$	TMTC	TMTC	TMTC		TMTC	TMTC	TMTC		TMTC	TMTC	TMTC	
	$x10^{-4}$	>300	>300	>300	(85+83+87)/3)x	>300	>300	>300	(65+63+69)/3)x	>300	>300	>300	(79+69+80)/3)x
	$x10^{-5}$	85	83	87	10^5/0.1	65	63	69	10^5/0.1	79	69	80	10^5/0.1
	$x10^{-6}$	33	39	40	8.50 $x10^7$	21	28	26	6.57 $x10^7$	27	25	35	7.60 $x10^7$
	$x10^{-7}$	13	11	16		3	1	1		4	4	3	
4 hour time point	$x10^{-1}$	TMTC	TMTC	TMTC	(125+136+130)/	TMTC	TMTC	TMTC	(99+103+105)/3)	TMTC	TMTC	TMTC	(121+117+139)/
	$x10^{-2}$	125	136	130	3)x 10^2/0.1	99	103	105	x 10^2/0.1	121	117	139	3)x 10^2/0.1
	$x10^{-3}$	37	33	35	1.30 $x10^5$	5	12	15	1.02 $x10^5$	23	28	30	1.26 $x10^5$
	$x10^{-4}$	5	-	1		-	-	-		2	1	-	
	$x10^{-5}$	-	-	-		-	-	-					
24 hour time point	$x10^{-1}$	TMTC	TMTC	TMTC	(128+135+133)/	TMTC	TMTC	TMTC	(101+103+108)/	TMTC	TMTC	TMTC	(129+133+130)/
	$x10^{-2}$	128	135	133	3)x 10^2/0.1	101	103	108	3)x 10^2/0.1	129	133	130	3)x 10^2/0.1
	$x10^{-3}$	39	37	43	1.32 $x10^5$	7	10	17	1.04 $x10^5$	29	27	33	1.31 $x10^5$
	$x10^{-4}$	1	1	1		-	-	-		2	1	-	
	$x10^{-5}$	-	-	-		-	-	-		-	-	-	

Biological Assay 2

Table C2.4: THP-1 cell count and MOI calculations for MTP biological assay 2

Wild type	**Mutant *mtp***	***mtp* comp**
Alive cells: 18+14+13+15	**Alive cells**: 14+12+16+14	**Alive cells:** 18+11+17+14
Cells/mL = $\frac{(\text{Total number of cells} \times \text{dilution factor}(6) \times 104}{\text{Number of quadrants}}$ $= \frac{(60 \times 6 \times 104)}{4}$ $= 9.0 \times 10^5$ cells/mL Total cell= 9. 20 mL = 1.87×10^7 MOI = $\frac{\text{Total number of bacterial cells}}{\text{Total number of THP}-1 \text{ cells}}$ $5 = \frac{(1 \times 10^8 \text{ cells/mL})\ (x)}{(9.0 \times 10^5 \text{ cells/mL})\ (20 \text{ mL})}$ Therefore: $x = \frac{(5)(9.0 \times 10^5 \text{ cells/mL})\ (20 \text{ mL})}{(1 \times 10^8 \text{ cells/mL})}$ x = 0.9 mL =900 µL	**Cells/mL** = $\frac{(\text{Total number of cells} \times \text{dilution factor}(6) \times 104}{\text{Number of quadrants}}$ $= \frac{(56 \times 6 \times 104)}{4}$ $= 8.40 \times 10^5$ Total cell= $8.40 \times 10^5 \times 20$ mL = 1.7×10^7 MOI = $\frac{\text{Total number of bacterial cells}}{\text{Total number of THP}-1 \text{ cells}}$ $5 = \frac{(1 \times 10^8 \text{ cells/mL})\ (x)}{(8.40 \times 10^5 \text{ cells/mL})\ (20 \text{ mL})}$ Therefore: $x = \frac{(5)(8.40 \times 10^5 \text{ cells/mL})\ (20 \text{ mL})}{(1 \times 10^8 \text{ cells/mL})}$ x = 0.84 mL =840 µL	**Cells/mL** = $\frac{(\text{Total number of cells} \times \text{dilution factor}(6) \times 104}{\text{Number of quadrants}}$ $= \frac{(60 \times 6 \times 104)}{4}$ $= 9.0 \times 10^5$ Total cell= $9.0 \times 10^5 \times 20$ mL = 1.80×10^7 MOI = $\frac{\text{Total number of bacterial cells}}{\text{Total number of THP}-1 \text{ cells}}$ $5 = \frac{(1 \times 10^8 \text{ cells/mL})\ (x)}{(9.0 \times 10^5 \text{ cells/mL})\ (20 \text{ mL})}$ Therefore: $x = \frac{(5)(9.0 \times 10^5 \text{ cells/mL})\ (20 \text{ mL})}{(1 \times 10^8 \text{ cells/mL})}$ x = 0.90 mL =900 µL

Table C2.5: Confirmation of MOI MTP biological assay 2

Wild-type	Mutant mtp	mtp comp
Selected dilution: 10^{-5} Average number of colonies = $\frac{(92+87+89)}{3}$ = 8.9 x 10^1 = 89 colonies CFU/mL = $\frac{\textbf{(average number of colonies} \times \textbf{dilution factor)}}{\textbf{volume plated out in mL}}$ = $\frac{(89)(10^5)}{(0.1)\text{mL}}$ = 8.90 ×10^7 CFU/mL MOI = $\frac{(\text{bacterial cells/mL of} \times \text{total volume of inoculum})}{(\text{THP}-1 \text{ cells/mL} \times \text{total volume})}$ = $\frac{(8.90\times 10^7 \text{ cells/mL})(0.900 \text{ mL})}{(9.00\times 10^5 \text{ cells/mL})\times(20 \text{ mL})}$ = 4.45	**Selected dilution: 10^{-5}** Average number of colonies = $\frac{(69+63+69)}{3}$ = 6.70 x 10^1 = 67 colonies CFU/mL = $\frac{\textbf{(average number of colonies} \times \textbf{dilution factor)}}{\textbf{volume plated out in mL}}$ = $\frac{(6.7x10^1)(10^5)}{(0.1)\text{mL}}$ = 6.7 ×10^7 CFU/mL MOI = $\frac{(\text{bacterial cells/mL of} \times \text{total volume of inoculum})}{(\text{THP}-1 \text{ cells/mL} \times \text{total volume})}$ = $\frac{(6.7\times 10^7 \text{ cells/mL})(0.840 \text{ mL})}{(8.40\times 10^5 \text{ cells/mL})\times(20 \text{ mL})}$ = 3.9	**Selected dilution: 10^{-5}** Average number of colonies = $\frac{(75+82+78)}{3}$ = 7.8 x 10^1 colonies CFU/mL = $\frac{\textbf{(average number of colonies} \times \textbf{dilution factor)}}{\textbf{volume plated out in mL}}$ = $\frac{(7.8x10^1)(10^5)}{(0.1)\text{mL}}$ = 7.8 ×10^7 CFU/mL MOI = $\frac{(\text{bacterial cells/mL of} \times \text{total volume of inoculum}}{(\text{THP}-1 \text{ cells/mL} \times \text{total volume})}$ = $\frac{(7.8\times 10^7 \text{ cells/mL})(0.900 \text{ mL})}{(9.0\times 10^5 \text{ cells/mL})\times(20 \text{ mL})}$ = 4.0

Table C2.6: CFU's for inoculum, 4-h and 24-h time done in triplicates for biological assay 2

	Dilution factor	Biological Assay 2										
		V9124 Wild-type (colonies count)			CFU/mL & MOI	*Mutant mtp* (colonies count)			CFU/mL calculation	*Mtp comp* (colonies count)			CFU/mL calculation
		Rep 1	Rep 2	Rep 3		Rep 1	Rep 2	Rep 3		Rep 1	Rep 2	Rep 3	
Inoculum	$x10^{-1}$	lawn	lawn	lawn		lawn	lawn	lawn		lawn	lawn	lawn	
	$x10^{-2}$	lawn	lawn	lawn		lawn	lawn	lawn		lawn	lawn		
	$x10^{-3}$	TMTC	TMTC	TMTC		TMTC	TMTC	TMTC		TMTC	TMTC	TMTC	
	$x10^{-4}$	>300	>300	>300	(92+87+89)/3) x	>300	>300	>300	(69+69+63)/3) x	>300	>300	>300	(73+71+78)/3)x
	$x10^{-5}$	92	87	89	10^5/0.1	69	69	63	10^5/0.1	73	71	78	10^5/0.1
	$x10^{-6}$	69	70	67	8.93×10^7	29	27	24	6.70×10^7	30	33	30	7.40×10^7
	$x10^{-7}$	14	08	12		1	2	1		3	3	1	
4 hour time point	$x10^{-1}$	TMTC	TMTC	TMTC	(130+137+147)/	TMTC	TMTC	TMTC	(84+89+101)/3)	TMTC	TMTC	TMTC	(123+128+133)/
	$x10^{-2}$	130	137	147	$3)x\ 10^2/0.1$	87	89	101	$x\ 10^2/0.1$	123	128	133	$3)x\ 10^2/0.1$
	$x10^{-3}$	43	40	48	1.38×10^5	10	13	13	$9.13x10^4$	35	35	38	1.28×10^5
	$x10^{-4}$	3	2	3		-	-	-		4	2	2	
	$x10^{-5}$	-	-	-		-	-	-					
24 hour time point	$x10^{-1}$	TMTC	TMTC	TMTC	(133+137+145)/	TMTC	TMTC	TMTC	(119+123+108)/	TMTC	TMTC	TMTC	(129+133+130)/
	$x10^{-2}$	133	137	145	$3)x\ 10^2/0.1$	119	123	108	$3)x\ 10^2/0.1$	129	133	130	$3)x\ 10^2/0.1$
	$x10^{-3}$	49	37	40	1.38×10^5	27	24	30	1.17×10^5	37	40	40	1.31×10^5
	$x10^{-4}$	4	1	3		-	-	-		1	3	3	
	$x10^{-5}$	-	-	-		-	-	-		-	-	-	

Biological assay 3

Table C2.7: THP-1 cell count and MOI calculations for MTP biological assay 3

Wild-type	**Mutant mtp**	**mtp comp**
Alive cells: 19+13+17+13	**Alive cells**: 09+18+14+08	**Alive cells:** 14+12+16+14
Cells/mL = $\frac{(\text{Total number of cells} \times \text{dilution factor}(6) \times 104}{\text{Number of quadrants}}$ $= \frac{(62 \times 6 \times 104)}{4}$ $= 9.30 \times 10^5$ Total cell= $9.30 \times 10^5 \times 20\ \text{mL} = 1.86 \times 10^7$ MOI = $\frac{\text{Total number of bacterial cells}}{\text{Total number of THP}-1\ \text{cells}}$ $5 = \frac{(1\text{x}10^8\ \text{cells/mL})\ (x)}{(9.30\text{x}10^5\ \text{cells/mL})\ (20\ \text{mL})}$ Therefore: $x = \frac{(5)(9.30\text{x}10^5\ \text{cells/mL})\ (20\ \text{mL})}{(1\text{x}10^8\ \text{cells/mL})}$ x = 0.93 mL =930 µL	**Cells/mL** = $\frac{(\text{Total number of cells} \times \text{dilution factor}(6) \times 104}{\text{Number of quadrants}}$ $= \frac{(59 \times 6 \times 104)}{4}$ $= 8.85 \times 10^5$ Total cell= $8.85 \times 10^5 \times 20\ \text{mL} = 1.77 \times 10^7$ MOI = $\frac{\text{Total number of bacterial cells}}{\text{Total number of THP}-1\ \text{cells}}$ $5 = \frac{(1\text{x}10^8\ \text{cells/mL})\ (x)}{(8.85\text{x}10^5\ \text{cells/mL})\ (20\ \text{mL})}$ Therefore: $x = \frac{(5)(8.85\text{x}10^5\ \text{cells/mL})\ (20\ \text{mL})}{(1\text{x}10^8\ \text{cells/mL})}$ x = 0.885 mL =885 µL	**Cells/mL** = $\frac{(\text{Total number of cells} \times \text{dilution factor}(6) \times 104}{\text{Number of quadrants}}$ $= \frac{(63 \times 6 \times 104)}{4}$ $= 9.45 \times 10^5$ Total cell= $9.45 \times 10^5 \times 20\ \text{mL} = 1.89 \times 10^7$ MOI = $\frac{\text{Total number of bacterial cells}}{\text{Total number of THP}-1\ \text{cells}}$ $5 = \frac{(1\text{x}10^8\ \text{cells/mL})\ (x)}{(9.45\text{x}10^5\ \text{cells/mL})\ (20\ \text{mL})}$ Therefore: $x = \frac{(5)(9.45\text{x}10^5\ \text{cells/mL})\ (20\ \text{mL})}{(1\text{x}10^8\ \text{cells/mL})}$ x = 0.945 mL =945 µL

Table C2.8: Confirmation of the MOI for biological assay 3

Wild-type	Mutant mtp	mtp comp
Selected dilution: 10^{-5} Average number of colonies = $\frac{(95+89+95)}{3}$ = 93 x 10^1 = 93 colonies CFU/mL = $\frac{(\textbf{average number of colonies} \times \textbf{dilution factor})}{\textbf{volume plated out in mL}}$ = $\frac{(93)(10^5)}{(0.1)\text{mL}}$ = 9.3 ×10^7 CFU/mL MOI = $\frac{(\text{bacterial cells/mL of} \times \text{total volume of inoculum})}{(\text{THP}-1 \text{ cells/mL} \times \text{total volume})}$ = $\frac{(9.3\times 10^7 \text{ cells/mL})(0.93 \text{ mL})}{(9.30\times 10^5 \text{ cells/mL})\times(20 \text{ mL})}$ = 4.7	**Selected dilution: 10^{-5}** Average number of colonies = $\frac{(72+65+89)}{3}$ = 7.5 x 10^1 = 75 colonies CFU/mL = $\frac{(\textbf{average number of colonies} \times \textbf{dilution factor})}{\textbf{volume plated out in mL}}$ = $\frac{(7.5x10^1)(10^5)}{(0.1)\text{mL}}$ = 7.5 ×10^7 CFU/mL MOI = $\frac{(\text{bacterial cells/mL of} \times \text{total volume of inoculum})}{(\text{THP}-1 \text{ cells/mL} \times \text{total volume})}$ = $\frac{(7.5\times 10^7 \text{ cells/mL})(0.885 \text{ mL})}{(8.85\times 10^5 \text{ cells/mL})\times(20 \text{ mL})}$ = 3.75	**Selected dilution: 10^{-5}** Average number of colonies = $\frac{(87+88+75)}{3}$ = 8.3 x 10^1 colonies CFU/mL = $\frac{(\textbf{average number of colonies} \times \textbf{dilution factor})}{\textbf{volume plated out in mL}}$ = $\frac{(8.3x10^1)(10^5)}{(0.1)\text{mL}}$ = 7.8 ×10^7 CFU/mL MOI = $\frac{(\text{bacterial cells/mL of} \times \text{total volume of inoculum}}{(\text{THP}-1 \text{ cells/mL} \times \text{total volume})}$ = $\frac{(8.3\times 10^7 \text{ cells/mL})(0.945 \text{ mL})}{(9.45\times 10^5 \text{ cells/mL})\times(20 \text{ mL})}$ = 4.2

Table C2.9: CFU's for inoculum, 4-h and 24-h time done in triplicates for biological assay 3

	Dilution factor	Biological Assay 3										
		V9124 Wild-type (colonies count)			CFU/mL & MOI	*Mutant mtp* (colonies count)			CFU/mL calculation	*Mtp comp* (colonies count)			CFU/mL calculation
		Rep 1	Rep 2	Rep 3		Rep 1	Rep 2	Rep 3		Rep 1	Rep 2	Rep 3	
Inoculum	$x10^{-1}$	lawn	lawn	lawn		lawn	lawn	lawn		lawn	lawn	lawn	
	$x10^{-2}$	lawn	lawn	lawn		lawn	lawn	lawn		lawn	lawn		
	$x10^{-3}$	TMTC	TMTC	TMTC		TMTC	TMTC	TMTC		TMTC	TMTC	TMTC	
	$x10^{-4}$	>300	>300	>300	(95+89+95)/3)x	>300	>300	>300	(72+65+89)/3)x	>300	>300	>300	(87+88+75)/3)x
	$x10^{-5}$	95	89	95	10^5/0.1	72	65	89	10^5/0.1	87	88	75	10^5/0.1
	$x10^{-6}$	65	70	73	9.30 $x10^7$	37	30	29	7.53 $x10^7$	39	29	43	8.33 $x10^7$
	$x10^{-7}$	11	08	05		2	3	3		3	5	2	
4 hour time point	$x10^{-1}$	TMTC	TMTC	TMTC	(127+143+124)/	TMTC	TMTC	TMTC	(75+82+89)/3)x	TMTC	TMTC	TMTC	(101+92+87)/3)x
	$x10^{-2}$	127	143	124	3)x 10^2/0.1	75	82	89	10^2/0.1	101	92	87	10^2/0.1
	$x10^{-3}$	33	33	28	1.31 $x10^5$	07	11	09	8.20 $x10^4$	26	29	33	6.33 $x10^4$
	$x10^{-4}$	02	02	05		-	-	1		1	1	3	
	$x10^{-5}$	-	-	-		-	-	-					
24 hour time point	$x10^{-1}$	TMTC	TMTC	TMTC	(135+129+149)/	TMTC	TMTC	TMTC	(89+87+92)/3)x	TMTC	TMTC	TMTC	(129+133+130)/
	$x10^{-2}$	135	129	149	3)x 10^2/0.1	89	87	92	10^2/0.1	129	133	130	3)x 10^2/0.1
	$x10^{-3}$	53	42	39	1.38 $x10^5$	09	11	13	8.93 $x10^4$	44	37	33	1.31 $x10^5$
	$x10^{-4}$	7	3	5		-	-	-		1	1	4	
	$x10^{-5}$	-	-	-		-	-	-		-	-	-	

Table C2.10: THP-1 cell count and MOI calculations for HBHA biological assay 1

Wild-type	**Mutant *hbhA***	***hbhA* comp**
Alive cells: 18+20+16+16	**Alive cells**: 09+18+14+08	**Alive cells:** 18+15+13+20
Cells/mL = $\frac{(\text{Total number of cells} \times \text{dilution factor}(6) \times 104}{\text{Number of quadrants}}$ $= \frac{(70 \times 6 \times 104)}{4}$ $= 1.1 \times 10^6$ Total cell= $1.1 \times 10^6 \times 20\ \text{mL} = 2.1 \times 10^7$ MOI = $\frac{\text{Total number of bacterial cells}}{\text{Total number of THP}-1\ \text{cells}}$ $5 = \frac{(1\text{x}10^8\ \text{cells/mL})\ (x)}{(1.1\text{x}10^6\ \text{cells/mL})\ (20\ \text{mL})}$ Therefore: $x = \frac{(5)(1.1\text{x}10^6\ \text{cells/mL})\ (20\ \text{mL})}{(1\text{x}10^8\ \text{cells/mL})}$ x = 1.05 mL	**Cells/mL** = $\frac{(\text{Total number of cells} \times \text{dilution factor}(6) \times 104}{\text{Number of quadrants}}$ $= \frac{(56 \times 6 \times 104)}{4}$ $= 8.40 \times 10^5$ Total cell= $8.40 \times 10^5 \times 20\ \text{mL} = 1.7 \times 10^7$ MOI = $\frac{\text{Total number of bacterial cells}}{\text{Total number of THP}-1\ \text{cells}}$ $5 = \frac{(1\text{x}10^8\ \text{cells/mL})\ (x)}{(8.40\text{x}10^5\ \text{cells/mL})\ (20\ \text{mL})}$ Therefore: $x = \frac{(5)(8.40\text{x}10^5\ \text{cells/mL})\ (20\ \text{mL})}{(1\text{x}10^8\ \text{cells/mL})}$ x = 0.840 mL =840 µL	**Cells/mL** = $\frac{(\text{Total number of cells} \times \text{dilution factor}(6) \times 104}{\text{Number of quadrants}}$ $= \frac{(66 \times 6 \times 104)}{4}$ $= 9.9 \times 10^5$ Total cell= $9.9 \times 10^5 \times 20\ \text{mL} = 2.0 \times 10^7$ MOI = $\frac{\text{Total number of bacterial cells}}{\text{Total number of THP}-1\ \text{cells}}$ $5 = \frac{(1\text{x}10^8\ \text{cells/mL})\ (x)}{(9.9\text{x}10^5\ \text{cells/mL})\ (20\ \text{mL})}$ Therefore: $x = \frac{(5)(9.9\text{x}10^5\ \text{cells/mL})\ (20\ \text{mL})}{(1\text{x}10^8\ \text{cells/mL})}$ x = 0.99 mL =990 µL

Table C2.12: Confirmation of the MOI for HBHA biological assay 1

Wild-type	Mutant *hbhA*	*hbhA* comp
Selected dilution: 10^{-5} Average number of colonies = $\frac{(103+101+105)}{3}$ = 1.0 x 10^2 = 103 colonies CFU/mL = $\frac{(\textbf{average number of colonies} \times \textbf{dilution factor})}{\textbf{volume plated out in mL}}$ = $\frac{(103)(10^5)}{(0.1)\text{mL}}$ = 1.03 ×10^8 CFU/mL MOI = $\frac{(\text{bacterial cells/mL of} \times \text{total volume of inoculum})}{(\text{THP}-1 \text{ cells/mL} \times \text{total volume})}$ = $\frac{(1.03\times 10^8 \text{ cells/mL})(1.05 \text{ mL})}{(1.1\times 10^6 \text{ cells/mL})\times(20 \text{ mL})}$ = 5.15	**Selected dilution: 10^{-5}** Average number of colonies = $\frac{(83+75+63)}{3}$ = 7.4 x 10^1 = 74 colonies CFU/mL = $\frac{(\textbf{average number of colonies} \times \textbf{dilution factor})}{\textbf{volume plated out in mL}}$ = $\frac{(7.4x10^1)(10^5)}{(0.1)\text{mL}}$ = 7.40 ×10^7 CFU/mL MOI = $\frac{(\text{bacterial cells/mL of} \times \text{total volume of inoculum})}{(\text{THP}-1 \text{ cells/mL} \times \text{total volume})}$ = $\frac{(7.40\times 10^7 \text{ cells/mL})(0.840 \text{ mL})}{(8.40\times 10^5 \text{ cells/mL})\times(20 \text{ mL})}$ = 3.70	**Selected dilution: 10^{-5}** Average number of colonies = $\frac{(95+97+106)}{3}$ = 9.9 x 10^1 colonies CFU/mL = $\frac{(\textbf{average number of colonies} \times \textbf{dilution factor})}{\textbf{volume plated out in mL}}$ = $\frac{(9.9x10^1)(10^5)}{(0.1)\text{mL}}$ = 9.9 ×10^7 CFU/mL MOI = $\frac{(\text{bacterial cells/mL of} \times \text{total volume of inoculum})}{(\text{THP}-1 \text{ cells/mL} \times \text{total volume})}$ = $\frac{(9.9\times 10^7 \text{ cells/mL})(0.99\text{mL})}{(9.9\times 10^5 \text{ cells/mL})\times(20 \text{ mL})}$ = 5.0

Table C2.13: CFU's for inoculum, 4-h and 24-h time done in triplicates for HBHA biological assay 1

	Dilution factor	Biological Assay 1										
		V9124 Wild-type (colonies count)			CFU/mL & MOI	*Mutant hbhA* (colonies count)			CFU/mL calculation	*hbhA comp* (colonies count)			CFU/mL calculation
		Rep 1	Rep 2	Rep 3		Rep 1	Rep 2	Rep 3		Rep 1	Rep 2	Rep 3	
Inoculum	$x10^{-1}$	lawn	lawn	lawn		lawn	lawn	lawn		lawn	lawn	lawn	
	$x10^{-2}$	lawn	lawn	lawn		lawn	lawn	lawn		lawn	lawn		
	$x10^{-3}$	TMTC	TMTC	TMTC		TMTC	TMTC	TMTC		TMTC	TMTC	TMTC	
	$x10^{-4}$	>300	>300	>300	(103+101+105)/	>300	>300	>300	(83+75+85)/3) x	>300	>300	>300	(95+97+106)/
	$x10^{-5}$	103	101	105	3) x 10^5/0.1	83	75	85	10^5/0.1	95	97	106	3) x 10^5/0.1
	$x10^{-6}$	49	56	63	1.03 $x10^8$	04	14	09	8.10 $x10^7$	17	18	11	9.93 $x10^7$
	$x10^{-7}$	07	13	17		03	03	07		02	03	07	
4 hour time point	$x10^{-1}$	TMTC	TMTC	TMTC	(230+215+211)/	TMTC	TMTC	TMTC	(125+146+159)/	TMTC	TMTC	TMTC	(159+160+18
	$x10^{-2}$	230	215	211	3) x 10^2/0.1	125	146	159	3) x 10^2/0.1	159	160	183	3) x 10^2/0.1
	$x10^{-3}$	45	33	35	2.2 $x10^5$	15	25	31	1.4 $x10^5$	29	36	43	1.70 $x10^5$
	$x10^{-4}$	5	3	1		-	-	-		04	02	13	
	$x10^{-5}$	-	-	-		-	-	-		-	-	-	
24 hour time point	$x10^{-1}$	TMTC	TMTC	TMTC	(205+215+197)/	TMTC	TMTC	TMTC	(154+146+159)/	TMTC	TMTC	TMTC	(165+179+18
	$x10^{-2}$	205	215	197	3) x 10^2/0.1	154	146	159	3) x 10^2/0.1	165	179	183	3)/3) x 10^2/0.1
	$x10^{-3}$	49	56	65	2.06 $x10^5$	54	43	59	1.5 $x10^5$	89	94	101	1.8 $x10^5$
	$x10^{-4}$	13	10	15		-	-	-		10	17	09	
	$x10^{-5}$	-	-	-		-	-	-		-	-	-	

Table C2.14: THP-1 cell count and MOI calculations for HBHA biological assay 2

Wild-type	**Mutant *hbhA***	***hbhA* comp**
Alive cells: 16+21+18+14	**Alive cells**: 13+18+13+14	**Alive cells:** 12+16+15+17
Cells/mL = $\frac{(\text{Total number of cells} \times \text{dilution factor}(6) \times 104}{\text{Number of quadrants}}$ $= \frac{(69 \times 6 \times 104)}{4}$ $= 1.04 \times 10^6$ Total cells = $1.1 \times 10^6 \times 20$ mL = 2.07×10^7 MOI = $\frac{\text{Total number of bacterial cells}}{\text{Total number of THP}-1\text{ cells}}$ $5 = \frac{(1\text{x}10^8\ \text{cells/mL})\ (x)}{(1.04\text{x}10^6\ \text{cells/mL})\ (20\ \text{mL})}$ Therefore: $x = \frac{(5)(1.04\text{x}10^6\ \text{cells/mL})\ (20\ \text{mL})}{(1\text{x}10^8\ \text{cells/mL})}$ x = 1.04 mL	**Cells/mL** = $\frac{(\text{Total number of cells} \times \text{dilution factor}(6) \times 104}{\text{Number of quadrants}}$ $= \frac{(58 \times 6 \times 104)}{4}$ $= 8.70 \times 10^5$ Total cell= $8.70 \times 10^5 \times 20$ mL = 1.74×10^7 MOI = $\frac{\text{Total number of bacterial cells}}{\text{Total number of THP}-1\text{ cells}}$ $5 = \frac{(1\text{x}10^8\ \text{cells/mL})\ (x)}{(8.70\text{x}10^5\ \text{cells/mL})\ (20\ \text{mL})}$ Therefore: $x = \frac{(5)(8.70\text{x}10^5\ \text{cells/mL})\ (20\ \text{mL})}{(1\text{x}10^8\ \text{cells/mL})}$ x = 0.870 mL =870 µL	**Cells/mL** = $\frac{(\text{Total number of cells} \times \text{dilution factor}(6) \times 104}{\text{Number of quadrants}}$ $= \frac{(60 \times 6 \times 104)}{4}$ $= 9.0 \times 10^5$ Total cell= $9.0 \times 10^5 \times 20$ mL = 1.8×10^7 MOI = $\frac{\text{Total number of bacterial cells}}{\text{Total number of THP}-1\text{ cells}}$ $5 = \frac{(1\text{x}10^8\ \text{cells/mL})\ (x)}{(9.0\text{x}10^5\ \text{cells/mL})\ (20\ \text{mL})}$ Therefore: $x = \frac{(5)(9.0\text{x}10^5\ \text{cells/mL})\ (20\ \text{mL})}{(1\text{x}10^8\ \text{cells/mL})}$ x = 0.900 mL =900 µL

Table C2.15: Confirmation of the MOI for HBHA biological assay 2

Wild type	Mutant *hbhA*	*hbhA* comp
Selected dilution: 10^{-5} Average number of colonies = $\frac{(106+111+109)}{3}$ = 1.1 x 10^2 = 108 colonies CFU/mL = $\frac{(\textbf{average number of colonies} \times \textbf{dilution factor})}{\textbf{volume plated out in mL}}$ = $\frac{(108)(10^5)}{(0.1)\text{mL}}$ = 1.09 ×10^8 CFU/mL MOI = $\frac{(\text{bacterial cells/mL of} \times \text{total volume of inoculum})}{(\text{THP}-1 \text{ cells/mL} \times \text{total volume})}$ = $\frac{(1.09\times 10^8 \text{ cells/mL})(1.05 \text{ mL})}{(1.04\times 10^6 \text{ cells/mL})\times(20 \text{ mL})}$ = 5	**Selected dilution: 10^{-5}** Average number of colonies = $\frac{(69+75+83)}{3}$ = 7.6 x 10^1 = 76 colonies CFU/mL = $\frac{(\textbf{average number of colonies} \times \textbf{dilution factor})}{\textbf{volume plated out in mL}}$ = $\frac{(7.6x10^1)(10^5)}{(0.1)\text{mL}}$ = 7.60 ×10^7 CFU/mL MOI = $\frac{(\text{bacterial cells/mL of} \times \text{total volume of inoculum})}{(\text{THP}-1 \text{ cells/mL} \times \text{total volume})}$ = $\frac{(7.60\times 10^7 \text{ cells/mL})(0.870 \text{ mL})}{(8.70\times 10^5 \text{ cells/mL})\times(20 \text{ mL})}$ = 3.8	**Selected dilution: 10^{-5}** Average number of colonies = $\frac{(79+83+101)}{3}$ = 8.8 x 10^1 colonies CFU/mL = $\frac{(\textbf{average number of colonies} \times \textbf{dilution factor})}{\textbf{volume plated out in mL}}$ = $\frac{(8.8x10^1)(10^5)}{(0.1)\text{mL}}$ = 8.8 ×10^7 CFU/mL MOI = $\frac{(\text{bacterial cells/mL of} \times \text{total volume of inoculum}$ $\frac{(\text{THP}-1 \text{ cells/mL} \times \text{total volume})}{}$ = $\frac{(8.8\times 10^7 \text{ cells/mL})(0.900\text{mL})}{(9.0\times 10^5 \text{ cells/mL})\times(20 \text{ mL})}$ = 4.4

Table C2.16: CFU's for inoculum, 4-h and 24-h time done in triplicates for biological assay 2

	Dilution factor	Biological Assay 2										
		V9124 Wild-type (colonies count)			CFU/mL & MOI	*Mutant hbhA* (colonies count)			CFU/mL calculation	*hbhA comp* (colonies count)			CFU/mL calculation
		Rep 1	Rep 2	Rep 3		Rep 1	Rep 2	Rep 3		Rep 1	Rep 2	Rep 3	
Inoculum	$x10^{-1}$	lawn	lawn	lawn		lawn	lawn	lawn		lawn	lawn	lawn	
	$x10^{-2}$	lawn	lawn	lawn		lawn	lawn	lawn		lawn	lawn		
	$x10^{-3}$	TMTC	TMTC	TMTC		TMTC	TMTC	TMTC		TMTC	TMTC	TMTC	
	$x10^{-4}$	>300	>300	>300	(106+111+109)/	>300	>300	>300	(69+75+83)/3) x	>300	>300	>300	(79+83+101)/
	$x10^{-5}$	106	111	109	3)x 10^5/0.1	69	75	83	10^5/0.1	79	83	101	3) x 10^5/0.1
	$x10^{-6}$	69	85	92	1.09 $x10^8$	25	36	32	7.57 $x10^7$	35	39	32	7.70 $x10^7$
	$x10^{-7}$	15	09	07		05	10	07		09	11	11	
4 hour time point	$x10^{-1}$	TMTC	TMTC	TMTC	(185+192+192)/	TMTC	TMTC	TMTC	(93+115+129)/3)	TMTC	TMTC	TMTC	(179+170+18
	$x10^{-2}$	185	192	192	3)x 10^2/0.1	93	115	129	x 10^2/0.1	179	170	187	7)/3) x 10^1/0.1
	$x10^{-3}$	73	89	98	1.90 $x10^5$	18	20	30	1.1$x10^5$	39	56	48	1.8 $x10^5$
	$x10^{-4}$	07	03	03		01	02	02		11	05	11	
	$x10^{-5}$	-	-	-		-	-	-		-	-	-	
24 hour time point	$x10^{-1}$	TMTC	TMTC	TMTC	(211+203+210)/	TMTC	TMTC	TMTC	(121+131+168)/	TMTC	TMTC	TMTC	(198+202+19
	$x10^{-2}$	211	203	210	3)x 10^2/0.1	121	131	168	3)x 10^2/0.1	198	202	196	6)/3)x 10^2/0.1
	$x10^{-3}$	85	73	92	2.08 $x10^5$	65	53	64	1.4 $x10^5$	69	87	82	2.0 $x10^5$
	$x10^{-4}$	07	05	13		04	04	01		11	15	20	
	$x10^{-5}$	-	-	-		-	-	-		03	01	03	

Table C2.17: THP-1 cell count and MOI calculations for HBHA biological assay 3

Wild-type	**Mutant hbhA**	**hbhA comp**
Alive cells: 19+13+18+14	**Alive cells**: 12+18+16+12	**Alive cells:** 18+16+14+12
Cells/mL = $\frac{(\text{Total number of cells} \times \text{dilution factor}(6) \times 104}{\text{Number of quadrants}}$ $= \frac{(64 \times 6 \times 10\text{^}4)}{4}$ $= 9.60 \times 10^5$ Total cells = $9.60 \times 10^5 \times 20$ mL = 1.92×10^7 MOI = $\frac{\text{Total number of bacterial cells}}{\text{Total number of THP}-1\text{ cells}}$ $5 = \frac{(1 \times 10^8 \text{ cells/mL})\,(x)}{(9.60 \times 10^5 \text{ cells/mL})\,(20 \text{ mL})}$ Therefore: $x = \frac{(5)(9.60 \times 10^5 \text{ cells/mL})\,(20 \text{ mL})}{(1 \times 10^8 \text{ cells/mL})}$ x = 0.96 mL	**Cells/mL** = $\frac{(\text{Total number of cells} \times \text{dilution factor}(6) \times 104}{\text{Number of quadrants}}$ $= \frac{(58 \times 6 \times 10\text{^}4)}{4}$ $= 8.70 \times 10^5$ Total cell= $8.70 \times 10^5 \times 20$ mL = 1.74×10^7 MOI = $\frac{\text{Total number of bacterial cells}}{\text{Total number of THP}-1\text{ cells}}$ $5 = \frac{(1 \times 10^8 \text{ cells/mL})\,(x)}{(8.70 \times 10^5 \text{ cells/mL})\,(20 \text{ mL})}$ Therefore: $x = \frac{(5)(8.70 \times 10^5 \text{ cells/mL})\,(20 \text{ mL})}{(1 \times 10^8 \text{ cells/mL})}$ x = 0.870 mL =870 µL	**Cells/mL** = $\frac{(\text{Total number of cells} \times \text{dilution factor}(6) \times 104}{\text{Number of quadrants}}$ $= \frac{(60 \times 6 \times 10\ \ 4)}{4}$ $= 9.0 \times 10^5$ Total cell= $9.0 \times 10^5 \times 20$ mL = 1.8×10^7 MOI = $\frac{\text{Total number of bacterial cells}}{\text{Total number of THP}-1\text{ cells}}$ $5 = \frac{(1 \times 10^8 \text{ cells/mL})\,(x)}{(9.0 \times 10^5 \text{ cells/mL})\,(20 \text{ mL})}$ Therefore: $x = \frac{(5)(9.0 \times 10^5 \text{ cells/mL})\,(20 \text{ mL})}{(1 \times 10^8 \text{ cells/mL})}$ x = 0.900 mL =900 µL

Table C2.18: Confirmation of the MOI for HBHA biological assay 3

Wild-type	Mutant *hbhA*	*hbhA* comp
Selected dilution: 10^{-5} Average number of colonies = $\frac{(101+96+98)}{3}$ = 9.9 x 10^1 = 98 colonies CFU/mL = $\frac{(\textbf{average number of colonies} \times \textbf{dilution factor})}{\textbf{volume plated out in mL}}$ = $\frac{(98)(10^5)}{(0.1)\text{mL}}$ = 9.8 ×10^7 CFU/mL MOI = $\frac{(\text{bacterial cells/mL of} \times \text{total volume of inoculum})}{(\text{THP}-1 \text{ cells/mL} \times \text{total volume})}$ = $\frac{(9.8\times 10^7 \text{ cells/mL})(0.96 \text{ mL})}{(9.60\times 10^5 \text{ cells/mL})\times(20 \text{ mL})}$ = 4.9	**Selected dilution: 10^{-5}** Average number of colonies = $\frac{(89+87+75)}{3}$ = 8.4 x 10^1 = 84 colonies CFU/mL = $\frac{(\textbf{average number of colonies} \times \textbf{dilution factor})}{\textbf{volume plated out in mL}}$ = $\frac{(8.4x10^1)(10^5)}{(0.1)\text{mL}}$ = 8.40 ×10^7 CFU/mL MOI = $\frac{(\text{bacterial cells/mL of} \times \text{total volume of inoculum})}{(\text{THP}-1 \text{ cells/mL} \times \text{total volume})}$ = $\frac{(8.40\times 10^7 \text{ cells/mL})(0.870 \text{ mL})}{(8.70\times 10^5 \text{ cells/mL})\times(20 \text{ mL})}$ = 4.2	**Selected dilution: 10^{-5}** Average number of colonies = $\frac{(85+92+96)}{3}$ = 9.1 x 10^1 colonies CFU/mL = $\frac{(\textbf{average number of colonies} \times \textbf{dilution factor})}{\textbf{volume plated out in mL}}$ = $\frac{(9.1x10^1)(10^5)}{(0.1)\text{mL}}$ = 9.1 ×10^7 CFU/mL MOI = $\frac{(\text{bacterial cells/mL of} \times \text{total volume of inoculum}}{(\text{THP}-1 \text{ cells/mL} \times \text{total volume})}$ = $\frac{(9.1\times 10^7 \text{ cells/mL})(0.900\text{mL})}{(9.0\times 10^5 \text{ cells/mL})\times(20 \text{ mL})}$ = 4.6

Table C2.19: CFU's for inoculum, 4-h and 24-h time done in triplicates for biological assay 3

	Dilution factor	Biological Assay 3										
		V9124 Wild-type (colonies count)			CFU/mL & MOI	*Mutant hbhA* (colonies count)			CFU/mL calculation	*hbhA comp* (colonies count)			CFU/mL calculation
		Rep 1	Rep 2	Rep 3		Rep 1	Rep 2	Rep 3		Rep 1	Rep 2	Rep 3	
Inoculum	$x10^{-1}$	lawn	lawn	lawn		lawn	lawn	lawn		lawn	lawn	lawn	
	$x10^{-2}$	lawn	lawn	lawn		lawn	lawn	lawn		lawn	lawn		
	$x10^{-3}$	TMTC	TMTC	TMTC		TMTC	TMTC	TMTC		TMTC	TMTC	TMTC	
	$x10^{-4}$	>300	>300	>300	(101+96+98)/3)x	>300	>300	>300	(89+87+75)/3)x	>300	>300	>300	(85+92+96)/3)x
	$x10^{-5}$	101	96	98	10^5/0.1	89	87	75	10^5/0.1	85	92	96	10^5/0.1
	$x10^{-6}$	56	65	67	9.83 $x10^7$	25	33	28	8.37 $x10^7$	36	49	54	9.10 $x10^7$
	$x10^{-7}$	11	15	15		01	07	07		05	05	09	
4 hour time point	$x10^{-1}$	TMTC	TMTC	TMTC	(200+189+197)/	TMTC	TMTC	TMTC	(169+171+150)/	TMTC	TMTC	TMTC	(198+189+205)/
	$x10^{-2}$	200	189	197	3)x 10^2/0.1	169	171	150	3)x 10^1/0.1	198	189	205	3)x 10^2/0.1
	$x10^{-3}$	65	52	39	1.95$x10^5$	25	35	33	1.6 $x10^5$	69	73	50	2.0$x10^5$
	$x10^{-4}$	11	09	07		11	09	05		09	13	06	
	$x10^{-5}$	-	-	-		-	-	-		-	-	-	
24 hour time point	$x10^{-1}$	TMTC	TMTC	TMTC	(246+235+200)/	TMTC	TMTC	TMTC	(189+178+190)/	TMTC	TMTC	TMTC	(209+199+210)/
	$x10^{-2}$	246	235	200	3)x 10^2/0.1	189	178	190	3)x 10^2/0.1	209	199	210	3)x 10^2/0.1
	$x10^{-3}$	76	71	82	2.25 $x10^5$	89	93	69	1.9 $x10^5$	101	109	97	2.1 $x10^5$
	$x10^{-4}$	16	07	07		15	09	17		29	29	31	
	$x10^{-5}$	-	-	-		03	-	01		11	09	13	

Table C2.20: THP-1 cell count and MOI calculations for MTP-HBHA biological assay 1

Wild type	**Mutant mtp-hbhA**	**Mtp-hbhA comp**
Alive cells: 16+12+18+14	**Alive cells**: 19+14+16+15	**Alive cells:** 12+16+19+17
Cells/mL = $\frac{(\text{Total number of cells} \times \text{dilution factor}(6) \times 104}{\text{Number of quadrants}}$ $= \frac{(60 \times 6 \times 104)}{4}$ $=9.0 \times 10^5$ Total cell= $9.0 \times 10^5 \times 20$ mL $= 1.8 \times 10^7$ MOI $= \frac{\text{Total number of bacterial cells}}{\text{Total number of THP}-1 \text{ cells}}$ $5 = \frac{(1\text{x}10^8 \text{ cells/mL})\ (x)}{(9.0\text{x}10^5 \text{ cells/mL})\ (20 \text{ mL})}$ Therefore: $x = \frac{(5)(9.0\text{x}10^5 \text{ cells/mL})\ (20 \text{ mL})}{(1\text{x}10^8 \text{ cells/mL})}$ x = 0.900 mL =900 µL	**Cells/mL** = $\frac{(\text{Total number of cells} \times \text{dilution factor}(6) \times 104}{\text{Number of quadrants}}$ $= \frac{(64 \times 6 \times 10\text{^}4)}{4}$ $=9.6 \times 10^5$ Total cell= $9.6 \times 10^5 \times 20$ mL $= 1.9 \times 10^7$ MOI $= \frac{\text{Total number of bacterial cells}}{\text{Total number of THP}-1 \text{ cells}}$ $5 = \frac{(1\text{x}10^8 \text{ cells/mL})\ (x)}{(9.6\text{x}10^5 \text{ cells/mL})\ (20 \text{ mL})}$ Therefore: $x = \frac{(5)(9.6\text{x}10^5 \text{ cells/mL})\ (20 \text{ mL})}{(1\text{x}10^8 \text{ cells/mL})}$ x = 0.96 mL =960 µL	**Cells/mL** = $\frac{(\text{Total number of cells} \times \text{dilution factor}(6) \times 104}{\text{Number of quadrants}}$ $= \frac{(64 \times 6 \times 104)}{4}$ $=9.6 \times 10^5$ Total cell= $9.6 \times 10^5 \times 20$ mL $= 1.9 \times 10^7$ MOI $= \frac{\text{Total number of bacterial cells}}{\text{Total number of THP}-1 \text{ cells}}$ $5 = \frac{(1\text{x}10^8 \text{ cells/mL})\ (x)}{(9.6\text{x}10^5 \text{ cells/mL})\ (20 \text{ mL})}$ Therefore: $x = \frac{(5)(9.6\text{x}10^5 \text{ cells/mL})\ (20 \text{ mL})}{(1\text{x}10^8 \text{ cells/mL})}$ x = 0.96 mL =960 µL

Table C2.21: Confirmation of the MOI for MTP-HBHA biological assay 1

Wild type	Mutant *mtp-hbhA*	*mtp-hbhA* comp
Selected dilution: 10^{-5} Average number of colonies $= \frac{(101+85+99)}{3}$ $= 9.8 \times 10^{1}$ $= 98$ colonies CFU/mL $= \frac{(\textbf{average number of colonies} \times \textbf{dilution factor})}{\textbf{volume plated out in mL}}$ $= \frac{(98)(10^5)}{(0.1)\text{mL}}$ $= 9.8 \times 10^7$ CFU/mL MOI $= \frac{(\text{bacterial cells/mL of} \times \text{total volume of inoculum})}{(\text{THP}-1 \text{ cells/mL} \times \text{total volume})}$ $= \frac{(9.8\times 10^7 \text{ cells/mL})(0.900\text{mL})}{(9.0\times 10^5 \text{ cells/mL})\times(20 \text{ mL})}$ $= 4.9$	**Selected dilution: 10^{-5}** Average number of colonies $= \frac{(87+95+105)}{3}$ $= 9.6 \times 10^{1}$ $= 96$ colonies CFU/mL $= \frac{(\textbf{average number of colonies} \times \textbf{dilution factor})}{\textbf{volume plated out in mL}}$ $= \frac{(9.6x10^1)(10^5)}{(0.1)\text{mL}}$ $= 9.60 \times 10^7$ CFU/mL MOI $= \frac{(\text{bacterial cells/mL of} \times \text{total volume of inoculum})}{(\text{THP}-1 \text{ cells/mL} \times \text{total volume})}$ $= \frac{(9.6\times 10^7 \text{ cells/mL})(0.870 \text{ mL})}{(9.60\times 10^5 \text{ cells/mL})\times(20 \text{ mL})}$ $= 4.8$	**Selected dilution: 10^{-5}** Average number of colonies = $\frac{(96+111+87)}{3}$ $= 9.8 \times 10^{1}$ colonies CFU/mL $= \frac{(\textbf{average number of colonies} \times \textbf{dilution factor})}{\textbf{volume plated out in mL}}$ $= \frac{(9.8x10^1)(10^5)}{(0.1)\text{mL}}$ $= 9.8 \times 10^7$ CFU/mL MOI $= \frac{(\text{bacterial cells/mL of} \times \text{total volume of inoculum}}{(\text{THP}-1 \text{ cells/mL} \times \text{total volume})}$ $= \frac{(9.8\times 10^7 \text{ cells/mL})(0.96\text{mL})}{(9.6\times 10^5 \text{ cells/mL})\times(20 \text{ mL})}$ $= 4.9$

Table C2.22: CFU's for inoculum, 4-h and 24-h time done in triplicates for *mtp-hbhA* biological assay 1

	Dilution factor	Biological Assay 1											
		V9124 Wild-type (colonies count)			CFU/mL & MOI	*Mutant mtp-hbhA* (colonies count)			CFU/mL calculation	*Mtp-hbhA comp* (colonies count)			CFU/mL calculation
		Rep 1	Rep 2	Rep 3		Rep 1	Rep 2	Rep 3		Rep 1	Rep 2	Rep 3	
Inoculum	$x10^{-1}$	lawn	lawn	lawn		lawn	lawn	lawn		lawn	lawn	lawn	
	$x10^{-2}$	lawn	lawn	lawn		lawn	lawn	lawn		lawn	lawn	lawn	
	$x10^{-3}$	TMTC	TMTC	TMTC		lawn	lawn	lawn		lawn	lawn	lawn	
	$x10^{-4}$	>300	>300	>300	(109+85+99)/3)x	TMTC	TMTC	TMTC	(87+95+105)/3)	TMTC	TMTC	TMTC	(96+111+87)/3)
	$x10^{-5}$	109	85	99	10^5/0.1	87	95	105	x 10^5/0.1	96	111	87	x 10^5/0.1
	$x10^{-6}$	69	71	64	9.8 $x10^7$	65	59	76	9.6 $x10^7$	11	08	15	9.8 $x10^7$
	$x10^{-7}$	09	21	13		47	32	41		01	01	03	
4 hour time point	$x10^{-1}$	TMTC	TMTC	TMTC	(239+243+203)/	125	146	159	(125+146+159)/	171	189	193	(171+189+193)/
	$x10^{-2}$	239	243	203	3)x 10^2/0.1	13	14	13	3) x 10^1/0.1	32	37	32	3) x 10^1/0.1
	$x10^{-3}$	46	59	54	2.28x10^5	03	07	10	1.4 $x10^4$	03	17	07	1.8 $x10^4$
	$x10^{-4}$	16	08	11		-	-	-		-	-	-	
	$x10^{-5}$	11	03	03		-	-	-		-	-	-	
24 hour time point	$x10^{-1}$	TMTC	TMTC	TMTC	(257+259+245)/	TMTC	TMTC	TMTC	(153+163+183)/	TMTC	TMTC	TMTC	(165+179+183)/
	$x10^{-2}$	257	259	245	3)x 10^2/0.1	153	163	183	3)x 10^1/0.1	165	179	183	3)x 10^2/0.1
	$x10^{-3}$	65	67	56	2.54 $x10^5$	02	01	-	1.7 $x10^4$	45	39	40	1.8 $x10^5$
	$x10^{-4}$	23	23	15		-	-	-		02	01	01	
	$x10^{-5}$	09	04	07		-	-	-		-	-	-	

Table C2.23: THP-1 cell count and MOI calculations for MTP-HBHA biological assay 2

Wild type	**Mutant mtp-hbhA**	**Mtp-hbhA comp**
Alive cells: 15+12+18+17	**Alive cells**: 12+14+19+11	**Alive cells:** 15+13+19+17
Cells/mL = $\frac{(\text{Total number of cells} \times \text{dilution factor}(6) \times 104}{\text{Number of quadrants}}$ = $\frac{(62 \times 6 \times 104)}{4}$ =9.3 x 10^5 Total cell= 9.3 x 10^5 x 20 mL = 1.9x 10^7 MOI = $\frac{\text{Total number of bacterial cells}}{\text{Total number of THP}-1 \text{ cells}}$ $5 = \frac{(1\text{x}10^8 \text{ cells/mL})\ (x)}{(9.3\text{x}10^5 \text{ cells/mL})\ (20 \text{ mL})}$ Therefore: x = $\frac{(5)(9.3\text{x}10^5 \text{ cells/mL})\ (20 \text{ mL})}{(1\text{x}10^8 \text{ cells/mL})}$ x = 0.93 mL =930 µL	**Cells/mL** = $\frac{(\text{Total number of cells} \times \text{dilution factor}(6) \times 104}{\text{Number of quadrants}}$ = $\frac{(60 \times 6 \times 10\text{^}4)}{4}$ =9.0 x 10^5 Total cell= 9.0 x 10^5 x 20 mL = 1.8 x 10^7 MOI = $\frac{\text{Total number of bacterial cells}}{\text{Total number of THP}-1 \text{ cells}}$ $5 = \frac{(1\text{x}10^8 \text{ cells/mL})\ (x)}{(9.0\text{x}10^5 \text{ cells/mL})\ (20 \text{ mL})}$ Therefore: x = $\frac{(5)(9.0\text{x}10^5 \text{ cells/mL})\ (20 \text{ mL})}{(1\text{x}10^8 \text{ cells/mL})}$ x = 0.900 mL =900 µL	**Cells/mL** = $\frac{(\text{Total number of cells} \times \text{dilution factor}(6) \times 104}{\text{Number of quadrants}}$ = $\frac{(64 \times 6 \times 10\text{^}4)}{4}$ =9.6 x 10^5 Total cell= 9.6 x 10^5 x 20 mL = 1.9 x 10^7 MOI = $\frac{\text{Total number of bacterial cells}}{\text{Total number of THP}-1 \text{ cells}}$ $5 = \frac{(1\text{x}10^8 \text{ cells/mL})\ (x)}{(9.6\text{x}10^5 \text{ cells/mL})\ (20 \text{ mL})}$ Therefore: x = $\frac{(5)(9.6\text{x}10^5 \text{ cells/mL})\ (20 \text{ mL})}{(1\text{x}10^8 \text{ cells/mL})}$ x = 0.96 mL =960 µL

Table C2.24: Confirmation of the MOI for MTP-HBHA biological assay 2

Wild type	Mutant *mtp-hbhA*	*mtp-hbhA* comp
Selected dilution: 10^{-5} Average number of colonies $= \frac{(103+109+95)}{3}$ $= 1.0 \times 10^2$ $= 102$ colonies CFU/mL $= \frac{(\textbf{average number of colonies} \times \textbf{dilution factor})}{\textbf{volume plated out in mL}}$ $= \frac{(102)(10^5)}{(0.1)\text{mL}}$ $= 1.0 \times 10^8$ CFU/mL MOI $= \frac{(\text{bacterial cells/mL of} \times \text{total volume of inoculum})}{(\text{THP}-1 \text{ cells/mL} \times \text{total volume})}$ $= \frac{(1.0\times 10^8 \text{ cells/mL})(0.930 \text{ mL})}{(9.3\times 10^5 \text{ cells/mL})\times(20 \text{ mL})}$ $= 5.0$	**Selected dilution: 10^{-5}** Average number of colonies $= \frac{(83+104+90)}{3}$ $= 9.2 \times 10^1$ $= 92$ colonies CFU/mL $= \frac{(\textbf{average number of colonies} \times \textbf{dilution factor})}{\textbf{volume plated out in mL}}$ $= \frac{(9.2\ x10^1)(10^5)}{(0.1)\text{mL}}$ $= 9.2 \times 10^7$ CFU/mL MOI $= \frac{(\text{bacterial cells/mL of} \times \text{total volume of inoculum})}{(\text{THP}-1 \text{ cells/mL} \times \text{total volume})}$ $= \frac{(9.2\times 10^7 \text{ cells/mL})(0.900 \text{ mL})}{(9.0\times 10^5 \text{ cells/mL})\times(20 \text{ mL})}$ $= 4.6$	**Selected dilution: 10^{-5}** Average number of colonies $= \frac{(93+115+98)}{3}$ $= 1.0 \times 10^2$ colonies CFU/mL $= \frac{(\textbf{average number of colonies} \times \textbf{dilution factor})}{\textbf{volume plated out in mL}}$ $= \frac{(1.0x10^2)(10^5)}{(0.1)\text{mL}}$ $= 1.0 \times 10^8$ CFU/mL MOI $= \frac{(\text{bacterial cells/mL of} \times \text{total volume of inoculum})}{(\text{THP}-1 \text{ cells/mL} \times \text{total volume})}$ $= \frac{(1.0\times 10^8 \text{ cells/mL})(0.96\text{mL})}{(9.6\times 10^5 \text{ cells/mL})\times(20 \text{ mL})}$ $= 5$

Table C2.25: CFU's for inoculum, 4-h and 24-h time done in triplicates for *mtp-hbhA* biological assay 2

	Dilution factor	Biological Assay 2										
		V9124 Wild type (colonies count)			CFU/mL & MOI	*Mutant mtp-hbhA* (colonies count)			CFU/mL calculation	*Mtp-hbhA comp* (colonies count)			CFU/mL calculation
		Rep 1	Rep 2	Rep 3		Rep 1	Rep 2	Rep 3		Rep 1	Rep 2	Rep 3	
Inoculum	$x10^{-1}$	lawn	lawn	lawn		lawn	lawn	lawn		lawn	lawn	lawn	
	$x10^{-2}$	lawn	lawn	lawn		lawn	lawn	lawn		lawn	lawn	lawn	
	$x10^{-3}$	TMTC	TMTC	TMTC		lawn	lawn	lawn		lawn	lawn	lawn	
	$x10^{-4}$	>300	>300	>300	(103+109+95)/3)	TMTC	TMTC	TMTC	(83+104+90)/3)	TMTC	TMTC	TMTC	(115+93+98)/3)
	$x10^{-5}$	103	109	95	x 10^5/0.1	83	104	90	x 10^5/0.1	115	93	98	x 10^5/0.1
	$x10^{-6}$	71	58	63	1.08 $x10^8$	25	39	49	9.2 $x10^7$	76	62	74	1.0 $x10^8$
	$x10^{-7}$	06	09	11		03	15	09		22	24	15	
4-hour time point	$x10^{-1}$	TMTC	TMTC	TMTC	(200+189+197)/	93	115	129	(95+115+129)/3)	179	170	187	(179+170+187)/
	$x10^{-2}$	200	189	197	3) x 10^2/0.1	18	20	30	x 10^1/0.1	27	39	33	3) x 10^1/0.1
	$x10^{-3}$	65	52	39	1.95$x10^5$	01	01	01	1.1 $x10^4$	03	07	07	1.8 $x10^4$
	$x10^{-4}$	11	09	07		-	-	-		-	-	-	
	$x10^{-5}$	-	-	-		-	-	-		-	-	-	
24-hour time point	$x10^{-1}$	TMTC	TMTC	TMTC	(246+235+200)/	TMTC	TMTC	TMTC	(111+98+101)/3)	TMTC	TMTC	TMTC	(131+159+145)/
	$x10^{-2}$	246	235	200	3) x 10^2/0.1	65	53	63	x 10^1/0.1	131	159	145	3) x 10^2/0.1
	$x10^{-3}$	76	71	82	2.25 $x10^5$	05	01	01	1.0 $x10^4$	45	39	46	1.5 $x10^5$
	$x10^{-4}$	16	07	07		-	-	-		02	01	01	
	$x10^{-5}$	-	-	-		-	-	-		-	-	-	

Table C2.26: THP-1 cell count and MOI calculations for MTP-HBHA biological assay 3

Wild type	**Mutant mtp-hbhA**	**Mtp-hbhA comp**
Alive cells: 18+16+17+14	**Alive cells**: 13+16+13+17	**Alive cells:** 13+13+19+17
Cells/mL = $\frac{(\text{Total number of cells} \times \text{dilution factor}(6) \times 104}{\text{Number of quadrants}}$ $= \frac{(65 \times 6 \times 104)}{4}$ $= 9.8 \times 10^5$ Total cell= $9.8 \times 10^5 \times 20\ mL = 2.0 \times 10^7$ MOI = $\frac{\text{Total number of bacterial cells}}{\text{Total number of THP}-1\text{ cells}}$ $5 = \frac{(1x10^8\ \text{cells/mL})\ (x)}{(9.8x10^5\ \text{cells/mL})\ (20\ \text{mL})}$ Therefore: $x = \frac{(5)(9.8x10^5\ \text{cells/mL})\ (20\ \text{mL})}{(1x10^8\ \text{cells/mL})}$ x = 0.98 mL =980 µL	**Cells/mL** = $\frac{(\text{Total number of cells} \times \text{dilution factor}(6) \times 104}{\text{Number of quadrants}}$ $= \frac{(59 \times 6 \times 10\text{^}4)}{4}$ $= 8.9 \times 10^5$ Total cell= $8.9 \times 10^5 \times 20\ mL = 1.8 \times 10^7$ MOI = $\frac{\text{Total number of bacterial cells}}{\text{Total number of THP}-1\text{ cells}}$ $5 = \frac{(1x10^8\ \text{cells/mL})\ (x)}{(8.9x10^5\ \text{cells/mL})\ (20\ \text{mL})}$ Therefore: $x = \frac{(5)(8.9x10^5\ \text{cells/mL})\ (20\ \text{mL})}{(1x10^8\ \text{cells/mL})}$ x = 089 mL = 890µL	**Cells/mL** = $\frac{(\text{Total number of cells} \times \text{dilution factor}(6) \times 104}{\text{Number of quadrants}}$ $= \frac{62 \times 6 \times 10\text{^}4)}{4}$ $= 9.3 \times 10^5$ Total cell= $9.3 \times 10^5 \times 20\ mL = 1.9 \times 10^7$ MOI = $\frac{\text{Total number of bacterial cells}}{\text{Total number of THP}-1\text{ cells}}$ $5 = \frac{(1x10^8\ \text{cells/mL})\ (x)}{(9.6x10^5\ \text{cells/mL})\ (20\ \text{mL})}$ Therefore: $x = \frac{(5)(9.3x10^5\ \text{cells/mL})\ (20\ \text{mL})}{(1x10^8\ \text{cells/mL})}$ x = 0.93 mL =930 µL

Table C2.27: Confirmation of the MOI for MTP-HBHA biological assay 3

Wild type	Mutant *mtp-hbhA*	*mtp-hbhA* comp
Selected dilution: 10^{-5} Average number of colonies $= \frac{(104+109+96)}{3}$ $= 1.0 \times 10^2$ $= 103$ colonies CFU/mL $= \frac{(\textbf{average number of colonies} \times \textbf{dilution factor})}{\textbf{volume plated out in mL}}$ $= \frac{(103)(10^5)}{(0.1)\text{mL}}$ $= 1.0 \times 10^8$ CFU/mL MOI $= \frac{(\text{bacterial cells/mL of} \times \text{total volume of inoculum})}{(\text{THP}-1 \text{ cells/mL} \times \text{total volume})}$ $= \frac{(1.0\times 10^8 \text{ cells/mL})(0.930 \text{ mL})}{(9.8\times 10^5 \text{ cells/mL})\times(20 \text{ mL})}$ $= 5.0$	**Selected dilution: 10^{-5}** Average number of colonies $= \frac{(101+93+86)}{3}$ $= 9.3 \times 10^1$ $= 93$ colonies CFU/mL $= \frac{(\textbf{average number of colonies} \times \textbf{dilution factor})}{\textbf{volume plated out in mL}}$ $= \frac{(9.3\ x10^1)(10^5)}{(0.1)\text{mL}}$ $= 9.3 \times 10^7$ CFU/mL MOI $= \frac{(\text{bacterial cells/mL of} \times \text{total volume of inoculum})}{(\text{THP}-1 \text{ cells/mL} \times \text{total volume})}$ $= \frac{(9.3\times 10^7 \text{ cells/mL})(0.900 \text{ mL})}{(8.9\times 10^5 \text{ cells/mL})\times(20 \text{ mL})}$ $= 4.7$	**Selected dilution: 10^{-5}** Average number of colonies $= \frac{(105+109+89)}{3}$ $= 1.0 \times 10^2$ colonies CFU/mL $= \frac{(\textbf{average number of colonies} \times \textbf{dilution factor})}{\textbf{volume plated out in mL}}$ $= \frac{(1.0x10^2)(10^5)}{(0.1)\text{mL}}$ $= 1.0 \times 10^8$ CFU/mL MOI $= \frac{(\text{bacterial cells/mL of} \times \text{total volume of inoculum})}{(\text{THP}-1 \text{ cells/mL} \times \text{total volume})}$ $= \frac{(1.0\times 10^8 \text{ cells/mL})(0.93\text{mL})}{(9.3\times 10^5 \text{ cells/mL})\times(20 \text{ mL})}$ $= 5$

Table C2.28: CFU's for inoculum, 4-h and 24-h time done in triplicates for *mtp-hbhA* biological assay 3

	Dilution factor	Biological Assay 3											
		V9124 Wild type (colonies count)			CFU/mL & MOI	*Mutant mtp-hbhA* (colonies count)			CFU/mL calculation	*Mtp-hbhA comp* (colonies count)			CFU/mL calculation
		Rep 1	Rep 2	Rep 3		Rep 1	Rep 2	Rep 3		Rep 1	Rep 2	Rep 3	
Inoculum	$x10^{-1}$	lawn	lawn	lawn		lawn	lawn	lawn		lawn	lawn	lawn	
	$x10^{-2}$	lawn	lawn	lawn		lawn	lawn	lawn		lawn	lawn	lawn	
	$x10^{-3}$	TMTC	TMTC	TMTC		lawn	lawn	lawn		lawn	lawn	lawn	
	$x10^{-4}$	>300	>300	>300	(104+109+96)/3)	TMTC	TMTC	TMTC	(101+93+86)/3)	TMTC	TMTC	TMTC	(105+109+89)/3)
	$x10^{-5}$	104	109	96	x 10^5/0.1	101	93	86	x 10^5/0.1	105	109	89	x 10^5/0.1
	$x10^{-6}$	69	71	75	1.0 $x10^8$	35	39	43	9.33 $x10^7$	49	62	52	1.0 $x10^8$
	$x10^{-7}$	09	11	13		15	09	25		09	09	15	
4-hour time point	$x10^{-1}$	TMTC	TMTC	TMTC	(213+199+201)/	98	92	101	(98+92+101)/3)	189	167	169	(189+167+169)/
	$x10^{-2}$	213	199	201	3) x 10^2/0.1	34	45	39	x 10^1/0.1	34	36	34	3) x 10^1/0.1
	$x10^{-3}$	56	65	61	2.04 $x10^5$	11	16	09	9.7 $x10^3$	12	11	09	1.8 $x10^4$
	$x10^{-4}$	13	16	13		01	01	05		01	-	-	
	$x10^{-5}$	08	03	05		-	-	-		-	-	-	
24-hour time point	$x10^{-1}$	TMTC	TMTC	TMTC	(224+215+219)/	TMTC	TMTC	TMTC	(94+93+89)/3) x	TMTC	TMTC	TMTC	(101+132+111)/
	$x10^{-2}$	224	215	219	3) x 10^2/0.1	94	93	89	10^2/0.1	101	132	111	3) x 10^2/0.1
	$x10^{-3}$	63	60	59	2.19 $x10^5$	28	29	39	9.2 $x10^4$	37	34	39	1.1 $x10^5$
	$x10^{-4}$	20	15	13		11	11	09		15	09	09	
	$x10^{-5}$	11	03	03		-	-	-		01	01	-	

Table C2.28: THP-1 cell count and MOI calculations for *Rv0309* biological assay 1

Wild-type	**Mutant Rv0309**	**Rv0309 comp**
Alive cells: 19+13+18+14	**Alive cells:** 18+16+14+12	Alive cells:15+13+21+14
Cells/mL = $\frac{(\text{Total number of cells} \times \text{dilution factor}(6) \times 104}{\text{Number of quadrants}}$ $= \frac{(64 \times 6 \times 10\text{^}4)}{4}$ $= 9.60 \times 10^5$ Total cells = $9.60 \times 10^5 \times 20\ \text{mL} = 1.92 \times 10^7$ MOI = $\frac{\text{Total number of bacterial cells}}{\text{Total number of THP}-1\ \text{cells}}$ $5 = \frac{(1 \times 10^8\ \text{cells/mL})\ (x)}{(9.60 \times 10^5\ \text{cells/mL})\ (20\ \text{mL})}$ Therefore: $x = \frac{(5)(9.60 \times 10^5\ \text{cells/mL})\ (20\ \text{mL})}{(1 \times 10^8\ \text{cells/mL})}$ x = 0.96 mL	**Cells/mL** = $\frac{(\text{Total number of cells} \times \text{dilution factor}(6) \times 104}{\text{Number of quadrants}}$ $= \frac{(60 \times 6 \times 10\ \ 4)}{4}$ $= 9.0 \times 10^5$ Total cell= $9.0 \times 10^5 \times 20\ \text{mL} = 1.8 \times 10^7$ MOI = $\frac{\text{Total number of bacterial cells}}{\text{Total number of THP}-1\ \text{cells}}$ $5 = \frac{(1 \times 10^8\ \text{cells/mL})\ (x)}{(9.0 \times 10^5\ \text{cells/mL})\ (20\ \text{mL})}$ Therefore: $x = \frac{(5)(9.0 \times 10^5\ \text{cells/mL})\ (20\ \text{mL})}{(1 \times 10^8\ \text{cells/mL})}$ x = 0.900 mL =900 µL	**Cells/mL** = $\frac{(\text{Total number of cells} \times \text{dilution factor}(6) \times 104}{\text{Number of quadrants}}$ $= \frac{(66 \times 6 \times 104)}{4}$ $= 9.9 \times 10^5$ Total cell= $9.9 \times 10^5 \times 20\ \text{mL} = 2.0 \times 10^7$ MOI = $\frac{\text{Total number of bacterial cells}}{\text{Total number of THP}-1\ \text{cells}}$ $5 = \frac{(1 \times 10^8\ \text{cells/mL})\ (x)}{(9.9 \times 10^5\ \text{cells/mL})\ (20\ \text{mL})}$ Therefore: $x = \frac{(5)(9.9 \times 10^5\ \text{cells/mL})\ (20\ \text{mL})}{(1 \times 10^8\ \text{cells/mL})}$ x = 0.99 mL =990 µL

Table C2.29: Confirmation of the MOI for MTP-HBHA biological assay 1

Wild-type	**Mutant *Rv0309***	***Rv0309* comp**
Selected dilution: 10^{-5} Average number of colonies $= \frac{(101+96+98)}{3}$ $= 9.9 \times 10^{1}$ $= 98$ colonies CFU/mL $= \frac{(\textbf{average number of colonies} \times \textbf{dilution factor})}{\textbf{volume plated out in mL}}$ $= \frac{(98)(10^{5})}{(0.1)\text{mL}}$ $= 9.8 \times 10^{7}$ CFU/mL MOI $= \frac{(\text{bacterial cells/mL of} \times \text{total volume of inoculum})}{(\text{THP}-1 \text{ cells/mL} \times \text{total volume})}$ $= \frac{(9.8\times 10^{7} \text{ cells/mL})(0.96 \text{ mL})}{(9.60\times 10^{5} \text{ cells/mL})\times(20 \text{ mL})}$ $= 4.9$	**Selected dilution: 10^{-5}** Average number of colonies = $\frac{(85+92+96)}{3}$ $= 9.1 \times 10^{1}$ colonies CFU/mL $= \frac{(\textbf{average number of colonies} \times \textbf{dilution factor})}{\textbf{volume plated out in mL}}$ $= \frac{(9.1x10^{1})(10^{5})}{(0.1)\text{mL}}$ $= 9.1 \times 10^{7}$ CFU/mL MOI $= \frac{(\text{bacterial cells/mL of} \times \text{total volume of inoculum})}{(\text{THP}-1 \text{ cells/mL} \times \text{total volume})}$ $= \frac{(9.1\times 10^{7} \text{ cells/mL})(0.900\text{mL})}{(9.0\times 10^{5} \text{ cells/mL})\times(20 \text{ mL})}$ $= 4.6$	**Selected dilution: 10^{-5}** Average number of colonies = $\frac{(95+97+106)}{3}$ $= 9.9 \times 10^{1}$ colonies CFU/mL $= \frac{(\textbf{average number of colonies} \times \textbf{dilution factor})}{\textbf{volume plated out in mL}}$ $= \frac{(9.9x10^{1})(10^{5})}{(0.1)\text{mL}}$ $= 9.9 \times 10^{7}$ CFU/mL MOI $= \frac{(\text{bacterial cells/mL of} \times \text{total volume of inoculum})}{(\text{THP}-1 \text{ cells/mL} \times \text{total volume})}$ $= \frac{(9.9\times 10^{7} \text{ cells/mL})(0.99\text{mL})}{(9.9\times 10^{5} \text{ cells/mL})\times(20 \text{ mL})}$ $= 5.0$

Table C2.30: CFU's for inoculum, 4-h and 24-h time done in triplicates for *Rv0309* biological assay 1

	Dilution factor	Biological Assay 1											
		V9124 Wild-type (colonies count)			CFU/mL & MOI	*Mutant Rv0309* (colonies count)			CFU/mL calculation	*Rv0309 comp* (colonies count)			CFU/mL calculation
		Rep 1	Rep 2	Rep 3		Rep 1	Rep 2	Rep 3		Rep 1	Rep 2	Rep 3	
Inoculum	$x10^{-1}$	lawn	lawn	lawn		lawn	lawn	lawn		lawn	lawn	lawn	
	$x10^{-2}$	lawn	lawn	lawn		lawn	lawn	lawn		lawn	lawn	lawn	
	$x10^{-3}$	TMTC	TMTC	TMTC		TMTC	TMTC	TMTC		TMTC	TMTC	TMTC	
	$x10^{-4}$	>300	>300	>300	(101+96+98)/3)x	>300	>300	>300	(85+92+96)/3)x	>300	>300	>300	(95+97+106)/3)x
	$x10^{-5}$	101	98	96	10^5/0.1	92	96	85	10^5/0.1	95	106	97	10^5/0.1
	$x10^{-6}$	69	73	67	9.83 $x10^7$	23	19	33	9.10 $x10^7$	33	45	23	9.93 $x10^7$
	$x10^{-7}$	20	08	18		14	09	11		23	12	12	
4 hour time point	$x10^{-1}$	TMTC	TMTC	TMTC	(109+99+121)/3) x	TMTC	TMTC	TMTC	(69+39+48)/3) x	TMTC	TMTC	TMTC	(61+100+94)/3)x
	$x10^{-2}$	109	99	121	10^2/0.1	69	39	48	10^2/0.1	61	100	94	10^2/0.1
	$x10^{-3}$	45	32	20	1.10$x10^5$	13	17	10	5.20 $x10^4$	24	20	17	8.50 $x10^4$
	$x10^{-4}$	11	09	07		-	02	01		01	03	-	
	$x10^{-5}$	-	-	-		-	-	-		-	-	-	
24 hour time point	$x10^{-1}$	TMTC	TMTC	TMTC	(189+193+200)/3)	TMTC	TMTC	TMTC	(165+154+117)/3)	TMTC	TMTC	TMTC	(164+209+176)/3)
	$x10^{-2}$	189	193	200	x 10^2/0.1	165	154	117	x 10^2/0.1	164	209	176	x 10^2/0.1
	$x10^{-3}$	113	89	123	1.94 $x10^5$	17	20	17	1.45 $x10^5$	31	29	37	1.83 $x10^5$
	$x10^{-4}$	39	28	17		02	02	01		08	04	01	
	$x10^{-5}$	07	01	05		01	-	-		01	01	-	

Table C2.31: THP-1 cell count and MOI calculations for *Rv0309* biological assay 2

Wild type	**Mutant Rv0309**	**Rv0309 comp**
Alive cells: 16+21+18+14	**Alive cells**: 13+18+13+14	**Alive cells:** 12+16+15+17
Cells/mL = $\frac{(\text{Total number of cells} \times \text{dilution factor}(6) \times 104}{\text{Number of quadrants}}$ $= \frac{(69 \times 6 \times 104)}{4}$ $= 1.04 \times 10^6$ Total cells = $1.1 \times 10^6 \times 20\ \text{mL} = 2.07 \times 10^7$ MOI = $\frac{\text{Total number of bacterial cells}}{\text{Total number of THP}-1\ \text{cells}}$ $5 = \frac{(1\text{x}10^8\ \text{cells/mL})\ (x)}{(1.04\text{x}10^6\ \text{cells/mL})\ (20\ \text{mL})}$ Therefore: $x = \frac{(5)(1.04\text{x}10^6\ \text{cells/mL})\ (20\ \text{mL})}{(1\text{x}10^8\ \text{cells/mL})}$ x = 1.04 mL	**Cells/mL** = $\frac{(\text{Total number of cells} \times \text{dilution factor}(6) \times 104}{\text{Number of quadrants}}$ $= \frac{(58 \times 6 \times 104)}{4}$ $= 8.70 \times 10^5$ Total cell= $8.70 \times 10^5 \times 20\ \text{mL} = 1.74 \times 10^7$ MOI = $\frac{\text{Total number of bacterial cells}}{\text{Total number of THP}-1\ \text{cells}}$ $5 = \frac{(1\text{x}10^8\ \text{cells/mL})\ (x)}{(8.70\text{x}10^5\ \text{cells/mL})\ (20\ \text{mL})}$ Therefore: $x = \frac{(5)(8.70\text{x}10^5\ \text{cells/mL})\ (20\ \text{mL})}{(1\text{x}10^8\ \text{cells/mL})}$ x = 0.870 mL =870 µL	**Cells/mL** = $\frac{(\text{Total number of cells} \times \text{dilution factor}(6) \times 104}{\text{Number of quadrants}}$ $= \frac{(60 \times 6 \times 104)}{4}$ $= 9.0 \times 10^5$ Total cell= $9.0 \times 10^5 \times 20\ \text{mL} = 1.8 \times 10^7$ MOI = $\frac{\text{Total number of bacterial cells}}{\text{Total number of THP}-1\ \text{cells}}$ $5 = \frac{(1\text{x}10^8\ \text{cells/mL})\ (x)}{(9.0\text{x}10^5\ \text{cells/mL})\ (20\ \text{mL})}$ Therefore: $x = \frac{(5)(9.0\text{x}10^5\ \text{cells/mL})\ (20\ \text{mL})}{(1\text{x}10^8\ \text{cells/mL})}$ x = 0.900 mL =900 µL

Table C2.32: Confirmation of the MOI for RV0309 biological assay 2

Wild type	Mutant *Rv0309*	*Rv0309* comp
Selected dilution: 10^{-5} Average number of colonies $= \frac{(106+111+109)}{3}$ $= 1.1 \times 10^{2}$ $= 108$ colonies CFU/mL $= \frac{(\textbf{average number of colonies} \times \textbf{dilution factor})}{\textbf{volume plated out in mL}}$ $= \frac{(108)(10^{5})}{(0.1)\text{mL}}$ $= 1.09 \times 10^{8}$ CFU/mL MOI $= \frac{(\text{bacterial cells/mL of} \times \text{total volume of inoculum})}{(\text{THP}-1 \text{ cells/mL} \times \text{total volume})}$ $= \frac{(1.09\times 10^{8} \text{ cells/mL})(1.05 \text{ mL})}{(1.04\times 10^{6} \text{ cells/mL})\times(20 \text{ mL})}$ $= 5$	**Selected dilution: 10^{-5}** Average number of colonies $= \frac{(69+75+83)}{3}$ $= 7.6 \times 10^{1}$ $= 76$ colonies CFU/mL $= \frac{(\textbf{average number of colonies} \times \textbf{dilution factor})}{\textbf{volume plated out in mL}}$ $= \frac{(7.6x10^{1})(10^{5})}{(0.1)\text{mL}}$ $= 7.60 \times 10^{7}$ CFU/mL MOI $= \frac{(\text{bacterial cells/mL of} \times \text{total volume of inoculum})}{(\text{THP}-1 \text{ cells/mL} \times \text{total volume})}$ $= \frac{(7.60\times 10^{7} \text{ cells/mL})(0.870 \text{ mL})}{(8.70\times 10^{5} \text{ cells/mL})\times(20 \text{ mL})}$ $= 3.8$	**Selected dilution: 10^{-5}** Average number of colonies $= \frac{(79+83+101)}{3}$ $= 8.8 \times 10^{1}$ colonies CFU/mL $= \frac{(\textbf{average number of colonies} \times \textbf{dilution factor})}{\textbf{volume plated out in mL}}$ $= \frac{(8.8x10^{1})(10^{5})}{(0.1)\text{mL}}$ $= 8.8 \times 10^{7}$ CFU/mL MOI $= \frac{(\text{bacterial cells/mL of} \times \text{total volume of inoculum})}{(\text{THP}-1 \text{ cells/mL} \times \text{total volume})}$ $= \frac{(8.8\times 10^{7} \text{ cells/mL})(0.900\text{mL})}{(9.0\times 10^{5} \text{ cells/mL})\times(20 \text{ mL})}$ $= 4.4$

Table C2.33: CFU's for inoculum, 4-h and 24-h time done in triplicates for *Rv0309* biological assay 2

	Dilution factor	Biological Assay 2											
		V9124 Wild-type (colonies count)			CFU/mL & MOI	*Mutant Rv0309* (colonies count)			CFU/mL calculation	*Rv0309 comp* (colonies count)			CFU/mL calculation
		Rep 1	Rep 2	Rep 3		Rep 1	Rep 2	Rep 3		Rep 1	Rep 2	Rep 3	
Inoculum	$x10^{-1}$	lawn	lawn	lawn		lawn	lawn	lawn		lawn	lawn	lawn	
	$x10^{-2}$	lawn	lawn	lawn		lawn	lawn	lawn		lawn	lawn	lawn	
	$x10^{-3}$	TMTC	TMTC	TMTC		TMTC	TMTC	TMTC		TMTC	TMTC	TMTC	
	$x10^{-4}$	>300	>300	>300	(106+111+109)/	>300	>300	>300	((69+75+83)/3)	>300	>300	>300	(79+83+101)/3)
	$x10^{-5}$	106	109	111	3)x 10^5/0.1	83	75	69	x 10^5/0.1	83	101	79	x 10^5/0.1
	$x10^{-6}$	87	56	69	1.09 $x10^8$	23	32	29	7.57 $x10^7$	19	27	19	7.70 $x10^7$
	$x10^{-7}$	09	14	11		09	05	11		05	03	06	
4 hour time point	$x10^{-1}$	TMTC	TMTC	TMTC	(215+223+187)/	TMTC	TMTC	TMTC	(59+44+66)/3) x	TMTC	TMTC	TMTC	(100+127+71)/3)
	$x10^{-2}$	215	223	187	3) x 10^2/0.1	59	44	66	10^2/0.1	100	127	71	x 10^2/0.1
	$x10^{-3}$	101	123	98	2.08$x10^5$	10	13	09	5.63 $x10^4$	12	20	17	6.27 $x10^4$
	$x10^{-4}$	18	11	09		-	02	01		01	03	-	
	$x10^{-5}$	01	06	08		-	-	-		-	-	-	
24 hour time point	$x10^{-1}$	TMTC	TMTC	TMTC	(275+237+229)/	TMTC	TMTC	TMTC	(152+174+113)/	TMTC	TMTC	TMTC	(175+183+171)/
	$x10^{-2}$	275	237	229	3) x 10^2/0.1	152	174	113	3) x 10^2/0.1	175	183	171	3)x 10^2/0.1
	$x10^{-3}$	115	135	116	2.47 $x10^5$	14	05	09	1.46 $x10^5$	40	28	21	1.76 $x10^5$
	$x10^{-4}$	25	15	09		-	-	01		02	01	01	
	$x10^{-5}$	07	11	05		-	-	-		01	-	-	

Table C2.34: THP-1 cell count and MOI calculations for *Rv0309* biological assay 3

Wild type	**Mutant Rv0309**	**Rv0309 comp**
Alive cells: 18+14+13+15	**Alive cells**: 14+12+16+14	**Alive cells:** 18+11+17+14
Cells/mL = $\frac{(\text{Total number of cells} \times \text{dilution factor}(6) \times 104}{\text{Number of quadrants}}$ $= \frac{(60 \times 6 \times 104)}{4}$ $= 9.0 \times 10^5$ cells/mL Total cell= 9. 20 mL = 1.87×10^7 MOI = $\frac{\text{Total number of bacterial cells}}{\text{Total number of THP}-1 \text{ cells}}$ $5 = \frac{(1 \times 10^8 \text{ cells/mL})\ (x)}{(9.0 \times 10^5 \text{ cells/mL})\ (20 \text{ mL})}$ Therefore: x = $\frac{(5)(9.0 \times 10^5 \text{ cells/mL})\ (20 \text{ mL})}{(1 \times 10^8 \text{ cells/mL})}$ x = 0.9 mL =900 µL	**Cells/mL** = $\frac{(\text{Total number of cells} \times \text{dilution factor}(6) \times 104}{\text{Number of quadrants}}$ $= \frac{(56 \times 6 \times 104)}{4}$ $= 8.40 \times 10^5$ Total cell= $8.40 \times 10^5 \times 20$ mL = 1.7×10^7 MOI = $\frac{\text{Total number of bacterial cells}}{\text{Total number of THP}-1 \text{ cells}}$ $5 = \frac{(1 \times 10^8 \text{ cells/mL})\ (x)}{(8.40 \times 10^5 \text{ cells/mL})\ (20 \text{ mL})}$ Therefore: x = $\frac{(5)(8.40 \times 10^5 \text{ cells/mL})\ (20 \text{ mL})}{(1 \times 10^8 \text{ cells/mL})}$ x = 0.84 mL =840 µL	**Cells/mL** = $\frac{(\text{Total number of cells} \times \text{dilution factor}(6) \times 104}{\text{Number of quadrants}}$ $= \frac{(60 \times 6 \times 104)}{4}$ $= 9.0 \times 10^5$ Total cell= $9.0 \times 10^5 \times 20$ mL = 1.80×10^7 MOI = $\frac{\text{Total number of bacterial cells}}{\text{Total number of THP}-1 \text{ cells}}$ $5 = \frac{(1 \times 10^8 \text{ cells/mL})\ (x)}{(9.0 \times 10^5 \text{ cells/mL})\ (20 \text{ mL})}$ Therefore: x = $\frac{(5)(9.0 \times 10^5 \text{ cells/mL})\ (20 \text{ mL})}{(1 \times 10^8 \text{ cells/mL})}$ x = 0.90 mL =900 µL

Table C2.35: Confirmation of the MOI for RV0309 biological assay 3

Wild type	Mutant Rv0309	Rv0309 comp
Selected dilution: 10^{-5} Average number of colonies $= \frac{(92+87+89)}{3}$ $= 8.9 \times 10^{1}$ $= 89$ colonies CFU/mL $= \frac{(\textbf{average number of colonies} \times \textbf{dilution factor})}{\textbf{volume plated out in mL}}$ $= \frac{(89)(10^5)}{(0.1)\text{mL}}$ $= 8.90 \times 10^7$ CFU/mL MOI $= \frac{(\text{bacterial cells/mL of} \times \text{total volume of inoculum})}{(\text{THP}-1 \text{ cells/mL} \times \text{total volume})}$ $= \frac{(8.90\times 10^7 \text{ cells/mL})(0.900 \text{ mL})}{(9.00\times 10^5 \text{ cells/mL})\times(20 \text{ mL})}$ $= 4.45$	**Selected dilution: 10^{-5}** Average number of colonies $= \frac{(69+63+69)}{3}$ $= 6.70 \times 10^{1}$ $= 67$ colonies CFU/mL $= \frac{(\textbf{average number of colonies} \times \textbf{dilution factor})}{\textbf{volume plated out in mL}}$ $= \frac{(6.7x10^1)(10^5)}{(0.1)\text{mL}}$ $= 6.7 \times 10^7$ CFU/mL MOI $= \frac{(\text{bacterial cells/mL of} \times \text{total volume of inoculum})}{(\text{THP}-1 \text{ cells/mL} \times \text{total volume})}$ $= \frac{(6.7\times 10^7 \text{ cells/mL})(0.840 \text{ mL})}{(8.40\times 10^5 \text{ cells/mL})\times(20 \text{ mL})}$ $= 3.9$	**Selected dilution: 10^{-5}** Average number of colonies $= \frac{(75+82+78)}{3}$ $= 7.8 \times 10^{1}$ colonies CFU/mL $= \frac{(\textbf{average number of colonies} \times \textbf{dilution factor})}{\textbf{volume plated out in mL}}$ $= \frac{(7.8x10^1)(10^5)}{(0.1)\text{mL}}$ $= 7.8 \times 10^7$ CFU/mL MOI $= \frac{(\text{bacterial cells/mL of} \times \text{total volume of inoculum})}{(\text{THP}-1 \text{ cells/mL} \times \text{total volume})}$ $= \frac{(7.8\times 10^7 \text{ cells/mL})(0.900 \text{ mL})}{(9.0\times 10^5 \text{ cells/mL})\times(20 \text{ mL})}$ $= 4.0$

Table C2.1: CFU's for inoculum, 4-h and 24-h time done in triplicates for *Rv0309* biological assay 3

	Dilution factor	Biological Assay 3										
		V9124 Wild-type (colonies count)			CFU/mL & MOI	*Mutant Rv0309* (colonies count)			CFU/mL calculation	*Rv0309 comp* (colonies count)			CFU/mL calculation
		Rep 1	Rep 2	Rep 3		Rep 1	Rep 2	Rep 3		Rep 1	Rep 2	Rep 3	
Inoculum	$x10^{-1}$	lawn	lawn	lawn		lawn	lawn	lawn		lawn	lawn	lawn	
	$x10^{-2}$	lawn	lawn	lawn		lawn	lawn	lawn		lawn	lawn	lawn	
	$x10^{-3}$	TMTC	TMTC	TMTC		TMTC	TMTC	TMTC		TMTC	TMTC	TMTC	
	$x10^{-4}$	>300	>300	>300	(92+87+89)/3) x	>300	>300	>300	(69+63+69)/3) x	>300	>300	>300	(73+71+78)/3) x
	$x10^{-5}$	92	89	87	10^5/0.1	69	63	69	10^5/0.1	73	71	78	10^5/0.1
	$x10^{-6}$	69	55	72	8.93 $x10^7$	15	23	19	6.70 $x10^7$	20	27	35	7.40 $x10^7$
	$x10^{-7}$	09	12	08		7	5	1		11	07	06	
4 hour time point	$x10^{-1}$	TMTC	TMTC	TMTC	(213+209+201)/	TMTC	TMTC	TMTC	(136+110+100)/	TMTC	TMTC	TMTC	(82+111+88)/3)
	$x10^{-2}$	213	209	201	3) x 10^2/0.1	136	110	100	3) x 10^2/0.1	82	111	88	x 10^2/0.1
	$x10^{-3}$	59	65	52	2.08$x10^5$	17	12	18	1.15 $x10^5$	11	08	11	9.37 $x10^4$
	$x10^{-4}$	17	12	17		01	-	01		03	02	-	
	$x10^{-5}$	07	09	04		-	-	-		-	-	-	
24 hour time point	$x10^{-1}$	TMTC	TMTC	TMTC	(255+231+210)/	TMTC	TMTC	TMTC	(130+145+136)/	TMTC	TMTC	TMTC	(180+163+197)/
	$x10^{-2}$	255	231	210	3) x 10^2/0.1	130	145	136	3) x 10^2/0.1	180	163	197	3) x 10^2/0.1
	$x10^{-3}$	67	71	71	2.32 $x10^5$	20	20	29	1.37 $x10^5$	38	29	35	1.80 $x10^5$
	$x10^{-4}$	11	15	31		02	04	02		03	02	05	
	$x10^{-5}$	06	09	09		01	-	-		01	-	-	

Appendix D: MOPS gel electrophoresis

Gel preparation:

1. Added 0.5 g of agarose (Sigma, Capital lab supplies, South Africa) into 36 mL DEPC-treated water.

2. Heated until agarose (Sigma, Capital lab supplies, South Africa) dissolved and cooled till 60 °C

3. Added 5 mL 10 x MOPS buffer (Sigma, Capital lab supplies, South Africa) and 9 mL 37 % formaldehyde (Sigma, Capital lab supplies, South Africa).

4. Poured gel into casting tray and allowed to set for 30 mins.

RNA sample preparation and Electrophoresis:

1. Added 2.5 µL of RNA to 2.5 µL of RNase-free water (1:1 dilution).

2. Incubated samples at 65 °C for 10 mins and cooled on ice for 2mins.

3. Added 5 µL of RNA gel loading dye (Thermofisher Scientific, South Africa).

4. Loaded and ran at 70 V until dye has migrated ¾ of gel.

5. Visualised in the G box. Expose for 80 ms.

Table D1.1. RNA concentrations and purity ratios obtained for all strains for 4-h.

Sample	Replicate	Concentration	260/280	260/230
	1	235.4	1.95	2.03
	2	252.5	1.99	1.89
Δ*mtp*	3	221.7	1.94	2.08
MTP	1	393.5	1.99	2.04
complement	2	313.1	1.98	2.00
	3	280.9	2.02	2.07
	1	147.7	1.90	1.99
Δ*hbhA*	2	139.7	1.98	1.68
	3	271.3	1.89	2.03
HBHA	1	236.3	2.01	1.93
complement	2	243.2	2.01	2.22
	3	351.9	2.01	2.18
	1	120.5	1.97	2.02
Δ*Rv0309*	2	229.1	1.95	2.22
	3	215.3	1.98	2.08
Rv0309	1	352.2	1.95	2.02
complement	2	358.3	1.92	2.05
	3	305.5	1.95	2.01
Wild-type	1	439.9	1.95	2.18
	2	514.5	1.95	2.19
	3	500.5	1.68	0.23
Δmtp-hbhA	1	200.2	1.85	1.03
	2	155.6	1.98	2.14
	3	136.4	1.98	2.24
mtp-hbhA-	1	278.2	2.03	2.27
mutant	2	121.9	2.01	2.17
	3	188.5	1.97	2.31

Table D1.2. RNA concentrations and purity ratios obtained for all strains for 24-h

Sample	Replicate	Concentration	260/280	260/230
	1	688.6	1.96	2.08
Δ*mtp*	2	733.9	1.97	2.32
	3	741.4	1.94	2.16
MTP	1	852.1	1.95	2.27
complement	2	908.8	1.95	2.22
	3	1003.9	1.93	2.23
	1	758.5	1.97	2.29
Δ*hbhA*	2	838.4	1.92	2.28
	3	748.4	2.02	2.24
	1	624.5	1.97	2.02
Δ*Rv0309*	2	729.1	1.95	2.22
	3	802.3	1.92	2.08
Rv0309	1	752.2	1.95	2.02
complement	2	658.3	1.92	2.05
	3		1.92	2.01
HBHA	1	954.5	2.02	1.94
complement	2	839.6	2.02	2.00
	3	991.1	1.98	2.13
Wild-type	1	1062.9	1.93	2.06
	2	1090.7	1.90	2.14
	3	972.0	1.86	2.18
Δmtp-hbhA	1	326.3	1.92	2.24
	2	558.7	2.0	2.24
	3	597	1.92	2.14
mtp-hbhA-	1	642.4	1.98	2.17
complement	2	640.5	1.94	2.19
	3	608.8	2.01	1.50

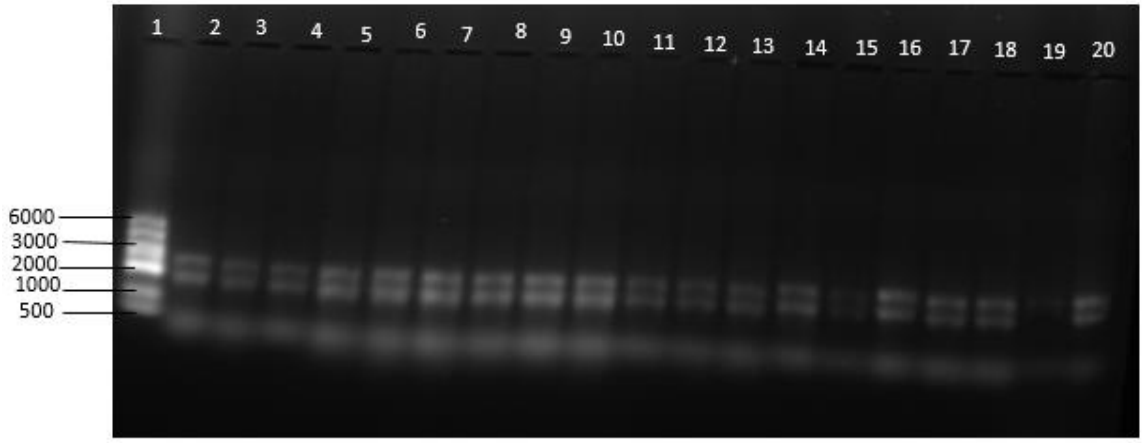

Figure D1.1: **Gel electrophoresis images of RNA extracted from intracellular *M. tuberculosis* strains from the infected THP-1 cells run at 70 V for 3 hours on a 1.5 % MOPS gel using a molecular riboruler marker.** (Lane 1) represents the molecular weight marker. Lanes 2-4 correspond to Δ*mtp* sample 4-h (Replicates 1-3) from Table D1.1 and D1.2 Lanes 5-7 correspond *mtp* comp at 24-h (Replicates 1-3). Lanes 8-10 correspond to wild-type (V9124) at 24-h (Replicates 1-3). Lanes 11-13 correspond Δ*hbhA* 4-h (Replicates 1-3). Lanes 14-16 correspond to Δ*mtp-hbhA* at 24-h (Replicates 1-3). Lanes 17-20 correspond to *hbhA*-complement (Replicates 1-3) at 24-h.

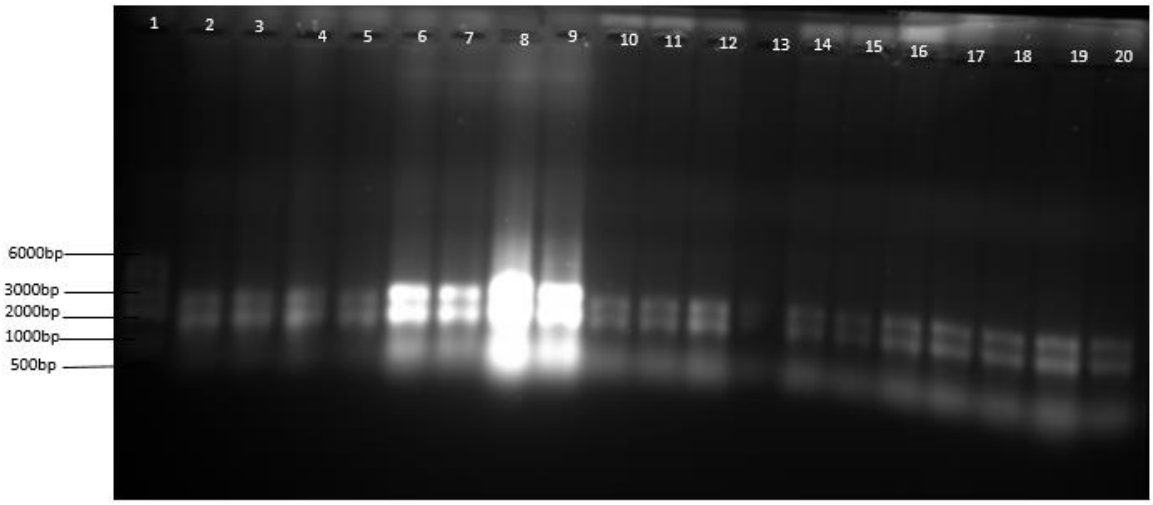

Figure D1.2: **Gel electrophoresis images of RNA extracted from intracellular *M. tuberculosis* strains from the infected THP-1 cells run at 70V for 3 hours on a 1.5% MOPS gel using a molecular riboruler marker.** (Lane 1) represents the molecular weight marker. Lanes 2-4 correspond to Δ*mtp* sample (Replicates 1-3) at 24-h from Table D1.1 and D1.2 (Lanes 5) Δ*mtp* 4-h, Lanes 6-9 correspond to wild-type (V9124) from the broth (Replicates 1-4). Lanes 10-12 correspond Δ*Rv309* (Replicates 1-3) at 24-h. Lanes 13-15 correspond to Δ *Rv0309* (Replicates 1-3) at 4-h. Lanes 16-18 correspond to *Rv0309*-complement (Replicates 1-3) at 24-h. Lane 19-20 correspond to *mtp-hbhA* complement (Replicate 1-2) at 24-h.

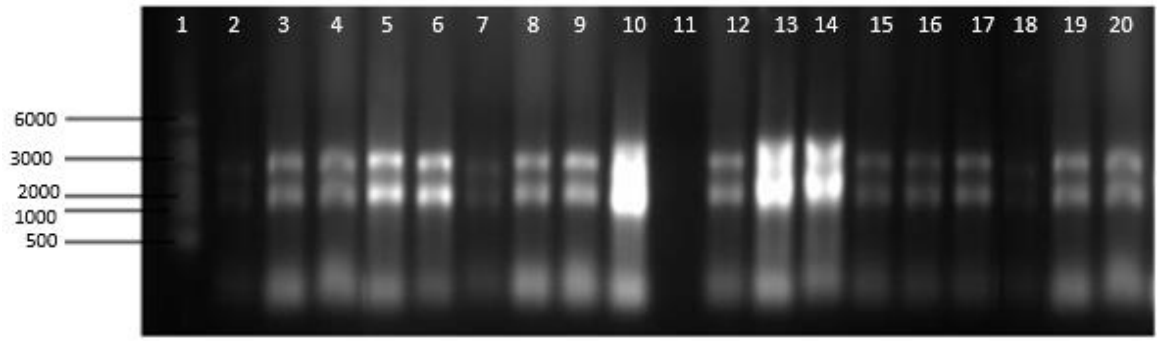

Figure D1.3: **Gel electrophoresis images of RNA extracted from intracellular *M. tuberculosis* strains from the infected THP-1 cells run at 70V for 3 hours on a 1.5% MOPS gel using a molecular riboruler marker.** (Lane 1) represents the molecular weight marker. Lanes 2-4 correspond to *hbhA* complement (Replicates 1-3) at 4-h from Table D1.1 and D1.2. Lanes 5-7 correspond to Δ*hbhA* (Replicates 1-3) at 24-h. Lane 8-9 (wild-type) at 24-h. Lane 10,13 and14 (wild-type from the broth). Lane 11 (blank). Lane 12,15 and 16 (*mtp* complement) at 4-h. Lane 17-18 (wild-type) at 4-h. Lane 19 and 20 wild-type at 24-h.

Table D1.3 Selection of primers – Adhesin genes that facilitate binding to THP-1 cells

Gene	Forward Primer	Reverse Primer	Product size
PstS-1 (Rv0934)	CTACCCGCTGTTCAACCTGT	GATGTTCATCAGCCCCTTGT	187 bp
DnaK (Rv0350)	GATTGGCTGGTGGACAAGTT	AGGTTGATCGAGGTGGACTG	137 bp
19 kDa (Rv3763)	GTCTTTCCGGATGTTCAAGC	CTTACCGTCGATGACGACCT	119 bp
Cpn60.2 (Rv0440)	AATTGCGTACGACGAAGAGG	CCACTTCTTTTCCAGGACGA	118 bp
Apa (Rv1860)	AACCTGTCCGGATCGACAAC	TTGCTGAGGAGTGCTGAACC	109 bp
Rv3804	CCGGTGCCCGACTACTACT	GTAGTCGCGGCTGTGGTC	129 bp
Type IV pili Rv3660	GAGCAGGAGGGTGAACTGGT	GGATCGAGATCGACCAACAG	176 bp

Primer reconstitution

Primers were reconstituted using nuclease-free water according to the volumes given by Inqaba. Primers were then aliquotted into 3 tubes containing 50 µl of 100 µM stocks. These were stored in the -20 ˚C freezer in the PCR mastermix room.

RT-qPCR raw data

To assess primer efficiency, WT genomic DNA (845.6 ng/L) was collected beforehand for PCR validation of the strains. The number of molecules in each piece of DNA was first determined. H37Rv was employed as a reference strain for measuring genome length. H37Rv has a genomic length of 4 411 532 bp.

Number of copies = (ng of DNA x 6.022x10^23)/ (genome length x 1x10^9 x 650)

= (845.6 x 6.022x10^{23})/ (4411532 bp x 1x10^{9} x 650)

= 1.77 x 10^{8} (number of genomes in 1 µL of DNA sample)

=1.78 x 10^{8}

A 10-fold dilution series was made to test primer efficiency. A 50 µL volume was used to make the first aliquot of the dilution series using the following calculation:

$C_1V_1 = C_2V_2$
(1.77x10^8) V_1 = (1x10^{7}) (50)
V_1 = 2.82 µL

From the above calculation, 2.82 of DNA stock was added to 47.18 µL of nuclease-free water to make the first aliquot of the dilution series i.e. tube A=1 x10^{7}.

Thereafter, dilute 10 fold across tube A-H (3 µL into 27 µL of nuclease-free water to make 1:10 dilution into a total volume of 30 µL).

Table D1.2: Dilution of genomic DNA

Tube	DNA dilution	Volume of a sample	Nuclease free water
A	10^{7}	50 µL	0
B	10^{6}	3 µL from tube A	27 µL
C	10^{5}	3 µL from tube B	27 µL
D	10^{4}	3 µL from tube C	27 µL
E	10^{3}	3 µL from tube D	27 µL
F	10^{2}	3 µL from tube E	27 µL
G	10^{1}	3 µL from tube F	27 µL
H	10^{0}	3 µL from tube G	27 µL

Primer dilutions of 10 µM working stocks were made. From the 100 µM aliquot, 3 µL of this was added to 27 µL nH_2O to make 30 µL aliquots and were labelled as follows:

1) Rv3763(F)
2) Rv3763(R)
3) Rv0934 (F)
4) Rv0934 (R)
5) Rv3804 (F)
6) Rv3804(R)
7) Rv0440 (F)
8) Rv0440(R)
9) Rv0350 (F)
10) Rvo350 (R)
11) Rv3660 (F)
12) Rv3660 (R)
13) 16S rRNA (R)
14) 16S rRNA (F)

Table D1.3 A qPCR mastermix was then prepared according to Suventha's protocol for a 10 µl reaction volume.

Reagent	X 1 reaction (µL)	X 10 reactions (µL)
SYBR Green	5	50
Primer (F)	1	10
Primer (R)	1	10
DNA	1	(1 µL added individually)
nH2O	2	20
Total	10	90

Ten (10) reactions consisted of 8 reactions (Tubes A – H for dilution series) and an extra 2 reactions for pipetting error. This was prepared for each primer set. Hence, 6 x 2 mL eppendorf tubes were labelled for each primer set and the above 90 µL mastermix was prepared in these tubes, with the addition of the respective F and R primers to each tube. From the 90 µL, 9 µL of the mastermix was pipetted into each strip well. Thereafter, 1 µL of the diluted DNA series (Tubes A - H) was added to each respective well.

Cycling conditions were as follows:

Holding stage @ 95 ˚C for 30 s

Cycling stage (40 cycles) @ 95 ˚C for 5 s then annealing temperature at 60 ˚C (changeable) for 30 s (documentation and imaging ON)

Melt curve stage @ 95 ˚C for 15 s than 60 ˚C for 1 min than (1% documentation and imaging ON) then 95 ˚C for 30 s and lastly, 60 ˚C for 15 s.

Change reaction volume to 10 µL and start run.

qPCR analysis of results

The amplification plot is expected to produce log-phase amplification curves that are equidistant from each other. This represents an idealistic dilution series and an optimal primer set. The lower dilution series often produce unamplified or low amplified products due to the low copy number of DNA in these tubes.

The standard curve produces the primer efficiency percentage and is represented as linear regression. If all points are plotted in a straight line, the primer is efficient.

Melt curve analysis shows amplified products. Unspecific peaks can be shown on these curves which means that your primer set is amplifying other genomic sections other than the target sequence. This is unfavourable. It could also mean that it is amplifying contaminants in the sample.

The primers were tested and the following images show the results of the run:

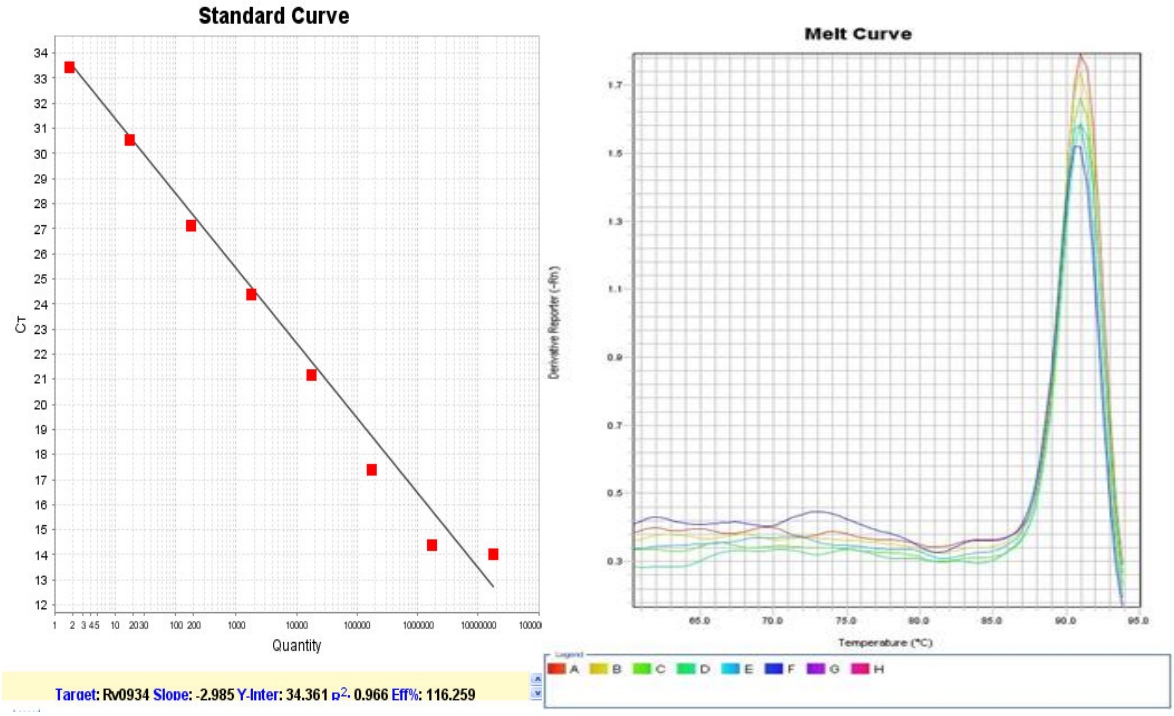

RT-qPCR analysis for *Rv0934*. Results generated a slope = -2.985, R^2 = 0.966, efficacy= 116.259% and Y-intercept =34.361, depicted by the standard curve (a), melt curve (b)

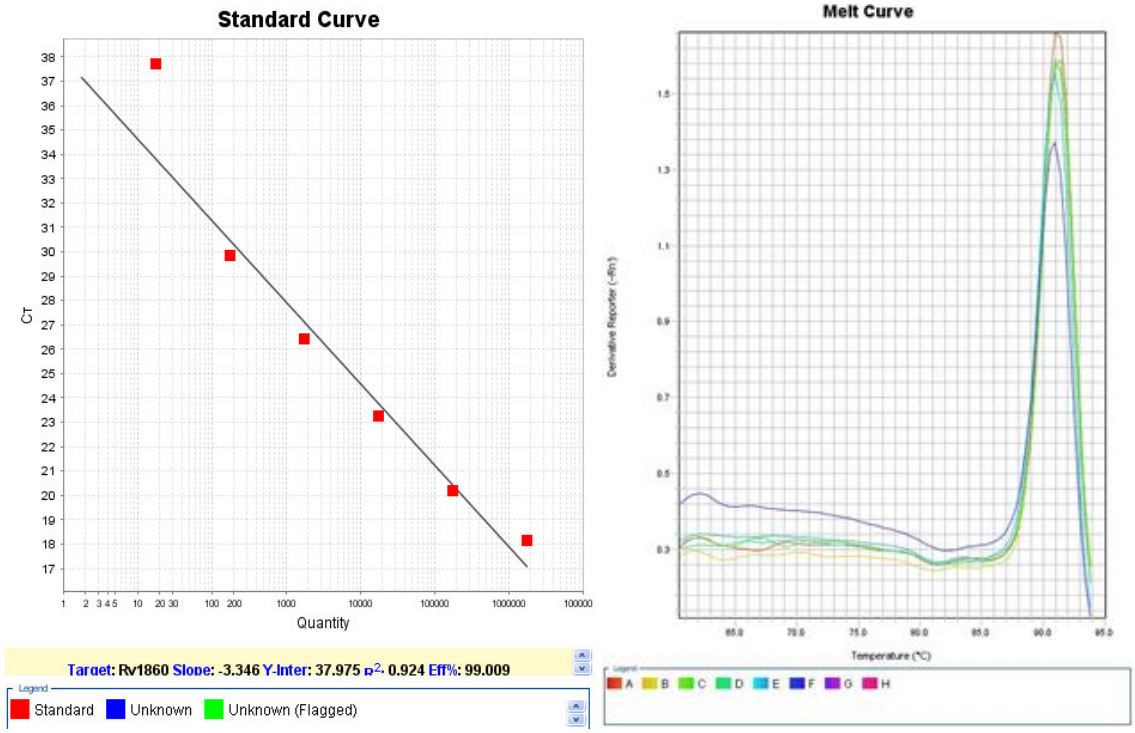

RT-qPCR analysis for *Rv1860*. Results generated a slope = -3.466, R^2 = 0.966, efficacy= 99.009 % and Y-intercept =37.975, depicted by the standard curve (a), melt curve (b)

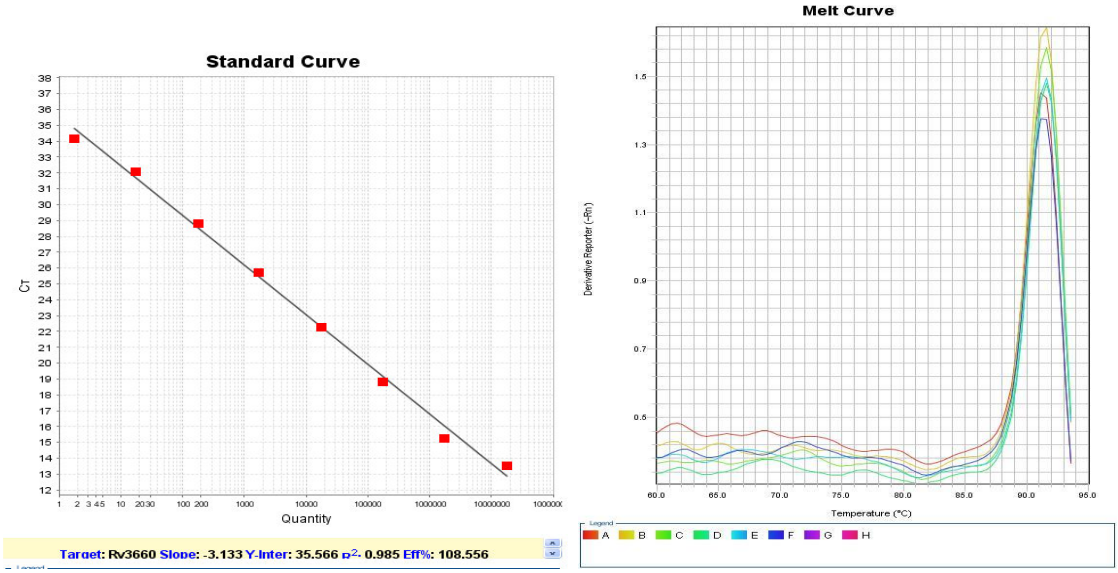

RT-qPCR analysis for *Rv3660*. Results generated a slope = -3.133, R^2 = 0.985, efficacy= 108,556 % and Y-intercept =35,560 depicted by the standard curve (a), melt curve (b).

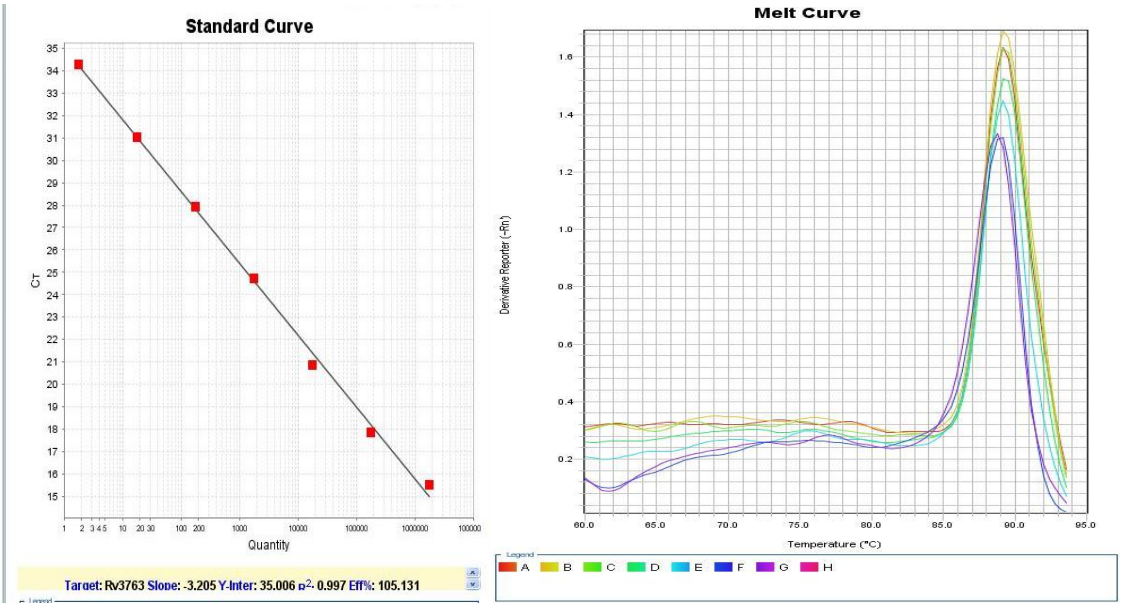

RT-qPCR analysis for *Rv3763*. Results generated a slope = -3.205, R^2 = 0.957, efficacy= 105,131 % and Y-intercept =35,096 depicted by the standard curve (a), melt curve (b).

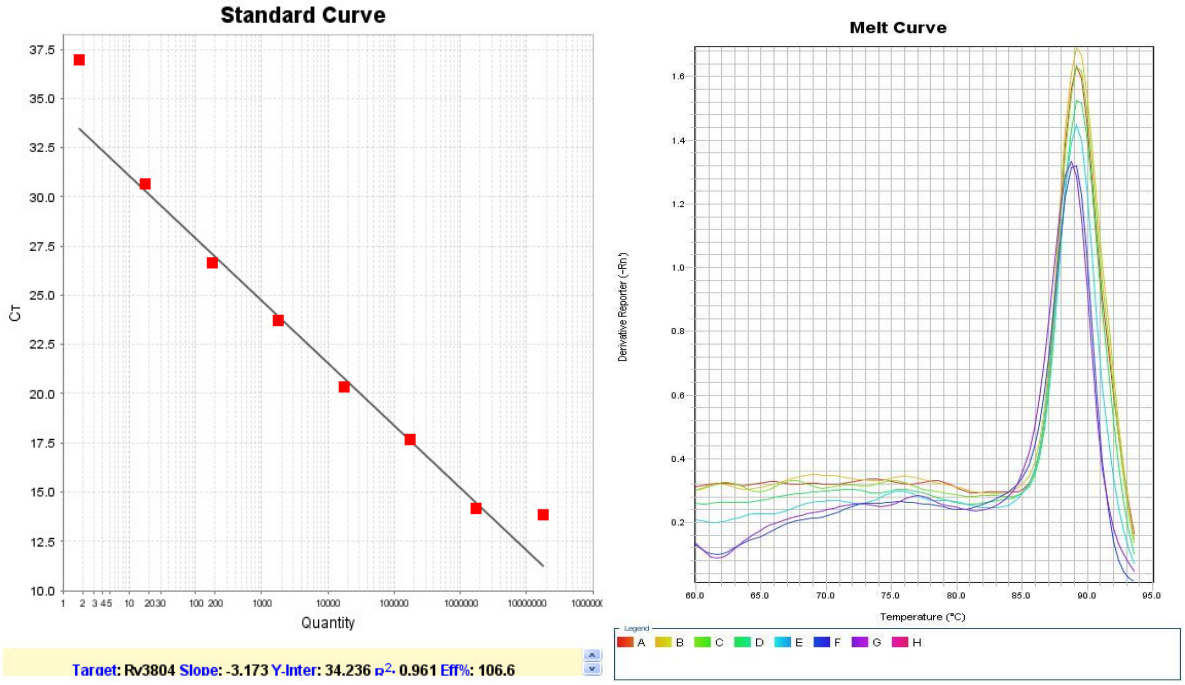

RT-qPCR analysis for *Rv3804*. Results generated a slope = -3,173, R^2 = 0.961, efficacy= 106.6 % and Y-intercept =34.236 depicted by the standard curve (a), melt curve (b).

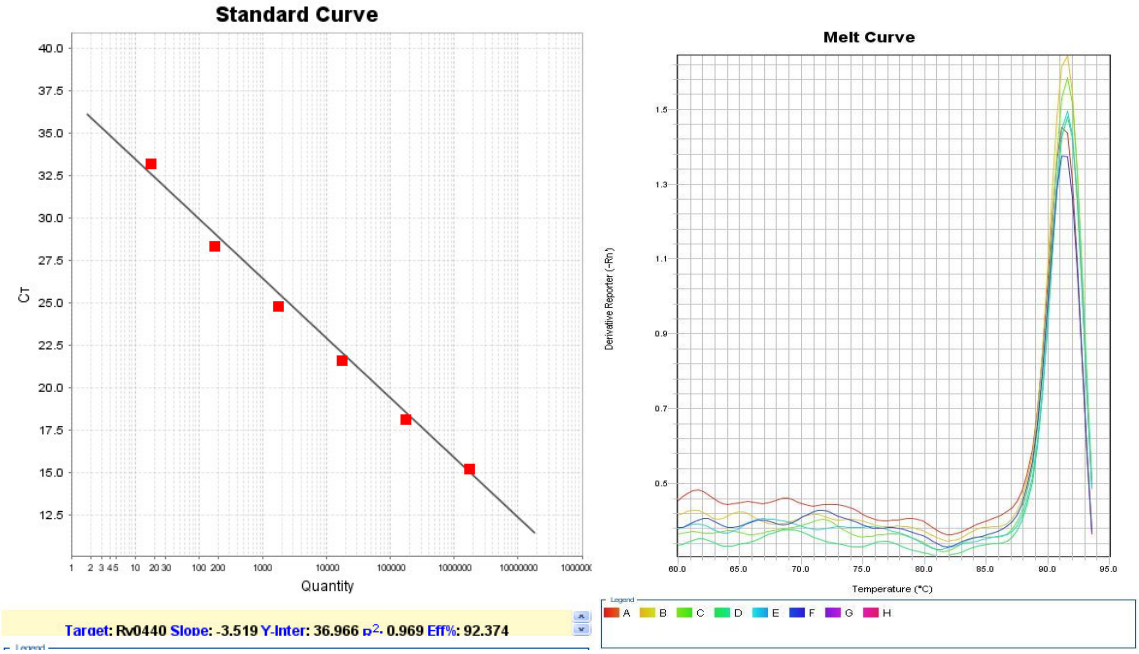

RT-qPCR analysis for *Rv0440*. Results generated a slope = -3,519, R^2 = 0.969, efficacy= 92.374 % and Y-intercept =36,966 depicted by the standard curve (a), melt curve (b).

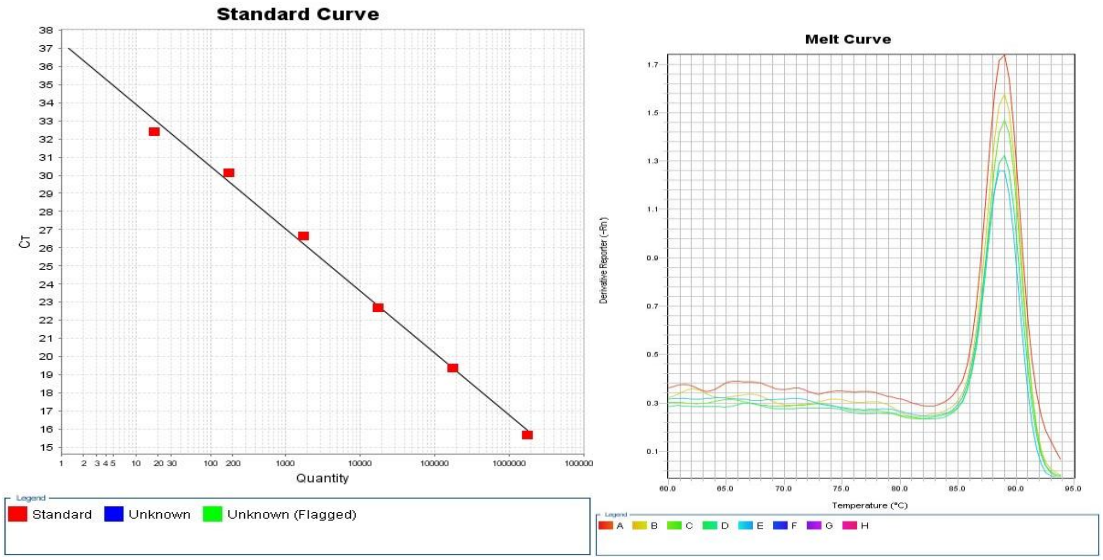

RT-qPCR analysis for 16S rRNA. Results generated a slope = -3,427, R^2 = 0.969, efficacy= 98.374 % and Y-intercept = 37,332 depicted by the standard curve (a), melt curve (b).

Standard curve values that were used to calculate gene expression.

primer	slope	y-intercept
Rv3763	-3,205	35,005
Rv0934	-2,985	34,361
Rv0350	-3,141	34,671
Rv3660	-3,133	35,56
Rv1860	-3,466	34,975
Rv0440	-3,519	36,966
Rv3804	-3,173	34,236
16S	-3,427	37,332

Gene expression data for each replicated and all biological assays was combined. This was then exported into Graphpad Prism for statistical analysis

These results were entered into an Excel spreadsheet and a linear regression equation for each primer was deduced using the slope value and y-intercept from the Primer Efficiency run. Using the individual Ct value for each sample as y, the value of x was solved which produced a transcriptome number. This value was then divided by the transcriptome number of 16S which was used as the housekeeping gene for normalisation.

Gene expression/16S for all three biological assays for 4 and 24-h time point

Table C3.4. Transcriptome number obtained for each gene and sample generated after the RT-qPCR run for 24-h

Strain	RV3763	RV3763	RV3763	RV0934	RV0934	RV0934	RV3804	RV3804	RV3804	RV0350	RV0350	RV0350	RV3660	RV3660	RV3660	RV1860	RV1860	RV1860	RV0440	RV0440	RV0440
WT	0,704589	0,655387	0,646434	0,558251	0,583964	0,56783	0,692965	0,635709	0,694973	0,551361	0,578839	0,566293	0,437197	0,501173	0,55776	0,633211	0,623219	0,683639	0,729807	0,735408	0,863861
MTP0	0,027847	0,154417	0,044493	0,041966	-0,0459	-0,1989	0,211135	-0,1958	-0,33444	5,719854	4,469567	5,207989	5,881497	4,595877	5,355166	0,282254	-0,13576	-0,07788	5,443393	4,253537	5,358497
MTPC	0,832915	0,806975	0,805945	0,572652	0,608058	0,586171	0,820667	0,737776	0,818069	0,356641	0,418589	0,387173	0,368619	0,305593	0,373426	0,741868	0,714998	0,811602	0,782104	0,784174	0,977785
HBHA0	0,605997	0,606073	0,593393	0,420848	0,460597	0,4357	0,513028	0,482997	0,520999	0,532827	0,564225	0,54969	0,383731	0,47984	0,540222	0,521139	0,519982	0,57968	0,652725	0,665454	0,801245
HBHAC	0,636408	0,632992	0,617841	0,468459	0,516199	0,486672	0,685426	0,626867	0,688748	0,477993	0,526396	0,503455	0,368594	0,412769	0,489878	0,63636	0,621482	0,71133	0,872154	0,863824	1,06556
RV0	0,822414	0,785907	0,781727	0,165809	0,286978	0,213756	0,776062	0,69297	0,775056	0,442656	-0,07985	-0,18959	0,588013	-0,24841	-0,21269	3,811902	3,166229	3,557042	0,536904	0,581492	0,853608
RVC	0,826678	0,796003	0,793637	0,494214	0,548218	0,515174	0,825333	0,736724	0,821865	0,240403	0,33196	0,284457	0,05274	0,194095	0,266946	0,844473	0,797477	0,925245	0,67155	0,689497	0,919687
DMS0	0,822127	0,79566	0,79357	0,550134	0,590838	0,565759	0,816297	0,73265	0,813702	0,264088	0,341843	0,301336	0,204787	0,220501	0,286225	0,797156	0,761568	0,86971	0,666831	0,683223	0,883117
DMSC	7,771684	5,614878	6,847526	0,025091	0,262669	0,127103	7,67761	5,135789	6,764639	7,854373	5,674619	6,920382	0,199759	5,834984	7,115952	7,180294	5,187612	6,326461	7,474743	5,400345	7,120378

Strain	RV3763	RV3763	RV3763	RV0934	RV0934	RV0934	RV3804	RV3804	RV3804	RV0350	RV0350	RV0350	RV3660	RV3660	RV3660	RV1860	RV1860	RV1860	RV0440	RV0440	RV0440
WT	0,713249	0,694209	0,644761	0,552607	0,533007	0,55503	0,706565	0,631149	0,690646	0,548374	0,555039	0,562867	0,414007	0,499832	0,540396	0,625821	0,621477	0,677149	0,717247	0,72404	0,872196
MTP0	0,032117	0,183238	0,04282	0,036322	0,016722	-0,2117	0,224735	-0,20036	-0,33877	5,716866	4,445767	5,204563	5,858307	4,594536	5,337802	0,274864	-0,1375	-0,08437	5,430833	4,242169	5,356823
MTPC	0,831575	0,905796	0,804272	0,567008	0,547408	0,573371	0,834267	0,733216	0,813742	0,353653	0,394789	0,383747	0,345429	0,304252	0,356062	0,734478	0,713256	0,805112	0,769544	0,772806	0,976111
HBHA0	0,604657	0,614895	0,59172	0,415204	0,395604	0,4229	0,526628	0,478437	0,516672	0,52984	0,540425	0,546264	0,360541	0,478499	0,522858	0,513749	0,51824	0,57319	0,640165	0,654086	0,799571
HBHAC	0,635068	0,631814	0,616168	0,462815	0,443215	0,473872	0,699026	0,622307	0,684421	0,475005	0,502596	0,500029	0,345404	0,411428	0,472514	0,62897	0,61974	0,70484	0,859594	0,852456	1,063886
RV0	0,821074	0,784728	0,780053	0,160165	0,140565	0,200956	0,789662	0,68841	0,770729	0,439668	-0,10365	-0,19302	0,564823	-0,24975	-0,23005	3,804512	3,164487	3,550552	0,524344	0,570124	0,851934
RVC	0,825338	0,794824	0,791963	0,48857	0,46897	0,502374	0,838933	0,732164	0,817538	0,237416	0,30816	0,281031	0,02955	0,192754	0,249582	0,837083	0,795735	0,918755	0,65899	0,678129	0,918013
DMS0	0,820787	0,794481	0,791897	0,54449	0,52489	0,552959	0,829897	0,72809	0,809375	0,2611	0,318043	0,29791	0,181597	0,21916	0,268861	0,789766	0,759826	0,86322	0,654271	0,671855	0,881444
DMSC	7,787828	5,613699	6,845853	0,019447	-0,00015	0,114303	7,69121	5,131229	6,760312	7,851385	5,650819	6,916956	0,176569	5,833643	7,098588	7,172904	5,18587	6,319971	7,462183	5,388977	7,118704

Strain	RV3763	RV3763	RV3763	RV0934	RV0934	RV0934	RV3804	RV3804	RV3804	RV0350	RV0350	RV0350	RV3660	RV3660	RV3660	RV1860	RV1860	RV1860	RV0440	RV0440	RV0440
WT	0,71305	0,694055	0,635805	0,552428	0,526567	0,554854	0,690921	0,631272	0,687099	0,552907	0,557026	0,563431	0,411831	0,497834	0,540262	0,625807	0,604727	0,660399	0,719031	0,71639	0,86874
MTP0	0,031919	0,183084	0,033863	0,036144	0,010283	-0,21187	0,209091	-0,20024	-0,34232	5,721399	4,447755	5,205127	5,856131	4,592538	5,337668	0,27485	-0,15425	-0,10112	5,432617	4,234519	5,353367
MTPC	0,831376	0,905642	0,795316	0,56683	0,540969	0,573195	0,818623	0,733339	0,810195	0,358186	0,396776	0,384311	0,343253	0,302254	0,355928	0,734464	0,696506	0,788362	0,771328	0,765156	0,972655
HBHA0	0,604458	0,614741	0,582764	0,415026	0,389164	0,422724	0,510984	0,47856	0,513125	0,534373	0,542412	0,546828	0,358365	0,476501	0,522724	0,513736	0,50149	0,55644	0,641949	0,646436	0,796115
HBHAC	0,634869	0,63166	0,607211	0,462637	0,436775	0,473696	0,683382	0,622431	0,680874	0,479538	0,504583	0,500593	0,343228	0,40943	0,47238	0,628957	0,60299	0,68809	0,861378	0,844806	1,06043
RV0	0,820875	0,784574	0,771097	0,159986	0,134125	0,20078	0,774018	0,688533	0,767182	0,444201	-0,10167	-0,19245	0,562647	-0,25175	-0,23019	3,804499	3,147737	3,533802	0,526128	0,562474	0,848478
RVC	0,825139	0,79467	0,783007	0,488392	0,462531	0,502198	0,823289	0,732288	0,813992	0,241949	0,310148	0,281595	0,027374	0,190756	0,249448	0,837069	0,778985	0,902005	0,660774	0,670479	0,914557
DMS0	0,820588	0,794327	0,78294	0,544311	0,51845	0,552783	0,814253	0,728214	0,805828	0,265633	0,32003	0,298474	0,179421	0,217162	0,268727	0,789753	0,743076	0,84647	0,656055	0,664205	0,877988
DMSC	7,78763	5,613545	6,836897	0,019269	-0,00659	0,114127	7,675566	5,131353	6,756765	7,855918	5,652806	6,91752	0,174393	5,831644	7,098454	7,172891	5,16912	6,303221	7,463967	5,381327	7,115248

Table C3.4. Transcriptome number obtained for each gene and sample generated after the RT-qPCR run 4-h.

Strain	RV3763	RV3763	RV3763	RV0934	RV0934	RV0934	RV3804	RV3804	RV3804	RV0350	RV0350	RV0350	RV3660	RV3660	RV3660	RV1860	RV1860	RV1860	RV0440	RV0440	RV0440
WT	0,138587	0,216457	0,207412	0,345695	0,384365	0,504906	0,512907	0,551447	0,489973	0	0	0	0	0	0	0,299706	0,324133	0,433983	0,906707	0,91099	1,039528
MTP0	0,235874	0,312869	0,309711	-0,07454	0,010521	0,118644	0,655274	0,683966	0,624609	0	0	0	0	0	0	1,361417	0,383748	0,402552	0,531471	1,329498	1,292018	1,463842
MTPC	0,996777	0,997735	1,04423	1,070346	1,040996	1,223829	1,029611	1,020896	0,985967	1,08859	1,059976	1,026771	0,60157	0,646261	0,426473	0,819232	0,794519	0,951855	2,082203	1,969506	2,190448
HBHA0	0,4328	0,45772	0,460787	0,498083	0,510185	0,570475	0,543695	0,561017	0,532503	0,424422	0,440837	0,408221	0,290265	0,323221	0,221641	0,383784	0,391958	0,445482	0,886305	0,889265	0,948834
HBHAC	0,402212	0,428342	0,43051	0,498375	0,51041	0,570427	0,429233	0,451428	0,419744	0,506493	0,519285	0,489184	0,302758	0,335025	0,234273	0,381116	0,389369	0,442566	0,976359	0,975411	1,0373
RV0	1,409753	1,346822	1,463674	1,759892	1,606499	1,970758	2,036852	1,866111	1,90899	0	0	0	0,518509	0,601238	0,238246	1,465468	1,32607	1,644831	2,488824	2,24945	2,642036
RVC	0,022751	0,084877	0,072757	0,039797	0,086336	0,156284	0,019165	0,077477	0,013865	0	0	0	0	0	0	0,007617	0,043259	0,106589	-0,01255	0,048529	0,098809
DMS0	0	0	0	0	0,007981	0,067646	0	0	0	0	0	0	0	0	0	0,29566	0,311395	0,379004	1,038927	1,034114	1,118757
DMSC	0,325308	0,363022	0,363279	0,496469	0,511983	0,58954	0,489034	0,514139	0,475667	0,475277	0,493383	0,453508	0,244079	0,288641	0,156741	0,407933	0,417014	0,486781	1,11628	1,107317	1,192364

Strain	RV3763	RV3763	RV3763	RV0934	RV0934	RV0934	RV3804	RV3804	RV3804	RV0350	RV0350	RV0350	RV3660	RV3660	RV3660	RV1860	RV1860	RV1860	RV0440	RV0440	RV0440
WT	0,207412	0,216457	0,207412	0,504906	0,384365	0,504906	0,512907	0,551447	0,489973	0	0	0	0	0	0	0,299706	0,324133	0,433983	1,039528	0,91099	1,039528
MTP0	0,309711	0,312869	0,309711	0,118644	0,010521	0,118644	0,655274	0,683966	0,624609	0	0	0	0	0	0	0,383748	0,402552	0,531471	1,463842	1,292018	1,463842
MTPC	1,04423	0,997735	1,04423	1,223829	1,040996	1,223829	1,029611	1,020896	0,985967	1,08859	1,059976	1,026771	0,60157	0,546261	0,546261	0,819232	0,794519	0,951855	2,190448	1,969506	2,190448
HBHA0	0,460787	0,45772	0,460787	0,570475	0,510185	0,570475	0,543695	0,561017	0,532503	0,424422	0,440837	0,408221	0,290265	0,333221	0,333221	0,383784	0,391958	0,445482	0,948834	0,889265	0,948834
HBHAC	0,43051	0,428342	0,43051	0,570427	0,51041	0,570427	0,429233	0,451428	0,419744	0,506493	0,519285	0,489184	0,302758	0,335025	0,335025	0,381116	0,389369	0,442566	1,0373	0,975411	1,0373
RV0	1,463674	1,346822	1,463674	1,970758	1,606499	1,970758	2,036852	1,866111	1,90899	0	0	0	0,518509	0,701238	0,701238	1,465468	1,32607	1,644831	2,642036	2,24945	2,642036
RVC	0,072757	0,084877	0,072757	0,156284	0,086336	0,156284	0,019165	0,077477	0,013865	0	0	0	0	0	0	0,007617	0,043259	0,106589	0,098809	0,048529	0,098809
DMS0	0	0	0	0,067646	0,007981	0,067646	0	0	0	0	0	0	0	0	0	0,29566	0,311395	0,379004	1,118757	1,034114	1,118757
DMSC	0,363279	0,363022	0,363279	0,58954	0,511983	0,58954	0,489034	0,514139	0,475667	0,475277	0,493383	0,453508	0,244079	0,298641	0,298641	0,407933	0,417014	0,486781	1,192364	1,107317	1,192364

Strain	RV3763	RV3763	RV3763	RV0934	RV0934	RV0934	RV3804	RV3804	RV3804	RV0350	RV0350	RV0350	RV3660	RV3660	RV3660	RV1860	RV1860	RV1860	RV0440	RV0440	RV0440
WT	0,138587	0,216457	0,207412	0,345695	0,384365	0,504906	0,512907	0,551447	0,489973	0	0	0	0	0	0	0,299706	0,324133	0,433983	0,906707	0,91099	1,039528
MTP0	0,235874	0,312869	0,309711	-0,07454	0,010521	0,118644	0,655274	0,683966	0,624609	0	0	0	0	0	0	1,361417	0,383748	0,402552	0,531471	1,329498	1,292018	1,463842
MTPC	0,996777	0,997735	1,04423	1,070346	1,040996	1,223829	1,029611	1,020896	0,985967	1,08859	1,059976	1,026771	0,60157	0,646261	0,426473	0,819232	0,794519	0,951855	2,082203	1,969506	2,190448
HBHA0	0,4328	0,45772	0,460787	0,498083	0,510185	0,570475	0,543695	0,561017	0,532503	0,424422	0,440837	0,408221	0,290265	0,323221	0,221641	0,383784	0,391958	0,445482	0,886305	0,889265	0,948834
HBHAC	0,402212	0,428342	0,43051	0,498375	0,51041	0,570427	0,429233	0,451428	0,419744	0,506493	0,519285	0,489184	0,302758	0,335025	0,234273	0,381116	0,389369	0,442566	0,976359	0,975411	1,0373
RV0	1,409753	1,346822	1,463674	1,759892	1,606499	1,970758	2,036852	1,866111	1,90899	0	0	0	0,518509	0,601238	0,238246	1,465468	1,32607	1,644831	2,488824	2,24945	2,642036
RVC	0,022751	0,084877	0,072757	0,039797	0,086336	0,156284	0,019165	0,077477	0,013865	0	0	0	0	0	0	0,007617	0,043259	0,106589	-0,01255	0,048529	0,098809
DMS0	0	0	0	0	0,007981	0,067646	0	0	0	0	0	0	0	0	0	0,29566	0,311395	0,379004	1,038927	1,034114	1,118757
DMSC	0,325308	0,363022	0,363279	0,496469	0,511983	0,58954	0,489034	0,514139	0,475667	0,475277	0,493383	0,453508	0,244079	0,288641	0,156741	0,407933	0,417014	0,486781	1,11628	1,107317	1,192364

Appendix E

Nano drop readings

Protein concentration for the wild type=**15mg/mL**

Mutant *hbhA*=**11.5 mg/mL**

Comp *hbhA*=**12 mg/mL**

$C_1V_1=C_2V_2$

$11.5 \times 15 = 12 \times V_2$

$V_2=11.5$ µL

Adding 11.5 µL of protein sample with 15 µL of loading dye to lane 4

$C_1V_1=C_2V_2$

$11.5 \times 15 = 14.4 \times V_2$

$V_2=11.9$ µL

Adding 11.9 µL of protein sample with 15 µL of loading dye to lane 3

$C_1V_1=C_2V_2$

$11.5 \times 15 = 11.5 \times V_2$

$V_2=15$ µL

Adding 15 µL of protein sample with 15 µL of loading dye to lane 2

Figure E1.1: Western blot analysis was performed in bacterial protein extracted from the intracellular *M. tuberculosis* (4-h and 24-h post infection). Proteins were transferred in to nitrocellulose membranes using Bio-Rad Trans-Blot Turbo Transfer System for 7 min. The blots were probed with primary antibody for Cpn60.2 (1:500) (sc-58170, Santa Cruz, USA) and detected by TMB using Goat anti-Mouse IgG (H+L) Secondary Antibody, HRP conjugate (Product #62-6520, 1:10000 dilution). A protein ladder (in lane 1) Spectra™ Multicolor High Range Protein Ladder (Catalog number**:** 26625). Only the protein ladder was visible after transfer demonstrating the transfer method worked.

Appendix F

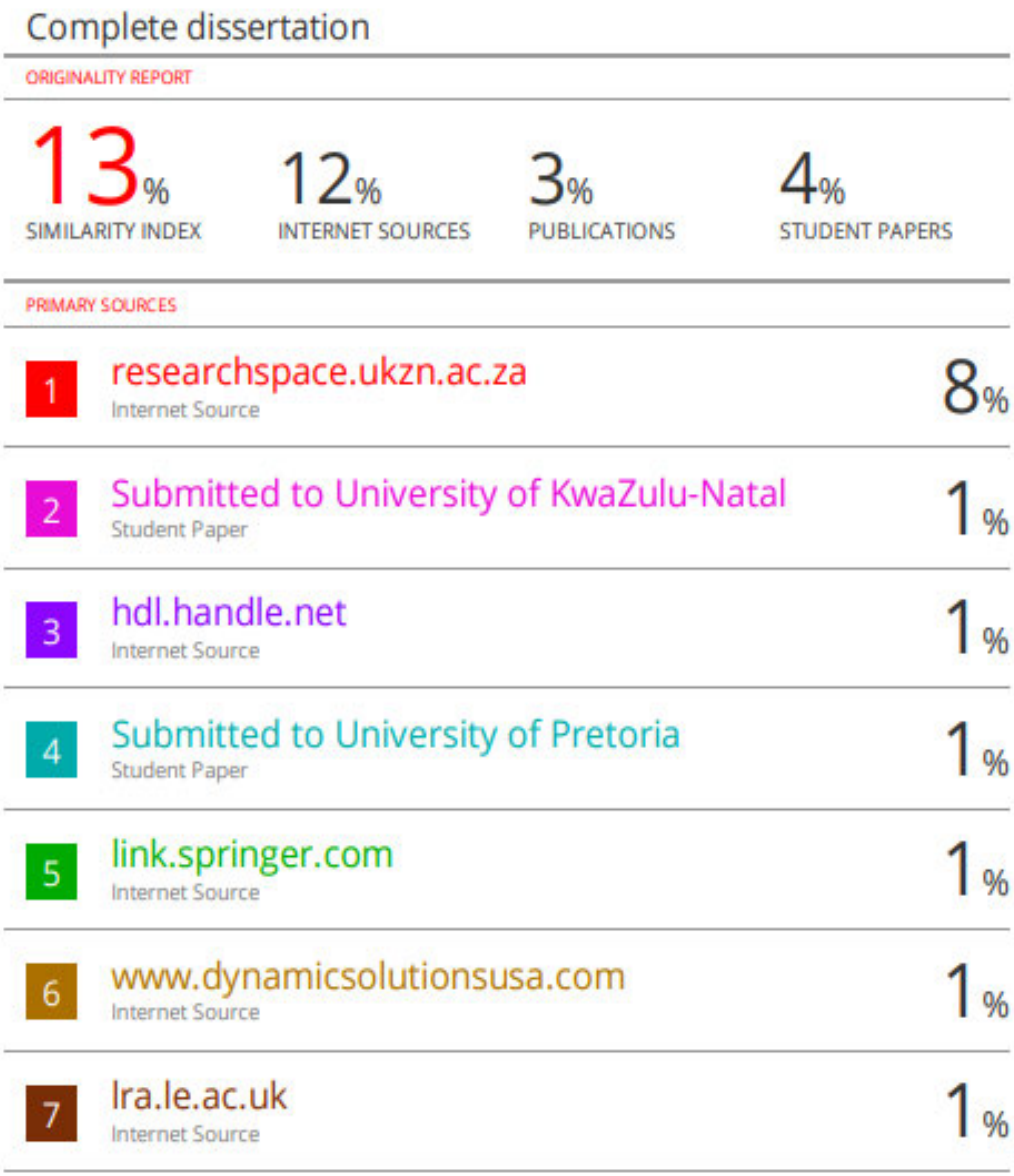

Complete dissertation

ORIGINALITY REPORT

13%	12%	3%	4%
SIMILARITY INDEX	INTERNET SOURCES	PUBLICATIONS	STUDENT PAPERS

PRIMARY SOURCES

1	researchspace.ukzn.ac.za Internet Source	8%
2	Submitted to University of KwaZulu-Natal Student Paper	1%
3	hdl.handle.net Internet Source	1%
4	Submitted to University of Pretoria Student Paper	1%
5	link.springer.com Internet Source	1%
6	www.dynamicsolutionsusa.com Internet Source	1%
7	lra.le.ac.uk Internet Source	1%